FREE VIBRATION OF ELASTIC PLATES WITH VARIOUS SHAPES AND BOUNDARY CONDITIONS

DOCTORAL DISSERTATION

Presented to the Graduate School of Engineering
Hokkaido University

by

Yoshihiro Narita

December, 1979

Acknowledgements

The author would like to express deepest gratitude to his academic adviser, Prof. Toshihiro Irie, for the useful suggestions and warm encouragements throughout the doctoral program at the graduate school of Hokkaido University. To Prof. Arthur W. Leissa, the author's adviser at The Ohio State University,for his continuous guidance during the period of September 1978 through June 1979. To Associate Prof. Gen Yamada of Hokkaido University for his encouragement and instructions on computer programming. Without their guidance, it would have been impossible to accomplish this study, and the author particularly wishes to thank them. To Mr.Suzuki and Mr.Nishikata, my thanks for their cooperation in drawing figures and doing experimental work. To Mr. Michael Nearhood, my appreciation for his assistance in improving the English expressions in this dissertation. The numerical computations of this study were carried out at The Hokkaido University Computing Center and The Ohio State University Computer Center.

Abstract

The free, transverse vibrations of thin isotropic plates of various shapes are investigated in the present study. The main objectives of the study are to demonstrate methods of obtaining series-type solutions for vibration of plates of arbitrary shape under various boundary (constraint) conditions, and to present accurate and extensive numerical results on the topic.

Analytical procedures are described in detail and the frequency equations obtained are expressed in convenient forms. The natural frequencies and nodal patterns of the plates are presented in figures and tables. Variations of these results with wide ranges of parameters are shown and their physical significances are thoroughly discussed.

CONTENTS

Acknowledgements

Abstract

Chapter 1 Preface

1-1 General statement of the problem 1

1-2 Comments on the methods of analyzing plate vibration 3

Chapter 2 Rectangular Plates with Internal Supports

2-1 Introduction 6

2-2 Analysis 6

2-3 Rectangular plate having uniform boundary conditions

2-3-1 Review 13

2-3-2 Application of the method 18

2-3-3 Results and discussion 25

2-4 Rectangular plate having internal supports

2-4-1 Review 26

2-4-2 Application of the method 27

2-4-3 Results and discussion 30

Chapter 3 Circular Plates with Various Boundary Conditions

3-1 Introduction 38

3-2 Circular plate having uniform boundary conditions

3-2-1 Review 39

3-2-2 Analysis 41

3-2-3 Results and discussion 46

3-3 Simply supported plate partially constrained by rotational springs

3-3-1 Review 57

3-3-2 Analysis 59

3-3-3 Results and discussion 64

3-4 Free plate partially constrained by translational and rotational springs

3-4-1 Review 82

3-4-2 Analysis 84

3-4-3 Results and discussion 89

3-5 Free plate with non-uniform edge mass

3-5-1 Review 100

3-5-2 Analysis 101

3-5-3 Results and discussion 104

Chapter 4 Clamped Polygonal Plates

4-1 Introduction 112

4-2 Analysis 112

4-3 Triangular plate

4-3-1 Review 116

4-3-2 Application of the method 117

4-3-3 Results and discussion 119

4-4 Pentagonal, hexagonal, septagonal and octagonal plate

4-4-1 Review 121

4-4-2 Application of the method 122

4-4-3 Results and discussion 125

Chapter 5 Clamped Plates of Irregular Shapes

5-1 Introduction 133

5-2 Review 133

5-3 Analysis 134

5-4 Cross-shaped plate

5-4-1 Application of the method 144

5-4-2 Results and discussion 149

5-5 I-shaped plate

5-5-1 Application of the method 152

5-5-2 Results and discussion 159

5-6 L-shaped plate

5-6-1 Application of the method 161

5-6-2 Results and discussion 164

5-7 L-shaped plate (Experiment)

5-7-1 Review on the experimental studies . . 166

5-7-2 Experimental procedure 167

5-7-3 Results and discussion 172

Chapter 6 Plates of Other Shapes (Bibliography)

6-1 Introduction 181

6-2 Trapezoidal plate 182

6-3 Parallelogramic plate 185

6-4 Annular plate 186

6-5 Sectorial and annular sectorial plate . . 187

6-6 Elliptical plate 188

6-7 Rectangular plate with narrow slits . . . 189

6-8 Rectangular plate with holes 190

Chapter 7 Conclusions 192

References 197

CHAP. I PREFACE

1-1. General statement of the problem

The attention of recent technology has been directed toward faster and larger, and therefore the need for more flexible and lighter structures is obvious. This trend has increased the practical importance of dynamic analysis in addition to the classical static analysis, and the numerical evaluation of vibrational characteristics of structural elements has become an important part of the design process. Particularly, thin flat plates of various shapes are found in many structures and the natural frequencies and mode shapes of the plates are indispensable information from a technical point of view. On the other hand, plate vibration has been an academic subject that famous physicists in the 1800's, such as Poisson, Kirchhoff and Rayleigh, have engaged in. For the reasons of both practical and academic interests, numerous publications concerned with the vibration of plates have been published.

The object of this work is, first, to present analytical methods to deal with the free transverse vibration of thin elastic plates of various shapes and edge conditions. The author introduces new series-type solutions which are mathematically exact, satisfying the differential equation of plate vibration, although truncation of the series is necessary. Secondly, extensive and

accurate numerical results are presented to demonstrate the effectiveness of the methods and to provide comprehensive data on the topic. Convergence study by succesive truncation of the series and comparison with other values in available, open literature are made to show the validity of the results. Frequency data are presented in terms of nondimensional frequency parameter. Both tabular and graphical results are given whenever possible, because tabular results are important for considering the accuracy of the method and the comparison by other researchers,and curves are useful for qualitative studies.

A survey was made to collect references mostly from technical journals published after 1967, thereby avoiding duplication with Leissa's monograph [1]. Since a thorough survey covering the recent development of this decade was not found, the author believes that this survey is a good supplement to Leissa's work. Inasmuch as the complicating effects of plates such as anisotropy, in-plane forces, variable thickness, surrounding media, large deflections, shear deformation and rotary inertia are not considered in the present work, literature involving these effects has been basically excluded in the survey.

1-2 Comments on the methods of analyzing plate vibration

The classical (thin) plate theory is used to analyze vibration of plates in the present study. This theory is based on some assumptions in deriving a governing differential equation of motion. For a thin plate whose deflection is small in comparison with its thickness, the governing equation can be derived by making use of the linearlized strain-displacement relation and the assumption that "Normals to the midplane of the undeformed plate remain straight and normal to the midplane during deformation."

For solving the differential equation thus obtained, it is naturally desirable to obtain the exact solutions. However, the exact solutions are found only in a limited number of problems such as a simply supported rectangular plate, and it is well known that the exact analytical methods cannot be applied to problems of plates with irregular boundaries. Approximate mathematical techniques have been developed to remedy the situation. Concerning bending problems of plates, a valuable study was made by Leissa et al.[2] to compare approximate methods, and it is the author's opinion that most of the comments in that study are useful also in considering vibration problems because the governing equation of plate vibration is obtained only by substituting the inertia force for the static load in the equation.

The approximate methods available in the plate vibration problems are classified into some categories

depending upon whether the solutions satisfy the differential equation or the boundary conditions. The Rayleigh-Ritz method consists of minimizing the Rayleigh quotient of the plate and using trial functions satisfying the given boundary conditions. This method is widely applied in the field and the products of beam functions are commonly used to represent the plate deflection. The Galerkin method requires that the residual of the differential equation be orthogonal to each term of the series that satisfy the boundary conditions. Point-matching is a convenient technique, utilizing the exact solutions of the differential equation and meeting the boundary conditions at discrete points along the boundary. The finite element method (FEM) has advanced recently with the development of computers and has its own practical advantage, particularly its applicability to problems having irregularly shaped boundaries.

Although various approximate methods, as described above, have been developed and a great number of technical papers are available using those methods, analytically oriented methods are still of importance. The present methods are good means to yield accurate numerical results since the solutions satisfy both the governing equation exactly and the boundary (constraint) conditions with an arbitrary degree of exactitude. Two types of the series solution are given in the present study, and both solutions employ Fourier series to deal with the boundary (constraint) conditions.

solution (a)—— Suppose that a plate is constrained along an internal segment. With the reaction force and bending moment acting on the segment regarded as unknown harmonic force and moment, the stationary response of the plate to these loads is obtained in terms of the Green function. The unknown force and moment distributed along the segment are expanded into Fourier (sine) series with unknown coefficients, and the frequency equation is given in a matrix form by using constraint conditions on the segment. This method is applied to elastically constrained rectangular plates (Chap.2) and extended to clamped polygonal plates (Chap.4) and irregularly shaped plates (Chap.5).

Solution (b)—— Suppose that a plate has a non-uniform edge condition. The boundary conditions along the edge are represented as accurately as necessary by expanding them into Fourier series. The exact solution of the differential equation of motion for the plate is substituted into the obtained boundary conditions. The frequency equation is then given by rewriting the products of trigonometric series into single series and equating coefficients of trigonometric functions having the same periodicity. This method is applied to circular plates having non-uniform elastic edge conditions and edge mass (Chap.3).

CHAP.2 RECTANGULAR PLATES WITH INTERNAL SUPPORTS

2-1. Introduction

This chapter presents an analytical method using Fourier series and its applications to rectangular plates having internal elastic supports. In Sec.2-2, a general analytical procedure is presented and a frequency equation is given in general form. The detailed equations are derived to determine natural frequencies and mode shapes for rectangular plates with combinations of simply supported and clamped edges (Sec. 2-3) and plates with internal line or rectangular supports (Sec.2-4).

Research on vibration of rectangular plates has a long established history, and more publications have been obtained than those on circular plates because a rectangular plate accommodates twenty-one distinct combinations of clamped, simply supported and free edges. Fifty seven pertinent references concerned with vibration of thin isotropic rectangular plates are reviewed and available results are presented for comparison purpose.

2-2 Analysis *

This section involves a general analysis to deal with vibration of rectangular plates having elastic constraints along some segments parallel to the edges. The analysis will be applied to various rectangular plates in the following sections.

* [56]

The differential equation of motion governing transverse vibration of thin isotropic plate is given, by use of the classical thin plate theory, as

$$D\nabla^4 w + \rho \frac{\partial^2 w}{\partial t^2} = P(x,y,t) \qquad (2\text{-}1)$$

where $w(x,y,t)$ is the transverse displacement of the plate, $P(x,y,t)$ is the external force, D is the flexural rigidity defined as $D = Eh^3/12(1-\nu^2)$ (E :Young's modulus, h :plate thickness and ν :Poisson's ratio), ρ is mass density per unit area of the plate, t is time, and ∇^2 is the Laplacian operator ($\nabla^4 = \nabla^2\nabla^2$) written as $\nabla^2 = \partial^2/\partial x^2 + \partial^2/\partial y^2$ in rectangular coordinates.

Figure 2-1 shows a rectangular plate elastically supported on some segments C_p (p =1,2,..., P) and $C_{p'}$ (p'=1,2, ..., P') located parallel to the edges. The xy plane of a rectangular coordinate o-xyz is taken in the neutral surface of the plate. Assuming harmonic displacement $W(x,y)e^{j\omega t}$ and regarding unknown reaction $P(x,y,t)$ acting on the internal support as unknown external force $Q(x,y)e^{j\omega t}$, equation(2-1)

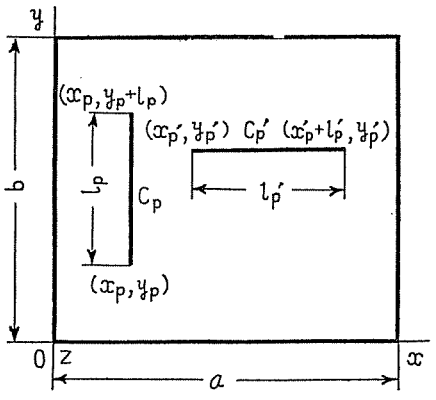

Fig.2-1

becomes

$$D\nabla^4 W - \rho\omega^2 W = Q(x,y) \tag{2-2}$$

$W(x,y)$ and $Q(x,y)$ are expanded into infinite series in terms of the normalized eigenfunction $W_{mn}(x,y)$ of a rectangular plate with no constraints.

$$W(x,y) = \sum_{m=1}^{\infty}\sum_{n=1}^{\infty} A_{mn} W_{mn}(x,y) \tag{2-3a}$$

$$Q(x,y) = \sum_{m=1}^{\infty}\sum_{n=1}^{\infty} Q_{mn} W_{mn}(x,y) \tag{2-3b}$$

where coefficient Q_{mn} in Eq.(2-3b) is expressed as

$$Q_{mn} = \int_0^b\int_0^a Q(u,v) W_{mn}(u,v)\, du\, dv \tag{2-4}$$

with (u, v) being a point where an external force is applied. Substituting Eqs.(2-3) into (2-2) and making use of the relation

$$D\nabla^4 W_{mn} - \rho\omega_{mn}^2 W_{mn} = 0 \tag{2-5}$$

yield

$$A_{mn} = Q_{mn} \big/ \rho(\omega_{mn}^2 - \omega^2) \tag{2-6}$$

and deflection $W(x,y)$ is expressed as

$$W(x,y) = \frac{1}{\rho}\sum_{m=1}^{\infty}\sum_{n=1}^{\infty} \frac{1}{\omega_{mn}^2 - \omega^2} W_{mn}(x,y) \int_0^a\int_0^b Q(u,v) W_{mn}(u,v)\, dv\, du \tag{2-7}$$

If harmonic bending moments $\{M_x(x,y)\ \ M_y(x,y)\}\, e^{j\omega t}$ act on a plate in addition to the force, the contribution of these moments to the plate deflection can be obtained by considering the moments as coupling forces. Suppose that

two sets of distributed forces $M_x\Delta v$, $M_x\Delta v$ and M_y Δu , $M_y\Delta u$ act along opposite sides of a rectangular plate element $\Delta u\Delta v$, the deflection caused by the coupling forces becomes

$$-M_x\Delta v\,G(x,y;u,v)+M_x\Delta v\,G(x,y;u+\Delta u,v)$$
$$-M_y\Delta u\,G(x,y;u,v)+M_y\Delta u\,G(x,y;u,v+\Delta v)$$
$$=M_x\frac{\partial G}{\partial u}(x,y;u,v)\,\Delta u\Delta v+M_y\frac{\partial G}{\partial v}(x,y;u,v)\,\Delta u\Delta v \qquad (2\text{-}8)$$

Then, the deflection by the force and moments is expressed as

$$W(x,y)=\int_0^a\int_0^b\Big\{Q(u,v)\,G(x,y;u,v)+M_x(u,v)\frac{\partial}{\partial u}G(x,y;u,v)$$
$$+M_y(u,v)\frac{\partial}{\partial v}G(x,y;u,v)\Big\}dv\,du \qquad (2\text{-}9)$$

where

$$G(x,y;u,v)=\frac{1}{\rho}\sum_{m=1}^{\infty}\sum_{n=1}^{\infty}\frac{1}{\omega_{mn}^2-\omega^2}W_{mn}(x,y)\,W_{mn}(u,v) \qquad (2\text{-}10)$$

is the Green function of the plate. When unknown force and moment $\{Q_x^{(p)}(y)\;\;M_x^{(p)}(y)\}e^{j\omega t}$ act on the segment $C_p\,[x=x_p=a_p,\ y_p\le y\le y_p+\ell_p]$ and $\{Q_y^{(p')}(x)\;\;M_y^{(p')}(x)\}e^{j\omega t}$ act on the segment $C_{p'}\,[x_{p'}\le x\le x_{p'}+\ell_{p'},\ y=y_{p'}=b_{p'}]$, $Q(u,v)$ and $M_x(u,v)$, $M_y(u,v)$ in Eq.(2-9) are written by

$$Q(u,v)=\sum_{p=1}^{P}Q_x^{(p)}(v)\,\delta(u-a_p)+\sum_{p'=1}^{P'}Q_y^{(p')}(u)\,\delta(v-b_{p'})$$
$$M_x(u,v)=\sum_{p=1}^{P}M_x^{(p)}(v)\,\delta(u-a_p),\quad M_y(u,v)=\sum_{p'=1}^{P'}M_y^{(p')}(u)\,\delta(v-b_{p'}) \qquad (2\text{-}11)$$

using Dirac's delta function. And the deflection is

$$W(x,y)=\sum_{p=1}^{P}\int_{y_p}^{y_p+l_p}\left\{Q_x^{(p)}(v)\,G(x,y;a_p,v)+M_x^{(p)}(v)\frac{\partial}{\partial a_p}G(x,y;a_p,v)\right\}dv$$

$$+\sum_{p'=1}^{P'}\int_{x_{p'}}^{x_{p'}+l_{p'}}\left\{Q_y^{(p')}(u)\,G(x,y;u,b_{p'})+M_y^{(p')}(u)\frac{\partial}{\partial b_{p'}}G(x,y;u,b_{p'})\right\}du \qquad (2\text{-}12)$$

The forces and moments distributed along the segments are expanded into Fourier sine series.

$$Q_x^{(p)}(v)=\sum_{i=1}^{\infty}Q_{x,i}^{(p)}\sin\frac{i\pi(v-y_p)}{l_p},\quad M_x^{(p)}(v)=\sum_{i=1}^{\infty}M_{x,i}^{(p)}\sin\frac{i\pi(v-y_p)}{l_p}$$
$$Q_y^{(p')}(u)=\sum_{i=1}^{\infty}Q_{y,i}^{(p')}\sin\frac{i\pi(u-x_{p'})}{l_{p'}},\quad M_y^{(p')}(u)=\sum_{i=1}^{\infty}M_{y,i}^{(p')}\sin\frac{i\pi(u-x_{p'})}{l_{p'}} \qquad (2\text{-}13)$$

Here it is also possible to use Fourier series with both sine and cosine terms or cosine terms only. Substituting Eqs.(2-13) into (2-12) yields

$$W(x,y)=\frac{1}{P}\sum_{m=1}^{\infty}\sum_{n=1}^{\infty}\frac{1}{\omega_{mn}^2-\omega^2}W_{mn}(x,y)$$
$$\times\sum_{i=1}^{\infty}\left[\sum_{p=1}^{P}\left\{Q_{x,i}^{(p)}I_{mn,i}(a_p)+M_{x,i}^{(p)}\frac{\partial}{\partial a_p}I_{mn,i}(a_p)\right\}+\sum_{p'=1}^{P'}\left\{Q_{y,i}^{(p')}I_{mn,i}(b_{p'})+M_{y,i}^{(p')}\frac{\partial}{\partial b_{p'}}I_{mn,i}(b_{p'})\right\}\right] \qquad (2\text{-}14)$$

where

$$I_{mn,i}(a_p)=\int_{y_p}^{y_p+l_p}W_{mn}(a_p,v)\sin\frac{i\pi(v-y_p)}{l_p}dv,\quad I_{mn,i}(b_{p'})=\int_{x_{p'}}^{x_{p'}+l_{p'}}W_{mn}(u,b_{p'})\sin\frac{i\pi(u-x_{p'})}{l_{p'}}du \qquad (2\text{-}15)$$

When both of the lateral deflection and rotation of a plate are elastically constrained along the segments, the following conditions must be satisfied.

$$Q_x^{(p)}(y)=-k_p W(a_p,y),\quad M_x^{(p)}(y)=-k_{x,p}\frac{\partial W}{\partial a_p}(a_p,y)$$
$$Q_y^{(p')}(x)=-k_{p'}W(x,b_{p'}),\quad M_y^{(p')}(x)=-k_{y,p'}\frac{\partial W}{\partial b_{p'}}(x,b_{p'}) \qquad (2\text{-}16)$$

where k_p, $k_{p'}$ and $k_{x,p}$, $k_{y,p'}$ are the stiffnesses per unit length of the internal supports for the lateral deflection and rotation, respectively.

$W_{mn}(a_p, y)$ and $W_{mn}(x, b_{p'})$ are also expanded into Fourier sine series

$$W_{mn}(a_p,y)=\frac{2}{l_p}\sum_{i=1}^{\infty}I_{mn,i}(a_p)\sin\frac{i\pi(y-y_p)}{l_p},\quad W_{mn}(x,b_{p'})=\frac{2}{l_{p'}}\sum_{i=1}^{\infty}I_{mn,i}(b_{p'})\sin\frac{i\pi(x-x_{p'})}{l_{p'}} \tag{2-17}$$

Substituting Eqs.(2-17) into the equations obtained by the substitution of Eq.(2-14) into (2-16) and equating all coefficients of $\sin\{j\pi(y-y_{p'})/l_p\}$ and $\sin\{j\pi(x-x_{p'})/l_{p'}\}$ to zero, the following equation is derived.

$$\left(\begin{bmatrix}\frac{l_p}{2k_p}\delta_{ij}\delta_{p\beta}\\ \frac{l_p}{2k_{x,p}}\delta_{ij}\delta_{p\beta}\\ \frac{l_{p'}}{2k_{p'}}\delta_{ij}\delta_{p\beta}\\ \frac{l_{p'}}{2k_{y,p'}}\delta_{ij}\delta_{p\beta}\end{bmatrix}+\frac{1}{\rho}\sum_{m=1}^{\infty}\sum_{n=1}^{\infty}\frac{1}{\omega_{mn}^2-\omega^2}\begin{Bmatrix}I_{mn,i}(a_p)\\ \frac{\partial}{\partial a_p}I_{mn,i}(a_p)\\ I_{mn,i}(b_{p'})\\ \frac{\partial}{\partial b_{p'}}I_{mn,i}(b_{p'})\end{Bmatrix}\begin{Bmatrix}I_{mn,j}(a_\beta)\\ \frac{\partial}{\partial a_\beta}I_{mn,j}(a_\beta)\\ I_{mn,j}(b_{\beta'})\\ \frac{\partial}{\partial b_{\beta'}}I_{mn,j}(b_{\beta'})\end{Bmatrix}^T\right)\begin{Bmatrix}Q_{x,j}^{(p)}\\ M_{x,j}^{(p)}\\ Q_{y,j}^{(p')}\\ M_{y,j}^{(p')}\end{Bmatrix}=0 \tag{2-18}$$

where δ_{ij} and $\delta_{p\beta}$ denotes Kronecker's delta. The natural frequencies ω of the plate are obtained by the calculation of the eigenvalues of Eq.(2-18) and the mode shapes are determined by obtaining the eigenvectors $\{Q_{x,j}^{(p)}\ M_{x,j}^{(p)}\ Q_{y,j}^{(p')}\ M_{y,j}^{(p')}\}^T$. In the numerical calculation, the number of terms (m, n) of the infinite series and terms (i, j) of the Fourier series may be truncated at appropriate finite number considering the convergence and accuracy of the solution.

If a rectangular plate with all edges simply supported is used as a plate without internal constraints, the natural frequencies and the normalized eigenfunctions are given by

$$\omega_{mn}^2=\frac{D}{\rho}\left\{\left(\frac{m\pi}{a}\right)^2+\left(\frac{n\pi}{b}\right)^2\right\}^2,\quad W_{mn}(x,y)=\frac{2}{\sqrt{ab}}\sin\frac{m\pi x}{a}\sin\frac{n\pi y}{b} \tag{2-19}$$

In this case, Eq.(2-18) can be written as

$$\left(\begin{bmatrix}\frac{1}{\kappa_p}\delta_{ij}\delta_{pq}\\ \frac{1}{\kappa_{xp}}\delta_{ij}\delta_{pq}\\ \frac{1}{\kappa_{p'}}\delta_{ij}\delta_{pq}\\ \frac{1}{\kappa_{xp'}}\delta_{ij}\delta_{pq}\end{bmatrix}+\sum_{m=1}^{\infty}\sum_{n=1}^{\infty}\frac{1}{f_{mn}(\lambda)}\begin{Bmatrix}\sin m\pi\alpha_p\,\phi_{n,i}(\zeta_p)\\ m\cos m\pi\alpha_p\,\phi_{n,i}(\zeta_p)\\ \sin n\pi\beta_{p'}\phi_{m,i}(\xi_{p'})\\ n\cos n\pi\beta_{p'}\phi_{m,i}(\xi_{p'})\end{Bmatrix}\begin{Bmatrix}\sin m\pi\alpha_q\,\phi_{n,j}(\zeta_q)\\ m\cos m\pi\alpha_q\,\phi_{n,j}(\zeta_q)\\ \sin n\pi\beta_{q'}\phi_{m,j}(\xi_{q'})\\ n\cos n\pi\beta_{q'}\phi_{m,j}(\xi_{q'})\end{Bmatrix}^T\right)\begin{Bmatrix}l_p\,Q_{x,j}^{(p)}\\ (\pi l_p/a)M_{x,j}^{(p)}\\ l_{p'}Q_{y,j}^{(p')}\\ (\pi l_{p'}/b)M_{y,j}^{(p')}\end{Bmatrix}=0 \tag{2-20}$$

where

$$\kappa_p=\frac{8\mu}{\pi^4}\frac{k_p l_p a^2}{D},\quad \kappa_{xp}=\frac{8\mu}{\pi^2}\frac{k_{xp}l_p}{D},\quad \kappa_{p'}=\frac{8\mu^3}{\pi^4}\frac{k_{p'}l_{p'}b^2}{D},\quad \kappa_{yp'}=\frac{8\mu^3}{\pi^2}\frac{k_{yp'}l_{p'}}{D} \tag{2-21}$$

denote nondimensional spring stiffness, $f_{mn}(\lambda)$ is

$$f_{mn}(\lambda)=(m^2+\mu^2n^2)^2-\lambda^4/\pi^4\quad(\mu=a/b) \tag{2-22}$$

and λ is frequency parameter

$$\lambda^4=\rho a^4\omega^2/D$$

$\phi_{n,i}(\zeta_p)$ and $\phi_{m,i}(\xi_{p'})$ in Eq.(2-20) express the definite integrals as follows.

$$\phi_{n,i}(\zeta_p)=\int_0^1\sin n\pi\zeta_p(z)\sin i\pi z\,dz,\quad \phi_{m,i}(\xi_{p'})=\int_0^1\sin m\pi\xi_{p'}(z)\sin i\pi z\,dz \tag{2-23}$$

where

$$\zeta_p(z)=(y_p+l_p z)/b,\quad \xi_{p'}(z)=(x_{p'}+l_{p'}z)/a,\quad \alpha_p=a_p/a,\quad \beta_{p'}=b_{p'}/b \tag{2-24}$$

The mode shapes are determined by

$$W(x,y) = \sum_{m=1}^{\infty}\sum_{n=1}^{\infty} \frac{1}{f_{mn}(\lambda)} W_{mn}(x,y) \begin{Bmatrix} \sin m\pi\alpha_p \phi_{n,i}(\gamma_p) \\ m\cos m\pi\alpha_p \phi_{n,i}(\gamma_p) \\ \sin n\pi\beta_{p'} \phi_{m,i}(\beta_{p'}) \\ n\cos n\pi\beta_{p'} \phi_{m,i}(\beta_{p'}) \end{Bmatrix}^T \begin{Bmatrix} l_p \; Q_{x,i}^{(p)} \\ (\pi l_p/a) \; M_{x,i}^{(p)} \\ l_{p'} \; Q_{y,i}^{(p')} \\ (\pi l_{p'}/b) \; M_{y,i}^{(p')} \end{Bmatrix} \qquad (2\text{-}25)$$

2-3 Rectangular plate having uniform boundary conditions

2-3-1 Review

In 1950's, several excellent papers dealing with vibration of rectangular plates were published. Young [5] employed the Ritz method and beam functions to represent the plate deflection. Iguchi [6] analyzed a free plate by the series method. Warburton [7] considered rectangular plates with all possible boundary conditions, and presented comprehensive solutions obtained by the Rayleigh method. Besides these studies, about a hundred and sixty pertinent references, published before 1967, were uncovered in [1].

Comparing with the recent increase of literature including the complicating effects of plates such as anisotropy, varying thickness and so forth, thin isotropic rectangular plates with uniform boundary conditions are not often dealt as before.

The outstanding comprehensive paper [8] was published attempting to present accurate analytical results for

natural frequencies of rectangular plates. Twenty-one combinations of clamp, free and simple support are considered. Exact characteristic frequency equations are given for six cases having Levy-type boundary conditions, namely a plate with two opposite sides simply supported, and the remaining cases are analyzed by the Ritz method by use of beam functions. Tabular results are available for all the cases.

Laura and Saffell [9] presented an analysis using the Galerkin method with a simple polynomial expression, and applied to a clamped square plate. This technique is used to determine the response of a clamped rectangular plate subjected to sinusoidal excitation [10]. To this work, Warburton [11] made a comment suggesting that the Rayleigh-Ritz method with beam functions is an alternate method of solution, which may be more accurate for higher excitation frequencies. Laura and his co-researchers widely applied this variational technique (the Galerkin or Ritz method with simple polynomials) to the fundamental frequencies of a rectangular plate having zero deflection and different rotational stiffness at the edge [12], and a plate both translational and rotational stiffness at four edges [13,14]. A rectangular plate elastically constrained against rotation along three edges and free on the fourth edge is also analyzed [15] to discuss a problem which has received no treatment.

Bassily and Dickinson [16] demonstrated the inadequacy of beam vibration modes when used in the Ritz method to obtain approximate solutions of plates involving adjacent free edges, and proposed the concept of "degenerated beam functions" which permit more accurate treatment of the problem and still remain the advantages in using beam functions. Vijayakumar and Ramaiah [17] presented an interesting procedure that the products of mode shapes determined from a modified Bolotin solution are used as admissible functions in the Rayleigh-Ritz method for the determination of the natural frequencies of a clamped square plate. It was shown that accuracy of this approach is better than that obtained from the modified Bolotin method alone or the Rayleigh-Ritz method with conventional beam functions. Dickinson [18] proposed to use the simply supported plate function in the Rayleigh method and made comparison with the values in [17].

Egle [19] studied the peak resonant response of a rectangular plate, simply supported on three edges and elastically restrained on the fourth, excited by a concentrated harmonic load. The effect of changing the elastic restraint on the peak resonance is discussed. Snowdon [20] has determined the mechanical impedance and force transmissibility for various internally damped simply supported rectangular plates. This author [21] also discussed use of centrally located masses and vibration absorbers to reduce vibration of rectangular plates. The effect of

location on the plate of point-force input is discussed. Ochs and Snowdon reported experimental determinations of natural frequencies and transmissibilities. Transmissibilities across rectangular plates with damping layers [22] and with loading masses and straight ribs [23] are studied.

Gorman and Sharma [24] introduced an interesting approach to vibration of rectangular plates, utilizing superposition of solutions for a homogeneous differental equation. This series-type solution is useful in dealing with a rectangular plate to which a Levy-type solution cannot be applied and an approximate solution derived by the enegy method has been applied. Gorman used this method to a cantilever plate [25] and a plate having combinations of simply supported and clamped edges [26]. The application on a completely free plate [27] yields good results when compared to a Ritz solution, although the conditions for free edges in this analysis does not satisfy the (Kirchhoff) shear condition accomodating the effect of twisting moment along the free edge.

Jones and Milne [28] used an extended Kantrovich method for a clamped plate. The idea extended by Kerr [29] was used, considering the Kantrovich method as a fisrt step of an iterative procedure. The Kantrovich method is a more general variational procedure which avoids a strong dependence of the Ritz and Galerkin methods on the chosen coordinate functions. Mukhopadhyay [30] obtained an ordi-

nary differential equation by substituting the basic function satisfying boundary conditions along two opposite edges into the partial differential equation of plate vibration, and solved the resulting equation in finite difference form.

Due to the difficulty arising in the analysis, a rectangular plate having nonuniform edge conditions has received sparse treatment. Kurata and Okamura [31] dealt with a simply supported rectangular plate partially clamped along central portion on two opposite or four edges. An analytical method presented is to satisfy the condition of clamped edge by introducing a resisting moment so as to keep zero slope along the relevant section, and the fundamental frequencies of the plate are obtained. This method was extended by Gajendar [32] to include free edges. A similar method was employed by Ota and Hamada [33]. Keer and Stahl [34] considered the problem, which was formulated as dual series equations and reduced to homogeneous Fredholm integral equations of the second kind. They presented numerical results including a free plate simply supported along adjacent edges symmetrically from the corners. Venkateswara et al. [35] employed the finite element method to demonstrate the effectiveness of the method in solving the problem with mixed boundary conditions, and the results were compared with those in [34].

2-3-2 Application of the method

Since the analysis in the previous section makes use of an eigenfunction for a simply supported rectangular plate, the present method is applicable to vibration of rectangular plates having combinations of simply supported and clamped edges as shown in Fig.2-2. Natural frequencies of a rectangular plate simply supported along the entire edges (Case(a)) are readily given by Eq.(2-19), and the exact frequency equation can be derived for a plate simply supported at opposite edges (Case(d)) [8]. Among the four remaining cases, a rectangular plate clamped along the entire edges is considered, when the aspect ratio is taken to be unity (a square plate), to show the validity of the method by comparing with other available results.

The segments constraining the plate rotation rigidly are located along the entire edges to form a clamped square plate on an original simply supported plate.

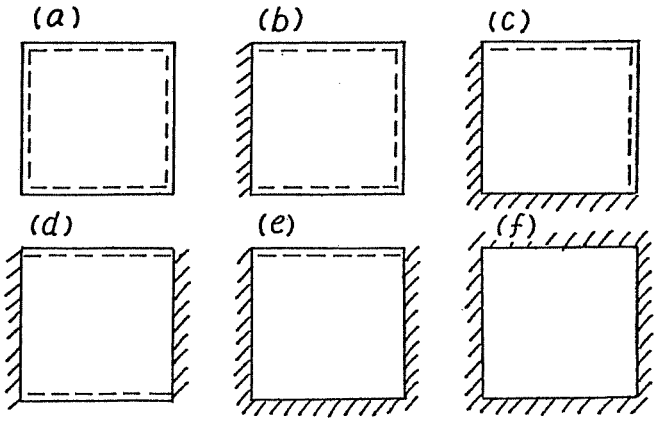

Fig.2-2 Square plates having possible combinations of simply supported and clamped edges

Since a rectangular plate has two axes of geometrical symmetry, symmetric and antisymmetric vibration with respect to the axes may arise and four types of vibration modes are expected as shown in Fig.2-3. SS-type vibration is symmetric vibration about both symmetric axes XX and YY. SA-type vibration is symmetric about XX axis and antisymmetric about YY axis. AS-type is essentially the same as SA-type if XX and YY axis are interchanged, and both types lead to identical frequencies in a square plate. AA-type vibration is antisymmetric about both axes. Antisymmetric mode has a nodal line (i.e., zero-deflection line) on the axis and therefore one nodal line, at least, appears in SA and AS-type mode and two nodal lines in AA-type mode as shown in the figure. m or n in Eq.(2-20) takes odd or even integer depending upon the type of vibration as presented in Table 2-1.

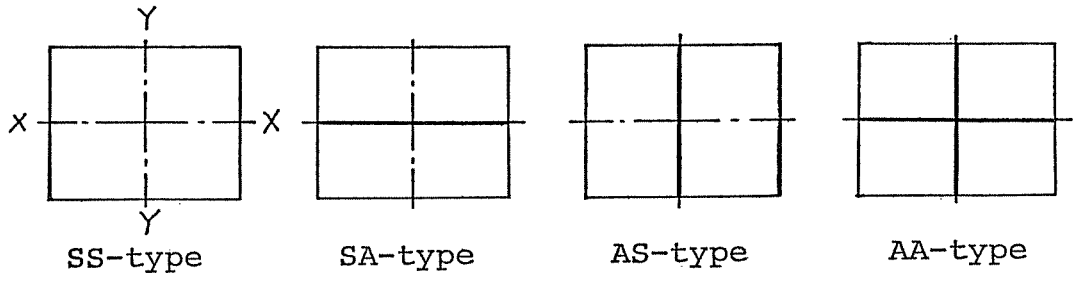

Fig.2-3 Four types of vibration modes for a rectangular plate

Table 2-1 Four types of vibration

	SS-type	SA-type	AS-type	AA-type
m	odd	odd	even	even
n	odd	even	odd	even

In Table 2-2, frequency equations obtained for a clamped square plate are presented. For a square plate, two more symmetric axes exist on the diagonal axes, and symmetry of vibration about these axes is taken into consideration. The natural frequencies are obtainable by calculating eigenvalues of the coefficient matrix in Eqs. (2-26,27).

Table 2-2 Clamped square plate

SSSS-type	SSAA-type	AASS-type	AAAAtype
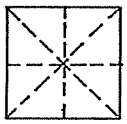	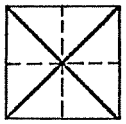	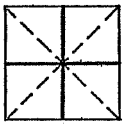	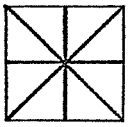

$$\left[\sum_m\sum_n \frac{1}{f_{mn}(\lambda)}\left\{n\cos n\pi\beta_p'\phi_{m,i}(\xi_p')\right\}\left\{n\cos n\pi\beta_q'\phi_{m,j}(\xi_q')\pm n\cos n\pi\beta_q'\phi_{m,j}(\xi_q')\right\}\right] \times\left\{M_{y,j}^{(i)}\right\}=0 \qquad (2\text{-}26)$$

$\xi_i'(z)=z/2$, $\beta_i'=0$

+	−	+	−
$m,n=1,3,\cdots$		$m,n=2,4,\cdots$	

SA-type

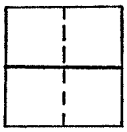

$$\left[\sum_m\sum_n \frac{1}{f_{mn}(\lambda)}\begin{Bmatrix} m\cos m\pi\alpha_p\phi_{n,i}(\eta_p) \\ n\cos n\pi\beta_p'\phi_{m,i}(\xi_p') \end{Bmatrix}\begin{Bmatrix} m\cos m\pi\alpha_q\phi_{n,j}(\eta_q) \\ n\cos n\pi\beta_q'\phi_{m,j}(\xi_q') \end{Bmatrix}^T\right]\begin{Bmatrix} M_{x,j}^{(i)} \\ M_{y,j}^{(i)} \end{Bmatrix}=0 \qquad (2\text{-}27)$$

$\xi_i'(z)=z/2$, $\beta_i'=0$, $\alpha_i=0$, $\eta_i(z)=z/2$

$m=1,3,\cdots$, $n=2,4,\cdots$

It is desirable, however, to improve accuracy of the solution by reducing the double infinite series into single series. The following formulas are used for such a manipulation.

$$\sum_{n(\ell)}^{\infty} \frac{n \sin nx}{n^2+a^2} = \frac{\pi}{4} \frac{\sinh a(\pi-x) \pm \sinh ax}{\sinh a\pi} \qquad \left(\pm : n = \begin{matrix} odd \\ even \end{matrix},\ 0<x<\pi\right) \tag{2-28}$$

$$\sum_{n(\ell)}^{\infty} \frac{\cos nx}{n^2+a^2} = \frac{\pi}{4a} \frac{\cosh a(\pi-x) \mp \cosh ax}{\sinh a\pi} - \frac{1}{4a^2}\left\{(-1)^n+1\right\} \left(\begin{matrix} \mp : n = \begin{matrix} odd \\ even \end{matrix} \\ 0 \le x \le \pi \end{matrix}\right)$$

The coefficient matrix in Eq.(2-27) is written in such a form as Eqs.(2-28) can be applied.

$$\sum_m \sum_n \frac{1}{f_{mn}(\lambda)} \begin{Bmatrix} m\cos m\pi\alpha_p \phi_{n,i}(\zeta_p) \\ n\cos n\pi\beta_p' \phi_{m,i}(\xi_p') \end{Bmatrix} \begin{Bmatrix} m\cos m\pi\alpha_q \phi_{n,j}(\zeta_q) \\ n\cos n\pi\beta_q' \phi_{n,j}(\zeta_q) \end{Bmatrix}^T$$

$$= \sum_m \begin{bmatrix} m\cos m\pi\alpha_p & 0 \\ 0 & \phi_{m,i}(\xi_p') \end{bmatrix} \begin{bmatrix} 0 & \sum_n \frac{n}{f_{mn}(\lambda)} \phi_{n,i}(\zeta_p) \cos n\pi\beta_q' \\ 0 & \sum_n \frac{n^2}{f_{mn}(\lambda)} \cos n\pi\beta_p' \cos n\pi\beta_q' \end{bmatrix} \begin{bmatrix} 0 & 0 \\ 0 & \phi_{m,j}(\xi_q') \end{bmatrix}$$

$$+ \sum_n \begin{bmatrix} \phi_{n,i}(\zeta_p) & 0 \\ 0 & n\cos n\pi\beta_p' \end{bmatrix} \begin{bmatrix} \sum_m \frac{m^2}{f_{mn}(\lambda)} \cos m\pi\alpha_p \cos m\pi\alpha_q & 0 \\ \sum_m \frac{m}{f_{mn}(\lambda)} \phi_{m,i}(\xi_p') \cos m\pi\alpha_q & 0 \end{bmatrix} \begin{bmatrix} \phi_{n,j}(\zeta_q) & 0 \\ 0 & 0 \end{bmatrix} \tag{2-29}$$

Summations in the brackets in Eq.(2-29) are calculated by applying the following equations derived from Eqs.(2-28).

$$\sum_{n(e)^{o}} \frac{n^2}{f_{mn(\lambda)}} \cos n\pi\beta_{p'} \cos n\pi\beta_{q'} = \frac{m_1}{\sinh m_1\pi}\left[-\cosh m_1\pi\begin{pmatrix}1-\beta_{p'}\\ \beta_{p'}\end{pmatrix}\cosh m_1\pi\begin{pmatrix}\beta_{q'}\\ 1-\beta_{q'}\end{pmatrix} \pm \cosh m_1\pi\beta_{p'}\cosh m_1\pi\beta_{q'}\right] - \frac{m_2}{\sinh m_2\pi}\left[m_1\to m_2\right] \quad (n=\text{even}^{\text{odd}}) \tag{2-30}$$

$$\sum_{m(e)^{o}} \frac{m^2}{f_{mn(\lambda)}} \cos m\pi\alpha_p \cos m\pi\alpha_q = \frac{\mu^2 n_1}{\sinh n_1\pi}\left[-\cosh n_1\pi\begin{pmatrix}1-\alpha_p\\ \alpha_p\end{pmatrix}\cosh n_1\pi\begin{pmatrix}\alpha_q\\ 1-\alpha_q\end{pmatrix} \pm \cosh n_1\pi\alpha_p\cosh n_1\pi\alpha_q\right] - \frac{\mu^2 n_2}{\sinh n_1\pi}\left[n_1\to n_2\right] \quad (m=\text{even}^{\text{odd}}) \tag{2-31}$$

$$\sum_{n(e)^{o}} \frac{n}{f_{mn(\lambda)}} \phi_{n,i}(\zeta_p)\cos n\pi\beta_{q'} = \int_0^1\left(\sum_{n(e)^{o}} \frac{n}{f_{mn(\lambda)}} \sinh n\pi\eta_p \cos n\pi\beta_{q'}\right)\sin i\pi z\,dz$$

$$= \frac{1}{\sinh m_1\pi}\left[\psi_{m,i}\begin{pmatrix}1-\eta_p\\ -\eta_p\end{pmatrix}\cosh m_1\pi\begin{pmatrix}\beta_{q'}\\ 1-\beta_{q'}\end{pmatrix} \pm \psi_{m,i}(\zeta_p)\cosh m_1\pi\beta_{q'}\right] - \frac{1}{\sinh m_2\pi}\left[m_1\to m_2\right] \quad (n=\text{even}^{\text{odd}}) \tag{2-32}$$

$$\sum_{m(e)^{o}} \frac{m}{f_{mn(\lambda)}} \phi_{m,i}(\xi_{p'})\cos m\pi\alpha_q = \int_0^1\left(\sum_{m(e)^{o}} \frac{m}{f_{mn(\lambda)}} \sinh m\pi\xi_{p'} \sin m\pi\alpha_q\right)\sin i\pi z\,dz$$

$$= \frac{\mu^2}{\sinh n_1\pi}\left[\psi_{n,i}\begin{pmatrix}1-\xi_{p'}\\ -\xi_{p'}\end{pmatrix}\cosh n_1\pi\begin{pmatrix}\alpha_q\\ 1-\alpha_q\end{pmatrix} \pm \psi_{n,i}(\xi_{p'})\cosh n_1\pi\alpha_q\right] - \frac{\mu^2}{\sinh n_2\pi}\left[n_1\to n_2\right] \quad (m=\text{even}^{\text{odd}}) \tag{2-33}$$

where $\cosh m_1\pi\begin{pmatrix}1-\beta_{p'}\\ \beta_{p'}\end{pmatrix}\cosh m_1\pi\begin{pmatrix}\beta_{q'}\\ 1-\beta_{q'}\end{pmatrix}$ represents $\cosh m_1\pi(1-\beta_{p'})\cosh m_1\pi\beta_{q'}$ for $\beta_{p'}\geq\beta_{q'}$ and $\cosh m_1\pi\beta_{p'}\cosh m_1\pi(1-\beta_{q'})$ for $\beta_p<\beta_{q'}$ and

$$m_1=\sqrt{m^2-(\lambda/\pi)^2}/\mu\ ,\quad m_2=\sqrt{m^2+(\lambda/\pi)^2}/\mu$$

$$n_1=\sqrt{\mu^2n^2-(\lambda/\pi)^2}\ ,\quad n_2=\sqrt{\mu^2n^2+(\lambda/\pi)^2} \tag{2-34}$$

$$\psi_{m,i}(\zeta_p)=\int_0^1 \sinh m_1\pi\eta_p(z)\sin i\pi z\,dz\ ,\quad \psi_{n,i}(\xi_p)=\int_0^1 \sinh n_1\pi\xi_{p'}(z)\sin i\pi z\,dz$$

Substitution of Eqs.(2-30) through (2-33) into (2-29) yields the frequency equation of the plate under consideration.

$$\left(M^{(p\,q\,p'\,q')}_{(1),ij} - M^{(p\,q\,p'\,q')}_{(2),ij} \right) \begin{Bmatrix} (l_p/a)\, M^{(p)}_{x,j} \\ (l_{p'}/b)\, M^{(p)}_{y,j} \end{Bmatrix} = 0 \tag{2-35}$$

where

$$M^{(p\,q\,p'\,q')}_{(1),ij} = \sum_{m(o)} \frac{1}{m_1} \begin{bmatrix} m\cos m\pi\alpha_p & 0 \\ 0 & m_1 \phi_{m,i}(\xi_{p'}) \end{bmatrix} \frac{1}{\sinh m_1\pi} \left(\begin{bmatrix} 0 & \psi_{m,i}\binom{1-\eta_p}{-\eta_p} \cosh m_1\pi \binom{\beta_{q'}}{1-\beta_{q'}} \\ 0 & -\cosh m_1\pi \binom{1-\eta_p}{\eta_p} \cosh m_1\pi \binom{\beta_{q'}}{1-\beta_{q'}} \end{bmatrix} \right.$$

$$\left. \underset{(n=\text{even})}{\overset{\text{odd}}{\pm}} \begin{Bmatrix} \psi_{m,i}(\eta_p) \\ \cosh m_1\pi\beta_{p'} \end{Bmatrix} \begin{Bmatrix} 0 \\ \cosh m_1\pi\beta_{q'} \end{Bmatrix}^T \right) \begin{bmatrix} 0 & 0 \\ 0 & m_1 \phi_{m,j}(\xi_{q'}) \end{bmatrix}$$

$$+ \sum_{n(e)} \frac{\mu^2}{n_1} \begin{bmatrix} n_1 \phi_{n,i}(\eta_p) & 0 \\ 0 & n\cosh n\pi\beta_{p'} \end{bmatrix} \frac{1}{\sinh n_1\pi} \left(\begin{bmatrix} -\cosh n_1\pi \binom{1-\alpha_p}{\alpha_p} \cosh n_1\pi \binom{\alpha_q}{1-\alpha_q} & 0 \\ \psi_{n,i}\binom{1-\xi_{p'}}{-\xi_{p'}} \cosh n_1\pi \binom{\alpha_q}{1-\alpha_q} & 0 \end{bmatrix} \right.$$

$$\left. \underset{(m=\text{even})}{\overset{\text{odd}}{\pm}} \begin{Bmatrix} \cosh n_1\pi\alpha_q \\ \psi_{n,i}(\xi_{p'}) \end{Bmatrix} \begin{Bmatrix} \cosh n_1\pi\alpha_q \\ 0 \end{Bmatrix}^T \right) \begin{bmatrix} n_1 \phi_{n,j}(\eta_q) & 0 \\ 0 & 0 \end{bmatrix} \tag{2-36}$$

Table 2-3 Comparison of frequency parameter $\lambda^2 = \omega a^2 \sqrt{\rho/D}$ for a clamped square plate

Authors	Methods	1	2	3	4	5	6	7	8
Present		35.9186	73.2934	108.217	131.236	132.115	164.915	210.207	219.668
Tomotika [36]	(1)	35.9866							
Iguchi [6]	(1)		73.40	108.22		132.18	164.99		
Young [5]	(2)	35.99	73.41	108.27	131.64	132.25	165.15		
Ödman [37]	(3)	35.998565	73.405	108.237	131.902		165.023	210.526	220.06
Vito et al. [38]	Up. (4)	35.98518			131.5731				219.9290
	Lw. (5)	35.98521			131.5808				
Laura et al. [9]	(6)	35.999	73.825	108.425					
Bazley [40]	Up. (2)	35.98221			131.5021				
	Lw. (7)	35.98533			131.5812				
Leissa [8]	(2)	35.992	73.413	108.27	131.64	132.24			
Jones et al. [28]	(8)	35.999	73.405	108.236	131.902		165.023	210.526	
Gorman [26]	(9)	35.98	73.40	108.2	131.6	132.2	165.0	210.5	220.0
Mukhopadhyay [30]	(10)	35.289	72.797	105.54	125.009	131.17			
Marangoni et al. [41]	Up.(2)	35.987	73.385	108.05	131.57				
	Lw.(7)	35.871	72.007						
Vijayakumar [17]	(11)	35.1124	72.8994	107.469	131.629		164.387	210.362	219.325
	(12)	36.0159	73.4175	108.252	131.581	132.234	165.035	210.530	220.070
	(13)	35.9854	73.3942	108.217	131.581	132.206	165.003	210.523	220.038

2-3-3 Results and discussion

The numerical results obtained by using Eq.(2-35) are presented in nondimensional form of $\lambda^2=\omega a^2\sqrt{\rho/D}$, with reference values by other authors in Table 2-3. The present values are calculated by 20x20 matrix with $m(n)=$ 48 terms. The methods used by other authors are indicated, and upper and lower bounds are given for [38,39,41]. It may be noted that the present method yields lower bounds for a clamped square plate. This can be shown by referring that all the present values are lower than those by the Rayleigh Ritz or Galerkin method which is known to give upper bounds of the solution.

Table 2-3 (continued)

Authors	(Mode) 9	10	11	12
present	242.154	296.024	308.498	340.509
Odman	242.66	296.35	309.038	340.59
Gorman	242.2	296.3	308.9	340.6
Vijayakumar	242.197	295.698	308.929	340.244
	242.154	296.376	308.902	340.596
	242.154	296.342	308.902	340.584

*method (1) series solution
(2) Ritz method with beam functions
(3) Galerkin method with hyperbolic functions
(4) Rayleigh-Ritz method with non-orthogonal polynomial
(5) method of orthogonal invariant
(6) Galerkin method with polynomial
(7) decomposition technique
(8) extended Kantrovich method
(9) method of superposition
(10) semi-analytic solution (Reduction into an ordinary differential equation and finite difference method)
(11) Bolotin method
(12) Ritz method with admissible function obtained from Bolotin method
(13) Rayleigh method with admissble function obtained from Bolotin method

2-4 Rectangular plate having internal supports

2-4-1 Review

As reviewed in Sec.2-3-1, rectangular plates constrained only along the edges have been extensively studied. In practice, however, many plate-like structural elements have internal constraints in addition to the boundary conditions, for instance, in form of rivet and spot welding.

Rectangular plates supported at some points have been studied by some researchers. Cox and Boxer [42] obtained the fundamental frequencies of a free plate point-supported at four corners. The lowest five frequencies are calculated by a finite difference procedure. John and Nataraja[43,44] also used the finite difference to solve the governing equation and the results are reported for a wide variation of support location. Reed [45] employed two approximate methods, the Ritz method and a series solution to the differential equation, to discuss advantages and disadvantages of the methods. Dowell [46] presented a Rayleigh-Ritz analysis with support conditions expressed by means of Lagrange multipliers, and the numerical results for a square plate with four internal point supports, located symmetrically on the diagonals. Venkateswara Rao et al. [47,48] have calculated by the finite element method the lower frequencies of square plates supported at four points on the diagonals. Comparison was made with the results in [42,44]. An experimental study was conducted

by Sadasiva et al. [49]. Leuner [50] studied the problem by a Rayleigh-Ritz analysis and by an experimental investigation through the use of holographic interferometry. Yang [52] formulated the eigenvalue problem of a point constraint and Damie et al.[51] used the finite element method.

In comparison with the number of references concerned with point-supported plates, only a limited amount of papers deal with vibration of rectangular plates constrained along internal segments. Klein [53] derived approximate solutions by using the Rayleigh-Ritz technique and Lagrange multipliers to account for the constraints. The method was applied to a clamped rectangular plate with an internal line of support, but the results presented are few. Stahl and Keer [54] also treated a plate with a centrally located rigid line support by an approach using integral equations. Takahashi and Chishaki[55] obtained a solution for a rectangular plate supported at oblique segments by replacing point constraints with the segment reactions. The natural frequencies and mode shapes are presented for the plate.

2-4-2 Application of the method

(a) Rectangular plate simply supported at the edges and elastically constrained at a cross-shaped support

Consider a rectangular plate simply supported at all edges and elastically constrained at a cross-shaped support located in the center as shown in Fig.2-4. In this

case, equation (2-20) is divided into four sets of equations corresponding to the four types of vibration modes.

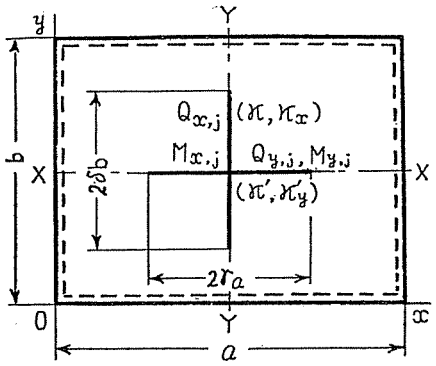

Fig.2-4

(1) SS-type mode (m, n = odd)

$$\left(\begin{bmatrix} \frac{1}{\gamma}\delta_{ij} & 0 \\ 0 & \frac{1}{\gamma'}\delta_{ij} \end{bmatrix} + \sum_m \sum_n \frac{1}{f_{mn}(\lambda)} \begin{Bmatrix} (-1)^{\frac{m-1}{2}} \phi_{n,i}(\gamma_i) \\ (-1)^{\frac{n-1}{2}} \phi_{m,i}(\xi_i') \end{Bmatrix} \begin{Bmatrix} (-1)^{\frac{m-1}{2}} \phi_{n,j}(\gamma_i) \\ (-1)^{\frac{n-1}{2}} \phi_{m,j}(\xi_i') \end{Bmatrix}^T \right) \begin{Bmatrix} \delta b Q_{x,j} \\ \gamma a Q_{y,j} \end{Bmatrix} = 0 \quad (2\text{-}37)$$

(2) SA-type mode (m = odd, n =even)

$$\left(\begin{bmatrix} \frac{1}{\gamma}\delta_{ij} & 0 \\ 0 & \frac{1}{\gamma_y'}\delta_{ij} \end{bmatrix} + \sum_m \sum_n \frac{1}{f_{mn}(\lambda)} \begin{Bmatrix} (-1)^{\frac{m-1}{2}} \phi_{n,i}(\gamma_i) \\ (-1)^{\frac{n}{2}} n \phi_{m,i}(\xi_i') \end{Bmatrix} \begin{Bmatrix} (-1)^{\frac{m-1}{2}} \phi_{n,j}(\gamma_i) \\ (-1)^{\frac{n}{2}} n \phi_{m,j}(\xi_i') \end{Bmatrix}^T \right) \begin{Bmatrix} \delta b Q_{x,j} \\ \pi\gamma\mu M_{y,j} \end{Bmatrix} = 0 \quad (2\text{-}38)$$

(3) AS-type mode (m = even, n = odd)

$$\left(\begin{bmatrix} \frac{1}{\gamma_x}\delta_{ij} & 0 \\ 0 & \frac{1}{\gamma'}\delta_{ij} \end{bmatrix} + \sum_m \sum_n \frac{1}{f_{mn}(\lambda)} \begin{Bmatrix} (-1)^{\frac{m}{2}} m \phi_{n,i}(\gamma_i) \\ (-1)^{\frac{n-1}{2}} \phi_{m,i}(\xi_i') \end{Bmatrix} \begin{Bmatrix} (-1)^{\frac{m}{2}} m \phi_{n,j}(\gamma_i) \\ (-1)^{\frac{n-1}{2}} \phi_{m,j}(\xi_i') \end{Bmatrix}^T \right) \begin{Bmatrix} (\pi\delta/\mu) M_{x,j} \\ \gamma a Q_{y,j} \end{Bmatrix} = 0 \quad (2\text{-}39)$$

(4) AA-type mode (m , n = even)

$$\left(\begin{bmatrix} \frac{1}{\gamma_x}\delta_{ij} & 0 \\ 0 & \frac{1}{\gamma_y'}\delta_{ij} \end{bmatrix} + \sum_m \sum_n \frac{1}{f_{mn}(\lambda)} \begin{Bmatrix} (-1)^{\frac{m}{2}} m \phi_{n,i}(\gamma_i) \\ (-1)^{\frac{n}{2}} n \phi_{m,i}(\xi_i') \end{Bmatrix} \begin{Bmatrix} (-1)^{\frac{m}{2}} m \phi_{n,j}(\gamma_i) \\ (-1)^{\frac{n}{2}} n \phi_{m,j}(\xi_i') \end{Bmatrix}^T \right) \begin{Bmatrix} (\pi\delta/\mu) M_{x,j} \\ \pi\gamma\mu M_{y,j} \end{Bmatrix} = 0 \quad (2\text{-}40)$$

m and n in Eqs.(2-37) through (2-40) take odd or even integer as directed in the parentheses. SS-type mode is symmetric vibration about the two symmetric axes and not influenced by the rotational stiffnesses K_x, K_y' of the cross-support. Likewise, SA-type is not affected by K_x, K', AS-type is not done by K, K_y', and AA-type is not by K, K'. When the plate is clamped at the cross-support ($K = K' = K_x = K_y' = \infty$), all the first terms in the brackets of Eqs.(2-37) through (2-40) vanish. When the plate is simply supported at the support ($K = K' = \infty, K_x = K_y' = 0$), SS-type mode is the same as that of a plate clamped there. SA-type and AS-type mode are obtained by taking $M_{y,j} = 0$ in Eq.(2-38) and $M_{x,j} = 0$ in Eq.(2-39), respectively. In this case, equation(2-40) has no physical meanings, and AA-type mode is reduced to that of a plate with no constraints on it.

(b) Rectangular plate clamped at all edges and an internal rectangular support

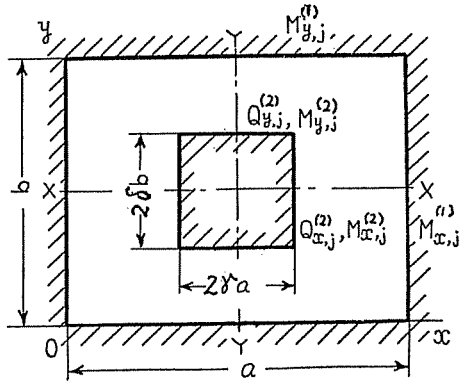

Fig.2-5

Figure 2-5 shows a symmetric rectangular plate clamped at the edges and an internal rectangular support. According to the same procedure explained in (a), the following equation is derived for the four types of vibration modes.

$$\left\{\begin{array}{c} m\,\phi_{n,i}(\gamma_1) \\ \sin m\pi\left(\frac{1}{2}-\gamma\right)\phi_{n,i}(\gamma_2) \\ m\cos m\pi\left(\frac{1}{2}-\gamma\right)\phi_{n,i}(\gamma_2) \\ n\,\phi_{m,i}(\xi_1') \\ \sin n\pi\left(\frac{1}{2}-\delta\right)\phi_{m,i}(\xi_2') \\ n\cos n\pi\left(\frac{1}{2}-\delta\right)\phi_{m,i}(\xi_2') \end{array}\right\}^T \left[\sum_m\sum_n \frac{1}{f_{mn}(\lambda)}\right] \left\{\begin{array}{c} m\,\phi_{n,j}(\gamma_1) \\ \sin m\pi\left(\frac{1}{2}-\gamma\right)\phi_{n,j}(\gamma_2) \\ m\cos m\pi\left(\frac{1}{2}-\gamma\right)\phi_{n,j}(\gamma_2) \\ n\,\phi_{m,j}(\xi_1') \\ \sin n\pi\left(\frac{1}{2}-\delta\right)\phi_{m,j}(\xi_2') \\ n\cos n\pi\left(\frac{1}{2}-\delta\right)\phi_{m,j}(\xi_2') \end{array}\right\} \left\{\begin{array}{c} (\pi/\mu)M_{x,j}^{(1)} \\ \gamma b\,Q_{x,j}^{(2)} \\ (\pi\delta/\mu)M_{x,j}^{(2)} \\ \pi\mu\,M_{y,j}^{(1)} \\ \gamma a\,Q_{y,j}^{(2)} \\ \pi\gamma\mu\,M_{y,j}^{(2)} \end{array}\right\} = 0 \qquad (2\text{-}41)$$

where $M_{x,j}^{(1)}$, $M_{y,j}^{(1)}$ denote the moments at the outer edge and $Q_{x,j}^{(2)}$, $M_{x,j}^{(2)}$, ... do the forces and moments at the inner boundary. For calculating each type of vibration, m and n take odd or even integer as explained in Table 2-1.

2-4-3 Results and discussion

Figure 2-6 presents the frequency parameters $\lambda = a(\omega\sqrt{\rho/D})^{1/2}$ and mode shapes of a square plate simply supported at the edges and the support (support length: $\gamma = \delta = 0.20$), wherein thick curve shows nodal line and thin curve denotes contour line of the deflection. SA and AS-type mode has the identical frequencies in a square plate. AA-type mode becomes that of a plate without the support as already explained.

Figure 2-7 shows the frequency parameters and mode shapes of a square plate simply supported at the edges and clamped at the support. There is no difference between SS-type modes of a plate simply supported at the support and a plate clamped there. However, SA and

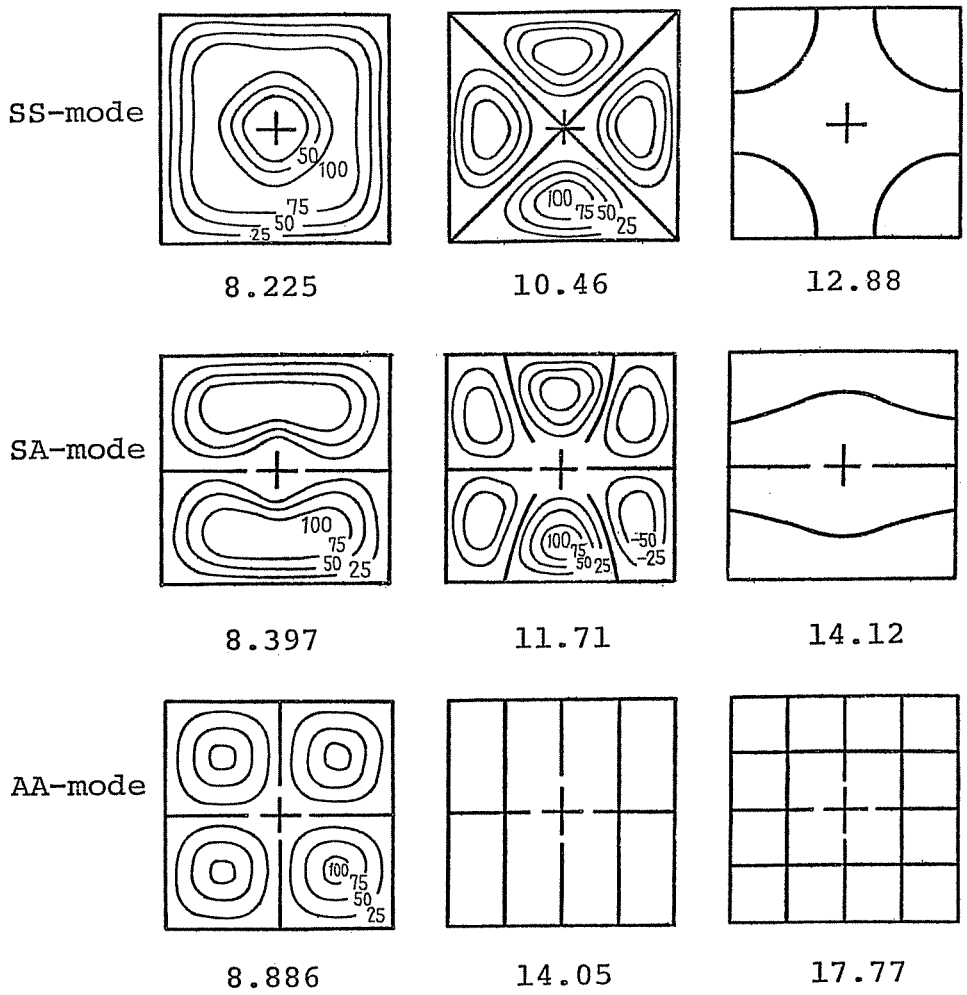

Fig.2-6 Frequency parameters λ and nodal patterns of a square plate simply supported at the edges and a cross-shaped support ($\gamma = \delta = 0.20$).

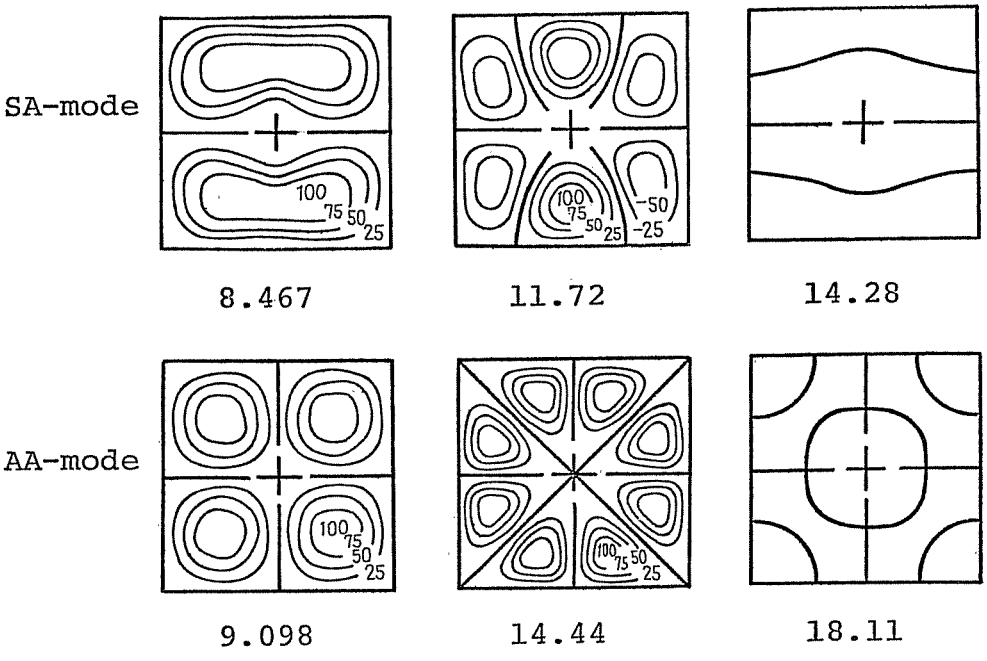

Fig.2-7 Frequency parameters λ and nodal patterns of a square plate simply supported at the edges and clamped at a cross-shaped support

AA -type mode of a plate clamped at the support have higher frequencies than that of a plate simply supported there, and different mode shapes appear on the plate.

Figure 2-8 shows the effect of length of the support on the frequencies of SS and SA-type modes of a square plate simply supported at the edges and the support. Although the frequencies increase monotonously as the length is extended, the rate of increase of the frequencies has different characteristics depending upon modes of vibration. The case of $\gamma = \delta = 0$ corresponds to a plate simply supported at a single point in the center and $\gamma = \delta = 1.0$ to a plate simply supported along XX and YY axes. The frequencies of such plates which have been already obtained [8,57] are shown with ∘. The frequencies obtained for these special cases are in good agreement with the reference values except for SA-type modes. The reason why the frequencies of SA-type modes of a plate supported at a small cross-shaped support is higher than those of a point-supported plate must be that even a small support constrains the rotation of plate, clamping the plate in the extending direction of the + (cross-shaped) support.

The effects of varying stiffness of the support on the frequencies are studied in Fig.2-9. With the increase of stiffness of the support, the frequencies also increase accordingly. When the stiffness parameters approach 0 or ∞, the plate becomes free and simply sup-

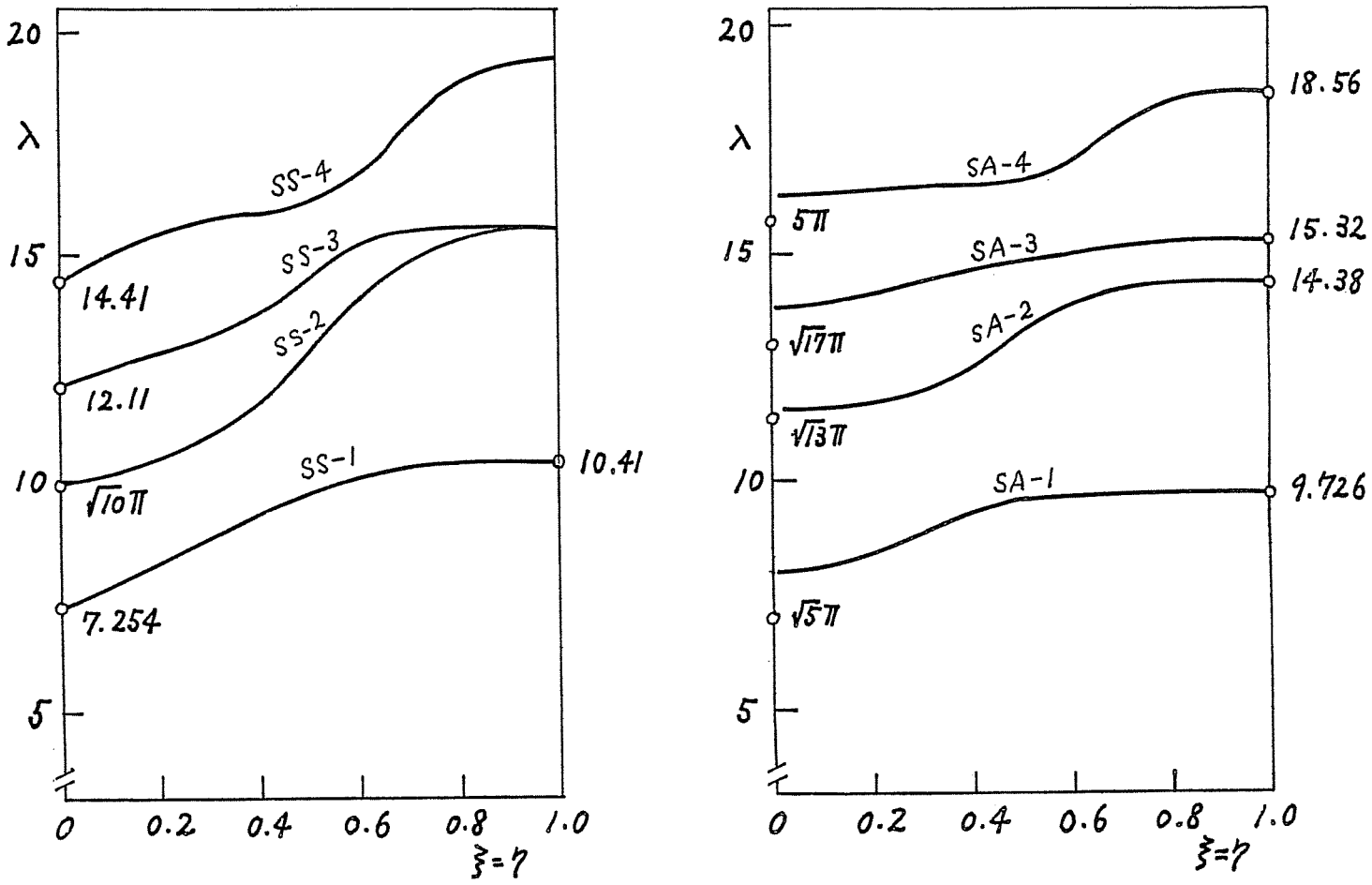

Fig.2-8 Variation of frequency parameters λ with the length of a cross-shaped support ($\kappa = \kappa' = \infty$, $\kappa_x = \kappa_y = 0$)

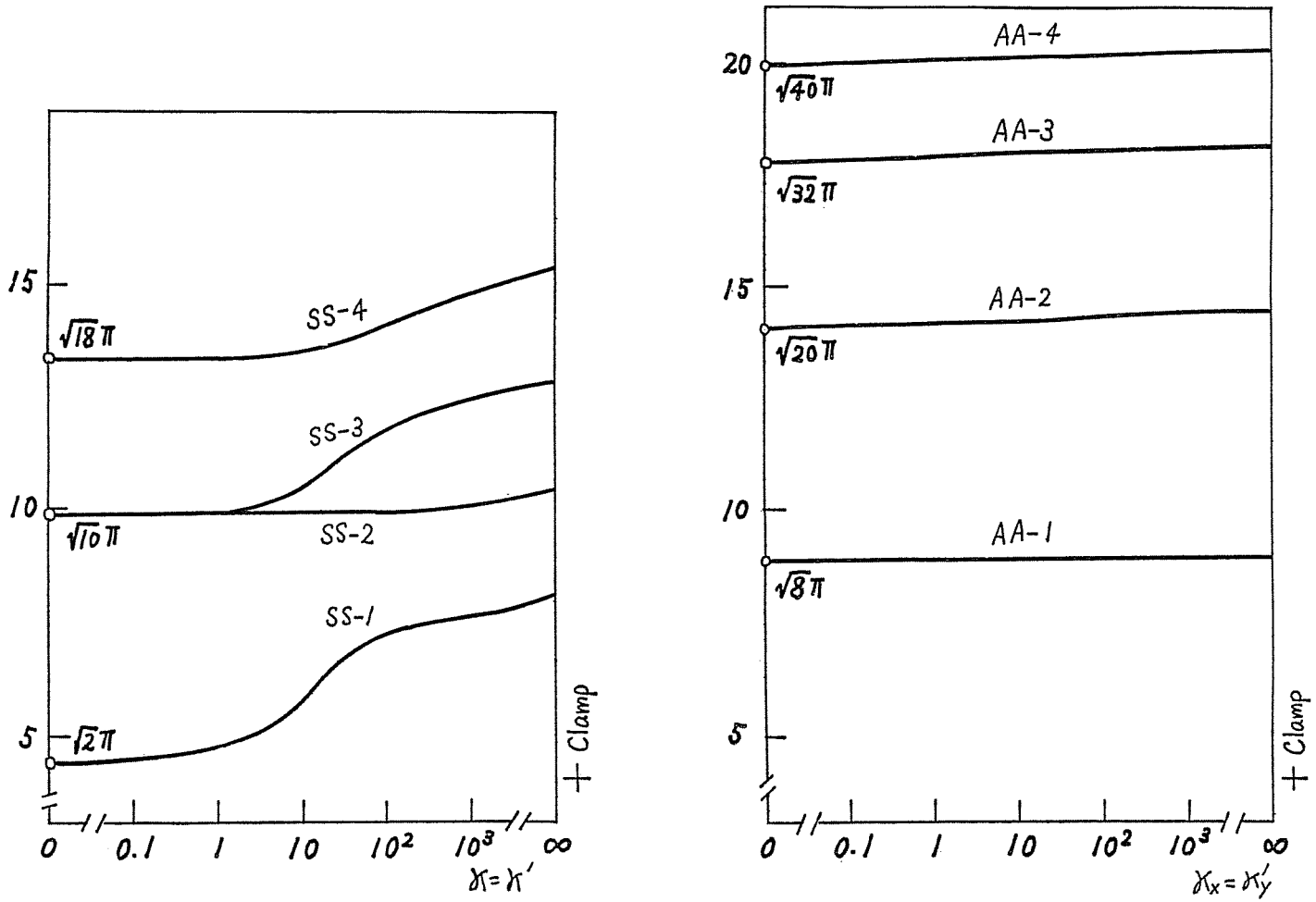

(a) SS-mode

(b) AA-mode

Fig.2-9 Variation of frequency parameters λ with the stiffness of a cross-shaped support ($\gamma = \delta = 0.20$)

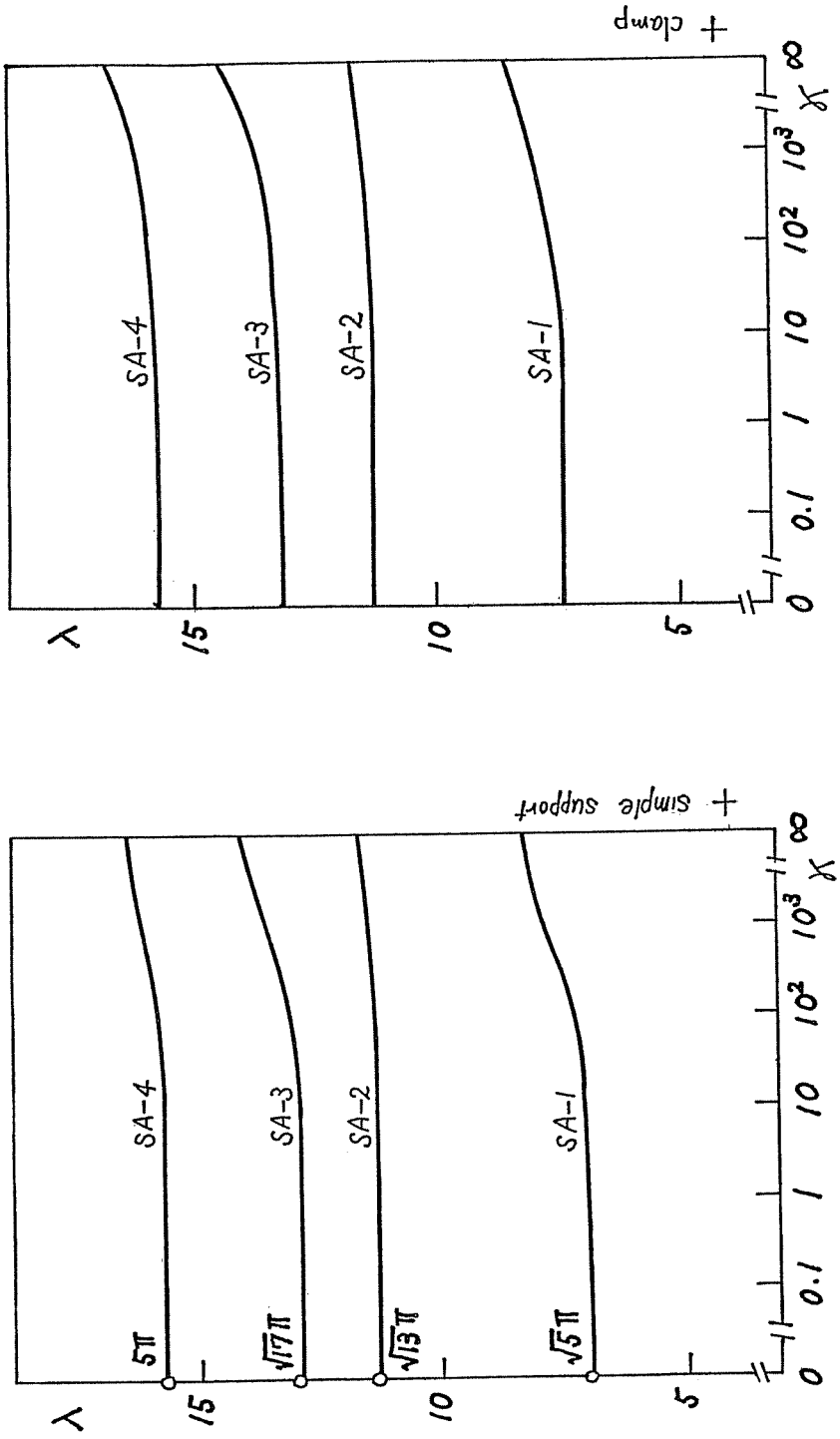

(c) SA-mode ($\chi_y' = 0$)

(d) SA-mode ($\chi_y' = \infty$)

Fig.2-9 (continued)

ported or clamped at the support, respectively. In SS-type mode, as shown in Fig.2-9(a), the difference between the frequencies of SS-2 and SS-3 disappears with the decrease of the stiffness, and finally both frequencies tend to the frequency of the second mode of a plate without internal constraints.

Figure 2-10 presents the convergence characteristics of the frequency parameters λ of SS-1 and SS-2 modes of a square plate clamped at the outer and inner square boundaries ($\gamma = \delta = 0.20$) when the number of Fourier series terms is increased. It may be noted that the rate of convergence depends on the mode of vibration.

Figure 2-11 shows the frequency parameters and mode shapes of a square plate clamped at both inner and outer edges. Frequency equation (2-41) was employed with $m \times n = 40 \times 40$ terms and $i \times j = 4 \times 4$ terms resulting 24x24 matrix. Therefore, about 1 percent error may be expected

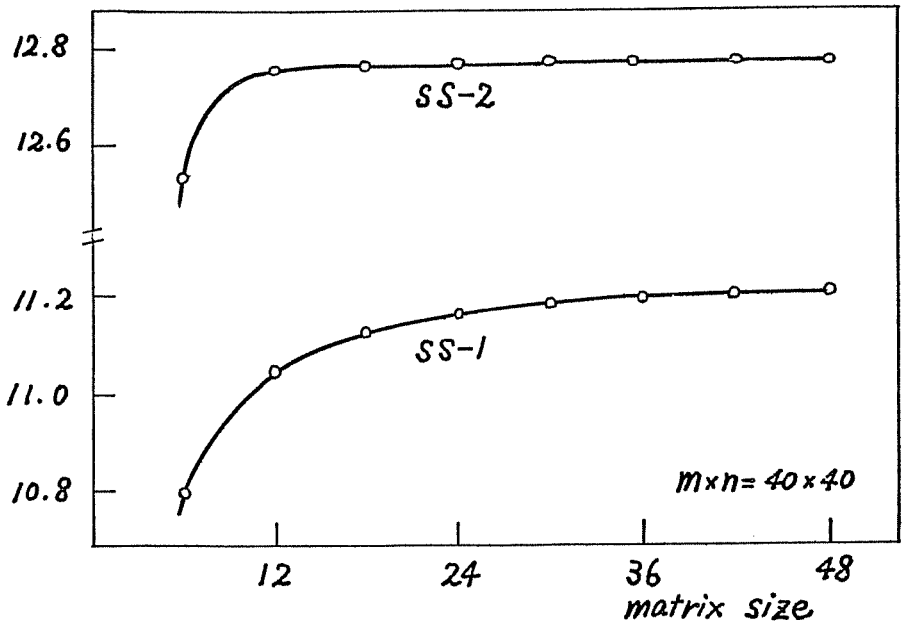

Fig.2-10 Convergence of frequency parameters λ

for the values in the figure. The frequencies of an internal clamped rectangular plate are also calculated in this procedure, but these values can easily be removed utilizing the known results for a clamped square plates.

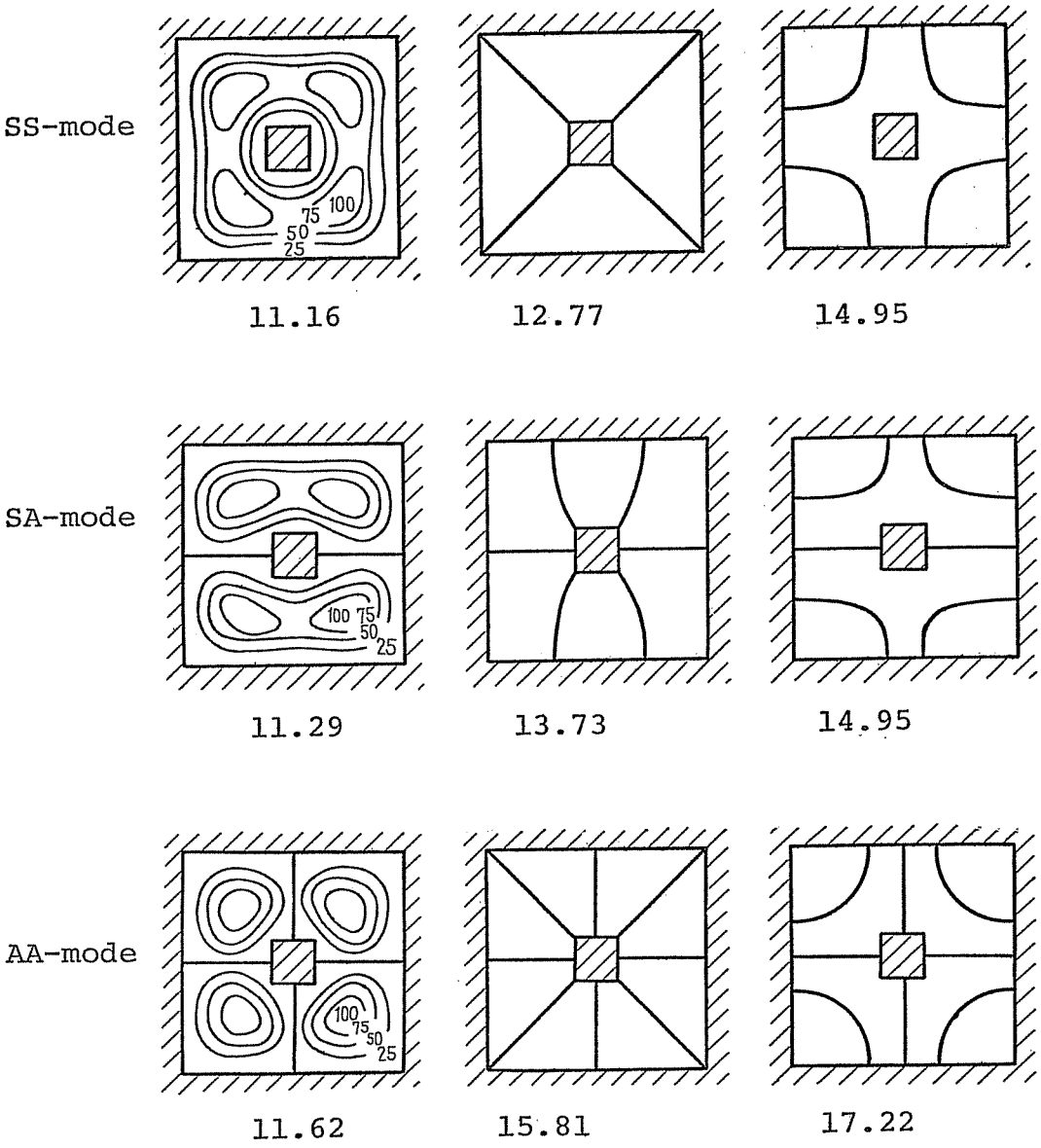

Fig.2-11 Frequency parameters λ and nodal patterns of a square plate clamped at the edges and an internal square support ($\gamma = \delta = 0.20$)

CHAP.3 CIRCULAR PLATES WITH VARIOUS BOUNDARY CONDITIONS

3-1 Introduction

The free vibration of circular plates has been a subject of considerable study for a century and a half. The first theoretical investigation was obtained by Poisson [58] in 1829 for axisymmetric vibration of a circular plate, and Kirchhoff [59] analyzed the more general case of asymmetric vibration in 1850. The summary compiled by Leissa [1] revealed that about fifty references had been obtained on the subject till 1967.

The main purposes of the chapter are to show how the presence of nonuniform spring and mass systems can be accommodated in the analysis, and to present interesting results showing how the frequencies and nodal patterns of the circular plates are affected by the addition of the nonuniform elastic constraints and masses.

The fundamental equations of circular plates are derived in Sec.3-2 and the numerical results are given only for the case when a reasonable number of accurate results is not available. Sections 3-3 and 3-4 deal with circular plates elastically constrained along parts of the edge by rotational springs only and by both translational and rotational springs, respectively. It is shown in Sec.3-5 that the method used in Sec.3-4 can be utilized to analyze a free circular plate having varying mass distributed along its boundary.

3-2 Circular plates having uniform boundary conditions

3-2-1 Review

This section is concerned with circular plates having uniform edge conditions. A reasonable number of literature is found in [1] for this case due to the fact that the uniform boundary conditions make the mathematical formulation quite simple. For a solid circular plate, number of combinations of boundary conditions is only three, compared to twenty-one distinct combinations for a rectangular plate, as long as the classical boundary conditions of free, simply support and clamp are considered. Blanch [60] and Carrington [61] obtained natural frequencies of a clamped plate, and Maruyama [62] experimentally determined the frequencies by use of holographic interferometry. Besides these studies, enough literature has been available for this case.

For a free plate, Colwell and Hardy [63] showed the frequencies for Poisson's ratio $\nu=0.33$ and Airey [64] for $\nu=0.25$. In the recent report by Itao and Crandall [65], the lowest 701 frequency parameters and corresponding modes are presented for a Poisson's ratio of 0.33.

For a simply supported plate, numerical results available are those published by Gontkevich [66] and Wah [67], and Pardoen[68,69] calculated the frequencies by the finite element method and the exact solution. Jones [70] noted that the fundamental frequency of a clamped elliptic plate, obtained by Mazumdar [71], does

not depend explicitly upon the geometry of the plates when the frequency is expressed in terms of the maximum deflection of a uniformly loaded plate. He extended the idea to other plates and boundary conditions, and presented an approximate formula for several different plates including a circular plate clamped or simply supported. Johns [72] also presented a two-term approximate solution which results the fundamental and second frequencies. Jaçquot and Lindsay [73] examined the influence of Poisson's ratio on the fundamental frequency of a simply supported plate. The number of useful results, however, is limited and a thorough and accurate study for a simply supported plate still needs to be done over a variety of Poisson's ratio from a technical point of view.

The elastically constrained boundary is a more general form of boundary condition, and in fact the classical boundary conditions of clamp, free and simply support are obtainable by taking two (translational and rotational) elastic constraints to be zero and/or infinity. Kantham [74] first dealt with a circular plate constrained rigidly against deflection and elastically by a rotational spring, and presented variation of frequency parameters between a simply supported and clamped plate. Laura et al.[75,76, 77] treated a problem having in-plane force by the Galerkin method used with a simple polynomial expression. This convenient method was extended to problems of a plate subjected to sinusoidal excitation [78], a plate holding

a concentrated mass [79] and a plate having two types of springs [80]. Singa Rao and Amba Rao [81] employed the Rayleigh-Ritz method with a three-term approximate expression for the elastically stiffened plate. Snowdon [82] considered response of simply supported or free circular plate possessing internal damping to a lateral, driving, central or concentric ring force. The same procedure was applied to a clamped circular plate [83]. Saito and Nakazawa [84] dealt with a circular plate mounted with an elastic annular support, taking the effect of the inertia of the support into consideration.

3-2-2 Analysis

The differential equation governing free vibration of a thin homogeneous plate is

$$D\nabla^4 W - \rho\omega^2 W = 0 \tag{3-1}$$

where the biharmonic operator in polar coordinates takes the form of

$$\nabla^2 = \frac{\partial^2}{\partial r^2} + \frac{1}{r}\frac{\partial}{\partial r} + \frac{1}{r^2}\frac{\partial^2}{\partial \theta^2} \tag{3-2}$$

An exact solution to Eq.(3-1) for a solid circular plate with a uniform edge is

$$W(r,\theta) = \left[A_n J_n(kr) + C_n I_n(kr)\right]\cos n\theta \quad (k^4 = \omega^2\rho/D) \tag{3-3}$$

with regular and modified Bessel functions J_n and I_n of the first kind, and undetermined coefficients A_n, C_n .

(a) clamped circular plate

When a circular plate is completely clamped along the edge as shown in Fig.3-1, the boundary conditions are given by

$$W(a,\theta)=0$$
$$\frac{\partial W}{\partial r}(a,\theta)=0 \qquad (3\text{-}4)$$

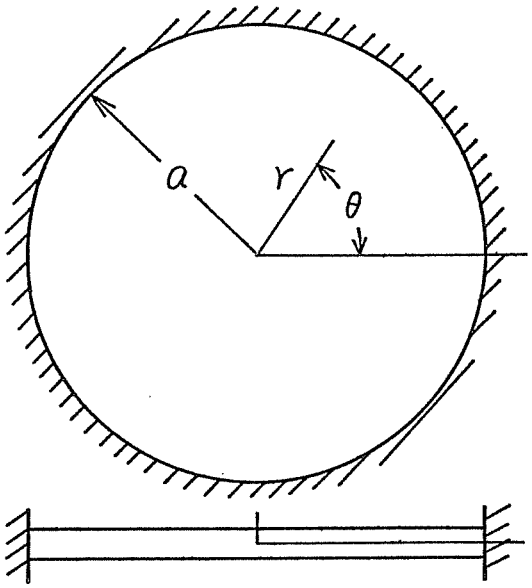

Fig.3-1

Substitution of Eq.(3-3) into (3-4) yields a frequency equation

$$J_{n+1}(\lambda)\,I_n(\lambda)+J_n(\lambda)\,I_{n+1}(\lambda)=0$$
$$(\lambda^4=a^4\omega^2\rho/D) \qquad (3\text{-}5)$$

after applying the formulas

$$J_n'(\lambda)=\frac{n}{\lambda}J_n(\lambda)-J_{n+1}(\lambda)$$
$$I_n'(\lambda)=\frac{n}{\lambda}I_n(\lambda)+I_{n+1}(\lambda) \qquad (3\text{-}6)$$

(b) simply supported circular plate *

For a simply supported plate as shown in Fig.3-2, the boundary conditions are

$$W(a,\theta)=0$$
$$M_r(a,\theta)=0 \qquad (3\text{-}7)$$

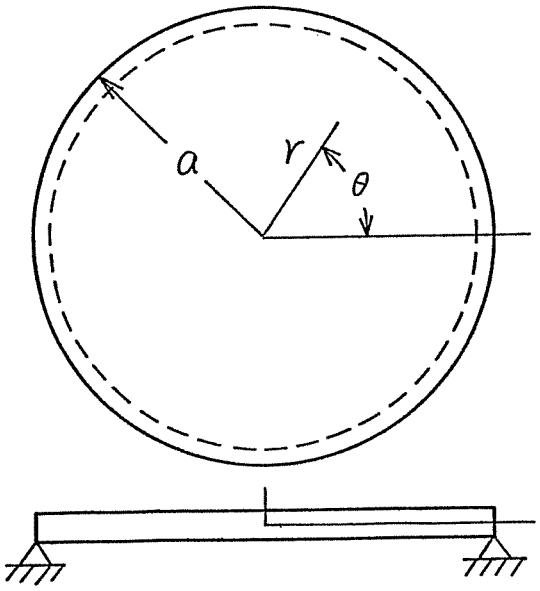

Fig.3-2

*[85]

where

$$M_r(r,\theta) = -D\left[\frac{\partial^2 W}{\partial r^2} + \nu\left(\frac{1}{r}\frac{\partial W}{\partial r} + \frac{1}{r^2}\frac{\partial^2 W}{\partial \theta^2}\right)\right] \tag{3-8}$$

Substitution of Eq.(3-3) into (3-7) results in

$$\frac{J_{n+1}(\lambda)}{J_n(\lambda)} + \frac{I_{n+1}(\lambda)}{I_n(\lambda)} = \frac{2\lambda}{1-\nu} \tag{3-9}$$

Formulas (3-6) and the recursion formula

$$\begin{aligned} J_{n+2}(\lambda) &= \frac{2}{\lambda}(n+1)J_{n+1}(\lambda) - J_n(\lambda) \\ I_{n+2}(\lambda) &= -\frac{2}{\lambda}(n+1)I_{n+1}(\lambda) + I_n(\lambda) \end{aligned} \tag{3-10}$$

are used to deal with the derivatives of second order in Eq.(3-8).

$$\begin{aligned} J_n''(\lambda) &= \left\{\frac{n(n-1)}{\lambda^2} - 1\right\}J_n(\lambda) + \frac{1}{\lambda}J_{n+1}(\lambda) \\ I_n''(\lambda) &= \left\{\frac{n(n-1)}{\lambda^2} + 1\right\}I_n(\lambda) - \frac{1}{\lambda}I_{n+1}(\lambda) \end{aligned} \tag{3-11}$$

(c) free circular plate

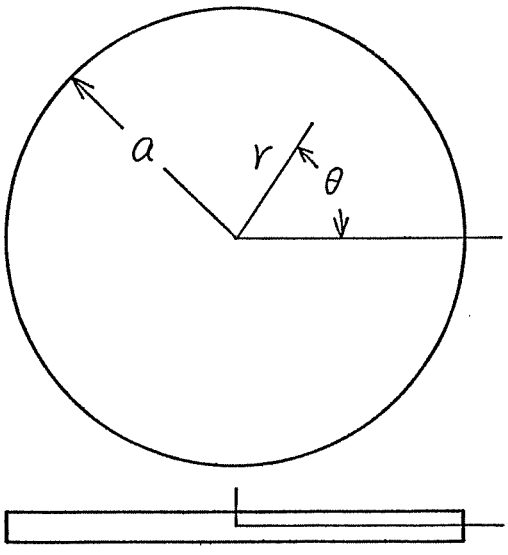

Fig.3-3

For a completely free plate as shown in Fig.3-3, the boundary conditions are

$$\begin{aligned} V_r(a,\theta) &= 0 \\ M_r(a,\theta) &= 0 \end{aligned} \tag{3-12}$$

where $$V_r(r,\theta) = -D\left[\frac{\partial}{\partial r}(\nabla^2 W) + \frac{1}{r}(1-\nu)\frac{\partial}{\partial r}\left(\frac{1}{r}\frac{\partial^2 W}{\partial \theta^2}\right)\right] \tag{3-13}$$

A determinant of the frequency matrix is written as

$$\begin{vmatrix} C_1 & C_2 \\ C_3 & C_4 \end{vmatrix} = 0 \tag{3-14}$$

where
$$\begin{aligned} C_1 &= n\{n(1-n)(1-\nu) - \lambda^2\}J_n + \lambda\{n^2(1-\nu) + \lambda^2\}J_{n+1} \\ C_2 &= n\{n(1-n)(1-\nu) + \lambda^2\}I_n - \lambda\{n^2(1-\nu) - \lambda^2\}I_{n+1} \\ C_3 &= \{n(n-1)(1-\nu) - \lambda^2\}J_n + \lambda(1-\nu)J_{n+1} \\ C_4 &= \{n(n-1)(1-\nu) + \lambda^2\}I_n - \lambda(1-\nu)I_{n+1} \end{aligned} \tag{3-15}$$

(d) Elastically supported circular plate

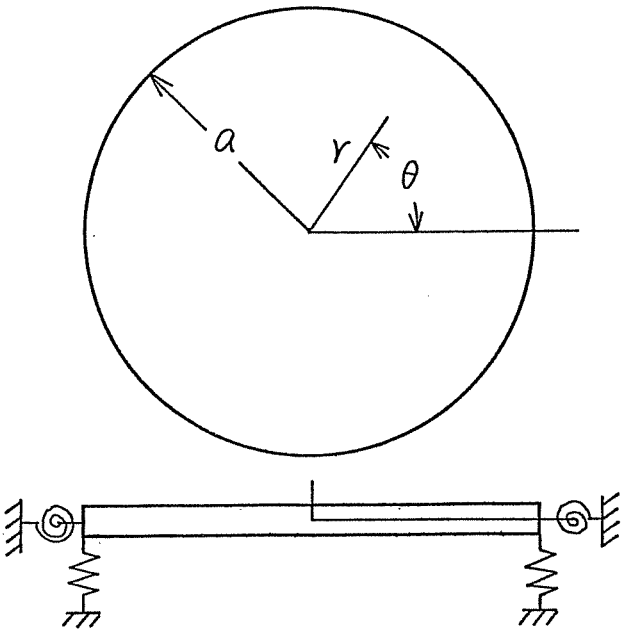

Fig.3-4

For a circular plate elastically constrained by a translational and rotational spring as shown in Fig.3-4, the boundary conditions are

$$\begin{aligned} V_r(a,\theta) &= -K_w W(a,\theta) \\ M_r(a,\theta) &= K_\psi \frac{\partial W}{\partial r}(a,\theta) \end{aligned} \tag{3-16}$$

Elements in the resulting determinant of the form Eq.(3-14) are

$$C_1=\{n^2(1-n)(1-\nu)-n\lambda^2-\bar{K}\}J_n+\lambda\{n^2(1-\nu)+\lambda^2\}J_{n+1}$$
$$C_2=\{n^2(1-n)(1-\nu)+n\lambda^2-\bar{K}\}I_n-\lambda\{n^2(1-\nu)-\lambda^2\}I_{n+1}$$
$$C_3=\{n(n-1)(1-\nu)-\lambda^2+n\bar{L}\}J_n+\lambda(1-\nu-\bar{L})J_{n+1} \quad (3\text{-}17)$$
$$C_4=\{n(n-1)(1-\nu)+\lambda^2+n\bar{L}\}I_n-\lambda(1-\nu-\bar{L})I_{n+1}$$

where

$$\bar{K}=a^3K_W/D\ ,\quad \bar{L}=aK_\psi/D$$

(e) elastically supported circular plate (rotational spring only)

The boundary conditions for a circular plate rigidly constrained against deflection and elastically against rotation are expressed as

$$W(a,\theta)=0\ ,\quad M_r(a,\theta)=K_\psi\frac{\partial W}{\partial r}(a,\theta) \quad (3\text{-}18)$$

In this case, the frequency equation in (d) is considerably simplified and takes a similar form of Eq.(3-9)

$$\frac{J_{n+1}(\lambda)}{J_n(\lambda)}+\frac{I_{n+1}(\lambda)}{I_n(\lambda)}=\frac{2\lambda}{1-\nu-\bar{L}} \quad (3\text{-}19)$$

(f) free plate with added mass to its boundary

For a free circular plate having a uniform distributed mass along the edge as shown in Fig.3-5, the boundary conditions become

$$V_r(a,\theta)=m\omega^2W(a,\theta)$$
$$M_r(a,\theta)=-I_G\omega^2\frac{\partial W}{\partial r}(a,\theta) \quad (I_G=k_G m) \quad (3\text{-}20)$$

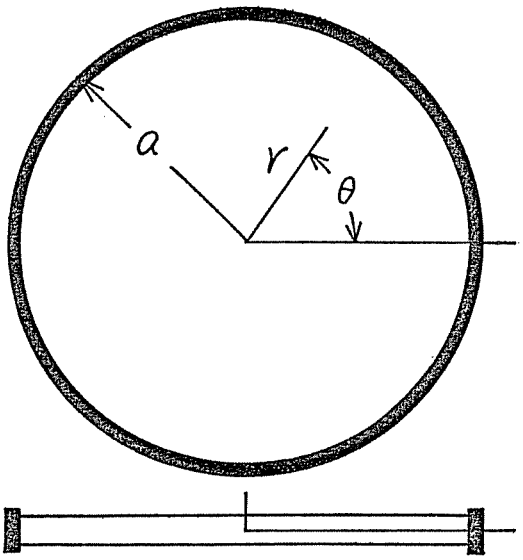

Fig.3-5

where I_G is mass moment of inertia per unit of circumferential length and k_g is radius of gyration of ring. Elements of the determinant are given by

$$
\begin{aligned}
C_1 &= \left\{ n^2(1-n)(1-\nu) - n\lambda^2 + \frac{\lambda^4}{2} R_m \right\} J_n + \lambda \left\{ n^2(1-\nu) + \lambda^2 \right\} J_{n+1} \\
C_2 &= \left\{ n^2(1-n)(1-\nu) + n\lambda^2 + \frac{\lambda^4}{2} R_m \right\} I_n - \lambda \left\{ n^2(1-\nu) - \lambda^2 \right\} I_{n+1} \\
C_3 &= \left\{ n(n-1)(1-\nu) - \lambda^2 - n \frac{\lambda^4 \bar{k}_g}{2} R_m \right\} J_n + \lambda \left(1-\nu + \frac{\lambda^4 \bar{k}_g}{2} R_m \right) J_{n+1} \\
C_4 &= \left\{ n(n-1)(1-\nu) + \lambda^2 - n \frac{\lambda^4 \bar{k}_g}{2} R_m \right\} I_n - \lambda \left(1-\nu + \frac{\lambda^4 \bar{k}_g}{2} R_m \right) I_{n+1}
\end{aligned}
\qquad (3\text{-}21)
$$

where $R_m = M_A / M_P$ (M_A: total mass of the added mass, M_P: total mass of a plate), $\bar{k}_g = k_g / a$.

3-2-3 Results and discussion

Some literature surveys [1,2,3] revealed that a reasonable number of numerical results had been obtained for the two cases when the plate boundary is either clamped or free, as pointed out in Sec.3-1-1, but that few results were available for the simply supported boundary. For this reason, natural frequencies of simply supported circular plates are calculated in this section by using Eq.(3-9), and the numerical results are summalized in Table 3-1 through 3-6 for the full range of physically possible Poisson ratios , ν = 0,0.1,0.2,0.3, 0.4 and 0.5. Results are given for all values of n and s having $n+s \leq 10$, where n denotes the number of nodal diameters and s the number of interior nodal circles.

Table 3-1 Frequency parameters $\lambda = a(\omega\sqrt{\rho/D})^{1/2}$ of a simply supported circular plate ($\nu = 0.0$)

s \ n	0	1	2	3	4	5	6	7	8	9	10
0	2.10799	3.67442	5.02440	6.29310	7.51641	8.71001	9.88232	11.0385	12.1819	13.3150	14.4393
1	5.41883	6.93802	8.35354	9.70661	11.0170	12.2961	13.5508	14.7861	16.0054	17.2112	
2	8.59202	10.1215	11.5747	12.9751	14.3364	15.6672	16.9734	18.2594	19.5282		
3	11.7471	13.2846	14.7609	16.1916	17.5867	18.9530	20.2955	21.6178			
4	14.8962	16.4393	17.9311	19.3829	20.8023	22.1947	23.5644				
5	18.0426	19.5897	21.0927	22.5601	23.9977	25.4103					
6	21.1875	22.7376	24.2491	25.7283	27.1803						
7	24.3315	25.8840	27.4020	28.8907							
8	27.4749	29.0293	30.5526								
9	30.6180	32.1739									
10	33.7608										

Table 3-2 Frequency parameters $\lambda = a(\omega\sqrt{\rho/D})^{1/2}$ of a simply supported circular plate ($\nu = 0.10$)

s \ n	0	1	2	3	4	5	6	7	8	9	10
0	2.14924	3.69301	5.03693	6.30266	7.52419	8.71658	9.88803	11.0435	12.1865	13.3191	14.4431
1	5.43001	6.94638	8.36032	9.71235	11.0220	12.3005	13.5548	14.7898	16.0088	17.2143	
2	8.59856	10.1270	11.5794	12.9793	14.3401	15.6706	16.9765	18.2623	19.5309		
3	11.7517	13.2887	14.7645	16.1949	17.5897	18.9558	20.2981	21.6203			
4	14.8998	16.4425	17.9341	19.3857	20.8048	22.1971	23.5666				
5	18.0455	19.5923	21.0952	22.5624	23.9999	25.4123					
6	21.1899	22.7399	24.2512	25.7304	27.1823						
7	24.3336	25.8860	27.4039	28.8925							
8	27.4768	29.0311	30.5543								
9	30.6197	32.1755									
10	33.7623										

Table 3-3 Frequency parameters $\lambda = a(\omega\sqrt{\rho/D})^{1/2}$ of a simply supported circular plate ($\nu = 0.20$)

s \ n	0	1	2	3	4	5	6	7	8	9	10
0	2.18691	3.71087	5.04911	6.31202	7.53183	8.72306	9.89366	11.0485	12.1909	13.3231	14.4468
1	5.44093	6.95460	8.36700	9.71803	11.0270	12.3049	13.5588	14.7934	16.0121	17.2174	
2	8.60502	10.1324	11.5841	12.9834	14.3438	15.6740	16.9797	18.2652	19.5336		
3	11.7563	13.2927	14.7681	16.1982	17.5927	18.9586	20.3007	21.6227			
4	14.9033	16.4457	17.9370	19.3884	20.8073	22.1994	23.5688				
5	18.0484	19.5950	21.0977	22.5647	24.0021	25.4144					
6	21.1924	22.7422	24.2533	25.7324	27.1842						
7	24.3358	25.8880	27.4058	28.8943							
8	27.4787	29.0329	30.5559								
9	30.6214	32.1771									
10	33.7638										

Table 3-4 Frequency parameters $\lambda = a(\omega\sqrt{\rho/D})^{1/2}$ of a simply supported circular plate ($\nu = 0.30$)

s \ n	0	1	2	3	4	5	6	7	8	9	10
0	2.22152	3.72802	5.06096	6.32118	7.53933	8.72944	9.89922	11.0535	12.1954	13.3272	14.4505
1	5.45160	6.96268	8.37359	9.72363	11.0319	12.3093	13.5627	14.7970	16.0154	17.2204	
2	8.61139	10.1377	11.5887	12.9875	14.3475	15.6773	16.9828	18.2680	19.5363		
3	11.7609	13.2967	14.7717	16.2014	17.5957	18.9613	20.3032	21.6251			
4	14.9069	16.4489	17.9399	19.3910	20.8098	22.2018	23.5710				
5	18.0513	19.5977	21.1001	22.5670	24.0042	25.4164					
6	21.1949	22.7445	24.2555	25.7344	27.1861						
7	24.3379	25.8900	27.4076	28.8961							
8	27.4806	29.0346	30.5576								
9	30.6230	32.1787									
10	33.7653										

Table 3-5 Frequency parameters $\lambda = a(\omega\sqrt{\rho/D})^{1/2}$ of a simply supported circular plate ($\nu = 0.40$)

s \ n	0	1	2	3	4	5	6	7	8	9	10
0	2.25348	3.74452	5.07249	6.33014	7.54671	8.73572	9.90470	11.0583	12.1998	13.3312	14.4542
1	5.46204	6.97062	8.38009	9.72916	11.0367	12.3136	13.5666	14.8005	16.0186	17.2235	
2	8.61768	10.1430	11.5933	12.9915	14.3512	15.6807	16.9858	18.2709	19.5389		
3	11.7654	13.3006	14.7752	16.2046	17.5986	18.9641	20.3058	21.6275			
4	14.9104	16.4521	17.9428	19.3937	20.8123	22.2041	23.5732				
5	18.0542	19.6003	21.1026	22.5693	24.0064	25.4184					
6	21.1973	22.7467	24.2576	25.7364	27.1879						
7	24.3400	25.8919	27.4095	28.8979							
8	27.4824	29.0364	30.5593								
9	30.6247	32.1803									
10	33.7669										

Table 3-6 Frequency parameters $\lambda = a(\omega\sqrt{\rho/D})^{1/2}$ of a simply supported circular plate (ν=0.50)

s \ n	0	1	2	3	4	5	6	7	8	9	10
0	2.28312	3.76041	5.08371	6.33892	7.55395	8.74190	9.91010	11.0631	12.2041	13.3351	14.4578
1	5.47225	6.97843	8.38650	9.73463	11.0415	12.3178	13.5705	14.8041	16.0219	17.2265	
2	8.62388	10.1482	11.5978	12.9956	14.3548	15.6840	16.9889	18.2737	19.5416		
3	11.7698	13.3045	14.7787	16.2078	17.6015	18.9668	20.3083	21.6298			
4	14.9139	16.4552	17.9457	19.3963	20.8148	22.2064	23.5754				
5	18.0570	19.6029	21.1050	22.5715	24.0085	25.4202					
6	21.1997	22.7490	24.2597	25.7384	27.1898						
7	24.3421	25.8939	27.4114	28.8996							
8	27.4843	29.0381	30.5610								
9	30.6264	32.1819									
10	33.7684										

Frequency parameters λ are given with six significant figures. The parameters λ^2 by other authors are presented in Table 3-7. It is seen that inaccuracy exists in the previous data except for Pardoen's values, probably due to errors in calculating the Bessel functions. Comparing Table 3-1 through 3-6, it can be known that the effect of Poisson's ratio upon the frequency parameter λ is significant only for the lowest frequencies. This effect is observed clearly in Table 3-8 wherein the ratio of $\lambda^2(0.5)/\lambda^2(0)$ is shown for selected modes of n and s with $\lambda^2(0.5)$ and $\lambda^2(0)$ being the values of λ^2 for $\nu=0.5$ and 0, respectively. The squared values λ^2 are used here to observe the difference more clearly. When the ratios of the frequencies themselves are compared, the effects of ν are more pronounced as seen in Table 3-8. The circumferential stiffening is particularly important in the lowest axisymmetric mode where the frequency can be differ by as much as 35 percent for different ν. The number of presented data in these tables must be sufficient for most practical needs.

Another significant lack of data on circular plates is variation of frequencies for a plate supported by a translational spring only. Table 3-9 presents frequency parameters of the plate with four significant figures by use of Eq.(3-14,17). The mode shapes are identified by (n, s). For a completely free plate $(\bar{K}=0)$, the lowest and second frequency vanish and the plate physically shows rigid body motions of translation and rotation,

Table 3-7 Comarison of frequency parameters with those by other authors for $\nu = 0.30$.

n	S	Gontkevich[66]	Wah[67]	Pardoen[69]	Present work
0	0	4.977	4.94	4.9352	4.93515
	1	29.76	29.72	29.7200	29.7200
	2	74.20	74.15	74.1561	74.1560
	3	138.34	——	138.3181	138.318
1	0	13.94	13.47	13.8982	13.8982
	1	48.51	47.89	48.4789	48.4789
	2	102.80	103.43	102.7734	102.773
	3	176.84	——	176.8012	176.801
2	0	25.65	25.60	25.6133	25.6133
	1	70.14	68.89	70.1170	70.1170
	2	134.33	134.56	134.2977	134.298
	3	218.24	——	218.2025	218.202

Table 3-8 Ratios of frequency parameters and frequencies for different Poisson's ratios

n	S	$\lambda^2(.5)/\lambda^2(0)$	$\omega(.5)/\omega(0)$
0	0	1.17307	1.35454
0	1	1.01981	1.17758
0	2	1.00743	1.16328
0	10	1.00045	1.15522
1	0	1.04736	1.20934
2	0	1.02375	1.18212
10	0	1.00257	1.15470

Table 3-9 Frequency parameters $\lambda = a(\omega\sqrt{\rho/D})^{1/2}$ of a circular plate uniformly constrained by a translational spring (ν =0.33)

mode (n,s) \ $\bar{K}_w$	0	10^{-1}	10^{0}	10^{1}	10^{2}	10^{4}	10^{6}	∞
1 (0,0)	0	0.668	1.172	1.861 1.86*	2.183 2.18*	2.231	2.231	2.231
2 (1,0)	0	0.795	1.410	2.440	3.479	3.731	3.733	3.733
3 (2,0)	2.294	2.305	2.398	2.983	4.370	5.057	5.064	5.064
4 (0,1)	3.012	3.016	3.052	3.390	4.701	5.447	5.455	5.455
5 (3,0)	3.499	3.503	3.536	3.822	5.068	6.308	6.324	6.324
6 (1,1)	4.529	4.530	4.541	4.648	5.567	6.949	6.965	6.965

* Laura et al. [80]

respectively. As the nondimensional stiffness $\bar{K} = a^3 K_w / D$ is increased, the frequency parameters become higher and coincide with those for a simply supported plate when $\bar{K} = 10^6$ is taken. The fundamental frequencies, obtained by Laura [80], for $\bar{K} = 10^1, 10^2$ are presented and they are found to agree.

Table 3-10 and Fig.3-6 show the effect of a uniform added mass to the edge on the frequency parameters of a free circular plate for the selected modes (0,1) and (3,0). Other frequencies and nodal patterns will be presented in Sec.3-5-3. Here the effect of rotary inertia of the edge mass is neglected. It is interesting to observe that the effect of a added mass appears on (3,0) mode more obviously than on (0,1) mode, as the mass ratio is increased.

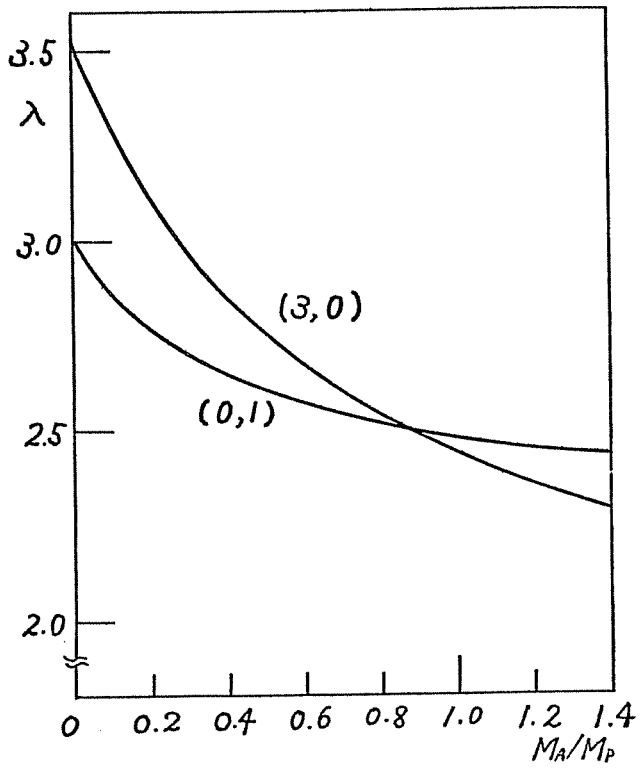

Fig.3-6

Table 3-10 Frequency parameters of a free plate with a uniform added mass

M_A/M_P \ (n,s)	(0,1)	(3,0)
0.0	3.001	3.527
0.2	2.770	3.108
0.4	2.646	2.855
0.6	2.569	2.679
0.8	2.516	2.546
1.0	2.477	2.441
1.2	2.448	2.354
1.4	2.424	2.281

(M_P:total mass of plate, M_A:total mass of edge mass)

3-3 Simply supported circular plate constrained by partial rotational springs

3-3-1 Review

In most works concerned with vibration of circular plates, the uniform boundary conditions have been used and circular plates with mixed boundary conditions have received sparce treatment. This is mainly attributed to the mathematical difficulty in obtaining analytical solutions of the problem.

Nowacki and Olesiak [86] have dealt with the problem using a Fredfolm integral equation but the results were few. Bartlett [87] obtained the fundamental frequency by use of a variational approach. The variational expressions were determined by separation of variables, and two different procedures gave upper and lower bounds of the solution. Numerical results are given in good accuracy. Noble [88] also obtained the fundamental frequency from an integral equation involving unknown functions along the circumference of the plate. The solution of a certain static problem was used to find an approximation to the fundamental frequency. Hirano and Okazaki [89] employed the variational method to obtain the lowest two frequencies for plates having three combinations of free, clamped and simply supported edge. Hemmig [90] obtained both finite element and experimental results for the problem, but the number of frequencies presented are few. Thus, these previous studies revealed only the lowest two frequencies.

Moreover, apparently no one has been able to deal with the mixed boundary conditions for the case when a plate is constrained by elastic springs along part of the boundary.

In this section, the author deals with the problem of a simply supported plate having some partial rotational springs, and shows natural frequencies and mode shapes up to higher modes. Numerical results are also shown for partially clamped plates, utilizing the concept that the edge condition of zero deflection and rotational elastic constraint is reached in the limit as the elastic spring constants are taken to be infinite. The analytical procedure used is an extension of a previously developed method [91] for accomodating spring stiffnesses which vary circumferentially around the boundary. The method is straightfoward and applicable to wide variations of edge constraints. An analytical solution of the differential equation of plate vibration is derived in a simple form, thereby avoiding a formidable task of the variational procedure. The natural frequncies are obtainable to the desired accuracy by using the frequency determinant of larger order. Numerical results presented in figures provide some interesting observations.

3-3-2 Analysis *

A general solution to Eq.(3-1) for a solid circular plate is given by

$$W(r,\theta)=\sum_{n=0}^{\infty}W_n(kr)\cos n\theta+\sum_{n=1}^{\infty}W_n^*(kr)\sin n\theta \tag{3-22}$$

where

$$\begin{aligned}W_n(kr)&=A_nJ_n(kr)+C_nI_n(kr)\\ W_n^*(kr)&=A_n^*J_n(kr)+C_n^*I_n(kr)\quad(k^4=\rho\omega^2/D)\end{aligned} \tag{3-23}$$

Consider a simply supported circular plate having rotational springs along parts of the edge as shown in Fig.3-7. Edge slope is opposed by the rotational springs having distributed stiffness K_ψ (moment/unit length). The boundary conditions are therefore

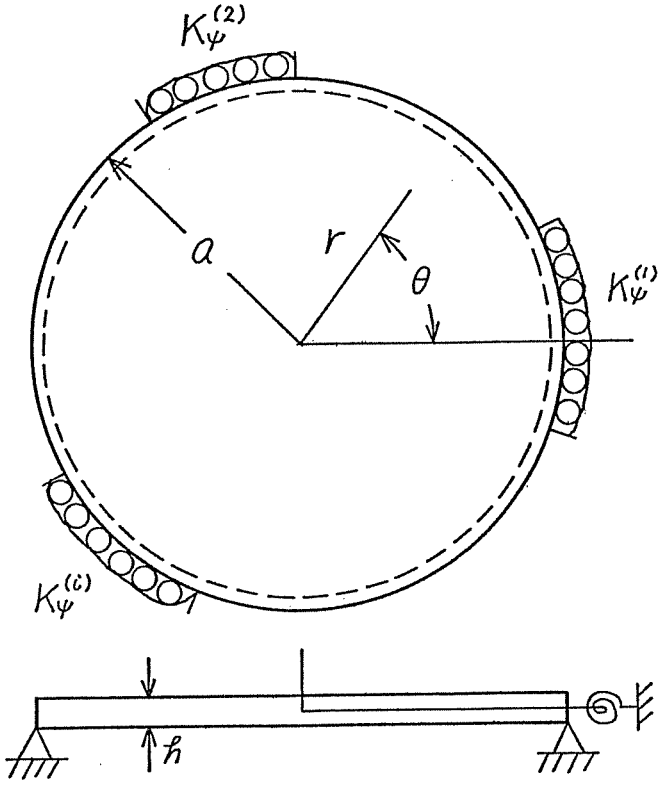

Fig.3-7

$$\begin{aligned}W(a,\theta)&=0\\ M_r(a,\theta)&=K_\psi\frac{\partial W}{\partial r}(a,\theta)\end{aligned} \tag{3-24}$$

where $M_r(r,\theta)$ is the radial bending moment per unit length given by Eq.(3-8). Since $K_{\psi(\theta)}$ varies along the boundary, it is reasonable to expand the spring stiffness in Fourier series.

$$K_\psi(\theta)=\sum_{m=0}^{\infty}L_m\cos m\theta+\sum_{m=1}^{\infty}L_m^*\sin m\theta \tag{3-25}$$

*[92]

where L_m and L_m^* are Fourier coefficients determined in the usual manner. Substituting Eqs.(3-8,22,25) into the boundary conditions (3-24) yields

$$
\begin{aligned}
& W_n(\lambda)\cos n\theta + W_n^*(\lambda)\sin n\theta = 0 \\
& \sum_{n=0}^{\infty}\left\{ \lambda^2 W_n''(\lambda) + \nu\lambda W_n'(\lambda) - \nu n^2 W_n(\lambda) \right\}\cos n\theta \\
& + \sum_{n=1}^{\infty}\left\{ \lambda^2 W_n^{*\prime\prime}(\lambda) + \nu\lambda W_n^{*\prime}(\lambda) - \nu n^2 W_n^*(\lambda) \right\}\sin n\theta \\
& = -\lambda\left\{ \vartheta_1(\theta) + \vartheta_2(\theta) + \vartheta_3(\theta) + \vartheta_4(\theta) \right\}
\end{aligned}
\tag{3-26}
$$

where λ is the nondimensional frequency parameter given by $\lambda^2 = (ka)^2 = \omega a^2\sqrt{\rho/D}$ and ϑ_1, ϑ_2, ϑ_3 and ϑ_4 are expressed as the products

$$
\begin{aligned}
\vartheta_1(\theta) &= \sum_{m=0}^{\infty}\bar{L}_m\cos m\theta \sum_{n=0}^{\infty} W_n'\cos n\theta \\
\vartheta_2(\theta) &= \sum_{m=0}^{\infty}\bar{L}_m\cos m\theta \sum_{n=1}^{\infty} W_n^{*\prime}\sin n\theta \\
\vartheta_3(\theta) &= \sum_{m=1}^{\infty}\bar{L}_m^*\sin m\theta \sum_{n=0}^{\infty} W_n'\cos n\theta \\
\vartheta_4(\theta) &= \sum_{m=1}^{\infty}\bar{L}_m^*\sin m\theta \sum_{n=1}^{\infty} W_n^{*\prime}\sin n\theta
\end{aligned}
\tag{3-27}
$$

using nondimensional spring coefficients $\bar{L}_m = aL_m/D$ and $\bar{L}_m^* = aL_m^*/D$. These products of trigonometric functions are removed by use of the trigonometric identities such as

$$
\begin{aligned}
\cos m\theta\cos n\theta &= \frac{1}{2}\left\{\cos(m+n)\theta + \cos(m-n)\theta\right\} \\
\cos m\theta\sin n\theta &= \frac{1}{2}\left\{\sin(m+n)\theta - \sin(m-n)\theta\right\}
\end{aligned}
\tag{3-28}
$$

Suppose that the edge constraint has an axis of symmetry at $\theta = 0$. Vibration modes in that case are separated into symmetric and antisymmetric mode with respect to the axis. Then,

$$W_n(\lambda)\begin{pmatrix}\cos n\theta\\ \sin n\theta\end{pmatrix} = 0 \tag{3-29a}$$

$$\left\{\lambda^2 W_n''(\lambda) + \nu\lambda W_n'(\lambda) - \nu n^2 W_n(\lambda)\right\}\begin{pmatrix}\cos n\theta\\ \sin n\theta\end{pmatrix} = -\lambda\begin{pmatrix}\vartheta_1(\theta)\\ \vartheta_2(\theta)\end{pmatrix} \tag{3-29b}$$

where

$$\vartheta_1(\theta) = \begin{cases} \bar{L}_0 W_0' + \frac{1}{2}\sum_{i=1}^{\infty}\bar{L}_i W_i' & (n=0) \\ \left[\bar{L}_0 W_n' + \frac{1}{2}\left\{\bar{L}_n W_0' + \sum_{i=1}^{\infty}\bar{L}_i\left(W_{n+i}' + W_{|n-i|}'\right)\right\}\right]\cos n\theta & (n=1,2,\cdots) \end{cases} \tag{3-30}$$

$$\vartheta_2(\theta) = \left[\bar{L}_0 W_n' + \frac{1}{2}\left\{\bar{L}_n W_0' + \sum_{i=1}^{\infty}\bar{L}_i\left(W_{n+i}' \pm W_{|n-i|}'\right)\right\}\right]\sin n\theta \qquad \left(\pm : \begin{matrix} n>i \\ n\le i \end{matrix}\right) \quad (n=1,2,\cdots)$$

Derivatives of Bessel functions with respect to kr are evaluated by formulas (3-8,16,17). From Eqs.(3-23,29a), one obtains

$$C_n = -\frac{J_n}{I_n}A_n \tag{3-31}$$

Substituting Eq.(3-31) into (3-29b) and equating coefficients of $\cos n\theta$ (or $\sin n\theta$) yield for

(1) Symmetric vibration mode

$$
\begin{aligned}
&2\{2\lambda J_0-(1-\nu-\bar{L}_0)(J_1 I_0+J_0 I_1)/I_0\}A_0 \\
&\qquad+\sum_{i=1}^{\infty}\{\bar{L}_i(J_{i+1}I_i+J_i I_{i+1})/I_i\}A_i=0 \qquad (n=0) \\
&2\{2\lambda J_n-(1-\nu-\bar{L}_0)(J_{n+1}I_n+J_n I_{n+1})/I_n\}A_n \\
&\qquad+\{\bar{L}_n(J_1 I_0+J_0 I_1)/I_0\}A_0 \\
&+\sum_{i=1}^{\infty}\bar{L}_i\left[\{(J_{n+i+1}I_{n+i}+J_{n+i}I_{n+i+1})/I_{n+i}\}A_{n+i}\right. \\
&\qquad\left.+\{(J_{|n-i|+1}I_{|n-i|}+J_{|n-i|}I_{|n-i|+1})/I_{|n-i|}\}A_{|n-i|}\right]=0 \\
&\qquad\qquad (n=1,2,\cdots)
\end{aligned}
\tag{3-32}
$$

or in matrix form

$$
\begin{bmatrix} e_{00} & e_{01} & e_{02} & \cdots\cdots \\ e_{10} & e_{11} & e_{12} & \cdots\cdots \\ e_{20} & e_{21} & e_{22} & \ddots \\ \vdots & & & \end{bmatrix}\begin{bmatrix} A_0 \\ A_1 \\ A_2 \\ \vdots \end{bmatrix}=0 \tag{3-33}
$$

where

$$
\begin{aligned}
e_{00} &= 4\lambda J_0-2(1-\nu-\bar{L}_0)\,b_0 \\
e_{0j} &= \bar{L}_i\,b_j \\
e_{i0} &= 2\bar{L}_i\,b_0 \\
e_{ij} &= \begin{cases} 4\lambda J_i+\{\bar{L}_{2i}-2(1-\nu-L_0)\}b_i & (i=j) \\ (\bar{L}_{|i-j|}+\bar{L}_{i+j})\,b_j & (i\neq j) \end{cases}
\end{aligned}
\tag{3-34}
$$

and

$$
b_j=(I_{j+1}I_j+J_j I_{j+1})/I_j
$$

(2) Antisymmetric vibration mode

$$
\begin{aligned}
&2\left\{2\lambda J_n-(1-\nu-\bar{L}_0)(J_{n+1}I_n+J_nI_{n+1})/I_n\right\}A_n\\
&\quad+\left\{\bar{L}_n(J_1I_0+J_0I_1)/I_0\right\}A_0\\
&+\sum_{i=1}^{\infty}\bar{L}_i\left[\left\{(J_{n+i+1}I_{n+i}+J_{n+i}I_{n+i+1})/I_{n+i}\right\}A_{n+i}\right.\\
&\quad\left.\pm\left\{(J_{|n-i|+1}I_{|n-i|}+J_{|n-i|}I_{|n-i|+1})/I_{|n-i|}\right\}A_{|n-i|}\right]=0 \qquad (3\text{-}35)\\
&\left(\pm:\begin{matrix}n>i\\ n\le i\end{matrix}\right) \qquad\qquad (n=1,2,\cdots)
\end{aligned}
$$

or in matrix form

$$
\begin{bmatrix} e_{11} & e_{12} & e_{13} & \cdots \\ e_{21} & e_{22} & e_{23} & \cdots \\ e_{31} & e_{32} & e_{33} & \ddots \\ \vdots & & & \end{bmatrix}\begin{bmatrix} A_1 \\ A_2 \\ A_3 \\ \vdots \end{bmatrix}=0 \qquad (3\text{-}36)
$$

where

$$
e_{ij}=\begin{cases}4\lambda J_i-\left\{\bar{L}_{2i}+2(1-\nu-L_0)\right\}b_j & (i=j)\\ (\bar{L}_{|i-j|}-\bar{L}_{i+j})\,b_j & (i\neq j)\end{cases} \qquad (3\text{-}37)
$$

The natural frequencies of the plate are obtained by calculating eigenvalues λ of the coefficient matrices of Eqs. (3-33,36). The mode shapes are determined by

$$
\begin{aligned}
W(r,\theta)=\sum_{n=0}^{\infty}A_n\begin{pmatrix}\cos n\theta\\ \sin n\theta\end{pmatrix}&\left\{J_n(\lambda\tfrac{r}{a})I_n(\lambda)\right.\\
&\left.-J_n(\lambda)I_n(\lambda\tfrac{r}{a})\right\}/I_n(\lambda) \qquad (3\text{-}38)
\end{aligned}
$$

after solving simultaneous equations in terms of amplitude ratios A_i/A_0 or A_i/A_1.

3-3-3 Results and discussion

Arbitrary spring systems are physically meaningful as long as they are passive spring systems ($K_\psi > 0$) for all values of θ. We now consider simply supported circular plate having one, two or three rotational springs on the boundary. For simplicity, it is assumed that each spring has the same degree of stiffness, although it is possible to utilize springs having different stiffnesses. They are symmetrically spaced with respect to $\theta = 0$. That is, (1) one spring is located on $-\alpha < \theta < \alpha$ of the boundary, (2) two springs are located $-\alpha < \theta < \alpha$ and $\pi - \alpha < \theta < \pi + \alpha$, and (3) three springs are located on $-\alpha < \theta < \alpha$, $2\pi/3 - \alpha < \theta < 2\pi/3 + \alpha$ and $4\pi/3 - \alpha < \theta < 4\pi/3 + \alpha$. Fourier coefficients of three spring systems are determined by

$$L_m = \frac{L_m a}{D} = \frac{1}{\pi} \int_0^{2\pi} \left(\frac{a K_\psi}{D} \right) \cos m\theta \, d\theta \qquad (3\text{-}39)$$

and are shown in Table 3-11.

Table 3-11

	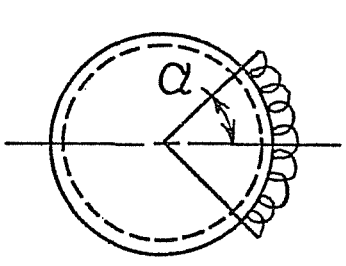	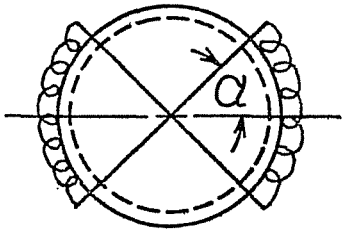	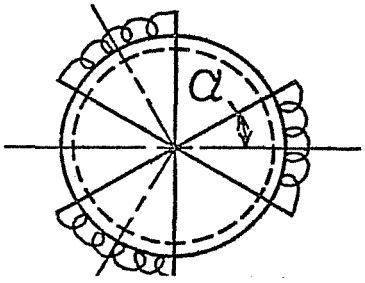
L_0	$\frac{\alpha}{\pi} \frac{a K_\psi}{D}$	$\frac{2\alpha}{\pi} \frac{a K_\psi}{D}$	$\frac{3\alpha}{\pi} \frac{a K_\psi}{D}$
L_m	$\frac{2 \sin m\alpha}{m\pi} \left(\frac{a K_\psi}{D} \right)$	$\frac{4 \sin m\alpha}{m\pi} \left(\frac{a K_\psi}{D} \right)$ $(m = 2, 4, 6 \cdots)$ $0 \quad (m = 1, 3, 5, \cdots)$	$\frac{6 \sin m\alpha}{m\pi} \left(\frac{a K_\psi}{D} \right)$ $(m = 3, 6, 9 \cdots)$ $0 \quad (m = 1, 2, 4, 5, \cdots)$

The rate of convergence of the fundamental frequency parameter using larger order determinants can be seen in Fig.3-8 for a simply supported circular plate having one rotational spring ($\alpha = \pi/4$, $aK_\psi/D = 10^4$). Poisson's ratio is taken as 0.25 for comparability. Since no known results are available on circular plates constrained by some partial rotational springs, it is appropriate to compare the present results for the limiting case with other known ones. It is obvious that the frequency parameter approaches that of a plate clamped along one quarter of its boundary as the nondimensional stiffness goes to infinity. It will be shown in Fig.3-10 that frequency parameters for $aK_\psi/D = 10^4$ and $\alpha = \pi$ show very good agreement with the exact values of a entirely clamped plate. Hence, $aK_\psi/D = 10^4$ can be regarded as "almost clamped." Bartlett [87] and Hemmig [90] presented the fundamental frequency for a circular plate partially clamped and simply supported at the remaining edge. These values are shown in the figure. It is noted that λ approaches Bartlett's value when larger order determinants are used.

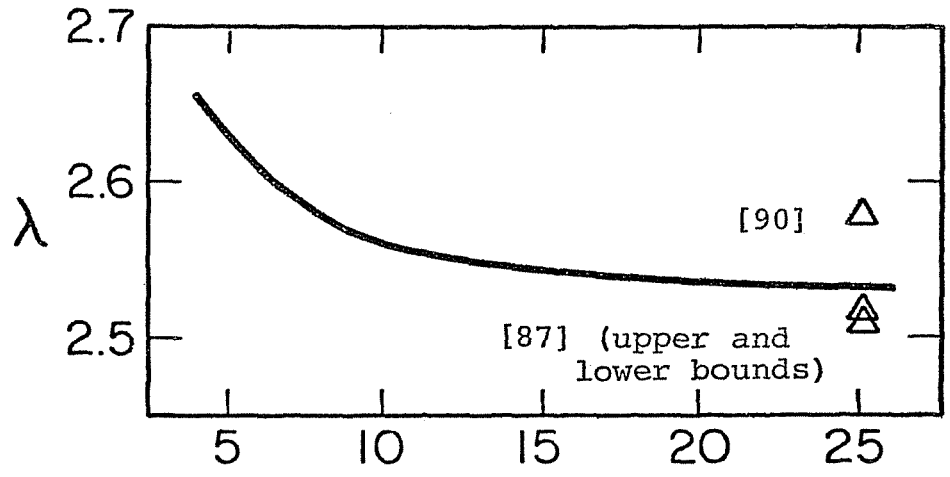

Fig.3-8 Convergence of the fundamental frequency parameter λ ($\alpha = \pi/4$, $aK_\psi/D = 10^4$).

Figure 3-9 presents frequency parameters and nodal patterns of a simply supported circular plate having one rotational spring of varying elastic stiffness ($\alpha = \pi/4$, $\nu = 0.3$). Frequency parameters were calculated by use of 20x20 matrices and errors are expected to be less than 1 percent for most cases according to the previous convergence study. Solid lines shown inside the plate boundary are nodal lines, corresponding to zero displacement of the plate. No nodal patterns are shown for the fundamental mode, because there are no nodal lines present. Nondimensional spring stiffness is taken as 0, 10^0, 10^2 and 10^4. The frequency equation is reduced to the exact one for a simply supported plate for $aK_\psi/D = 0$. As the stiffness is increased and discontinuity of the boundary condition becomes significant, frequencies of the plate increase and nodal lines become deformed. No major difference, however, is observed between $aK_\psi/D = 10^2$ and 10^4 in nodal patterns.

Figure 3-10 shows frequency parameters and nodal patterns of a simply supported circular plate having one rotational spring of varying angle ($aK_\psi/D = 10^4$, $\nu = 0.3$). Nondimensional stiffness is taken as constant 10^4 (almost clamped) and the angle α of the spring is taken $\pi/4$, $\pi/2$ $3\pi/4$ and π. The case of $\alpha = \pi/4$ corresponds to that of $aK_\psi/D = 10^4$ in Fig.3-9. Frequency parameters in the parentheses at $\alpha = \pi$ are the exact values for a clamped circular plate, and by comparing them with the previous ones, it is clear that $aK_\psi/D = 10^4$ is proper rigidity to represent clamping at the edge. Interesting variations of frequency

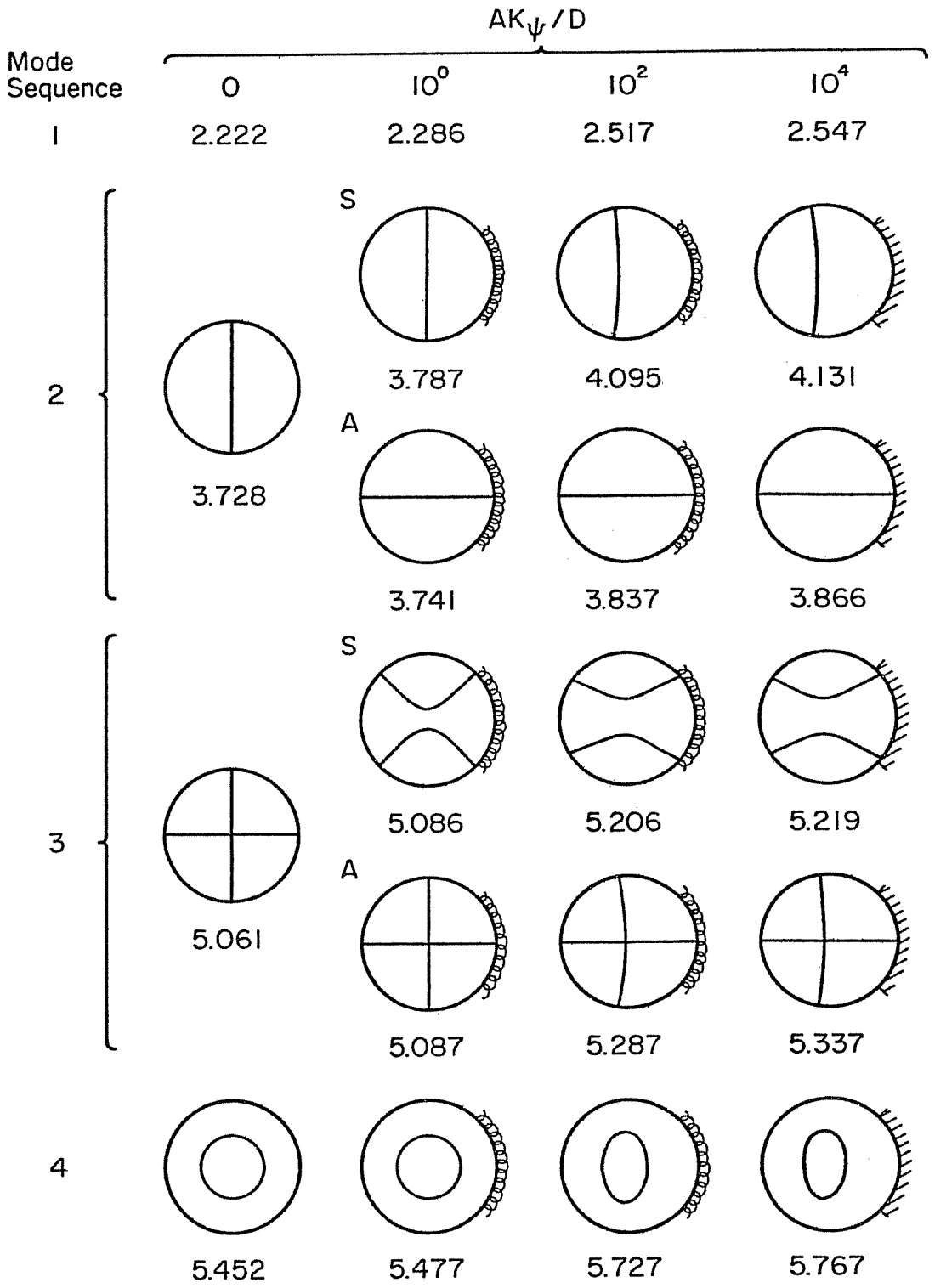

Fig.3-9 Frequency parameters and nodal patterns of simply supported plates with elastic constraint ($\alpha = \pi/4$, $\nu = 0.30$, 20 x 20 matrix).

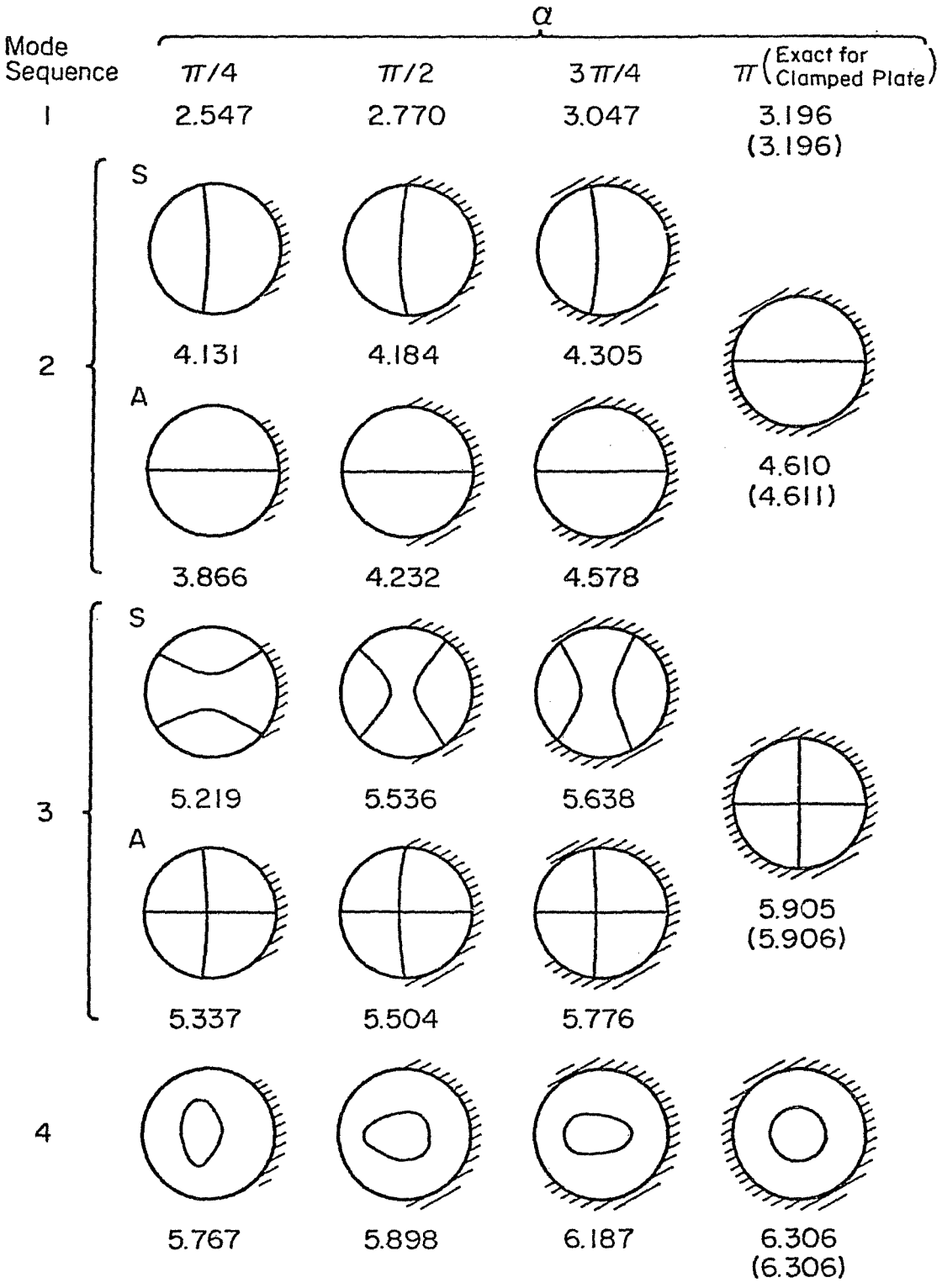

Fig.3-10 Frequency parameters and nodal patterns of plates clamped along one segment and simply supported on the remainder ($aK\psi/D = 10^4$, ν=0.30, 20x20 matrix).

parameters and nodal patterns are observed with the change of α. In the 2nd and 3rd modes, frequencies of symmetric or antisymmetric modes derived from one degenerated mode at $\alpha=0$ alternate in being higher or lower, and a nodal circle of the 4th mode changes its shape considerably. These nodal lines move so as to equalize the stiffness in each segment of the plate between the lines.

Figures 3-11,12 and 13 show the variations of the lowest five frequency parameters with the spring stiffness parameter when the plate is constrained by one, two and three springs, respectively. Solid lines denote symmetric modes and broken lines antisymmetric modes. For the case of $aK_\psi/D=0$ the exact values of a circular plate simply supported all around are presented. All frequencies increase monotonically and considerable changes take place between 10^0 and 10^2. Degeneracies exist for all values of aK_ψ/D for modes of the plate having three equally spaced springs. In this case, the frequencies of the symmetric and antisymmetric modes are the same. The values used in plotting these figures are presented in Table 3-12, 13 and 14.

The variations of the frequency parameter with the angle of spring constraint are shown in Fig.3-14, 15 and 16 when the plate is constrained by one, two and three springs, respectively. Since a nondimensional spring constant 10^4 is taken, the rotationally constrained parts of the edge can be considered as clamped, as suggested by the preceding example. As αM (M:number of springs) approaches π, the

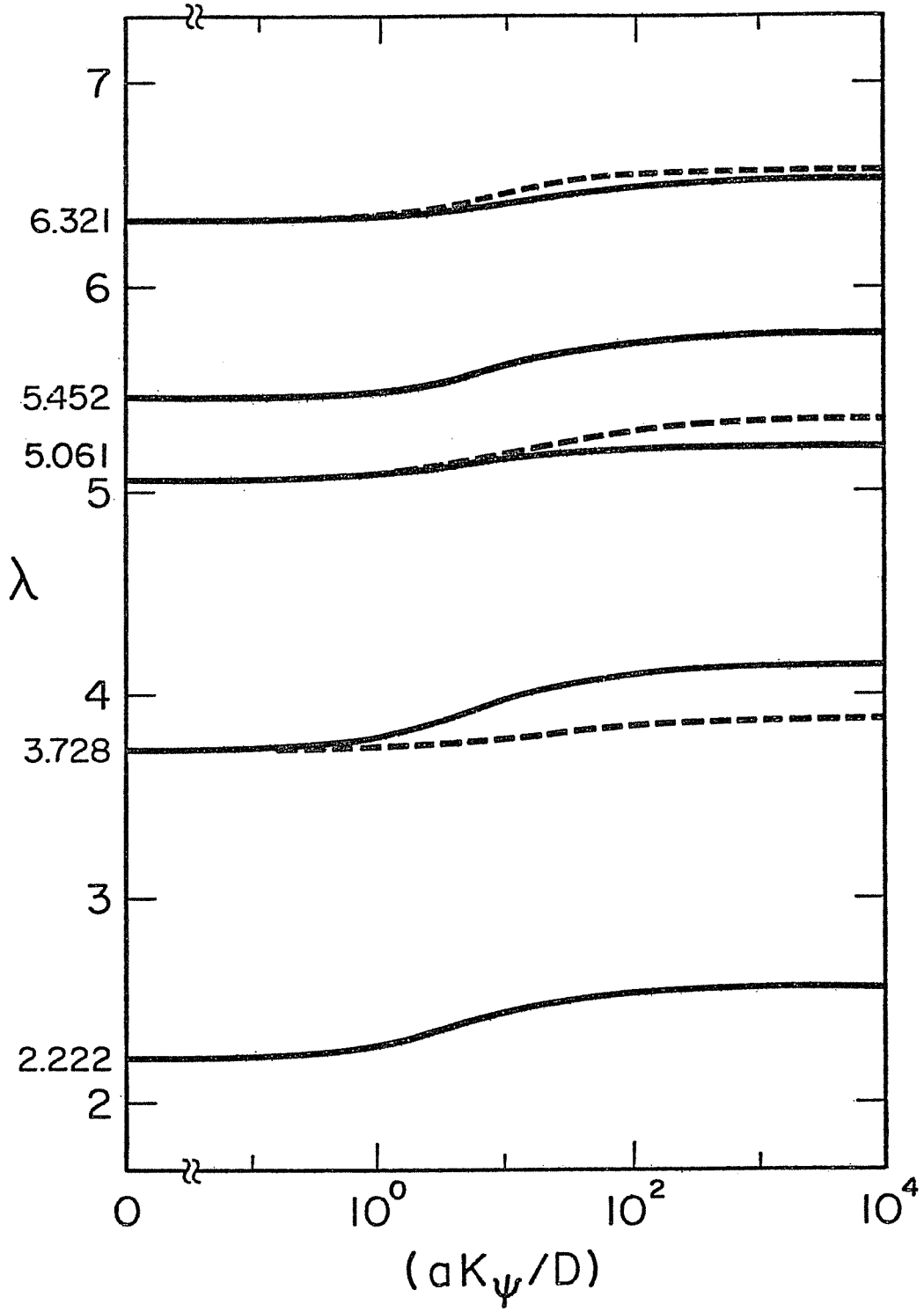

Fig.3-11 Variations of the frequency parameters for a simply supported plate elastically constrained along one segment ($\alpha = \pi/4, \nu = 0.30$).

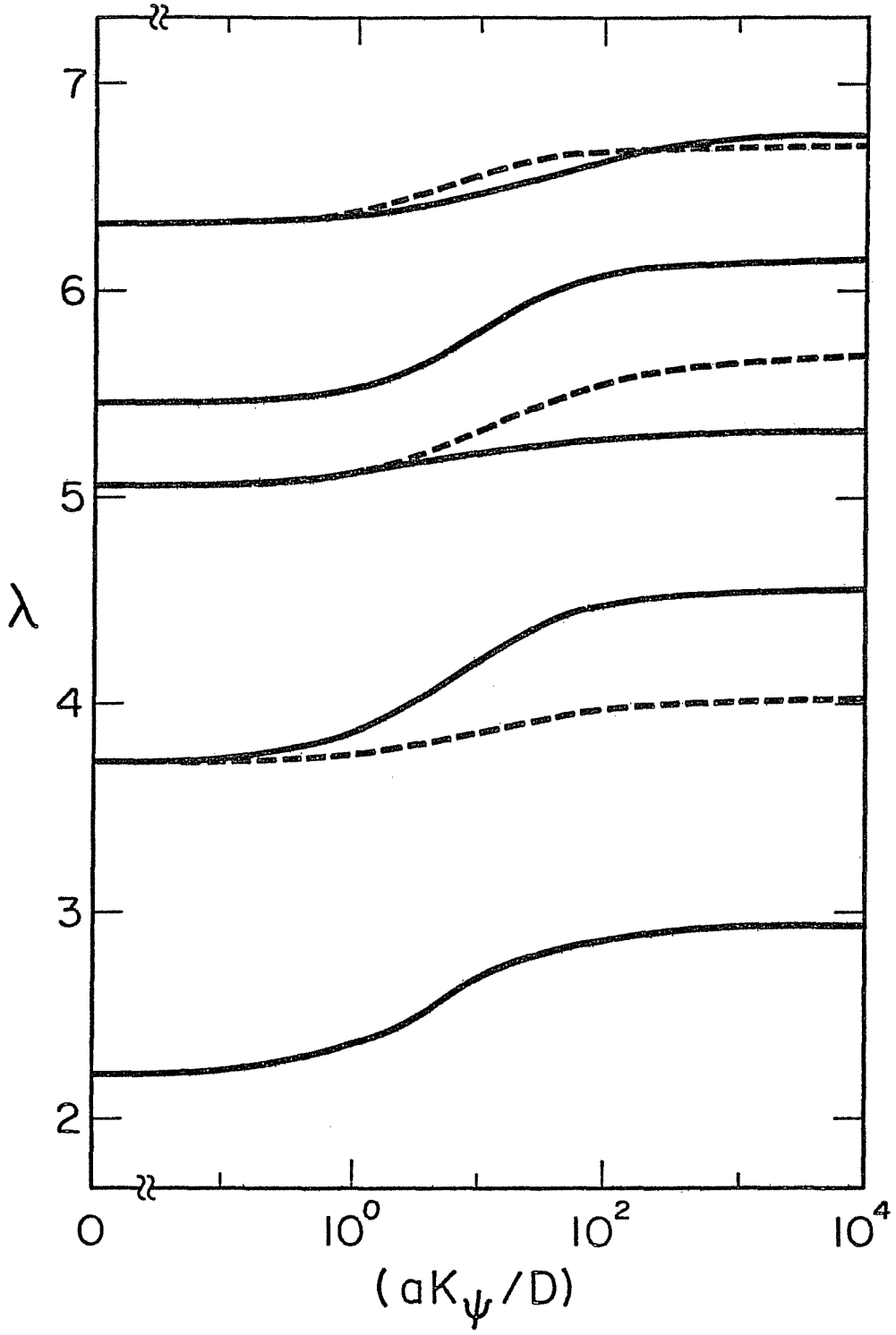

Fig.3-12 Variations of the frequency parameters for a simply supported plate elastically constrained along <u>two</u> segments ($\alpha = \pi/4$, $\nu = 0.30$).

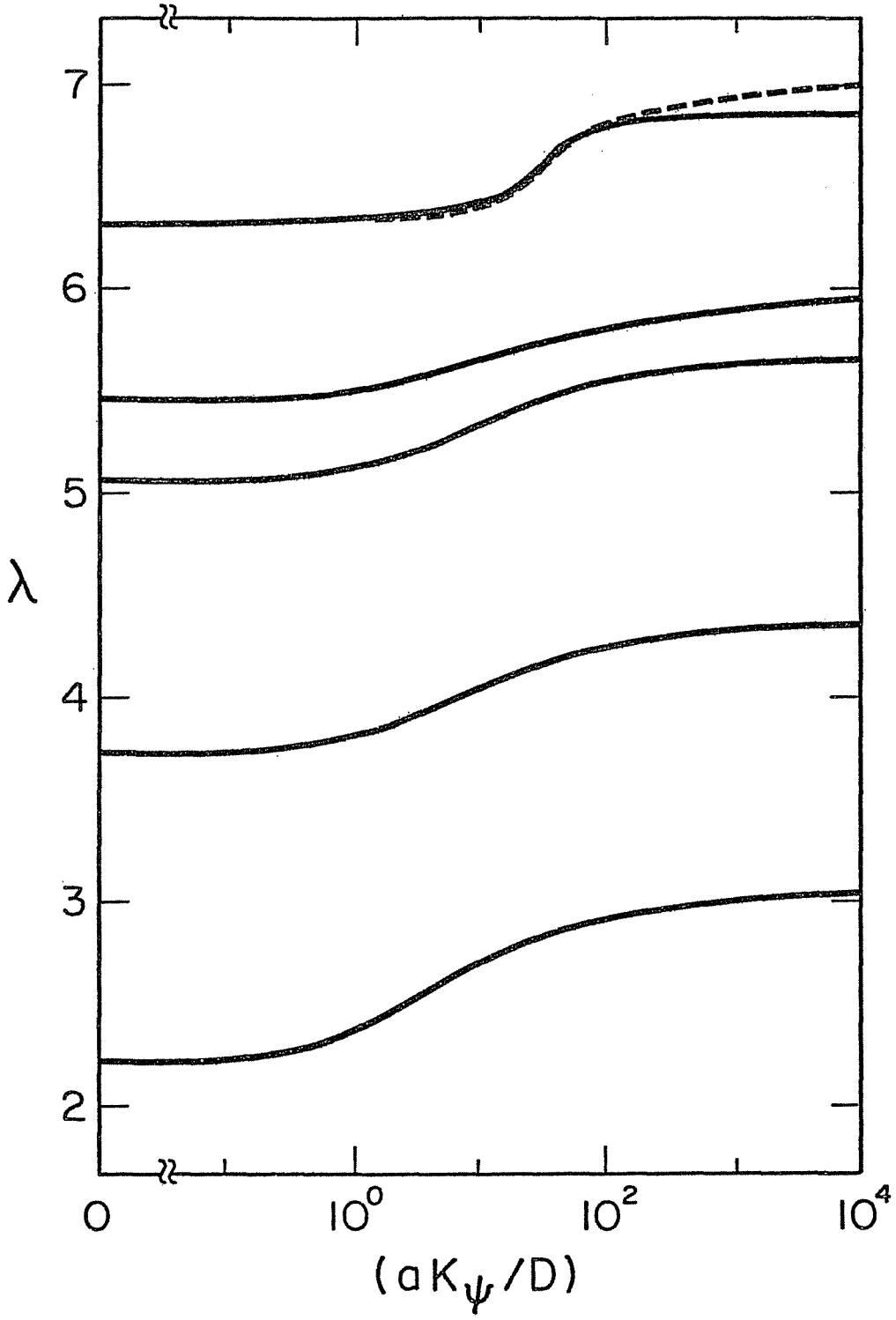

Fig.3-13 Variations of the frequency parameters for a simply supported plate elastically constrained along three segments ($\alpha = \pi/6$, $\nu = 0.30$).

Table 3-12

mode num.	type of mode	0	10^{-1}	10^{0}	10^{1}	10^{2}	10^{3}	10^{4}
1	S	2.222	2.22	2.29	2.45	2.52	2.55	2.56
2	S	3.728	3.73	3.79	3.98	4.10	4.13	4.15
	A	3.728	3.73	3.74	3.78	3.84	3.86	3.89
3	S	5.061	5.06	5.09	5.15	5.21	5.22	5.23
	A	5.061	5.06	5.09	5.19	5.30	5.34	5.38
4	S	5.452	5.45	5.48	5.62	5.73	5.77	5.78
5	S	6.321	6.32	6.34	6.41	6.48	6.53	6.56
	A	6.321	6.32	6.35	6.44	6.54	6.56	6.56

Table 3-13

mode num.	type of mode	0	10^{-1}	10^{0}	10^{1}	10^{2}	10^{3}	10^{4}
1	S	2.222	2.22	2.35	2.66	2.85	2.90	2.93
2	S	3.728	3.73	3.84	4.21	4.47	4.53	4.56
	A	3.728	3.73	3.75	3.85	3.96	4.01	4.05
3	S	5.061	5.06	5.11	5.21	5.27	5.30	5.31
	A	5.061	5.06	5.11	5.32	5.55	5.64	5.70

Table 3-13 (continued)

mode num.	type of mode	0	10^{-1}	10^{0}	10^{1}	10^{2}	10^{3}	10^{4}
4	S	5.452	5.45	5.50	5.79	6.08	6.14	6.16
5	S	6.321	6.32	6.35	6.48	6.63	6.71	6.76
	A	6.321	6.32	6.37	6.56	6.67	6.69	6.69

Table 3-14

mode num.	type of mode	0	10^{-1}	10^{0}	10^{1}	10^{2}	10^{3}	10^{4}
1	S	2.222	2.22	2.35	2.70	2.91	2.99	3.05
2	S	3.728	3.73	3.80	4.04	4.24	4.31	4.36
	A	3.728	3.73	3.80	4.04	4.24	4.31	4.36
3	S	5.061	5.06	5.11	5.34	5.56	5.62	5.67
	A	5.061	5.06	5.11	5.33	5.56	5.62	5.66
4	S	5.452	5.45	5.50	5.66	5.80	5.88	5.96
5	S	6.321	6.32	6.36	6.57	6.81	6.85	6.86
	A	6.321	6.32	6.36	6.56	6.82	6.93	7.01

partially clamped plate becomes a plate clamped along the entire edge. The exact figures are presented at $\alpha M = \pi$. On the other hand, as α approaches zero, the frequency parameters of the symmetric modes decrease rapidly in the vicinity of $\alpha = 0$. Physically speaking, however, the effect of moment constraint might remain even for small α. It is observed in the figures that the frequencies of two modes which generate from one mode at $\alpha = 0$ cross each other. This crossing takes place (2N-1) times (N: number of nodal diameters) for the plate with one spring and (N-1) times for two springs. Bartlett [87] obtained the fundamental variation with the angle of a clamped edge, and Hirano and Okazaki [89] also presented the variation for the lowest symmetric and antisymmetric modes. Both variations show excellent agreement with those in Fig.3-14, although the present results are slightly higher than those by the other authors due to the different Poisson's ratio. The values used in plotting these figures are presented in Table 3-15, 16 and 17.

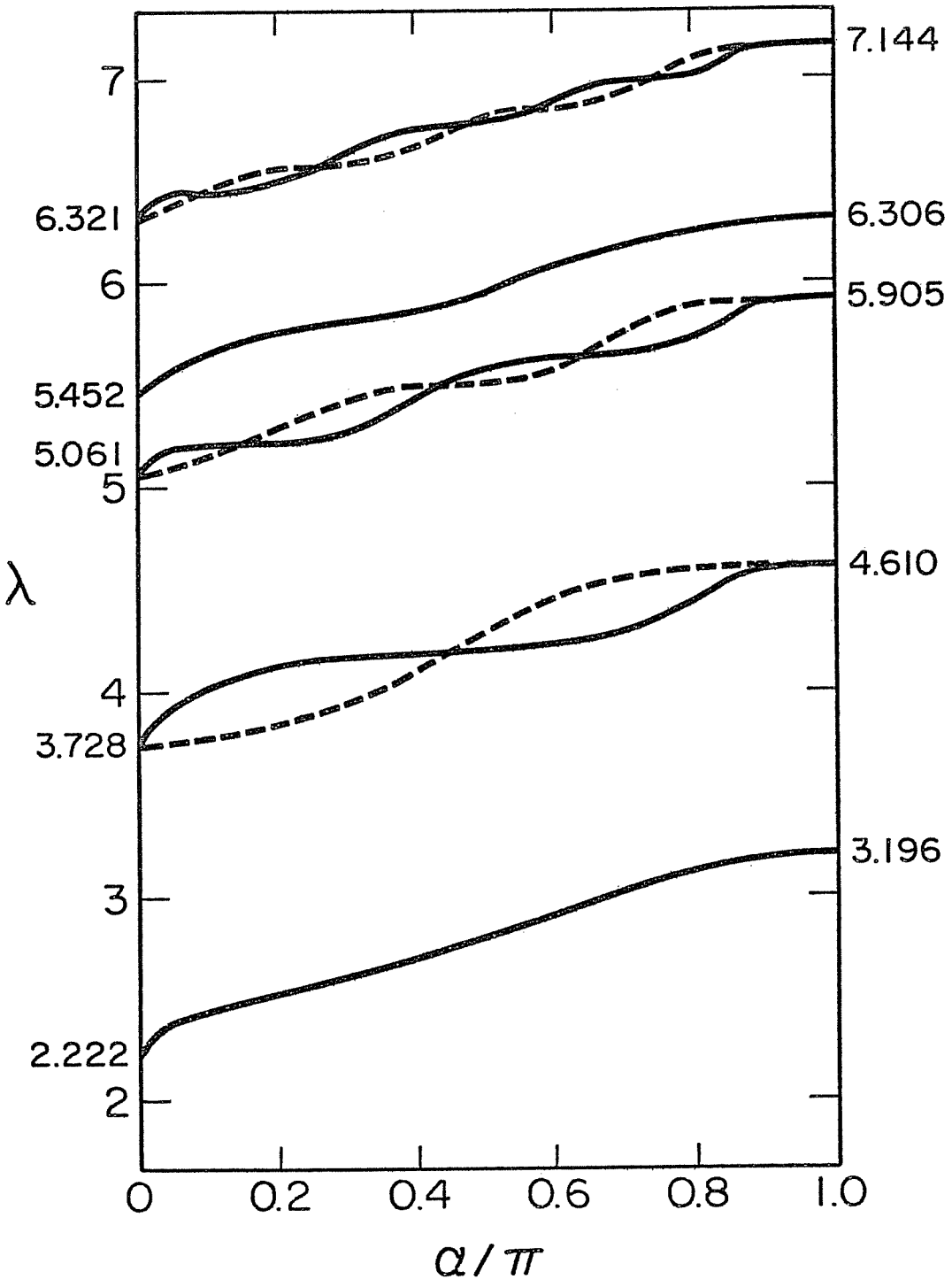

Fig.3-14 ariations of the frequency parameters for a simply supported plate clamped along one segment ($aKw/D = 10^4$, $\nu = 0.30$).

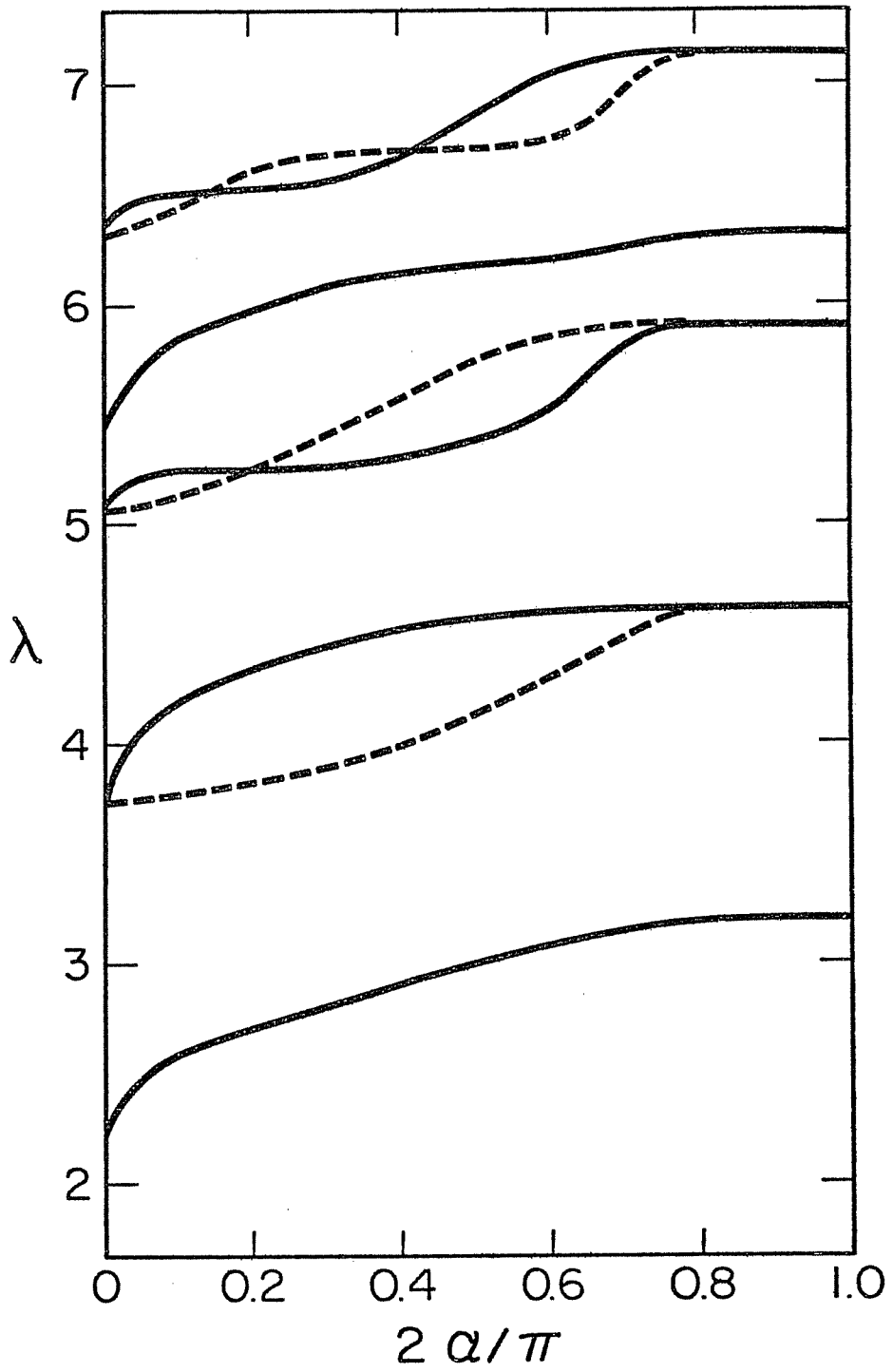

Fig.3-15 Variations of the frequency parameters for a simply supported plate clamped along <u>two</u> segments ($aK\Psi/D = 10^4$, $\nu = 0.30$).

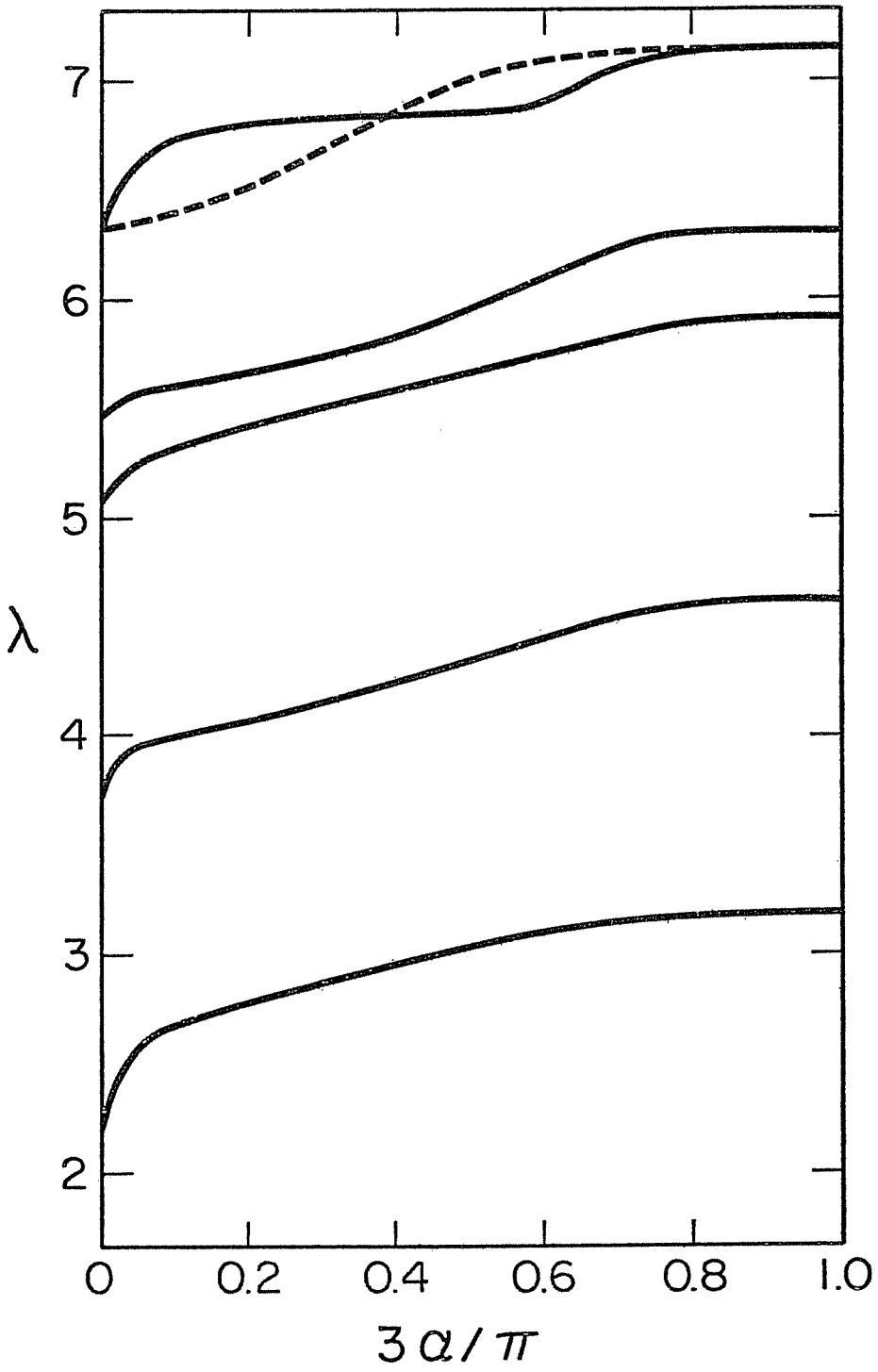

Fig.3-16 Variations of the frequency parameters for a simply supported plate clamped along <u>three</u> segments ($aK_\Psi/D = 10^4$, $\nu = 0.30$).

Table 3-15 One Rotational Spring (Matrix Size 10x10)

Mode Sequence	Type of Mode	α/π 0	0.1	0.2	0.3	0.4	0.5	0.6	0.7	0.8	0.9	1.0
1	S	2.222	2.44	2.52	2.61	2.70	2.80	2.91	3.02	3.12	3.19	3.196
2	S	3.728	4.01	4.11	4.17	4.18	4.19	4.21	4.28	4.43	4.61	4.610
	A	3.728	3.76	3.83	3.95	4.10	4.28	4.45	4.56	4.60	4.61	4.610
3	S	5.061	5.21	5.21	5.28	5.42	5.58	5.63	5.64	5.71	5.90	5.905
	A	5.061	5.15	5.29	5.43	5.50	5.51	5.57	5.74	5.88	5.90	5.905
4	S	5.452	5.64	5.75	5.81	5.85	5.94	6.09	6.17	6.22	6.30	6.306
5	S	6.321	6.45	6.50	6.65	6.76	6.77	6.88	6.98	7.00	7.14	7.144
	A	6.321	6.46	6.56	6.57	6.66	6.82	6.85	6.91	7.09	7.14	7.144

Table 3-16 Two Rotational Springs (Matrix Size 10x10)

Mode Sequence	Type of Mode	$2\alpha/\pi$ 0	0.1	0.2	0.3	0.4	0.5	0.6	0.7	0.8	0.9	1.0
1	S	2.222	2.61	2.69	2.81	2.89	3.00	3.06	3.16	3.19	3.19	3.196
2	S	3.728	4.21	4.32	4.44	4.52	4.57	4.60	4.61	4.61	4.61	4.610
	A	3.728	3.75	3.81	3.89	3.97	4.14	4.26	4.47	4.60	4.61	4.610
3	S	5.061	5.25	5.26	5.26	5.29	5.38	5.49	5.81	5.90	5.90	5.905
	A	5.061	5.12	2.25	5.42	5.56	5.75	5.83	5.90	5.90	5.90	5.905
4	S	5.452	5.86	5.96	6.09	6.14	6.18	6.20	6.26	6.30	6.31	6.306
5	S	6.321	6.50	6.51	6.54	6.68	6.83	7.05	7.14	7.14	7.14	7.144
	A	6.321	6.43	6.60	6.68	6.70	6.70	6.74	6.97	7.13	7.14	7.144

Table 3-17 Three Rotational Springs (Matrix Size 15x15)

Mode Sequence	Type of Mode	$3\alpha/\pi$ 0	0.1	0.2	0.3	0.4	0.5	0.6	0.7	0.8	0.9	1.0
1	S	2.222	2.69	2.76	2.87	2.95	3.04	3.08	3.16	3.18	3.18	3.196
2	S	3.728	4.00	4.07	4.16	4.26	4.36	4.46	4.55	4.60	4.60	4.610
	A	3.728	4.00	4.06	4.16	4.25	4.36	4.45	4.55	4.60	4.60	4.610
3	S	5.061	5.33	5.41	5.51	5.59	5.67	5.74	5.83	5.90	5.90	5.905
	A	5.061	5.32	5.41	5.51	5.58	5.66	5.74	5.82	5.90	5.90	5.905
4	S	5.452	5.62	5.66	5.74	5.81	5.96	6.06	6.25	6.30	6.30	6.306
5	S	6.321	5.76	6.82	6.85	6.86	6.86	6.90	7.05	7.13	7.14	7.144
	A	6.321	6.38	6.52	6.70	6.83	7.01	7.08	7.13	7.14	7.14	7.144

3-4 Free plate partially constrained by translational and rotational springs

3-4-1 Review

Several references were found on vibration of circular plates supported either inside the plate or along the edge. Bodine presented the fundamental [93] and higher frequencies [94] of a circular plate supported on a concentric circle, and Singh and Mizra [95] treated axisymmetric vibration of a plate supported on two concentric circles. Nagaya et al. [96] obtained a solution for a plate with an eccentric circular elastic support. The boundary conditions at the edge were satisfied by means of the Fourier expansion method. For circular plates supported on some arcs, Irie and Yamada [102] analyzed vibration of a plate whose lateral deflection and rotation are elastically constrained on some circular arcs inside the plate. Okazaki et al. [103] dealt with the problem by the weighted residual method.

Free circular plates supported on some discrete points are also important structural elements and are found, for instance, in point-supported large optical mirrors [97]. Nakazawa [98] dealt with a free plate whose lateral deflection is elastically supported at some points on the boundary. Chi [99] employed a similar procedure to obtain natural freqencies and nodal patterns of a plate supported on three equally spaced points on the boundary. Irie and Yamada [100] analyzed more general case of a plate whose deflection, rotation and torsion are elastically constrained by some points.

Ichinomiya and Maruyama [101] compared experimental results by the holographic interferometry with the values in [100], and good agreement was reported.

Difficulty in obtaining analytical solutions arises when non-uniform edge support is taken into consideration. In addition to the difficulty in the mathematical formulation, another difficulty may take place in the numerical calculation to obtain good convergence of the solution. Generally, analytical solutions for mixed boundary conditions cause bad convergence, particaularly for the case involving free edges. In contrast, it is relatively easy to have convergent values for mixed boundary conditions of simple support and clamp. Hemmig [90] presented some results for a free plate partially clamped along a portion of the edge, by the F.E.M. program (NASTRAN) and an experiment using the holography technique. Hirano and Okazaki [89] employed the same method as used in [103]. A method developed by Irie and Yamada [102] is also applicable to problems having nonuniform edge conditions only by taking circular arc supports along the edge. However, these methods introduced here are too complicated to practical engineers, and it is necessary to develop a simple and straightfoward method.

In this section, a method shown in the previous section is extended under more general boundary conditions, namely a free circular plate elastically constrained by partial translational and rotational springs.

3-4-2 Analysis *

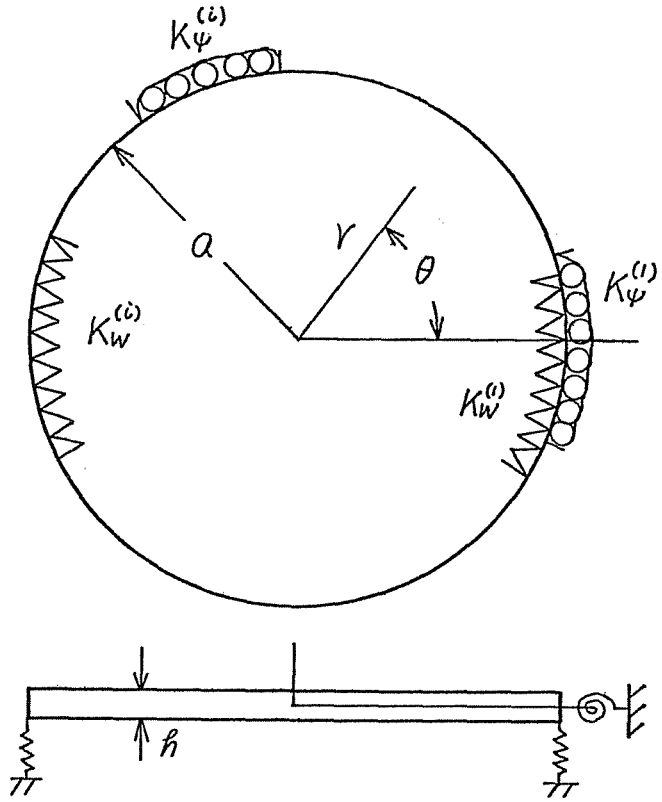

Fig.3-17

Consider a free circular plate elastically constrained along parts of the edge as shown in Fig. 3-17. Some translational and rotational springs having stiffnesses $K_w^{(i)}$ and $K_\psi^{(i)}$, respectively, are attached to portions of the edge. The differential equation (3-1) and the solution (3-22) are used, and the following boundary conditions are required along constrained parts of the edge.

$$V_r(a,\theta) = -K_w^{(i)} W(a,\theta) \qquad (3\text{-}40a)$$

$$M_r(a,\theta) = K_\psi^{(i)} \frac{\partial W}{\partial r}(a,\theta) \qquad (3\text{-}40b)$$

where the edge reaction and bending moment are given by Eqs. (3-8) and (3-13), respectively. Because the stiffnesses K_w, K_ψ of the entire spring system is assumed to vary along the edge, it is reasonable to expand them into Fourier series.

*[104]

$$K_w(\theta)=\sum_{m=0}^{\infty}K_m\cos m\theta+\sum_{m=1}^{\infty}K_m^{*}\sin m\theta$$
$$K_\psi(\theta)=\sum_{m=0}^{\infty}L_m\cos m\theta+\sum_{m=1}^{\infty}L_m^{*}\sin m\theta \qquad (3\text{-}41)$$

where K_m, K_m^{*}, L_m and L_m^{*} are the Fourier coefficients determined in the usual manner. Substitution of Eqs.(3-8,13,22,41) into (3-40) yields

$$\sum_{n=0}^{\infty}\left\{\lambda^3 W_n'''+\lambda^2 W_n''-\lambda\left[1+n^2(2-\nu)\right]W_n'+n^2(3-\nu)W_n\right\}\cos n\theta$$
$$+\sum_{n=1}^{\infty}\left\{\lambda^3 W_n^{*'''}+\lambda^2 W_n^{*''}-\lambda\left[1+n^2(2-\nu)\right]W_n^{*'}+n^2(3-\nu)W_n^{*}\right\}\sin n\theta$$
$$=f_1(\theta)+f_2(\theta)+f_3(\theta)+f_4(\theta) \qquad (3\text{-}42)$$

$$\sum_{n=0}^{\infty}\left\{\lambda^2 W_n''+\nu\lambda W_n'-\nu n^2 W_n\right\}\cos n\theta+\sum_{n=1}^{\infty}\left\{\lambda^2 W_n^{*''}+\nu\lambda W_n^{*'}-\nu n^2 W_n^{*}\right\}\sin n\theta$$
$$=-\lambda\left\{g_1(\theta)+g_2(\theta)+g_3(\theta)+g_4(\theta)\right\} \qquad (3\text{-}43)$$

where

$$f_1(\theta)=\sum_{m=0}^{\infty}\overline{K}_m\cos m\theta\sum_{n=0}^{\infty}W_n\cos n\theta,\quad f_2(\theta)=\sum_{m=0}^{\infty}\overline{K}_m\cos m\theta\sum_{n=1}^{\infty}W_n^{*}\sin n\theta$$
$$f_3(\theta)=\sum_{m=1}^{\infty}\overline{K}_m^{*}\sin m\theta\sum_{n=0}^{\infty}W_n\cos n\theta,\quad f_4(\theta)=\sum_{m=1}^{\infty}\overline{K}_m^{*}\sin m\theta\sum_{n=1}^{\infty}W_n^{*}\sin n\theta \qquad (3\text{-}44)$$
$$g_1(\theta)=\sum_{m=0}^{\infty}\overline{L}_m\cos m\theta\sum_{n=1}^{\infty}W_n'\cos n\theta,\quad g_2(\theta)=\sum_{m=0}^{\infty}\overline{L}_m\cos m\theta\sum_{n=1}^{\infty}W_n^{*'}\sin n\theta$$
$$g_3(\theta)=\sum_{m=1}^{\infty}\overline{L}_m^{*}\sin m\theta\sum_{n=1}^{\infty}W_n'\cos n\theta,\quad g_4(\theta)=\sum_{m=1}^{\infty}\overline{L}_m^{*}\sin m\theta\sum_{n=1}^{\infty}W_n^{*'}\sin n\theta$$

with $\overline{K}_m = a^3 K_m / D$, $\overline{K}_m^* = a^3 K_m^* / D$, $\overline{L}_m = a L_m / D$, $\overline{L}_m^* = a L_m^* / D$

and the primes denote derivatives with respect to kr.

Suppose that the spring system has an axis of symmetry at $\theta = 0$. In this case, vibration modes reflect this symmetry and are separated into symmetric and antisymmetric modes with respect to the axis. Thus, one obtains

$$\sum_{n=0}^{\infty} \left\{ \lambda^3 W_n''' + \lambda^2 W_n'' - \lambda \left[1 + n^2 (2-\nu) \right] W_n' + n^2 (3-\nu) W_n \right\} \begin{pmatrix} \cos n\theta \\ \sin n\theta \end{pmatrix} = \begin{pmatrix} f_1(\theta) \\ f_2(\theta) \end{pmatrix} \tag{3-45}$$

$$\sum_{n=0}^{\infty} \left\{ \lambda^2 W_n'' + \nu \lambda W_n' - \nu n^2 W_n \right\} \begin{pmatrix} \cos n\theta \\ \sin n\theta \end{pmatrix} = -\lambda \begin{pmatrix} g_1(\theta) \\ g_2(\theta) \end{pmatrix}$$

and $f_3(\theta) = f_4(\theta) = g_3(\theta) = g_4(\theta) = 0$.

The functions $f_1(\theta), f_2(\theta), \ldots$ can be rewritten as

$$f_1(\theta) = \begin{cases} \overline{K}_0 W_0 + \frac{1}{2} \sum_{i=1}^{\infty} \overline{K}_i W_i \\ \sum_{n=0}^{\infty} \left[\overline{K}_0 W_n + \frac{1}{2} \left\{ \overline{K}_n W_0 + \sum_{i=1}^{\infty} \overline{K}_i \left(W_{n+i} + W_{|n-i|} \right) \right\} \right] \cos n\theta \end{cases} \tag{3-46}$$

$$f_2(\theta) = \sum_{n=1}^{\infty} \left[\overline{K}_0 W_n + \frac{1}{2} \left\{ \overline{K}_n W_0 + \sum_{i=1}^{\infty} \overline{K}_i \left(W_{n+i} \pm W_{|n-i|} \right) \right\} \right] \sin n\theta \qquad \begin{pmatrix} + : n > i \\ - : n \le i \end{pmatrix}$$

$$g_1(\theta) = \begin{cases} \overline{L}_0 W_0' + \frac{1}{2} \sum_{i=1}^{\infty} \overline{L}_i W_i' \\ \sum_{n=1}^{\infty} \left[\overline{L}_0 W_n' + \frac{1}{2} \left\{ \overline{L}_n W_0' + \sum_{i=1}^{\infty} \overline{L}_i \left(W_{n+i}' + W_{|n-i|}' \right) \right\} \right] \cos n\theta \end{cases} \tag{3-47}$$

$$g_2(\theta) = \sum_{n=1}^{\infty} \left[\overline{L}_0 W_n' + \frac{1}{2} \left\{ \overline{L}_n W_0' + \sum_{i=1}^{\infty} \overline{L}_i \left(W_{n+i}' \pm W_{|n-i|}' \right) \right\} \right] \sin n\theta \qquad \begin{pmatrix} + : n > i \\ - : n \le i \end{pmatrix}$$

by use of the trigonometric identities such as Eqs.(3-28). Derivatives of Bessel functions with respect to kr are evaluated by formulas (3-6,11).

Equating the coefficients of $\cos n\theta$ or $\sin n\theta$ in Eqs.(3-45) and substituting Eq.(3-23) yield the following frequency equations in matrix form.

(1) Symmetric vibration mode

$$\begin{bmatrix} \mathcal{E}_{00} & \mathcal{E}_{01} & \mathcal{E}_{02} & \cdots\cdots \\ \mathcal{E}_{10} & \mathcal{E}_{11} & \mathcal{E}_{12} & \\ \mathcal{E}_{20} & \mathcal{E}_{21} & \mathcal{E}_{22} & \ddots \\ \vdots & & & \end{bmatrix} \begin{bmatrix} C_0 \\ C_1 \\ C_2 \\ \vdots \end{bmatrix} = 0 \qquad (3\text{-}48)$$

where

$$\mathcal{E}_{00} = 2\begin{bmatrix} -P(0) & -\bar{P}(0) \\ \frac{1}{\lambda}Q(0) & \frac{1}{\lambda}\bar{Q}(0) \end{bmatrix}, \quad \mathcal{E}_{0j} = \begin{bmatrix} \bar{K}_j J_j & \bar{K}_j I_j \\ \bar{L}_j J_j' & \bar{L}_j I_j' \end{bmatrix} \quad (j=1,2,\cdots) \qquad (3\text{-}49)$$

$$\mathcal{E}_{jj} = \begin{bmatrix} -2P(j)+\bar{K}_{2j}J_j & -2\bar{P}(j)+\bar{K}_{2j}I_j \\ \frac{2}{\lambda}Q(j)+\bar{L}_{2j}J_j' & \frac{2}{\lambda}\bar{Q}(j)+\bar{L}_{2j}I_j' \end{bmatrix} \quad (j=1,2,\cdots) \qquad (3\text{-}50)$$

$$\underset{(i\neq j)}{\mathcal{E}_{ij}} = \begin{bmatrix} (\bar{K}_{|i-j|}+\bar{K}_{i+j})J_j & (\bar{K}_{|i-j|}+\bar{K}_{i+j})I_j \\ (\bar{L}_{|i-j|}+\bar{L}_{i+j})J_j' & (\bar{L}_{|i-j|}+\bar{L}_{i+j})I_j' \end{bmatrix} \quad (i=1,2,\cdots;\ j=0,1,2\cdots) \qquad (3\text{-}51)$$

$$\mathbb{C}_i = \begin{bmatrix} A_i \\ C_i \end{bmatrix} \qquad (i = 0, 1, 2, \cdots) \tag{3-52}$$

and

$$\begin{aligned}
p(n) &= \left\{ n^2(1-n)(1-\nu) - n\lambda^2 - \bar{K}_0 \right\} J_n + \lambda \left\{ n^2(1-\nu) + \lambda^2 \right\} J_{n+1} \\
\bar{p}(n) &= \left\{ n^2(1-n)(1-\nu) + n\lambda^2 - \bar{K}_0 \right\} I_n - \lambda \left\{ n^2(1-\nu) - \lambda^2 \right\} I_{n+1} \\
q(n) &= \left\{ n(n-1)(1-\nu) - \lambda^2 + n\bar{L}_0 \right\} J_n + \lambda(1-\nu-\bar{L}_0) J_{n+1} \\
\bar{q}(n) &= \left\{ n(n-1)(1-\nu) + \lambda^2 + n\bar{L}_0 \right\} I_n - \lambda(1-\nu-\bar{L}_0) I_{n+1}
\end{aligned} \tag{3-53}$$

(2) Antisymmetric vibration mode

$$\begin{bmatrix} \mathbb{e}_{11} & \mathbb{e}_{12} & \mathbb{e}_{13} & \cdots\cdots \\ \mathbb{e}_{21} & \mathbb{e}_{22} & \mathbb{e}_{23} & \\ \mathbb{e}_{31} & \mathbb{e}_{32} & \mathbb{e}_{33} & \\ \vdots & & & \ddots \end{bmatrix} \begin{bmatrix} \mathbb{C}_1 \\ \mathbb{C}_2 \\ \mathbb{C}_3 \\ \vdots \end{bmatrix} = 0 \tag{3-54}$$

where

$$\mathbb{e}_{jj} = \begin{bmatrix} -2p(j) - \bar{K}_{2j} J_j & -2\bar{p}(j) - \bar{K}_{2j} I_j \\ \frac{2}{\lambda} q(j) - \bar{L}_{2j} J_j' & \frac{2}{\lambda} \bar{q}(j) - \bar{L}_{2j} I_j' \end{bmatrix} \quad (j = 1, 2, \cdots) \tag{3-55}$$

$$\underset{(i\neq j)}{C_{ij}} = \begin{bmatrix} (\bar{K}_{1i-j1} - \bar{K}_{i+j})\, J_j & (\bar{K}_{1i-j1} - \bar{K}_{i+j})\, I_j \\ (\bar{L}_{1i-j1} - \bar{L}_{i+j})\, J_j' & (\bar{L}_{1i-j1} - \bar{L}_{i+j})\, I_j' \end{bmatrix} \quad (i,j = 1,2,\cdots) \tag{3-56}$$

The natural frequencies of the plate are obtained by calculating the eigenvalues of the coefficient matrices of Eqs.(3-48,54) and the corresponding mode shapes are determined by Eq.(3-22) after solving Eqs.(3-48,54) in terms of amplitude ratio C_i/A_0 or C_i/A_1.

3-4-3 Results and discussion

Consider a free circular plate elastically constrained by uniform translational and rotational springs along some parts of the edge. The stiffness of each spring may vary independently from the others. As shown in Sec.3-3, when a plate is constrained along two opposite circular parts $(-\alpha<\theta<\alpha\ ,\ \pi-\alpha<\theta<\pi-\alpha)$ of the edge, the spring system along the entire edge is expanded into a Fourier cosine series with coefficients

$$K_m = \frac{1}{\pi}\int_0^{2\pi}\left(\frac{a^3 K_w}{D}\right)\cos m\theta\, d\theta$$

$$= \frac{2}{m\pi}\left(\bar{K}_w^{(1)} + \bar{K}_w^{(2)}\cos m\pi\right)\sin m\alpha \quad (m = 1, 2, \cdots) \tag{3-57}$$

for the translational spring, and

$$L_m = \frac{2}{m\pi}\left(\bar{K}_\psi^{(1)} + \bar{K}_\psi^{(2)}\cos m\pi\right)\sin m\alpha \quad (m = 1, 2, \cdots) \tag{3-58}$$

for the rotational spring in the same fashion, with

$\bar{K}_w^{(1)} = a^3 K_w^{(1)}/D$, $\bar{K}_w^{(2)} = a^3 K_w^{(2)}/D$, $\bar{K}_\psi^{(1)} = a K_\psi^{(1)}/D$ and $\bar{K}_\psi^{(2)} = a K_\psi^{(2)}/D$.

Figure 3-18 shows the lowest six frequency parameters and nodal patterns of circular plates elastically constrained by translational and rotational springs along a quarter part of the edge. The solid lines shown inside the circular boundary denote nodal lines; i.e.,lines of zero deflection. The fundamental modes have no internal nodal lines. In this figure, moving from left to right, the stiffness of a translational spring is gradually increased, starting from a completely free plate and going to a plate simply supported along a quarter of its boundary. Then, sufficient rotational rigidity is added to make the boundary segment effectively clamped. The generation of two sets of modes, symmetric and antisymmetric, from the degenerate modes of a completely free circular plate having one and two nodal diameters, is clearly seen.

A more comprehensive study of the variations of the frequency parameters with increasing spring stiffness is shown in Fig.3-19. Solid lines denote symmetric modes and broken lines antisymmetric modes. It is observed from the figures that considerable increases of frequency parameters take place between nondimensional rigidity 10^0 and 10^3 in both types of springs. The values used in plotting these figures are presented in Table 3-18 and 19.

Table 3-20 shows the convergence study of frequency parameters for the lowest six modes of a plate constrained along a quarter part of the edge ($\bar{K}_w^{(i)} = \bar{K}_\psi^{(i)} = 10^6$) presented

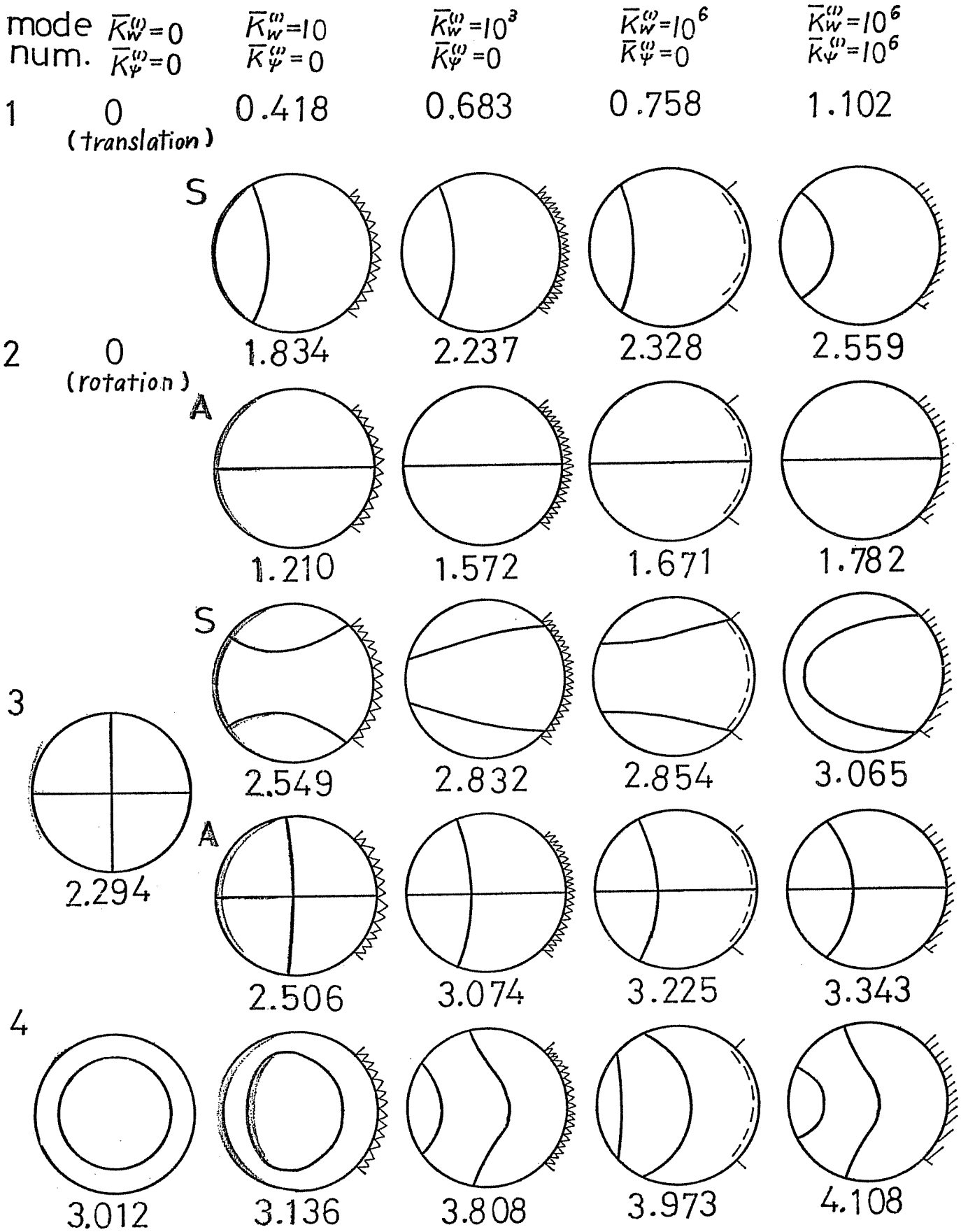

Fig.3-18 Frequency parameters and nodal patterns of circular plates elastically constrained by translational and rotational springs along a quarter of the edge ($\nu=0.33$).

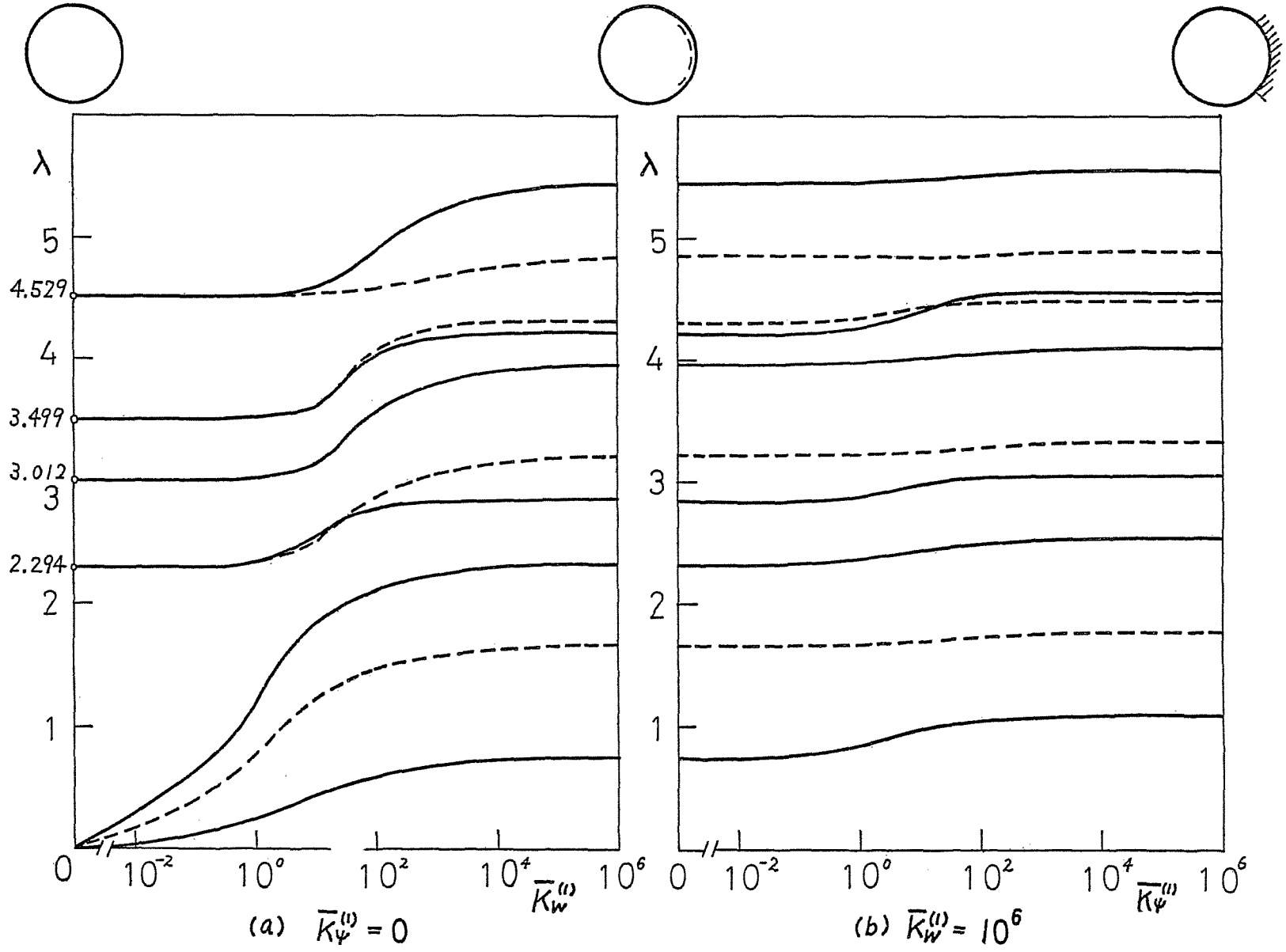

Fig.3-19 Variation of frequency parameters of circular plates elastically constrained by translational and rotational springs along a quarter part of the edge ($\alpha/\pi = 0.25, \nu = 0.33$).

Table 3-18 Frequency parameters λ of a free circular plate elastically constrained along a portion of the edge ($\bar{K}_\psi^{(i)} = 0$, $\alpha/\pi = 0.25$, $\nu = 0.33$).

mode \ $\bar{K}_w^{(i)}$		0	10^1	10^2	10^3	10^4	10^6
1		0	0.42	0.60	0.68	0.72	0.76
2	S	0	1.83	2.12	2.24	2.29	2.33
	A	0	1.21	1.47	1.57	1.62	1.67
3	S	2.294	2.55	2.80	2.83	2.84	2.85
	A	2.294	2.51	2.89	3.07	3.15	3.23
4		3.012	3.14	3.59	3.81	3.90	3.97
5	S	3.499	3.58	4.03	4.19	4.21	4.22
	A	3.499	3.61	4.06	4.27	4.31	4.32
6	S	4.529	4.58	4.90	5.22	5.35	5.46
	A	4.529	4.54	4.58	4.68	4.76	4.85

Table 3-19 ($\bar{K}_w^{(i)} = 10^6$, $\alpha/\pi = 0.25$, $\nu = 0.33$)

mode \ $\bar{K}_\psi^{(i)}$		10^{-1}	10^0	10^1	10^2	10^4	10^6
1		0.77	0.85	0.99	1.05	1.08	1.10
2	S	2.33	2.36	2.45	2.50	2.54	2.56
	A	1.67	1.67	1.70	1.73	1.76	1.78
3	S	2.85	2.88	2.99	3.05	3.06	3.07
	A	3.22	3.23	3.25	3.29	3.33	3.34
4		3.97	3.98	4.02	4.06	4.10	4.11
5	S	4.23	4.27	4.40	4.54	4.56	4.57
	A	4.31	4.33	4.43	4.46	4.48	4.49
6	S	5.46	5.46	5.48	5.51	5.56	5.56
	A	4.85	4.85	4.85	4.86	4.89	4.89

Table 3-20 Convergence study of frequency parameters for a partially constrained circular plate ($\bar{K}_w^{(\omega)} = \bar{K}_\varphi^{(\omega)} = 10$, $\alpha/\pi = 0.25$, $\nu = 0.33$)

matrix size \ mode	1	2-A	2-S	3-S	3-A	4
20x20	1.18	1.87	2.67	3.10	3.47	4.28
30x30	1.14	1.82	2.61	3.08	3.39	4.18
40x40	1.12	1.80	2.59	3.07	3.37	4.14
50x50	1.11	1.79	2.57	3.07	3.35	4.12
60x60	1.10	1.78	2.56	—	3.34	4.11
70x70	1.10	1.78	2.55		3.34	4.10
80x80	—	—	2.55		—	4.09
90x90			—			4.09

also in Fig.3-18. The frequency parameters apparently converge within the range of three significant figures, as the matrix size (twice as the employed terms of Fourier series) is increased. It is noted that the rate of convergence is different depending upon the mode of vibration. Since the numerical calculation in Fig.3-18 through 21 was carried out by use of 60 x 60 matrix, good accuracy is expected for all the results presented. Poisson's ratio is taken as 0.33.

Figure 3-20 shows variations of frequency parameters with the change of angle α for a plate constrained along one part of the edge. Since the stiffness are taken as $\bar{K}_w^{(\omega)} = 10^6$ and $\bar{K}_\varphi^{(\omega)} = 0$, the constrained part of the plate can

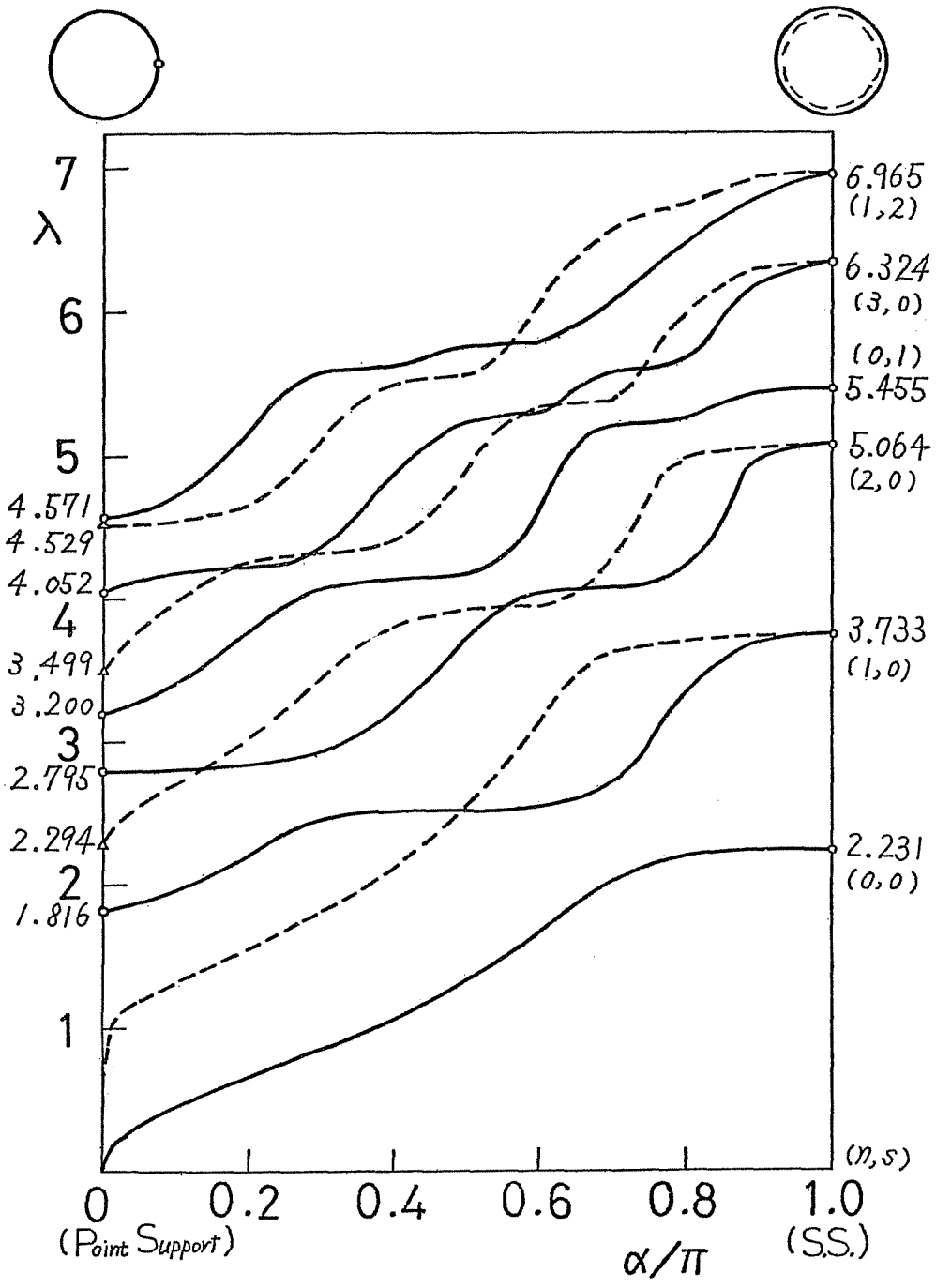

Fig.3-20 Variation of frequency parameters of circular plates constrained along a part of the the edge ($\overline{K}_w^w=10^6$, $\overline{K}_\psi^w=0$ [simply supported], $\nu=0.33$), △ :Irie and Yamada [100].

Table 3-21 Frequency parameters λ of a circular plate simply supported along one segment

mode \ α/π		0	0.01	0.05	0.1	0.2	0.3	0.4	0.5	0.6	0.7	0.8	0.9	1.0
1		0		0.33	0.45	0.66	0.85	1.07	1.32	1.66	2.02	2.20	2.23	2.231
2	S	1.816	1.816	1.88	1.98	2.21	2.42	2.51	2.51	2.53	2.68	3.33	3.71	3.733
	A	0		1.18	1.31	1.54	1.80	2.12	2.54	3.11	3.65	3.72	3.73	3.733
3	S	2.795	2.796	2.81	2.82	2.83	2.91	3.21	3.72	4.05	4.06	4.19	5.01	5.064
	A	2.294		2.57	2.71	3.03	3.42	3.80	3.93	3.94	4.27	5.00	5.06	5.064
4		3.200	3.202	3.29	3.41	3.77	4.10	4.14	4.16	4.62	5.21	5.24	5.43	5.455
5	S	4.052	4.057	4.15	4.19	4.20	4.32	4.88	5.25	5.28	5.58	5.63	6.18	6.324
	A	3.499		3.79	3.96	4.27	4.34	4.39	4.88	5.33	5.35	5.97	6.32	6.324
6	S	4.571	4.573	4.61	4.74	5.19	5.60	5.62	5.76	5.77	6.06	6.47	6.78	6.965
	A	4.529		4.53	4.53	4.65	5.11	5.51	5.55	6.08	6.59	6.73	6.96	6.965

be considered as almost simply supported. Irie and Yamada [100] have obtained the frequencies of a free circular plate supported at a point, and the present values for symmetric modes are in good agreement with their values in the vicinity of $\alpha = 0$. The differences of these values of λ are less than 0.1 percent, when $\alpha = 0.01$ is taken. For antisymmetric modes, the frequency parameters approach those for a free plate because the effect of a zero deflection constraint is diminished for small α on a nodal line. On the other hand, the plate becomes a uniformly simply supported plate as approaches π. The limiting values of λ for $\alpha = 0$ and π are presented in the figure. The number of nodal diameters (n) and interior nodal circles (s) for these limiting cases are also given. The values used in plotting the figures are presented in Table 3-21.

In Fig.3-21, stiffnesses are taken as $\bar{K}_w^{(0)} = \bar{K}_\psi^{(0)} = 10^6$ and the constrained part is therefore almost clamped. The frequency parameters vary between those of a point clamped ($\alpha = 0$) and completely clamped ($\alpha = \pi$) circular plate. In the vicinity of $\alpha = 0$, the frequency parameters for antisymmetric modes tend to approach those of a completely free plate. However, the values for symmetric modes are not very close to those of a point supported plate even when $\alpha = 0.005$ is taken. Comparing Fig.3-20 with 3-21, it is observed that variations of the corresponding modes in both figures show similar trends, although in Fig.3-21 frequencies of different modes approach each other and veer away, for example, near $\lambda = 4.6$ and 5.9. The values in the figure is presented in Table 3-22.

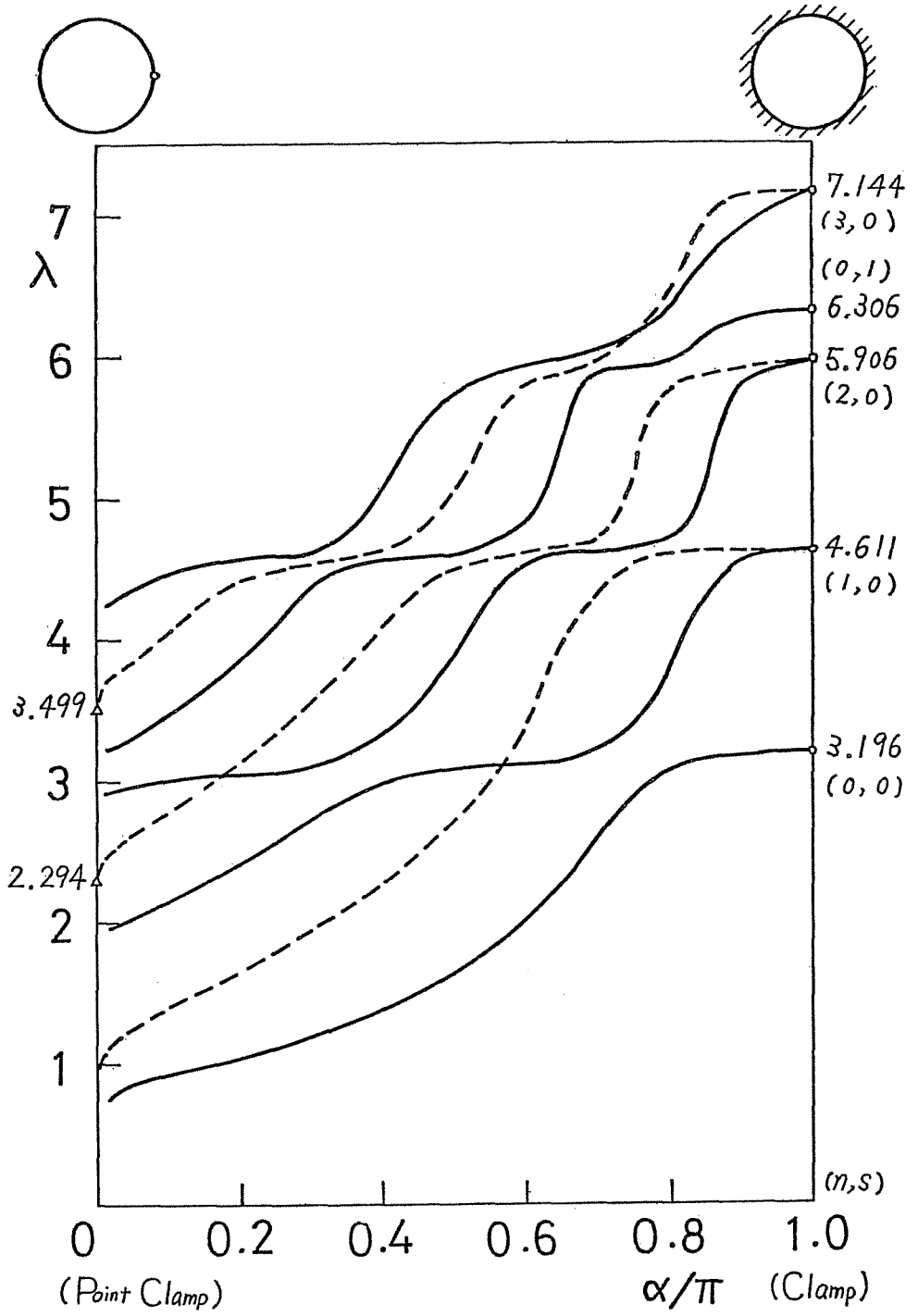

Fig.3-21 Variation of frequency parameters of circular plates constrained along a part of the edge ($\overline{K_w^\omega} = \overline{K_\psi^\omega} = 10^6$ [clamped], $\nu = 0.33$).

Table 3-22 Frequency parameters λ of a circular plate clamped along one segment

mode \ α/π		0	0.05	0.1	0.2	0.3	0.4	0.5	0.6	0.7	0.8	0.9	1.0
1		0.737	0.86	0.92	1.03	1.17	1.36	1.61	2.00	2.56	3.09	3.17	3.196
2	S	1.943	2.03	2.14	2.40	2.72	2.99	3.07	3.11	3.19	3.79	4.56	4.611
	A	1.026	1.24	1.41	1.64	1.92	2.26	2.71	3.35	4.30	4.60	4.61	4.611
3	S	2.904	2.96	2.99	3.04	3.09	3.31	3.87	4.52	4.58	4.68	5.81	5.906
	A	2.437	2.62	2.79	3.13	3.56	4.09	4.49	4.59	4.69	5.79	5.90	5.906
4		3.227	3.31	3.47	3.86	4.37	4.57	4.57	4.81	5.90	5.93	6.26	6.306
5	S		4.35	4.47	4.55	4.58	5.05	5.77	5.91	6.05	6.30	6.90	7.144
	A	3.630	3.84	4.05	4.42	4.53	4.62	5.03	5.82	5.94	6.44	7.14	7.144

3-5 Free plate with nonuniform edge mass

3-5-1 Review

It is shown in this section that how the method developed in Sec.3-4 can be utilized to analyze a free circular plate having varying mass distributed around its boundary, a type of problem which can be encountered in practical situation. This problem has received practically no treatment, but several references were found for the case when circular plates are reinforced by uniform rings. Kirk and Leissa [105] studied axisymmetric vibration of a circular plate reinforced by a concentric ring and presented the variation of the fundamental frequencies with some ring parameters. Takahashi treated a circular plate with its inner boundary built-in and a rigid ring around its outer boundary [106] and a plate having weights or a bar on the outer boundary [107]. The analysis was conducted by minimizing the Lagrangian of the plates. Stuart et al. [108] presented a short note discussing the effect of edge beam on the frequencies.

These references dealt with internal or edge ring having uniform mass and stiffness, and there are no literature concerned with circular plates having nonuniform edge mass. In the present study, it is assumed that mass distributed along the edge has no stiffness, but the more general problem of a plate having a nonuniform edge ring with both translational and rotational mass and stiffness can be treated by the same general method.

3-5-2 Analysis

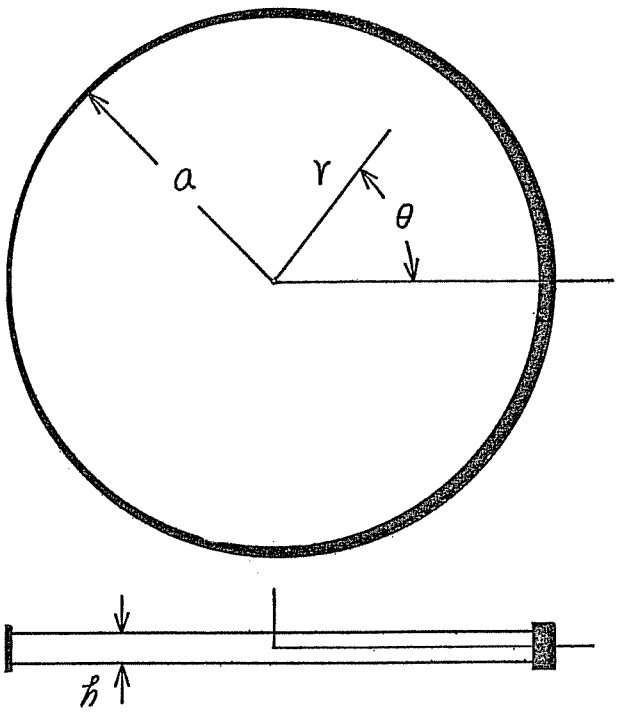

Fig.3-22

Consider a free circular plate of radius a having an additional strip of mass added along its boundary, as shown in Fig.3-22. The density of the added mass is m (mass per unit length) and, in general, $m = m(\theta)$; that is, the mass density is not uniform, but varies around the circumference. The boundary conditions for the problem are determined from the equations of motion for a infinitesimal length of the edge mass, namely:

$$V_r(a,\theta) = m\omega^2 W(a,\theta) \tag{3-59a}$$

$$M_r(a,\theta) = -I_G\omega^2 \frac{\partial W}{\partial r}(a,\theta) \tag{3-59b}$$

where V_r and M_r are the shearing force and bending moment given by Eq.(3-8) and (3-13), respectively. Equation (3-59b) was written in a form to account for the rotary inertia of the edge mass, with I_G being mass moment of inertia per unit of circumferential length. Inasmuch as it is difficult

to envision a physical body attached to the edge having significant rotary inertia, the right hand side of Eq. (3-59b) will be taken zero in subsequent work.

The distributed mass is now expressed in the form of a Fourier series,

$$m(\theta) = \sum_{i=0}^{\infty} m_i \cos i\theta + \sum_{i=1}^{\infty} m_i^* \sin i\theta \qquad (3\text{-}60)$$

where the m_i and m_i^* are determined in the usual manner. Substituting Eqs.(3-22,60) into (3-59) yields

$$\sum_{n=0}^{\infty}\Big[\lambda^3 W_n'''(\lambda)+\lambda^2 W_n''(\lambda)-\lambda\{1+n^2(2-\nu)\}W_n'(\lambda) + n^2(3-\nu)W_n(\lambda)\Big]\cos n\theta$$

$$+\sum_{n=1}^{\infty}\Big[\lambda^3 W_n^{*'''}(\lambda)+\lambda^2 W_n^{*''}(\lambda)-\lambda\{1+n^2(2-\nu)\}W_n^{*'}(\lambda) + n^2(3-\nu)W_n^{*}(\lambda)\Big]\sin n\theta$$

$$= -\{f_1(\theta)+f_2(\theta)+f_3(\theta)+f_4(\theta)\} \qquad (3\text{-}61a)$$

$$\sum_{n=0}^{\infty}\{\lambda^2 W_n''(\lambda)+\nu\lambda W_n'(\lambda)-\nu n^2 W_n(\lambda)\}\cos n\theta$$

$$+\sum_{n=1}^{\infty}\{\lambda^2 W_n^{*''}(\lambda)+\nu\lambda W_n^{*'}(\lambda)-\nu n^2 W_n^{*}(\lambda)\}\sin n\theta = 0 \qquad (3\text{-}61b)$$

where

$$
\begin{aligned}
f_1(\theta) &= \sum_{i=0}^{\infty} \overline{m}_i \cos i\theta \sum_{n=0}^{\infty} W_n(\lambda) \cos n\theta \\
f_2(\theta) &= \sum_{i=0}^{\infty} \overline{m}_i \cos i\theta \sum_{n=1}^{\infty} W_n^*(\lambda) \sin n\theta \\
f_3(\theta) &= \sum_{i=1}^{\infty} \overline{m}_i^* \sin i\theta \sum_{n=0}^{\infty} W_n(\lambda) \cos n\theta \\
f_4(\theta) &= \sum_{i=1}^{\infty} \overline{m}_i^* \sin n\theta \sum_{n=1}^{\infty} W_n^*(\lambda) \sin n\theta
\end{aligned}
\tag{3-62}
$$

the primes denote differentiation with respect to kr, and where m_i, m_i^* and λ are nondimensional parameters defined by

$$
(\overline{m}_i, \overline{m}_i^*) = (m_i, m_i^*)\frac{\omega^2 a^3}{D} = (m_i, m_i^*)\frac{\lambda^4}{\rho a}
\qquad (\lambda^4 = \omega^2 a^4 \rho / D)
\tag{3-63}
$$

Expanding the right-hand-side of Eq.(3-61a) by the use of trigonometric identities such as Eqs.(3-28) and equating coefficients of trigonometric functions having the same periodicity, Eqs.(3-61) yield an infinite set of homegeneous, algebraic equations in the undetermined constants $A_n, \ldots, C_n^*$.

For plates with edge mass distributed symmetrically about $\theta = 0$, the frequency equations thus derived take the same form as Eqs.(3-48,54) and can be determined by substituting $-\lambda^4\left(\frac{m_i}{a\rho}\right)$ into $\overline{K}_i$ and taking $\overline{L}_i$ to be zero. The eigenvalues of the determinant of the coefficient matrix give the nondimensional frequencies λ.

3-5-3 Results and discussion

To demonstrate the application of the method of analysis described in the previous section, consider a circular plate having its boundary a completely free of external constraints, but having a uniformly distributed mass attached along part of its boundary. Let the total added mass be M_A, with

$$M_A = m_c (2\beta a) \tag{3-64}$$

where m_c is the constant density (per unit length) of the added mass and 2β is the included angle of the boundary segment to which it is attached, as shown in Fig.3-23.

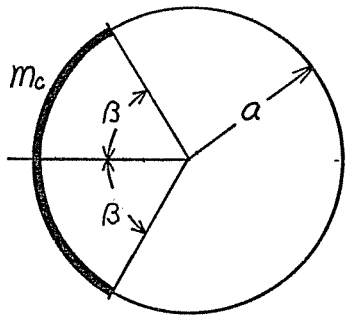

Fig.3-23

Choosing the coordinate system to take advantage of the symmetry of the problem, the free vibration modes divide into two classes, those symmetric and antisymmetric with respect to $\theta = 0$. Then, $m_i^* = \bar{m}_i^* = f_3(\theta) = f_4(\theta) = 0$ in Eq.(3-61a), and typical values of the nondimensional Fourier cosine mass coefficients are

$$\bar{m}_i = \lambda^4 \left(\frac{M_A}{M_P}\right) \frac{\sin i\beta}{i\beta} \tag{3-65}$$

where M_P is the mass of the plate by itself, $\pi a^2 \rho$.

Numerical results for frequency parameters and nodal patterns are shown in Fig.3-24 for various segments 2β of added mass. In this figure, it is assumed that the density of the added mass remains a constant as β is increased (i.e., $M_A/M_P = \beta/\pi$), with $M_A/M_P = 1$ when added mass occurs completely around the boundary; that is, the total mass added proportional to its circumferential strip length. Results are given also in Table 3-23.

With no added mass ($\beta/\pi = 0$) the frequencies and nodal patterns are those of the classical free plate. The fundamental frequency (other than the zero frequencies corresponding to rigid body translation and rotation) has a pattern of nodal lines consisting of two equally spaced diameters. The nodal pattern corresponding to the second frequency has one interior nodal circle, and the third one yields three equally spaced diameters.

As strip mass is added around the boundary (i.e., increasing β/π), as can be expected, the natural frequencies all decrease. However, the decreases are not at a steady rate, as seen in Fig.3-25. Furthermore, the frequency changes are accompanied by drastic changes in nodal patterns within the same symmetry class, as seen in Fig.3-24.

Of particular interest is the behavior of the modes which are degenerate at $\beta/\pi = 0$, giving $\lambda = 2.315$ and 3.527. The lower curves of Fig.3-25, begining at $\lambda = 2.315$ cross each other three times as β/π is increased, yielding a

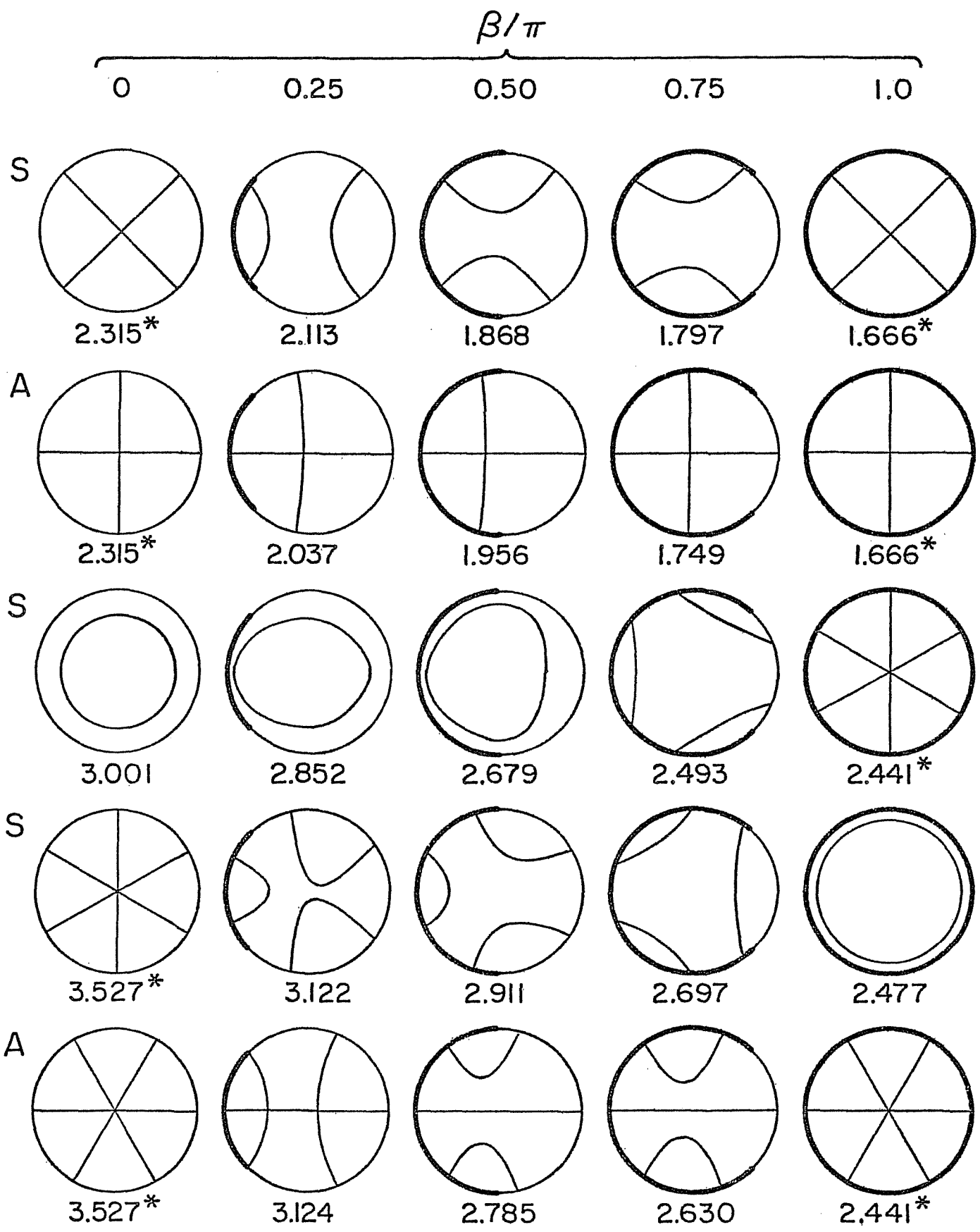

Fig.3-24 Frequency parameters and nodal patterns of a circular plate having a partial edge mass ($M_A/M_p = \theta/\pi$, ν =0.30, * degeneracy).

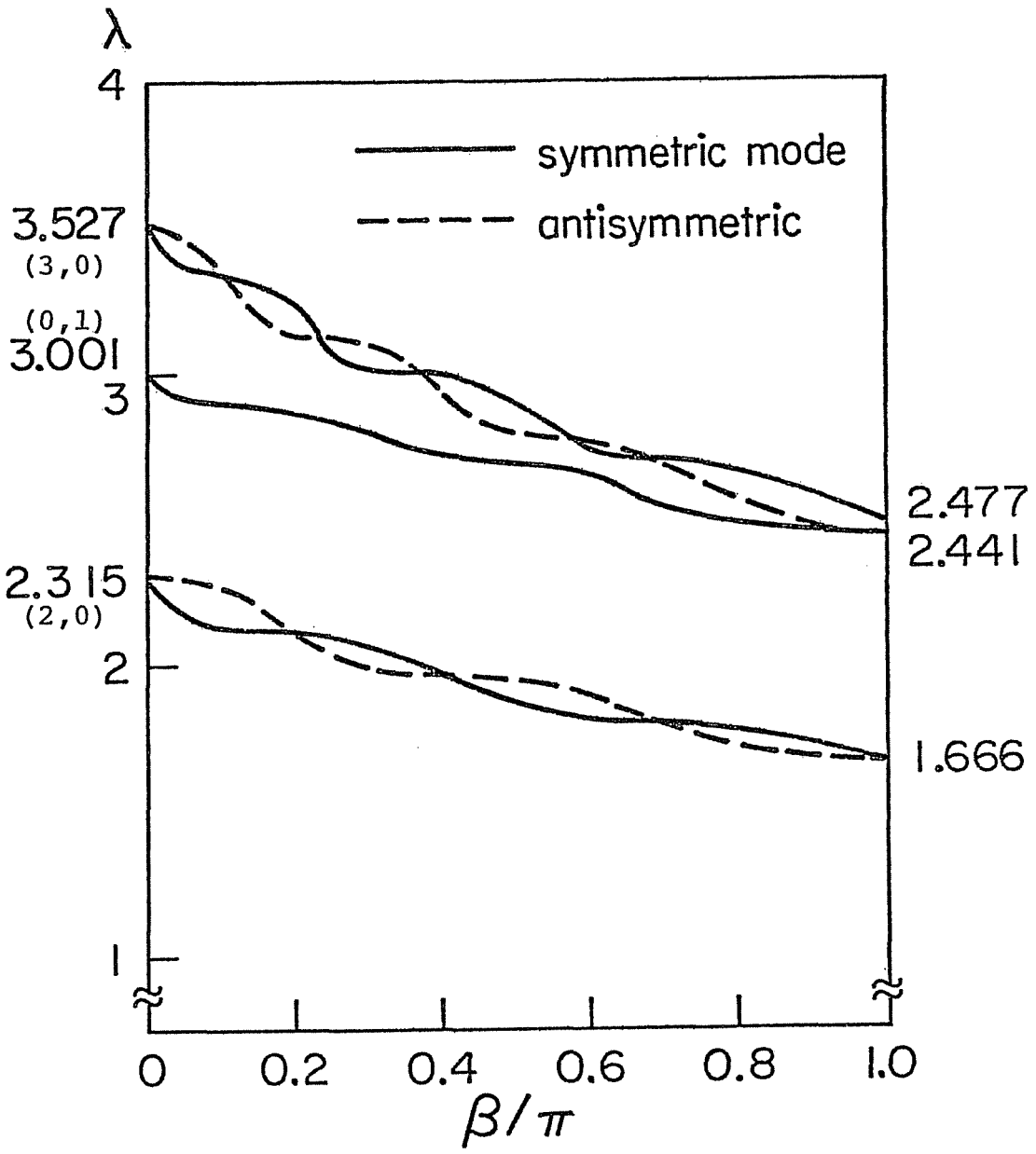

Fig.3-25 Variation of frequency parameters with the angle of a partial edge mass —— constant added mass density ($M_A/M_P=\beta/\pi$, $\nu=0.30$).

Table 3-23 Frequency parameters with the angle of a partial edge mass—constant added mass density ($M_A/M_p = \beta/\pi$, ν =0.30, 20 x 20 matrix)

mode \ β/π		0.0	0.1	0.2	0.3	0.4	0.5	0.6	0.7	0.8	0.9	1.0
3	S	2.315	2.11	2.10	2.07	1.96	1.87	1.80	1.79	1.76	1.70	1.666
	A	2.315	2.27	2.11	1.99	1.96	1.96	1.88	1.79	1.71	1.67	1.666
4		3.001	2.90	2.86	2.78	2.70	2.68	2.65	2.51	2.46	2.46	2.441
5	S	3.527	3.34	3.25	3.01	3.00	2.91	2.73	2.70	2.66	2.58	2.477
	A	3.527	3.37	3.13	3.11	2.94	2.79	2.76	2.69	2.56	2.46	2.441

fundamental mode shape which can be either symmetric or antisymmetric, but returning to the same degenerate (2,0) mode for $\beta/\pi = 1$. But the curves begining with the degenerate (3,0) mode, after crossing each other five times, do not coalesce at $\beta/\pi = 1$ but, rather, one of them joins with a completely different curve, degenerating into the roots λ=2.441.

Additional results are presented in Fig.3-26 for the change in λ as a function of β when the total added strip mass M_A remains constant, such that $M_A/M_p = 1$. Thus, as $\beta \to 0$ the limiting case becomes one of a point mass equal to that of the plate, and the frequencies for the symmetric modes are distinct (i.e., not degenerate) and lower than those of the corresponding antisymmetric modes. The curves for the symmetric modes are drawn to stop short of $\beta/\pi = 0$, for no numerical results could straightfowardly be obtained for this singular value. However, the antisymmetric modes and frequencies are unaffected by the presence of a point mass at the end of a diametral nodal line.

All numerical results presented here obtained from using 20th order determinants truncated from the infinite characteristic determinant. Convergence studies showed that results of sufficient accuracy were obtained from this order of truncation. A typical example of the rate of convergence of λ is shown in Table 3-25, which corresponds to three points in Fig.3-25. As could be expected, convergence for the higher frequencies requires higher order determinants than for the lower ones.

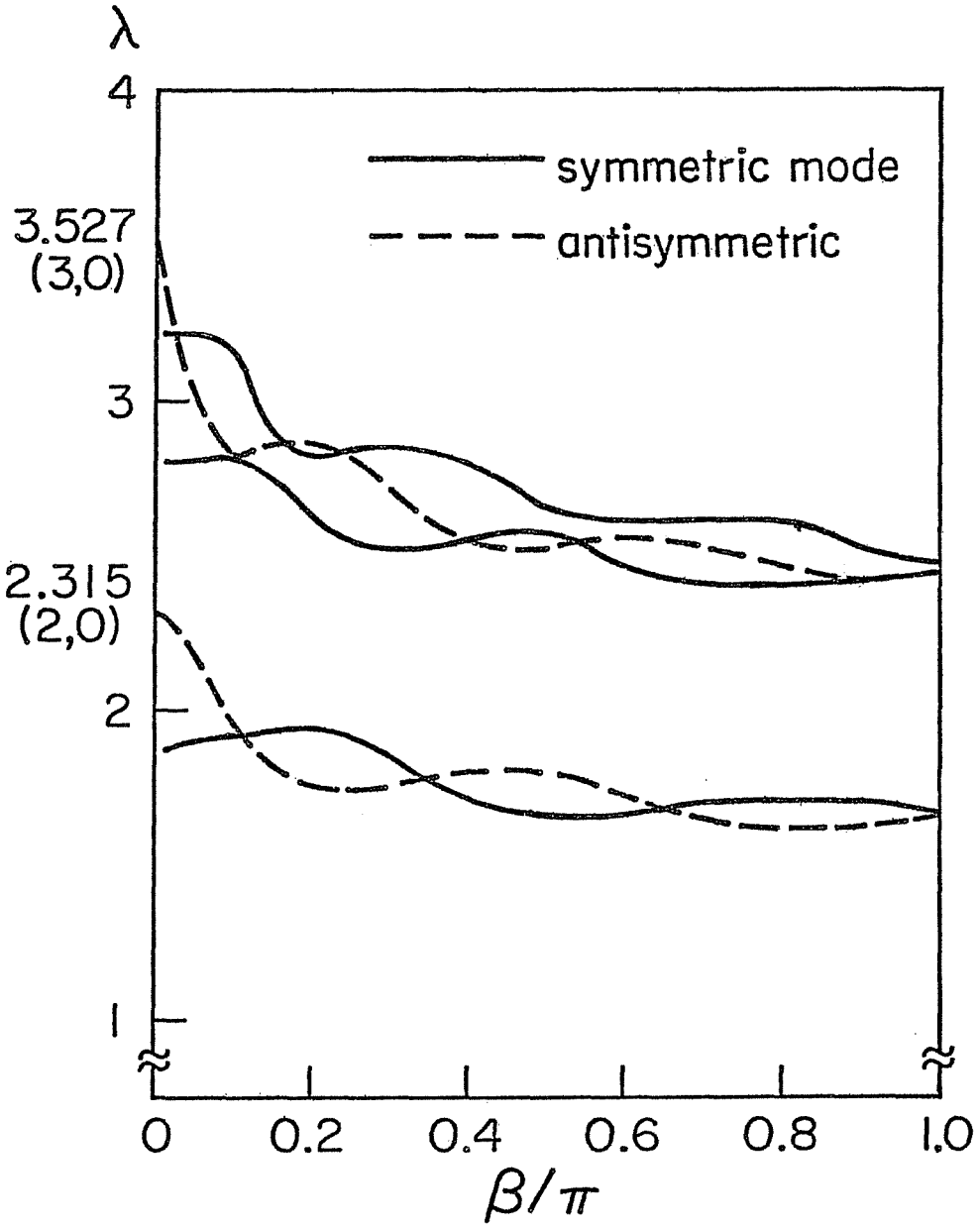

Fig.3-26 Variation of frequncy parameters with the angle of a partial edge mass —— constant added mass (M_A/M_P=1.0, ν=0.30).

Table 3-24 Frequency parameters with the angle of a partial edge mass—constant added mass ratio (M_A/M_p=1.0, ν=0.30, 20 x 20 matrix).

mode \ β/π		0.01	0.1	0.2	0.3	0.4	0.5	0.6	0.7	0.8	0.9	1.0
3	S	1.86	1.90	1.94	1.85	1.71	1.65	1.65	1.70	1.70	1.70	1.666
	A	2.30	1.95	1.75	1.75	1.80	1.80	1.73	1.65	1.61	1.61	1.666
4		2.80	2.81	2.66	2.51	2.55	2.58	2.46	2.40	2.40	2.42	2.441
5	S	3.21	3.17	2.82	2.85	2.80	2.65	2.60	2.61	2.60	2.51	2.477
	A	3.50	2.80	2.85	2.71	2.55	2.51	2.56	2.51	2.45	2.40	2.441

Table 3-25 Convergence of frequency parameter ($M_A/M_p = \beta/\pi$ =0.5, ν=0.30, symmetric modes).

determinant	(2,0)	(0,1)	(3,0)
10x10	1.868	2.679	2.927
20x20	1.868	2.679	2.911
30x30	1.868	2.679	2.910

CHAP.4 CLAMPED POLYGONAL PLATES

4-1. Introduction

Free vibration of clamped polygonal plates is studied in this chapter, and "polygon" here refers a regular polygon with the equal sides and angles between the adjacent sides. Polygonal plates are less encountered in practical situations when compared to rectangular or circular plates. Furthermore, it is difficult mathematically to obtain a deflection function which satisfies the given boundary conditions exactly. For these reasons, there has been only a limited number of technical papers concerned with vibration of polygonal plates.

A general analysis is presented for the determination of natural frequencies and mode shapes of the plates, and the analysis is applied to triangular and polygonal plates in Sec.4-3 and 4-4, respectively.

4-2 Analysis*

Figure 4-1 shows a rectangular plate which is simply supported at the edges and clamped along some segments C_p ($p=1,2,\ldots,P$) located inside the plate or along the edges. Denoting the length of two edges a, b, the xy plane of a rectangular coordinate $o\text{-}xyz$ is taken in the neutral surface of the plate. The differential equation of motion governing vibration of the plate is given by

$$D\nabla^4 W - \rho\omega^2 W = Q(x,y) \tag{4-1}$$

*[129]

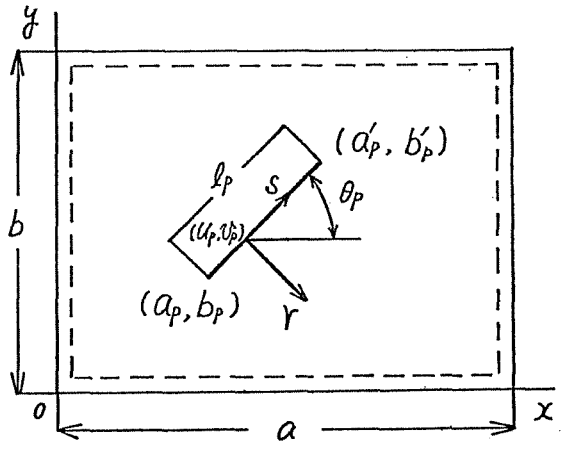

Fig.4-1

Regarding unknown reaction force and moment acting along the segment as unknown harmonic force and moment $\{Q(x,y)\ M_r(x,y)\}$ $e^{j\omega t}$ acting on the plate, the deflection of the plate is written as

$$W(x,y)=\int_0^a\int_0^b\left\{Q(u,v)G(x,y;u,v)+M_r(u,v)\frac{\partial}{\partial r}G(x,y;u,v)\right\}dvdu \qquad (4\text{-}2)$$

by use of the Green's function of the plate

$$G(x,y;u,v)=\frac{1}{\rho}\sum_{m=1}^{\infty}\sum_{n=1}^{\infty}\frac{1}{\omega_{mn}^2-\omega^2}W_{mn}(x,y)W_{mn}(u,v) \qquad (4\text{-}3)$$

where ρ is the mass per unit area and r is the length in the direction normal to the segment. The derivation of Eqs.(4-2,3) and its physical interpretation were made in Sec.2-2. ω_{mn} and $W_{mn}(x,y)$ are the natural frequency and normalized eigenfunction of a simply supported rectangular plate, respectively, which are expressed as

$$\omega_{mn}^2=\frac{D}{\rho}\left\{\left(\frac{m\pi}{a}\right)^2+\left(\frac{n\pi}{b}\right)^2\right\}^2,\quad W_{mn}(x,y)=\frac{2}{\sqrt{ab}}\sin\frac{m\pi x}{a}\sin\frac{n\pi y}{b} \qquad (4\text{-}4)$$

where D is the flexural rigidity of the plate given by $D=Eh^3/12(1-\nu^2)$ (E :Young's modulus, h :plate thickness, ν :Poisson's ratio).

When external force $Q^{(p)}(s)e^{j\omega t}$ and bending moment $M_r^{(p)}(s)e^{j\omega t}$ act on the segment

$$C_p : u_p(s) = a_p + s\cos\theta_p , \quad v_p(s) = b_p + s\sin\theta_p \quad (p=1,2,\cdots P) \tag{4-5}$$

the deflection of the plate is written as

$$W(x,y) = \sum_{p=1}^{P}\int_0^{\ell_p} \Big\{ Q^{(p)}(s)\, G(x,y;u_p(s),v_p(s)) + M_r^{(p)}(s)\left(\sin\theta_p\frac{\partial}{\partial u_p} - \cos\theta_p\frac{\partial}{\partial v_p}\right) G(x,y;u_p(s),v_p(s))\Big\} ds \tag{4-6}$$

where ℓ_p is the length of the segment C_p and s denotes the length measured along it and θ_p the angle between the segment and x axis. Expanding the force and moment distributed along the segment into Fourier sine series with unknown coefficients

$$Q^{(p)}(s) = \sum_{i=1}^{\infty} Q_i^{(p)} \sin\frac{i\pi s}{\ell_p} , \quad M_r^{(p)}(s) = \sum_{i=1}^{\infty} M_{r,i}^{(p)} \sin\frac{i\pi s}{\ell_p} \tag{4-7}$$

Equation (4-6) is written as

$$W(x,y) = \frac{1}{\rho}\sum_{m=1}^{\infty}\sum_{n=1}^{\infty}\frac{1}{\omega_{mn}^2 - \omega^2} W_{mn}(x,y) \sum_{i=1}^{\infty}\sum_{p=1}^{P}\left\{ Q_i^{(p)} I_{mn,i}^{(p)} + M_{r,i}^{(p)} J_{mn,i}^{(p)}\right\} \tag{4-8}$$

by use of Eqs.(4-3,7). $I_{mn,i}^{(p)}$ and $J_{mn,i}^{(p)}$ denote the definite intergrals

$$I_{mn,i}^{(p)} = \int_0^{\ell_p} W_{mn}(u_p(s),v_p(s)) \sin\frac{i\pi s}{\ell_p}\, ds$$
$$J_{mn,i}^{(p)} = \int_0^{\ell_p}\left(\sin\theta_p\frac{\partial}{\partial u_p} - \cos\theta_p\frac{\partial}{\partial v_p}\right) W_{mn}(u_p(s),v_p(s)) \sin\frac{i\pi s}{\ell_p}\, ds \tag{4-9}$$

When the plate is clamped along the segments, the following constraint conditions must be satisfied.

$$W(u_p(s),v_p(s)) = 0 , \quad \left(\sin\theta_p\frac{\partial}{\partial u_p} - \cos\theta_p\frac{\partial}{\partial v_p}\right) W(u_p(s),v_p(s)) = 0 \tag{4-10}$$

$W_{mn}(u_p(\alpha), v_p(\alpha))$ and $(\partial/\partial r) W_{mn}(u_p(\alpha), v_p(\alpha))$ are also expanded into the Fourier sine series

(4-11)

$$W_{mn}(u_p(\alpha), v_p(\alpha)) = \frac{2}{l_p} \sum_{j=1}^{\infty} I_{mn,j}^{(p)} \sin \frac{j\pi\alpha}{l_p}, \quad \left(\sin\theta_p \frac{\partial}{\partial u_p} - \cos\theta_p \frac{\partial}{\partial v_p}\right) W_{mn}(u_p(\alpha), v_p(\alpha)) = \frac{2}{l_p} \sum_{j=1}^{\infty} J_{mn,j}^{(p)} \sin \frac{j\pi\alpha}{l_p}$$

By substituting Eqs.(4-11) into the equations obtained by the substitution of Eq.(4-8) into (4-10), and equating all coefficients of $\sin(j\pi\alpha/l_p)$ to zero, the following equation is derived.

$$\left| \sum_{m=1}^{\infty} \sum_{n=1}^{\infty} \frac{1}{\omega_{mn}^2 - \omega^2} \begin{Bmatrix} I_{mn,i}^{(p)} \\ J_{mn,i}^{(p)} \end{Bmatrix} \begin{Bmatrix} I_{mn,j}^{(q)} & J_{mn,j}^{(q)} \end{Bmatrix} \right| \begin{Bmatrix} Q_j^{(p)} \\ M_{r,j}^{(p)} \end{Bmatrix} = 0 \qquad (4\text{-}12)$$

$$(p, q = 1, 2, \ldots, P;\ i, j = 1, 2, \ldots)$$

By introducing nondimensional expressions

$$f_{mn}(\lambda) = (m^2 + \mu^2 n^2)^2 - \lambda^4/\pi^4, \quad \lambda^4 = \rho a^4 \omega^2 / D \quad (\mu = a/b) \qquad (4\text{-}13)$$

and

$$g_{mn,i}^{(p)} = \int_0^1 \sin m\pi\xi_p(z) \sin n\pi\eta_p(z) \sin i\pi z \, dz$$

$$h_{mn,i}^{(p)} = m \sin\theta_p \int_0^1 \cos m\pi\xi_p(z) \sin n\pi\eta_p(z) \sin i\pi z \, dz \qquad (4\text{-}14)$$

$$- \mu n \cos\theta_p \int_0^1 \sin m\pi\xi_p(z) \cos n\pi\eta_p(z) \sin i\pi z \, dz$$

$$\xi_p(z) = \frac{1}{a}(a_p + l_p z \cos\theta_p), \quad \eta_p(z) = \frac{1}{b}(b_p + l_p z \sin\theta_p) \quad (z = x/l_p) \qquad (4\text{-}15)$$

Equation (4-12) is rewritten in the convenient form

$$\left| \sum_{m=1}^{\infty} \sum_{n=1}^{\infty} \frac{1}{f_{mn}(\lambda)} \begin{Bmatrix} g_{mn,i}^{(p)} \\ h_{mn,i}^{(p)} \end{Bmatrix} \begin{Bmatrix} g_{mn,j}^{(q)} & h_{mn,j}^{(q)} \end{Bmatrix} \right| \begin{Bmatrix} \frac{a}{\pi} Q_j^{(p)} \\ M_{r,j}^{(p)} \end{Bmatrix} = 0 \qquad (4\text{-}16)$$

$$(p, q = 1, 2, \cdots, P;\ i, j = 1, 2, \cdots)$$

where { } denotes a column vector, and the product of the column vector and the transposed vector in the parentheses ( ) gives a square coefficient matrix. The natural frequencies ω of the plate are obtainable by calculating the eigenvalues of Eq.(4-16) and the mode shapes are determined by

$$W(x,y)=\sum_{m=1}^{\infty}\sum_{n=1}^{\infty}\frac{1}{f_{mn}(\lambda)}\sin\frac{m\pi x}{a}\sin\frac{n\pi y}{b}\sum_{i=1}^{\infty}\sum_{p=1}^{P}\left\{g_{mn,i}^{(p)}\ h_{mn,i}^{(p)}\right\}\begin{Bmatrix}\frac{a}{\pi}Q_i^{(p)}\\ M_{r,i}^{(p)}\end{Bmatrix} \quad (4\text{-}17)$$

from the calculation of the eigenvectors $\{(a/\pi)Q_i^{(p)}\ M_{r,i}^{(p)}\}^T$. In the numerical calculations, the number of terms (m , n) of the infinite series and terms of the Fourier sine series (i,j) may be truncated at appropriate finite number, considering the convergence and accuracy of the solution.

4-3 Triangular plate

4-3-1 Review

A number of studies concerned with triangular plates with combinations of boundary conditions were introduced in [1], but most of them dealt with only the fundamental modes and the number of accurate results is still limited. Chopra and Durvasula [109,110] has treated simply supported symmetric and antisymmetric trapezoidal plates, and shown the frequencies for a triangular plate as a special case of the trapezoids. Orris and Petyt [111] conducted a finite element study for trapezoidal plates and also

presented the frequencies for a triangular plate. Williams et al [112] used trilinear coordinates to obtain analytical solutions for a simply supported triangular plate.

For a clamped triangular plate, Cox and Klein [113] used a deflection function satisfying the boundary conditions exactly but the results obtained were insufficient. Hersch [114] presented a lower bound for a clamped equilateral triangle, and Ota et al. [115] obtained fundamental frequencies of clamped isosceles triangular plates. In [111] Orris and Petyt also calculated frequencies of clamped isosceles triangles but no results are given for a equilateral triangle. In most references, only the fundamental frequencies were considered and the lack of accurate results including higher modes is quite obvious. This problem was also considered by Reid[116] and Koerner et al.[117].

4-3-2 Application of the method

A triangular plate can be formed on a simply supported rectangular plate by appropriately setting several clamping segments inside the plate or along the edges. Three segments C_1, C_2 and C_3 of equal length make an equilateral triangle on the original plate of aspect ratio $\mu = 2\sqrt{3}$ as shown in the figure of Table 4-1. One of the segments is at least located on the x axis. By the location of some segments and application of the theory, the natural frequencies and mode shapes are calculated numerically.

As there is one geometrical symmetric axis on an isosceles triangle, symmetric and antisymmetric vibration

modes arise with respect to the axis. By separating both types of vibration and considering only a half domain of the plate, the size of matrix in the frequency equation can be reduced into half.

Table 4-1 presents the frequency equation for an isosceles triangular plate, and also the way of locating the segments and taking integers (m, n) for each type of vibration and aspect ratio $\mu = a/b$ of an original rectangular plate where the actual plate is placed. The S-type mode denotes symmetric vibration about the symmetric axis (broken line) and A-type mode antisymmetric vibration about the axis with a nodal line (solid line) on it.

Table 4-1 Clamped triangular plate

S-type mode	A-type mode
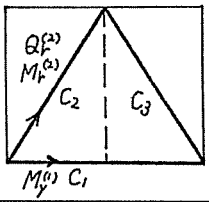	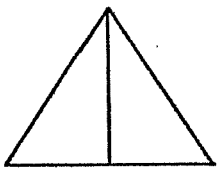

$$\left(\sum_{m=1}^{\infty}\sum_{n=1}^{\infty} \frac{1}{f_{mn}(\lambda)} \begin{Bmatrix} h_{mn,i}^{(1)} \\ g_{mn,i}^{(2)} \\ h_{mn,i}^{(2)} \end{Bmatrix} \left\{ h_{mn,j}^{(1)} \; g_{mn,j}^{(2)} \; h_{mn,j}^{(2)} \right\} \right) \left\{ \begin{matrix} M_{y,j}^{(1)} \\ \frac{a}{\pi} Q_j^{(2)} \\ M_{n,j}^{(2)} \end{matrix} \right\} = 0 \qquad (4\text{-}18)$$

$\xi_1 = \pi/2$, $\eta_1 = 0$ $(\theta_1 = 0)$, $\xi_2 = \pi/2$, $\eta_2 = \pi$ $(\theta_2 = \pi/3)$

$m = 1, 3, \cdots$	$m = 2, 4, \cdots$

$n = 1, 2, 3 \cdots$

4-3-3 Results and discussions

Figure 4-2 presents frequency parameters and nodal patterns of a clamped equilateral triangular plate. The frequency parameters obtained were converted into the values in terms of apothem γ_i (radius of a circle inscribed in the actual plate). Solid lines inside the plates are nodal lines. In the figure, sets of two frequency parameters have close values and denoted with *. They are "degenerated" frequencies and supposed to have the identical values. The slight errors between them are caused by the different equations used and the truncation of terms employed in the infinte series. 2-S mode, for example, can be made by the superposition of 2-A mode. The number of terms used in the series are presented in the

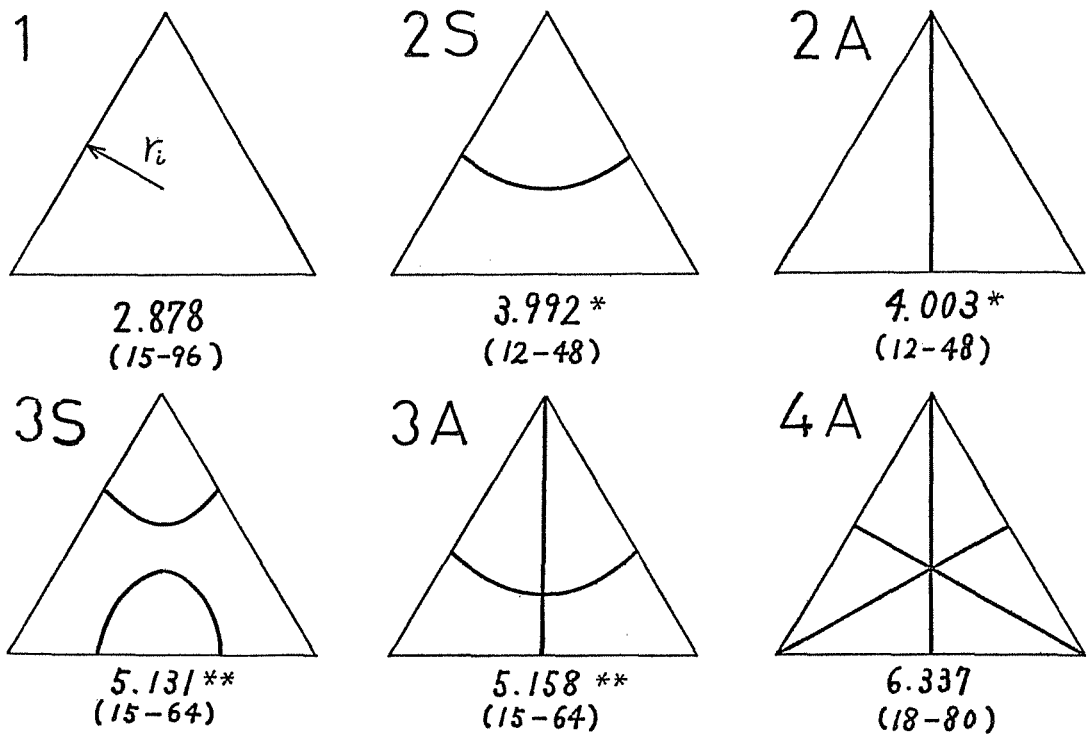

Fig.4-2 Frequency parameters $\lambda = \gamma_i(\omega\sqrt{\rho/D})^{1/2}$ (γ_i :apothem) and nodal patterns of a clamped equilateral triangular plate (*: degeneracy).

parentheses. (15-96) denotes that 15x15 matrix was used with 96 terms for (m,n) in Eq.(4-18).

The convergence of the fundamental frequency was examined in Fig.4-3 by successive truncation of terms for both (m,n) and (i,j) in the series. As more terms are employed for (m,n), the frequency parameter becomes lower. In contrast, with the increase of terms for (i,j) resulting the frequency matrix of $3i$ x$3j$ order, the parameter goes higher. In both cases, the convergent characteristics are obvious.

Table 4-2 compares the fundamental frequency obtained by the present method with those by other authors. The value by Hersch [114] is a lower bound and all other values are higher than his value. The present value is in good

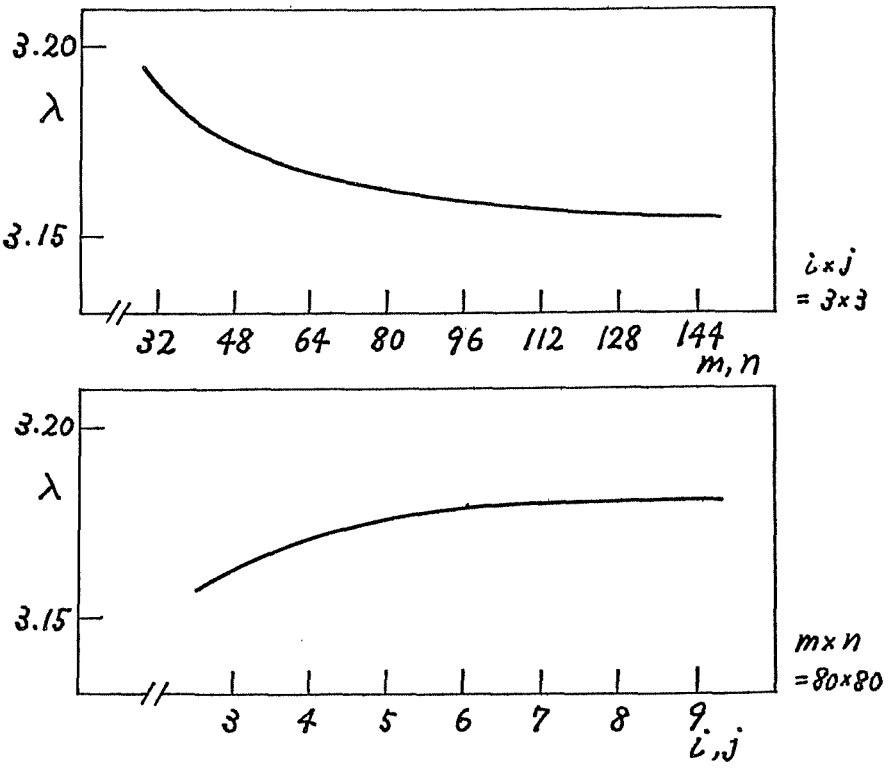

Fig.4-3 Convergence of the fundamental frequency parameter with the number of terms in the infinite and Fourier series.

agreement with those by Ota et al.[115] and Walkinshaw [122].

Table 4-2 Comparison of the fundamental frequencies

Present	Hersch [114]	Ota [115]	Walkinshaw [122]	Yu [124]
2.878	2.617	2.88	2.873	3.077

4-4 Pentagonal, hexagonal, septagonal and octagonal plates

4-4-1 Review

Waller [118] experimentally obtained nodal patterns of completely free pentagonal, hexagonal and octagonal plates. Kaczkowski [119] determined the fundamental freqency of a pentagonal, hexagonal and octagonal plate. Conway [120] has used a point-matching technique, the method of meeting the boundary conditions at discrete points, together with the membrane analogy [121] and presented the fundametal frequency for a simply supported hexagonal plate. Walkinshaw and Kennedy [122] also employed the point-matching method to deal with forced axisymmetric response of polygonal plates and the frequency parameters were shown for the plates with three through twelve edges.

Shahady et al. [123] introduced an interesting approach to treat the plates of complicated shapes by making use of conformal mapping and the Galerkin method, and the fundamental frequencies of simply supported polygonal plates were determined. Yu [124] presented a similar procedure by use of conformal mapping and the Rayleigh-Ritz method but the results obtained differ from those

in [123]. Laura and Marinelli [125] made a comment on this point. Roberts [126] also used the conformal mapping method to determine the fundamental frequency for simply supported plates of polygonal and rhombic shapes. His values agree well with those in [120,123]. Cheung and Cheung [127] dealt with simply supported polygonal plates by the finite strip method.

In these studies, however, only fundamental frequencies were considered and practically no analytical results are found for higher modes of polygonal plates except for a work by Gutierrez et al. [128] who obtained the second natural frequency of simply supported polygonal plates by use of the method developed in [123].

4-4-2 Application of the method

According to the same procedure in 4-3-2, inscribed polygons are formed on the original plates and lateral deflection and rotation of the plate are clamped along the entire boundary of the polygonal plates. One of the segments is conveniently located on the χ axis. The frequency equations derived by the procedure are presented for pentagonal ~ octagonal plates in Table 4-3 through 4-6. These tables also provide other necessary equations and aspect ratios. In the numerical calculations, 48 or 64 terms of the double infinite series and several terms of the Fourier series were used for each mode by considering convergence characteristics of the solution. 80 terms of the infinite series

were employed for the calculation of the fundamental frequencies. The rate of convergence of the solution with the increase of the terms for these polygonal plates was better than that for a triangular plate shown in Fig. 4-3.

The frequencies of small pieces of plate made by the separation of a polygonal plate from the original plate are calculated together, but these values can easily be removed because they give the known values or relatively higher values than those of the actual plate. When they cannot removed easily, mode shapes of the plate were drawn to distinguish them.

Table 4-3 Clamped regular pentagonal plate

S-type mode	A-type mode
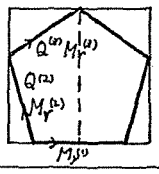	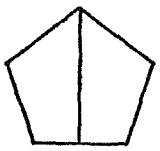

$$\left[\sum_m\sum_n \frac{1}{f_{mn(\lambda)}} \begin{Bmatrix} h^{(1)}_{mn,i} \\ g^{(2)}_{mn,i} \\ h^{(2)}_{mn,i} \\ g^{(3)}_{mn,i} \\ h^{(3)}_{mn,i} \end{Bmatrix} \left\{ h^{(1)}_{mn,j}\ g^{(2)}_{mn,j}\ h^{(2)}_{mn,j}\ g^{(3)}_{mn,j}\ h^{(3)}_{mn,j} \right\}\right] \begin{Bmatrix} M^{(1)}_{y,j} \\ (a/\pi)\,Q^{(2)}_j \\ M^{(2)}_{r,j} \\ (a/\pi)\,Q^{(3)}_j \\ M^{(3)}_{r,j} \end{Bmatrix} = 0 \qquad (4\text{-}19)$$

$\xi_1=\beta_1+(1/2-\beta_1)z,\ \eta_1=0\ (\theta_1=0);\ \xi_2=\beta_1(1-z),\ \eta_2=\beta_2 z\ (\theta_2=3\pi/5);\ \xi_3=z/2,\ \eta_3=\beta_2+(1-\beta_2)z$
$(\theta_3=\pi/5);\quad \mu=(1+2\cos 2\pi/5)/2\cos\pi/5\cos\pi/10,\ \beta_1=\cos 2\pi/5/(1+2\cos 2\pi/5),\ \beta_2=1/2\cos\pi/5$

$m=1,3,\cdots$	$m=2,4,\cdots$
$n=1,2,3,\cdots$	

Table 4-4 Clamped regular hexagonal plate

SS-type	SA-type	AS-type	AA-type
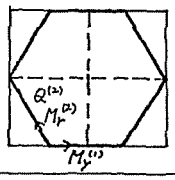	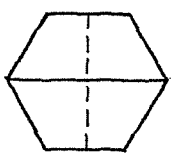	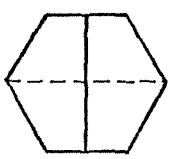	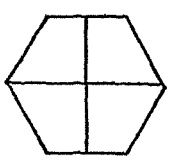

$$\left(\sum_m\sum_n \frac{1}{f_{mn}(\lambda)} \begin{Bmatrix} h_{mn,i}^{(1)} \\ g_{mn,i}^{(2)} \\ h_{mn,i}^{(2)} \end{Bmatrix} \left\{ h_{mn,j}^{(1)} \;\; g_{mn,j}^{(2)} \;\; h_{mn,j}^{(2)} \right\}\right) \begin{Bmatrix} M_{y,j}^{(1)} \\ (a/\pi) Q_j^{(2)} \\ M_{r,j}^{(2)} \end{Bmatrix} = 0 \qquad (4\text{-}20)$$

$\xi_1 = (1+\bar{z})/4$, $\eta_2 = 0$ $(\theta_1 = 0)$; $\xi_2 = (1-\bar{z})/4$, $\eta_2 = \bar{z}/2$ $(\theta_2 = 2\pi/3)$ $(\mu = 2/\sqrt{3})$

$m, n = 1, 3, \cdots$	$m = 1, 3, \cdots$ $n = 2, 4, \cdots$	$m = 2, 4, \cdots$ $n = 1, 3, \cdots$	$m, n = 2, 4, \cdots$

Table 4-5 Clamped regular septagonal plate

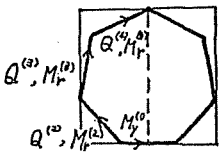	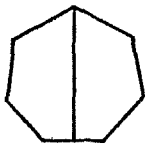

$$\left(\sum_m\sum_n \frac{1}{f_{mn}(\lambda)} \begin{Bmatrix} h_{mn,i}^{(1)} \\ g_{mn,i}^{(2)} \\ h_{mn,i}^{(2)} \\ g_{mn,i}^{(3)} \\ h_{mn,i}^{(3)} \\ g_{mn,i}^{(4)} \\ h_{mn,i}^{(4)} \end{Bmatrix} \left\{ h_{mn,j}^{(1)} \; g_{mn,j}^{(2)} \; h_{mn,j}^{(2)} \; g_{mn,j}^{(3)} \; h_{mn,j}^{(3)} \; g_{mn,j}^{(4)} \; h_{mn,j}^{(4)} \right\}\right) \begin{Bmatrix} M_{y,j}^{(1)} \\ (a/\pi) Q_j^{(2)} \\ M_{r,j}^{(2)} \\ (a/\pi) Q_j^{(3)} \\ M_{r,j}^{(3)} \\ (a/\pi) Q_j^{(4)} \\ M_{r,j}^{(4)} \end{Bmatrix} = 0 \qquad (4\text{-}21)$$

$\xi_1 = g_1 + (1/2 - g_1)\bar{z}$, $\eta_1 = 0$ $(\theta_1 = 0)$; $\xi_2 = g_1(1-\bar{z})$, $\eta_2 = g_2\bar{z}$ $(\theta_2 = 5\pi/7)$ $(u = e_2/e_1)$

$\xi_3 = g_3\bar{z}$, $\eta_3 = g_2 + (g_4 - g_2)\bar{z}$ $(\theta_3 = 3\pi/7)$; $\xi_4 = g_3 + (1/2 - g_3)\bar{z}$, $\eta_4 = g_4 + (1-g_4)\bar{z}$ $(\theta_4 = \pi/7)$

$g_1 = e_1 \cos 2\pi/7$, $g_2 = e_2 \cos 3\pi/14$, $g_3 = e_1 \sin \pi/14$, $g_4 = 2e_2 \cos \pi/7 \cos \pi/14$

$e_1 = 1/(1 + 2\cos 2\pi/7)$, $e_2 = 1/(\cos \pi/14 + \cos 3\pi/14 + \cos 5\pi/14)$

$m = 1, 3, \cdots$	$m = 2, 4, \cdots$
$n = 1, 2, 3, \cdots$	

Table 4-6 Clamped regular octagonal plate

SSSS-type	SSAA-type	AAAA-type	SA-type
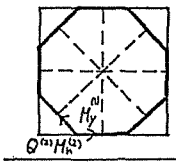	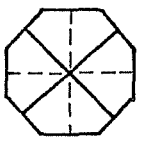	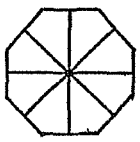	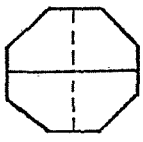

$$\left[\sum_m\sum_n \frac{1}{f_{mn}(\lambda)} \begin{Bmatrix} h_{mn,i}^{(1)} \\ g_{mn,i}^{(2)} \\ h_{mn,i}^{(2)} \end{Bmatrix} \left(\begin{Bmatrix} h_{mn,j}^{(1)} \\ g_{mn,j}^{(2)} \\ h_{mn,j}^{(2)} \end{Bmatrix} \pm \begin{Bmatrix} h_{mn,j}^{(1)} \\ g_{mn,j}^{(2)} \\ h_{mn,j}^{(2)} \end{Bmatrix}^T \right) \begin{Bmatrix} M_{y,j}^{(1)} \\ (a/\pi) Q_j^{(2)} \\ M_{r,j}^{(2)} \end{Bmatrix} = 0 \qquad (4\text{-}22)$$

$$\left(\sum_m\sum_n \frac{1}{f_{mn}(\lambda)} \begin{Bmatrix} h_{mn,i}^{(1)} \\ g_{mn,i}^{(2)} \\ h_{mn,i}^{(2)} \\ g_{mn,i}^{(3)} \end{Bmatrix} \begin{Bmatrix} h_{mn,j}^{(1)} \\ g_{mn,j}^{(2)} \\ h_{mn,j}^{(2)} \\ g_{mn,j}^{(3)} \end{Bmatrix}^T \right) \begin{Bmatrix} M_{y,j}^{(1)} \\ (a/\pi) Q_j^{(2)} \\ M_{r,j}^{(2)} \\ M_{r,j}^{(3)} \end{Bmatrix} = 0 \qquad (4\text{-}23)$$

$\xi_1 = g_1(1/2 - g_1)\bar{z}$, $\eta_1 = 0$ $(\theta_1 = 0)$ $g_1 = 1 - 1/\sqrt{2}$ $(\mu = 1)$

$\xi_2 = g_1(1 - \bar{z}/2)$, $\eta_2 = g_1\bar{z}/2$ $(\theta_2 = 3\pi/4)$		$\xi_2 = g_1(1-\bar{z})$, $\eta_2 = g_1\bar{z}$ $(\theta_2 = 3\pi/4)$ $\xi_3 = 0$, $\eta_3 = g_1 + (1/2 - g_1)\bar{z}$ $(\theta_3 = \pi/2)$
+	−	
$m, n = 1, 3, \cdots$	$m, n = 2, 4, \cdots$	$m = 1, 3, \cdots$, $n = 2, 4, \cdots$

4-4-3 Results and discussion

Table 4-7 compares the present frequency parameters with those obtained by other authors for the fundamental and second axisymmetric mode. The present values agree well with those by Shahady et al. [123], but are slightly higher than the values of Walkinshaw and Kennedy [122] by the point-matching method which is known to yield lower values than the exact ones in general. Laura and Marinelli [125] pointed out that Yu's results [124] were several percent higher than those by other authors and the exact values for a rectangular plate.

Table 4-7 Comparison of frequency parameters

	pentagon	hexagon	septagon	octagon
Present	3.068	3.106	3.128	3.145
Shahady et al. [123]	3.074	3.105	3.125	3.138
Yu [124]	3.144	3.155	3.165	3.171
Walkinshaw et al. [122]	3.061	3.098	3.120	3.137

Figures 4-4 through 4-7 show frequency parameters and nodal patterns of a clamped pentagonal, hexagonal, septagonal and octagonal plate, respectively. The frequency parameters obtained from Eqs.(4-19)through (4-23) were converted by multiplying λ by r_i/a (r_i: apothem—radius of a circle inscribed inside a polygon). Since regular polygonal plates have some symmetric axes, vibration modes reflect the symmetry and degeneracy of frequencies takes place. Physically, the degenerated modes are supposed to have the identical

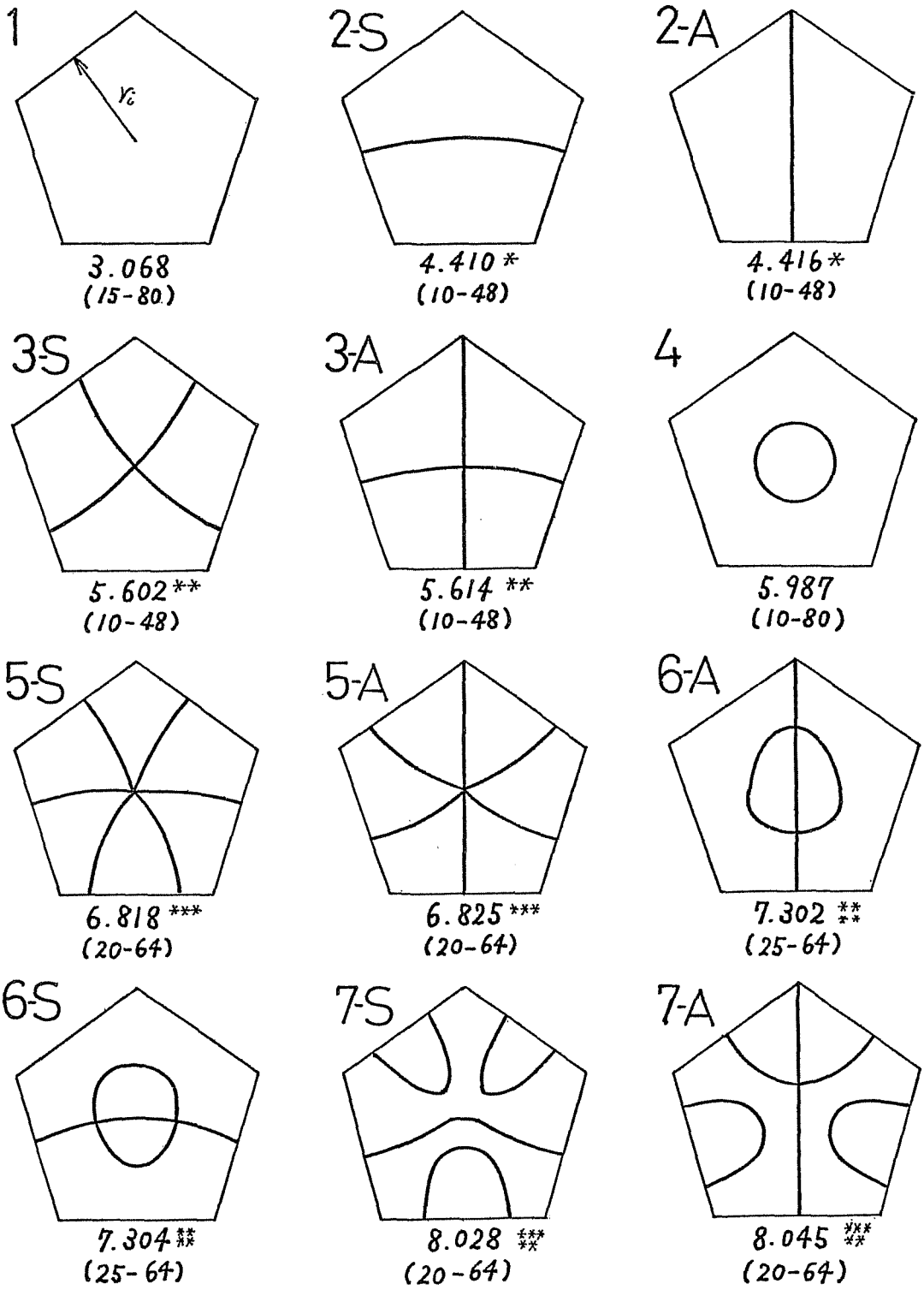

Fig.4-4 Frequency parameters $\lambda = r_i(\omega\sqrt{\rho/D})$ (r_i :apothem) and nodal patterns of a clamped regular pentagonal plate (* :degeneracy).

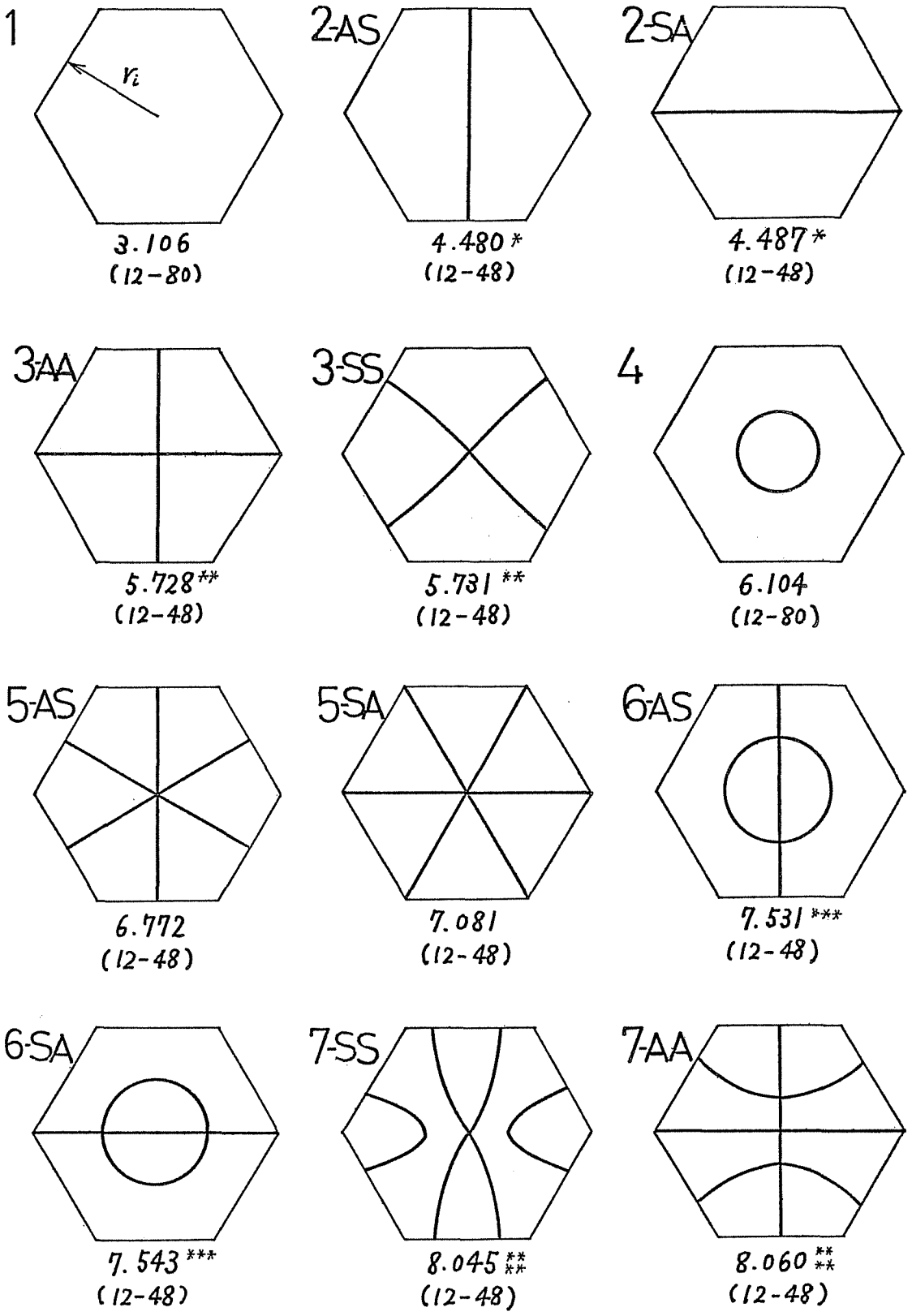

Fig.4-5 Frequency parameters and nodal patterns of a clamped regular hexagonal plate, (*:degeneracy).

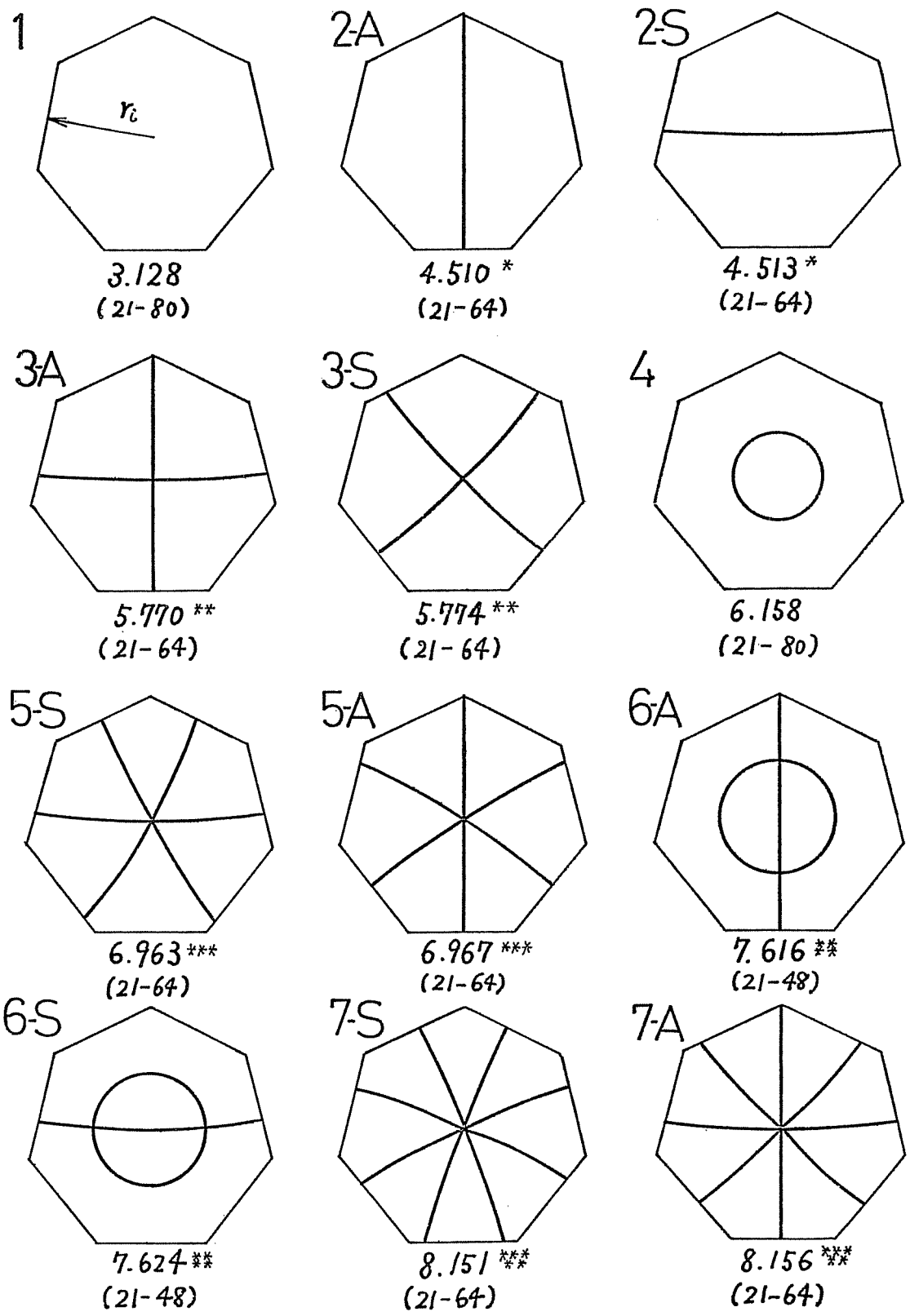

Fig.4-6 Frequency parameters and nodal patterns of a clamped regular septagonal plate, (*:degeneracy).

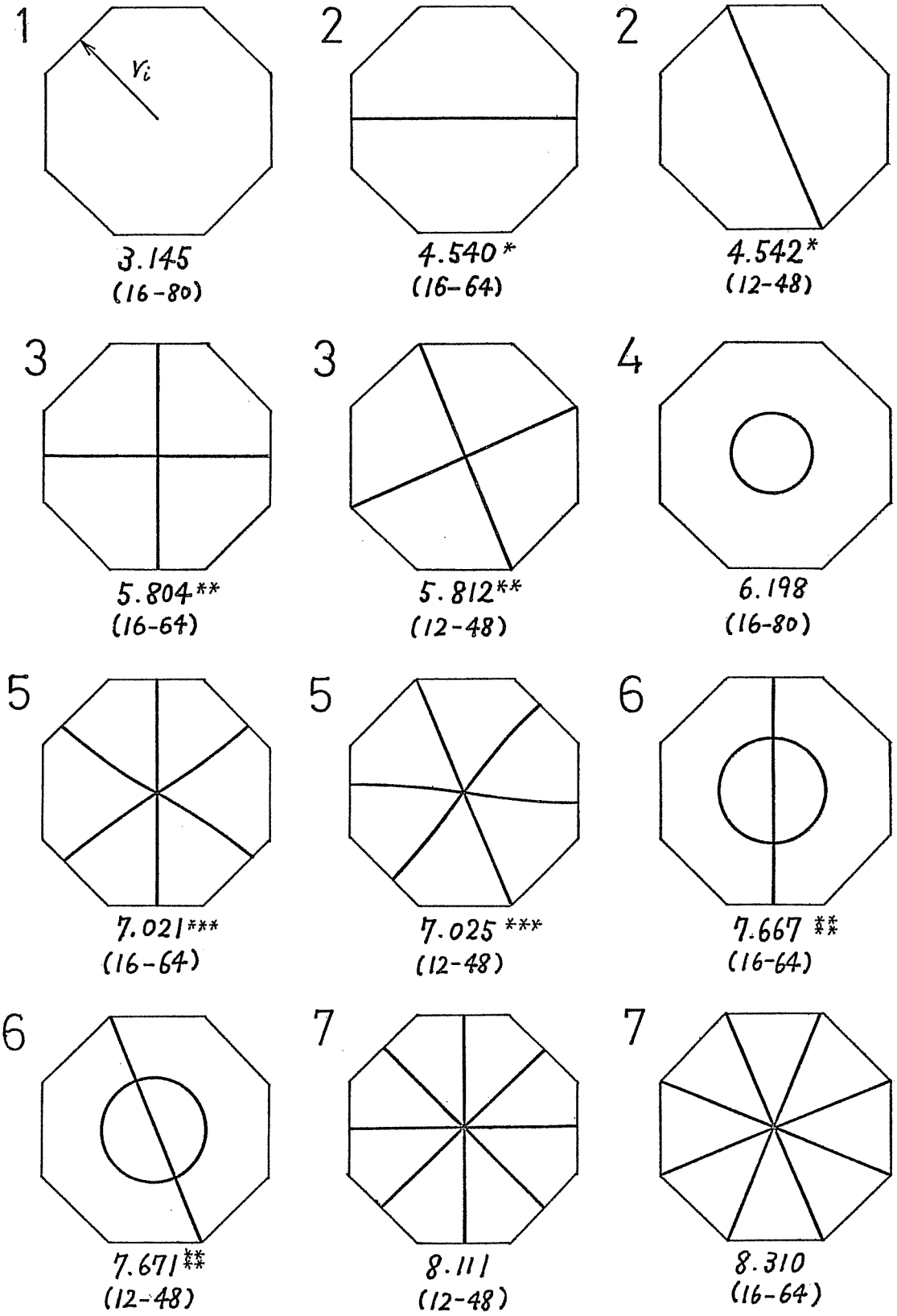

Fig.4-7 Frequency parameters and nodal patterns of a clamped regular octagonal plate (*:degeneracy).

frequencies, but the values obtained here for the same class of modes are slightly different (e.g., λ=4.410 for 2-S mode and λ=4.416 for 2-A mode in Fig.4-4) due to different equations used and the truncation of the series. The differences of the frequency parameters are, however, less than 0.4 percent for most cases. It is pointed out that the frequency parameters take different values without the occurrence of degeneracy for 5th mode of a hexagon and 7th mode of an octagon as seen in Figs.4-5 and 4-7. In this case, one mode shape cannot be made by the superposition of the other mode. For axisymmetric modes with no nodal diameters on it, degeneracy does not occur as seen in the fundamental and 4th modes of polygonal plates.

When the nodal patterns of the same mode number are examined in the figures, it may be noted that there are certain similarities among the patterns. In Fig.4-8(a), the frequency parameters presented in Figs.4-4 through 4-7 are plotted to show the variation with the number of sides. The values for a clamped triangular, square and circular plate are also presented in the figure. As seen clearly, the frequencies become higher as the number of sides is increased. Conversely, the frequencies are decreased with the increase of sides as seen in Fig.4-8(b) when the frequencies are expressed in terms of r_0 (r_0: radius of a circle circumscribed of a polygon). To eliminate the effect of different area of polygons on the frequencies, the parameters are converted into the values $\lambda = r_e(\omega\sqrt{\rho/D})^{1/2}$

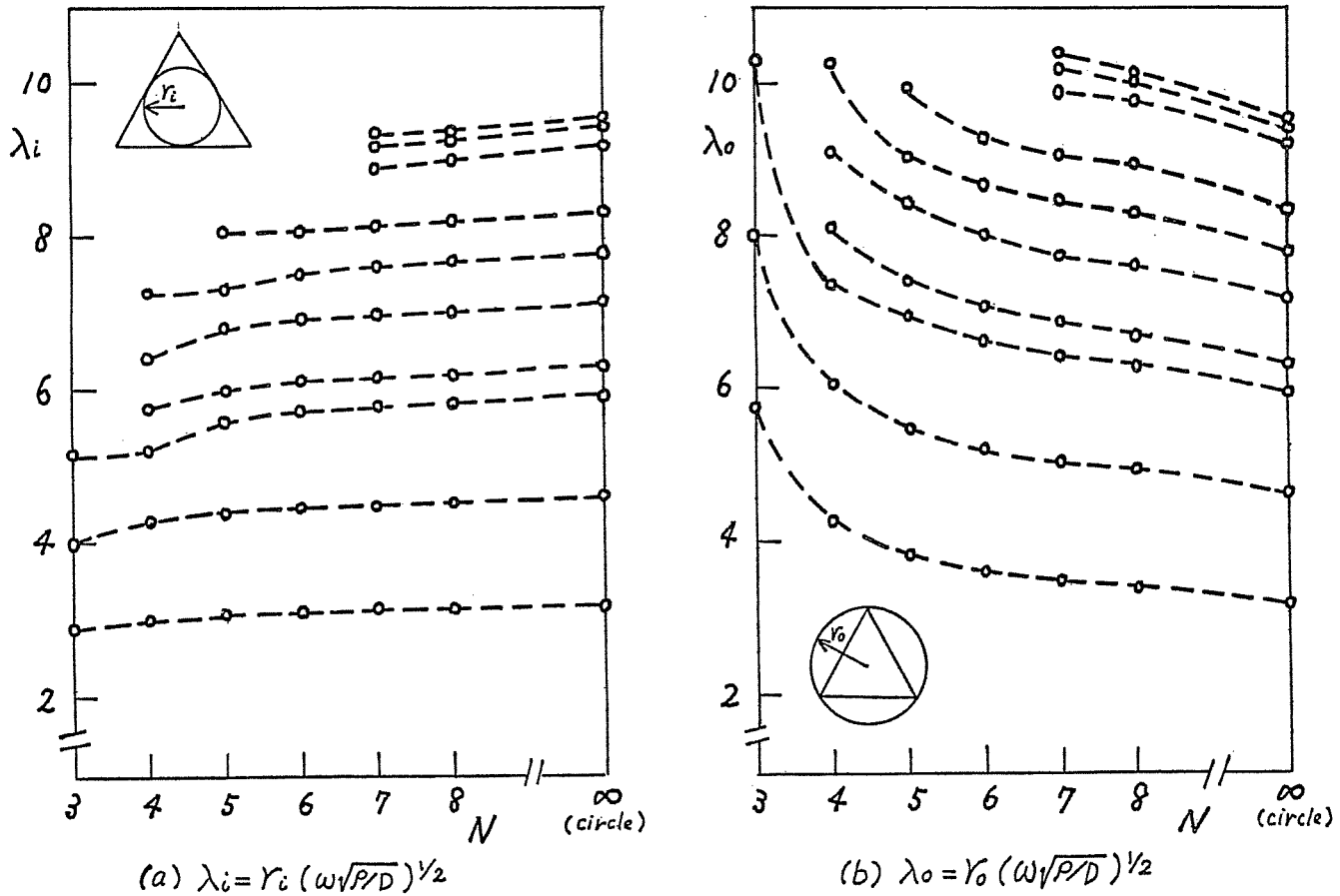

Fig.4-8 Variations of frequency parameters with the number of sides for polygonal plates.

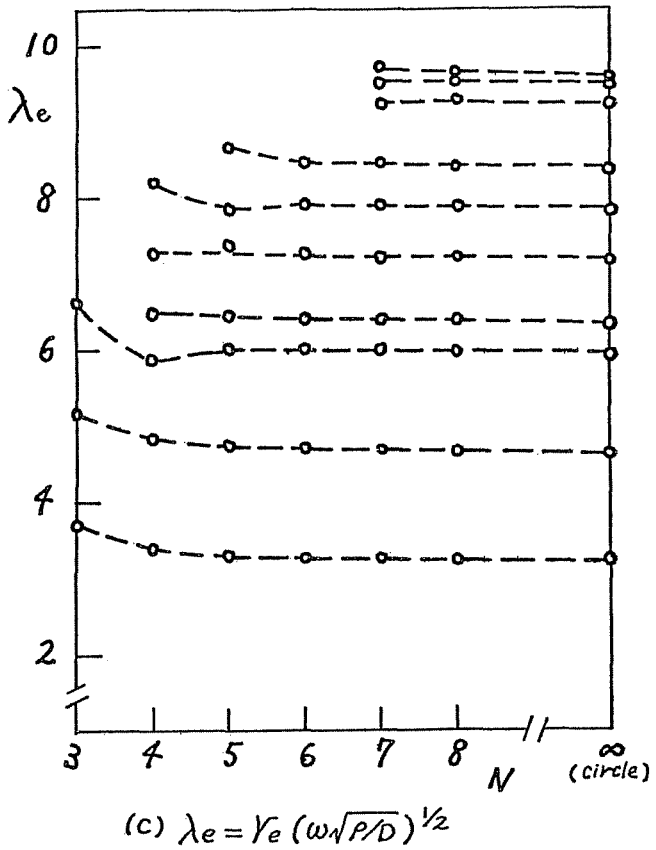

Fig.4-8 (continued)

(γ_e :radius of plates with the equal area). The frequency parameters of polygonal plates of mean radius become lower slightly with the increase of the number of sides, but they take almost equal values to those of a clamped circular plate when the number of sides are more than six. The effect of plate shape is found in polygonal plates whose sides are less than six. These plates have higher frequencies than other polygons with many sides , and inevitably have different mode shapes.

CHAP.5 CLAMPED PLATES OF IRREGULAR SHAPE

5-1.Introduction

This chapter presents an analytical and experimental study on vibration of clamped plates of irregular shape. A general analysis developed in Sec.5-3 is applied to a clamped cross-shaped, I-shaped and L-shaped plate in Secs. 5-4, 5 and 6, respectively. In Sec.5-7, natural frequencies and nodal patterns of a clamped L-shaped plate are experimentally determined by use of the Chladni method. The experimental results are compared with the numerical results obtained in Sec.5-6.

5-2 Review

Only a limited number of literature was found on vibration of plates of arbitrary shape, probably due to difficulty in obtaining an analytical solution. When a plate shape is slightly changed from a circle, the conformal mapping [123, 130,131] or perturbation technique [132] has been used for the analysis. For more general problems, Pnueli [133] presented a method to calculate lower bounds for simply supported or clamped plates of arbitrary shape, but the results shown were insufficient in accuracy. Vivoli and Fillippi [136] employed layer potentials for the analysis of a clamped semicircular plate and Khurasia and Rawtani [137] studied arc aerofoil shaped plates. Рвачев and Ракова [138] analyzed vibration of M-shaped and trapezoidal plates simply supported

or clamped at the edges. Interesting variations of the freq-encies and nodal patterns were presented with the change of plate shapes, starting from a rectangle.

Some experimental studies have been obtained, for example, to simulate a marine and impeller blade [134] and turbine blade [135]. Maruyama and Ichinomiya [139] experimentally obtained the natural frequencies and corresponding mode shapes of a clamped I-shaped plate. A technique of time averaged holographic interferometry was used for the determination of vibration modes.

Despite the fact that irregularly shaped plates are found in many practical situations, no analytical results have been obtained on vibration of the plates considered here.

5-3 Analysis

The frequency equation for a simply supported rectangular plate clamped along some segments inside the plate,as shown in Fig.5-1, can be obtained from Eq.(2-20).

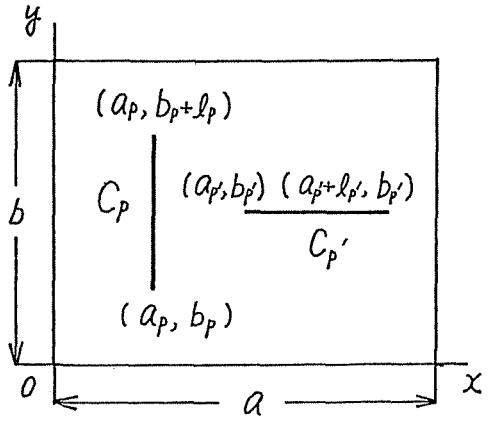

Fig.5-1

$$\left\{\sum_{m=1}^{\infty}\sum_{n=1}^{\infty}\frac{1}{f_{mn}(\lambda)}\begin{Bmatrix}\sin m\pi\alpha_p\,\phi_{n,i}(\eta_p)\\ m\cos m\pi\alpha_p\,\phi_{n,i}(\eta_p)\\ \sin n\pi\beta_{p'}\,\phi_{m,i}(\xi_{p'})\\ n\cos n\pi\beta_{p'}\,\phi_{m,i}(\xi_{p'})\end{Bmatrix}\begin{Bmatrix}\sin m\pi\alpha_q\,\phi_{n,j}(\eta_q)\\ m\cos m\pi\alpha_q\,\phi_{n,j}(\eta_q)\\ \sin n\pi\beta_{q'}\,\phi_{m,j}(\xi_{q'})\\ n\cos n\pi\beta_{q'}\,\phi_{m,j}(\xi_{q'})\end{Bmatrix}^{T}\right\}\begin{Bmatrix}\ell_p Q_{x,j}^{(p)}\\ \frac{\pi\ell_p}{a}M_{x,j}^{(p)}\\ \ell_{p'}Q_{y,j}^{(p')}\\ \frac{\pi\ell_{p'}}{b}M_{y,j}^{(p')}\end{Bmatrix}=0 \qquad (5\text{-}1)$$

where $$\phi_{n,i}(\eta_p)=\int_0^1 \sin n\pi\eta_p(z)\sin i\pi z\,dz\ ,\quad \phi_{m,i}(\xi_{p'})=\int_0^1 \sin m\pi\xi_{p'}(z)\sin i\pi z\,dz \qquad (5\text{-}2)$$

and $$\alpha_p=a_p/a\ ,\quad \eta_p(z)=(b_p+\ell_p z)/b\ ,\quad \beta_{p'}=b_{p'}/b\ ,\quad \xi_{p'}(z)=(a_{p'}+\ell_{p'}z)/a \qquad (5\text{-}3)$$

$$f_{mn}(\lambda)=(m^2+\mu^2n^2)^2-\lambda^4/\pi^4\quad(\mu=a/b) \qquad (5\text{-}4)$$

It is possible to apply Eq.(5-1) directly to irregularly shaped plates clamped along the edges, but the plates of irregular shapes considered here have sharp corners inside the plates which may cause bad convergence of the solution in the numerical calculations. Therefore, the matrix equation (5-1) is rewritten in the form of single series, and procedures for such manipulation are different depending upon geometry of the plates considered.

(a) Plate with two symmetric axes XX and YY

For a rectangular plate having some internal segments located symmetrically about XX and YY axes as shown in Fig.5-2, four types of vibration modes (SS,SA,AS and AA

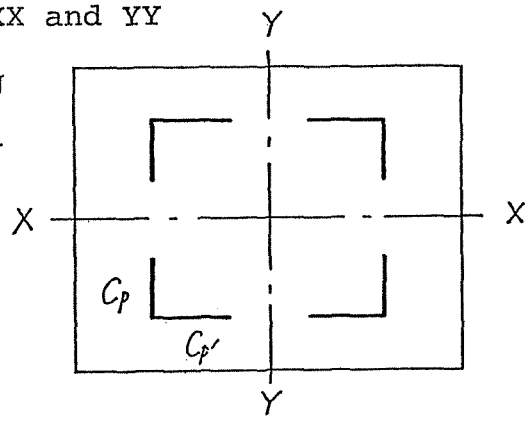

Fig.5-2

type) arise and the integers m and n in Eq.(5-1) must take odd or even number depending upon the mode. The following formulas are used for the summation of the series

$$\sum_{n(\substack{o\\e})}^{\infty} \frac{n\sin nx}{n^2+a^2} = \frac{\pi}{4}\frac{\sinh a(\pi-x) \pm \sinh ax}{\sinh a\pi} \quad \left(\pm : n=\substack{\text{odd}\\\text{even}}\right)(0<x<\pi) \tag{5-5}$$

$$\sum_{n(\substack{o\\e})}^{\infty} \frac{\cos nx}{n^2+a^2} = \frac{\pi}{4a}\frac{\cosh a(\pi-x) \mp \cosh ax}{\sinh a\pi} - \frac{1}{4a^2}\left\{(-1)^n+1\right\}\left(\mp : n=\substack{\text{odd}\\\text{even}}\right) \quad (0\le x\le\pi)$$

The coefficient matrix of Eq.(5-1) is first written in the form to which the formulas (5-5) can be applied.

$$\sum_{m(\substack{o\\e})}\begin{bmatrix} \mathcal{A}_m(\alpha_p) & 0 \\ 0 & \mathcal{B}_{m,i}(\vec{\xi}_{p'}) \end{bmatrix}\begin{bmatrix} 0 & \mathcal{A}_{m,i}(\vec{\eta}_p,\beta_{q'},\lambda) \\ 0 & \mathcal{B}_m(\beta_{p'},\beta_{q'},\lambda) \end{bmatrix}\begin{bmatrix} 0 & 0 \\ 0 & \mathcal{B}_{m,j}(\vec{\xi}_{q'}) \end{bmatrix}$$
$$+\sum_{n(\substack{o\\e})}\begin{bmatrix} \mathcal{B}_{n,i}(\vec{\eta}_p) & 0 \\ 0 & \mathcal{A}_n(\beta_{p'}) \end{bmatrix}\begin{bmatrix} \mathcal{B}_n(\alpha_p,\alpha_q,\lambda) & 0 \\ \mathcal{A}_{n,i}(\vec{\xi}_{p'},\alpha_q,\lambda) & 0 \end{bmatrix}\begin{bmatrix} \mathcal{B}_{n,j}(\vec{\eta}_q) & 0 \\ 0 & 0 \end{bmatrix} \tag{5-6}$$

where

$$\mathcal{A}_m(\alpha_p) = \begin{bmatrix} \sin m\pi\alpha_p & 0 \\ 0 & m\cos m\pi\alpha_p \end{bmatrix}, \quad \mathcal{B}_{m,i}(\vec{\xi}_{p'}) = \phi_{m,i}(\vec{\xi}_{p'})\begin{bmatrix} 1 & 0 \\ 0 & 1 \end{bmatrix} \tag{5-7}$$

$$\mathcal{A}_{m,i}(\vec{\eta}_p,\beta_{q'},\lambda) = \sum_{n(\substack{o\\e})}\frac{1}{f_{mn}(\lambda)}\begin{bmatrix} \phi_{n,i}(\vec{\eta}_p)\sin n\pi\beta_{q'} & \phi_{n,i}(\vec{\eta}_p)\, n\cos n\pi\beta_{q'} \\ \phi_{n,i}(\vec{\eta}_p)\sin n\pi\beta_{q'} & \phi_{n,i}(\vec{\eta}_p)\, n\cos n\pi\beta_{q'} \end{bmatrix} \tag{5-8}$$

$$\mathcal{B}_m(\beta_{p'},\beta_{q'},\lambda) = \sum_{n(\substack{o\\e})}\frac{1}{f_{mn}(\lambda)}\begin{bmatrix} \sin n\pi\beta_{p'}\sin n\pi\beta_{q'} & n\sin n\pi\beta_{p'}\cos n\pi\beta_{q'} \\ n\cos n\pi\beta_{p'}\sin n\pi\beta_{q'} & n^2\cos n\pi\beta_{p'}\cos n\pi\beta_{q'} \end{bmatrix} \tag{5-9}$$

If the infinite series in Eqs.(5-8) and (5-9) are expressable in terms of certain functions, the coefficient matrix (5-6) can be written by use of single series in m or n only. The summations in Eqs.(5-8) and (5-9) are written as

$$\sum_{n(e,o)} \frac{1}{f_{mn}(\lambda)} \begin{Bmatrix} \phi_{n,i}(\eta_p) \sin n\pi\beta_{q'} \\ \phi_{n,i}(\eta_p)\, n \cos n\pi\beta_{q'} \end{Bmatrix} = \frac{1}{m_1 \sinh m_1\pi} \left(\begin{Bmatrix} \psi_{m,i}\begin{pmatrix} 1 \\ \eta_p \end{pmatrix} \sinh m_1\pi \begin{pmatrix} \beta_{q'} \\ 1-\beta_{q'} \end{pmatrix} \\ \psi_{m,i}\begin{pmatrix} 1-\eta_p \\ -\eta_p \end{pmatrix} m_1 \cosh m_1\pi \begin{pmatrix} \beta_{q'} \\ 1-\beta_{q'} \end{pmatrix} \end{Bmatrix} \right.$$

$$\left. \underset{(\pm : n = \text{even}^{\text{add}})}{\pm} \begin{Bmatrix} \psi_{m,i}(\eta_p) \sinh m_1\pi\beta_{q'} \\ \psi_{m,i}(\eta_p)\, m_1 \cosh m_1\pi\beta_{q'} \end{Bmatrix} \right) - \frac{1}{m_2 \sinh m_2\pi} \left(m_1 \to m_2 \right) \qquad (5\text{-}10)$$

for $A l_{m,i}(\eta_p, \beta_{q'}, \lambda)$

$$\sum_{m(e,o)} \frac{1}{f_{mn}(\lambda)} \begin{Bmatrix} \phi_{m,i}(\xi_{p'}) \sin m\pi\alpha_q \\ \phi_{m,i}(\xi_{p'})\, m \cos m\pi\alpha_q \end{Bmatrix} = \frac{\mu^2}{n_1 \sinh n_1\pi} \left(\begin{Bmatrix} \psi_{n,i}\begin{pmatrix} 1-\xi_{p'} \\ \xi_{p'} \end{pmatrix} \sinh n_1\pi \begin{pmatrix} \alpha_q \\ 1-\alpha_q \end{pmatrix} \\ \psi_{n,i}\begin{pmatrix} 1-\xi_{p'} \\ -\xi_{p'} \end{pmatrix} n_1 \cosh n_1\pi \begin{pmatrix} \alpha_q \\ 1-\alpha_q \end{pmatrix} \end{Bmatrix} \right.$$

$$\left. \underset{(\pm : m = \text{even}^{\text{odd}})}{\pm} \begin{Bmatrix} \psi_{n,i}(\xi_{p'}) \sinh n_1\pi\alpha_q \\ \psi_{n,i}(\xi_{p'})\, n_1 \cosh n_1\pi\alpha_q \end{Bmatrix} \right) - \frac{\mu^2}{n_2 \sinh n_2\pi} \left(n_1 \to n_2 \right) \qquad (5\text{-}11)$$

for $A l_{n,i}(\xi_{p'}, \alpha_q, \lambda)$

$$\sum_{n(e,o)} \frac{1}{f_{mn}(\lambda)} \begin{Bmatrix} \sin n\pi\beta_{p'} \sin n\pi\beta_{q'} \\ n \sin n\pi\beta_{p'} \cos n\pi\beta_{q'} \\ n^2 \cos n\pi\beta_{p'} \cos n\pi\beta_{q'} \end{Bmatrix} = \frac{1}{m_1 \sinh m_1\pi} \begin{Bmatrix} \sinh m_1\pi \begin{pmatrix} 1-\beta_{p'} \\ \beta_{p'} \end{pmatrix} \sinh m_1\pi \begin{pmatrix} \beta_{q'} \\ 1-\beta_{q'} \end{pmatrix} \\ m_1 \sinh m_1\pi \begin{pmatrix} 1-\beta_{p'} \\ -\beta_{p'} \end{pmatrix} \cosh m_1\pi \begin{pmatrix} \beta_{q'} \\ 1-\beta_{q'} \end{pmatrix} \\ -m_1^2 \cosh m_1\pi \begin{pmatrix} 1-\beta_{p'} \\ \beta_{p'} \end{pmatrix} \cosh m_1\pi \begin{pmatrix} \beta_{q'} \\ 1-\beta_{q'} \end{pmatrix} \end{Bmatrix}$$

$$\pm_{(\pm:n\ \text{odd}\atop\text{even})}\left\{\begin{array}{l}\sinh m_1\pi\beta_p'\sinh m_1\pi\beta_q'\\ m_1\sinh m_1\pi\beta_p'\cosh m_1\pi\beta_q'\\ m_1^2\cosh m_1\pi\beta_p'\cosh m_1\pi\beta_q'\end{array}\right\}-\frac{1}{m_2\sinh m_2\pi}\left\{m_1\to m_2\right\} \qquad (5\text{-}12)$$

for $IB_m(\beta_p',\beta_q',\lambda)$

$$\sum_{m(\neq q)}\frac{1}{f_{mn}(\lambda)}\left\{\begin{array}{l}\sin m\pi\alpha_p\sin m\pi\alpha_q\\ m\sin m\pi\alpha_p\cos m\pi\alpha_q\\ m^2\cos m\pi\alpha_p\cos m\pi\alpha_q\end{array}\right\}=\frac{\mu^2}{n_1\sinh n_1\pi}\left\{\begin{array}{l}\sinh n_1\pi\binom{1-\alpha_p}{\alpha_p}\sinh n_1\pi\binom{\alpha_q}{1-\alpha_q}\\ n_1\sinh n_1\pi\binom{1-\alpha_p}{-\alpha_p}\cosh n_1\pi\binom{\alpha_q}{1-\alpha_q}\\ -n_1^2\cosh n_1\pi\binom{1-\alpha_p}{\alpha_p}\cosh n_1\pi\binom{\alpha_q}{1-\alpha_q}\end{array}\right\}$$

$$\pm_{(\pm:m\ \text{odd}\atop\text{even})}\left\{\begin{array}{l}\sinh n_1\pi\alpha_p\sinh n_1\pi\alpha_q\\ n_1\sinh n_1\pi\alpha_p\cosh n_1\pi\alpha_q\\ n_1^2\cosh n_1\pi\alpha_p\cosh n_1\pi\alpha_q\end{array}\right\}-\frac{\mu^2}{n_2\sinh n_2\pi}\left\{n_1\to n_2\right\} \qquad (5\text{-}13)$$

for $IB_n(\alpha_p,\alpha_q,\lambda)$, where $\psi_{m,i}\binom{1-\eta_p}{\eta_p}\sinh m_1\pi\binom{\beta_q'}{1-\beta_q'}$ represents $\psi_{m,i}(1-\eta_p)\sinh m_1\pi\beta_q'$ for $\eta_p>\beta_q'$ and $\psi_{m,i}(\eta_p)\sinh m_1\pi(1-\beta_q')$ for $\beta_p<\beta_q'$

and

$$m_1=\sqrt{m^2-(\lambda/\pi)^2}/\mu,\quad m_2=\sqrt{m^2+(\lambda/\pi)^2}/\mu$$
$$n_1=\sqrt{\mu^2n^2-(\lambda/\pi)^2},\quad n_2=\sqrt{\mu^2n^2+(\lambda/\pi)^2}\quad(\mu=a/b) \qquad (5\text{-}14)$$

$$\psi_{m,i}(\eta_p)=\int_0^1\sinh m_1\pi\eta_p\sin i\pi z\,dz$$
$$\psi_{n,i}(\xi_p')=\int_0^1\sinh n_1\pi\xi_p'\sin i\pi z\,dz \qquad (5\text{-}15)$$

Then, each element in Eq.(5-6) is given by

$$A_{m,i}(\gamma_p,\beta_\beta',\lambda)=\frac{1}{m_1\sinh m_1\pi}\left(\begin{bmatrix}\psi_{m,i}\begin{pmatrix}1-\gamma_p\\ \gamma_p\end{pmatrix}\sinh m_1\pi\begin{pmatrix}\beta_\beta'\\ 1-\beta_\beta'\end{pmatrix} & \psi_{m,i}\begin{pmatrix}1-\gamma_p\\ -\gamma_p\end{pmatrix}m_1\cosh m_1\pi\begin{pmatrix}\beta_\beta'\\ 1-\beta_\beta'\end{pmatrix}\\ \psi_{m,i}\begin{pmatrix}1-\gamma_p\\ \gamma_p\end{pmatrix}\sinh m_1\pi\begin{pmatrix}\beta_\beta'\\ 1-\beta_\beta'\end{pmatrix} & \psi_{m,i}\begin{pmatrix}1-\gamma_p\\ -\gamma_p\end{pmatrix}m_1\cosh m_1\pi\begin{pmatrix}\beta_\beta'\\ 1-\beta_\beta'\end{pmatrix}\end{bmatrix}\right.$$

$$\left.\pm\begin{Bmatrix}\psi_{m,i}(\gamma_p)\\ \psi_{m,i}(\gamma_p)\end{Bmatrix}\left\{\sinh m_1\pi\beta_\beta'\ m_1\cosh m_1\pi\beta_\beta\right\}\right)-\frac{1}{m_2\sinh m_2\pi}\left(m_1\to m_2\right)\qquad(5\text{-}16)$$

(+:n=odd,−:n=even)

$$IB_m(\beta_p',\beta_\beta',\lambda)=\frac{1}{m_1\sinh m_1\pi}\left(\begin{bmatrix}\sinh m_1\pi\begin{pmatrix}1-\beta_p'\\ \beta_p'\end{pmatrix}\sinh m_1\pi\begin{pmatrix}\beta_\beta'\\ 1-\beta_\beta'\end{pmatrix} & m_1\sinh m_1\pi\begin{pmatrix}1-\beta_p'\\ -\beta_p'\end{pmatrix}\cosh m_1\pi\begin{pmatrix}\beta_\beta'\\ 1-\beta_\beta'\end{pmatrix}\\ m_1\cosh m_1\pi\begin{pmatrix}1-\beta_p'\\ \beta_p'\end{pmatrix}\sinh m_1\pi\begin{pmatrix}-\beta_\beta'\\ 1-\beta_\beta'\end{pmatrix} & -m_1^2\cosh m_1\pi\begin{pmatrix}1-\beta_p\\ \beta_p'\end{pmatrix}\cosh m_1\pi\begin{pmatrix}\beta_\beta'\\ 1-\beta_\beta'\end{pmatrix}\end{bmatrix}\right.$$

$$\left.\pm\begin{Bmatrix}\sinh m_1\pi\beta_p'\\ m_1\cosh m_1\pi\beta_p'\end{Bmatrix}\left\{\sinh m_1\pi\beta_\beta'\ m_1\cosh m_1\pi\beta_\beta\right\}\right)-\frac{1}{m_2\sinh m_2\pi}\left(m_1\to m_2\right)\qquad(5\text{-}17)$$

(+:n=odd,−:n=even)

$$A_{n,i}(\zeta_p',\alpha_\beta,\lambda)=\frac{\mu^2}{n_1\sinh n_1\pi}\left(\begin{bmatrix}\psi_{n,i}\begin{pmatrix}1-\zeta_p'\\ \zeta_p'\end{pmatrix}\sinh n_1\pi\begin{pmatrix}\alpha_\beta\\ 1-\alpha_\beta\end{pmatrix} & \psi_{n,i}\begin{pmatrix}1-\zeta_p'\\ -\zeta_p'\end{pmatrix}n_1\cosh n_1\pi\begin{pmatrix}\alpha_\beta\\ 1-\alpha_\beta\end{pmatrix}\\ \psi_{n,i}\begin{pmatrix}1-\zeta_p'\\ \zeta_p'\end{pmatrix}\sinh n_1\pi\begin{pmatrix}\alpha_\beta\\ 1-\alpha_\beta\end{pmatrix} & \psi_{n,i}\begin{pmatrix}1-\zeta_p'\\ -\zeta_p'\end{pmatrix}n_1\cosh n_1\pi\begin{pmatrix}\alpha_\beta\\ 1-\alpha_\beta\end{pmatrix}\end{bmatrix}\right.$$

$$\left.\pm\begin{Bmatrix}\psi_{n,i}(\zeta_p')\\ \psi_{n,i}(\zeta_p')\end{Bmatrix}\left\{\sinh n_1\pi\alpha_\beta\ n_1\cosh n_1\pi\alpha_\beta\right\}\right)-\frac{\mu^2}{n_1\sinh n_1\pi}\left(n_1\to n_2\right)\qquad(5\text{-}18)$$

(+:m=odd,−:m=even)

and

$$|B_n(\alpha_p,\alpha_q,\lambda)=\frac{\mu^2}{n_1\sinh n_1\pi}\left|\begin{bmatrix} \sinh n_1\pi\begin{pmatrix}1-\alpha_p\\ \alpha_p\end{pmatrix}\sinh n_1\pi\begin{pmatrix}\alpha_q\\ 1-\alpha_q\end{pmatrix} & n_1\sinh n_1\pi\begin{pmatrix}1-\beta_{p'}\\ -\beta_{p'}\end{pmatrix}\cosh n_1\pi\begin{pmatrix}\beta_{q'}\\ 1-\beta_{q'}\end{pmatrix} \\ n_1\cosh n_1\pi\begin{pmatrix}1-\alpha_p\\ \alpha_p\end{pmatrix}\sinh n_1\pi\begin{pmatrix}-\alpha_q\\ 1\ \alpha_q\end{pmatrix} & -n_1^2\cosh n_1\pi\begin{pmatrix}1-\beta_{p'}\\ \beta_{p'}\end{pmatrix}\cosh n_1\pi\begin{pmatrix}\beta_{q'}\\ 1-\beta_{q'}\end{pmatrix}\end{bmatrix}\right.$$

$$\left.\pm\begin{Bmatrix}\sinh n_1\pi\alpha_p\\ n_1\cosh n_1\pi\alpha_p\end{Bmatrix}\left\{\sinh n_1\pi\alpha_p \quad n_1\cosh n_1\pi\alpha_q\right\}\right| - \frac{\mu^2}{n_2\sinh n_2\pi}\left|\ n_1\to n_2\ \right| \qquad (5\text{-}19)$$

(+:m=odd, −:m=even)

The equation for determining the mode shapes is obtained from Eq. (2-25).

$$W(x,y)=\sum_{m(q)}\sum_{n(e)}\frac{1}{f_{mn(\lambda)}}\sin\frac{m\pi x}{a}\sin\frac{n\pi y}{b}$$

$$\times\sum_{i=1}^{\infty}\left(\sum_{p=1}^{P}\phi_{n,i}(y_p)\left\{\sinh m\pi\alpha_p \quad m\cosh m\pi\alpha_p\right\}\begin{Bmatrix}(l_p/\pi)\,Q_{x,i}^{(p)}\\ (l_p/a)\,M_{x,i}^{(p)}\end{Bmatrix}\right.$$

$$\left.+\sum_{p'=1}^{P'}\phi_{m,i}(y_{p'})\left\{\sinh n\pi\beta_{p'} \quad n\cosh n\pi\beta_{p'}\right\}\begin{Bmatrix}(l_p/\pi)\,Q_{y,i}^{(p')}\\ (l_{p'}/b)\,M_{y,i}^{(p')}\end{Bmatrix}\right)$$

$$=\begin{Bmatrix}\sum_{n(e)}\phi_{n,i}(y_p)\sin\frac{n\pi y}{b}\left(\sum_{m(q)}\frac{1}{f_{mn(\lambda)}}\sin\frac{m\pi x}{a}\sin m\pi\alpha_p\right)\\ \sum_{n(q)}\phi_{n,i}(y_p)\sin\frac{n\pi y}{b}\left(\sum_{m(q)}\frac{m}{f_{mn(\lambda)}}\sin\frac{m\pi x}{a}\cos m\pi\alpha_p\right)\\ \sum_{m(e)}\phi_{m,i}(y_{p'})\sin\frac{m\pi x}{a}\left(\sum_{n(e)}\frac{1}{f_{mn(\lambda)}}\sin\frac{n\pi y}{b}\sin n\pi\beta_{p'}\right)\\ \sum_{m(e)}\phi_{m,i}(y_{p'})\sin\frac{m\pi x}{a}\left(\sum_{n(e)}\frac{n}{f_{mn(\lambda)}}\sin\frac{n\pi y}{b}\cos n\pi\beta_{p'}\right)\end{Bmatrix}^{T}\begin{Bmatrix}(l_p/\pi)\,Q_{x,i}^{(p)}\\ (l_p/a)\,M_{x,i}^{(p)}\\ (l_{p'}/\pi)\,Q_{y,i}^{(p')}\\ (l_{p'}/b)\,M_{y,i}^{(p')}\end{Bmatrix} \qquad (5\text{-}20)$$

The formulas(5-12) and (5-13) are applied to Eq.(5-20) and the equation for the determination of the mode shapes is given by

$$W(x,y)\cos\left(N_{(1),ij}^{(p\beta p'\beta')}-N_{(2),ij}^{(p\beta p'\beta')}\right)\begin{Bmatrix}(l_p/\pi)\,Q_{x,i}^{(p)}\\(l_p/a)\,M_{x,i}^{(p)}\\(l_p/\pi)\,Q_{y,i}^{(p')}\\(l_p/b)\,M_{y,i}^{(p')}\end{Bmatrix} \tag{5-21}$$

where

$$N_{(1),ij}^{(p\beta p'\beta')}=\begin{Bmatrix}\mu^2\sum_{n(e^o)}\dfrac{\phi_{n,i}(\eta_p)\sin n\pi Y}{n_1\sinh n_1\pi}\left[\sinh n_1\pi\begin{pmatrix}1-X\\X\end{pmatrix}\sinh n_1\pi\begin{pmatrix}\alpha_p\\1-\alpha_p\end{pmatrix}\quad\sinh n_1\pi X\cdot\sinh n_1\pi\alpha_p\right]\\ \mu^2\sum_{n(e^o)}\dfrac{\phi_{n,i}(\eta_p)\sin n\pi Y}{n_1\sinh n_1\pi}\left[\sinh n_1\pi\begin{pmatrix}1-X\\-X\end{pmatrix}n_1\cosh n_1\pi\begin{pmatrix}\alpha_p\\1-\alpha_p\end{pmatrix}\quad\sinh n_1\pi X\cdot n_1\cosh n_1\pi\alpha_p\right]\\ \sum_{m(e^o)}\dfrac{\phi_{m,i}(\xi_{p'})\sin m\pi X}{m_1\sinh m_1\pi}\left[\sinh m_1\pi\begin{pmatrix}1-Y\\Y\end{pmatrix}\sinh n_1\pi\begin{pmatrix}\beta_{p'}\\1-\beta_{p'}\end{pmatrix}\quad\sinh m_1\pi Y\sinh m_1\pi\beta_{p'}\right]\\ \sum_{m(e^o)}\dfrac{\phi_{m,i}(\xi_{p'})\sin m\pi X}{m_1\sinh m_1\pi}\left[\sinh m_1\pi\begin{pmatrix}1-Y\\-Y\end{pmatrix}m_1\cosh m_1\pi\begin{pmatrix}\beta_{p'}\\1-\beta_{p'}\end{pmatrix}\quad\sinh m_1\pi Y\cdot m_1\cosh m_1\pi\beta_{p'}\right]\end{Bmatrix} \tag{5-22}$$

with $X=x/a$, $Y=y/b$.

(b) Plate with a symmetric axis on the diagonal

Figure 5-3 shows a square plate having some segments located symmetrically with respect to the diagonal axis ZZ. In this case, reactions $\overline{Q}_z$, $\overline{M}_z$ ($z=x,y$) along the

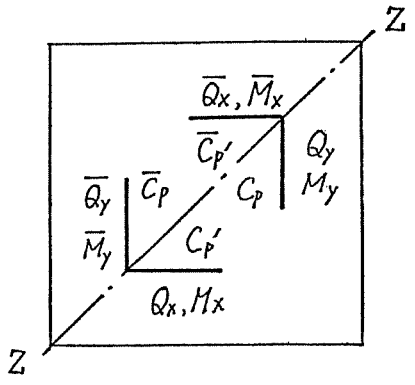

Fig.5-3

segments $\overline{C_p}$, $\overline{C_{p'}}$ can be expressed by reactions Q_z, M_z by interchanging m and n. Making use of these relations, the frequency matrix of 8x8 order obtained for a whole square domain in Fig.5-3 can be reduced to the following equation by considering only a half of the plate intersected by the diagonal line ZZ.

$$\sum_{m=1}^{\infty}\sum_{n=1}^{\infty}\frac{1}{f_{mn}(\lambda)}\begin{Bmatrix}\sin m\pi\alpha_p\,\phi_{n,i}(\zeta_p)\\ m\cos m\pi\alpha_p\,\phi_{n,i}(\zeta_p)\\ \sin n\pi\beta_{p'}\,\phi_{m,i}(\xi_{p'})\\ n\cos n\pi\beta_{p'}\,\phi_{m,i}(\xi_{p'})\end{Bmatrix}\begin{Vmatrix}\sin m\pi\alpha_q\,\phi_{n,j}(\zeta_q) & \sin n\pi\alpha_q\,\phi_{m,j}(\zeta_q)\\ m\cos m\pi\alpha_q\,\phi_{n,j}(\zeta_q) & n\cos n\pi\alpha_q\,\phi_{m,j}(\zeta_q)\\ \sin m\pi\beta_{q'}\,\phi_{n,j}(\xi_{q'}) & \sin n\pi\beta_{q'}\,\phi_{m,j}(\xi_{q'})\\ n\cos n\pi\beta_{q'}\,\phi_{m,j}(\xi_{q'}) & m\cos m\pi\beta_{q'}\,\phi_{n,j}(\xi_{q'})\end{Vmatrix}^{\pm}\begin{Bmatrix}\ell_p\,Q_{x,j}^{(p)}\\ \frac{\pi\ell_p}{a}M_{x,j}^{(p)}\\ \ell_{p'}\,Q_{y,j}^{(p')}\\ \frac{\pi\ell_{p'}}{b}M_{y,j}^{(p')}\end{Bmatrix}^{T}=0 \qquad (5\text{-}23)$$

(+:S-type, −:A-type)

The coefficient matrix of this equation is written as

$$\sum_{m=1}^{\infty}\left(\begin{bmatrix}a_m(\alpha_p) & 0\\ 0 & b_{m,i}(\xi_{p'})\end{bmatrix}\begin{Vmatrix}A_{m,i}(\zeta_p,\alpha_q,\lambda) & A_{m,i}(\zeta_p,\beta_{q'},\lambda)\\ B_m(\beta_{p'},\alpha_q,\lambda) & B_m(\beta_{p'},\beta_{q'},\lambda)\end{Vmatrix}\begin{bmatrix}\pm b_{m,j}(\zeta_q) & 0\\ 0 & b_{m,j}(\xi_{q'})\end{bmatrix}\right.$$

$$\left.+\begin{bmatrix}b_{m,i}(\zeta_p) & 0\\ 0 & a_m(\beta_{p'})\end{bmatrix}\begin{Vmatrix}B_m(\alpha_p,\alpha_q,\lambda) & B_m(\alpha_p,\beta_{q'},\lambda)\\ A_{m,i}(\xi_{p'},\alpha_q,\lambda) & A_{m,i}(\xi_{p'},\beta_{q'},\lambda)\end{Vmatrix}\begin{bmatrix}b_{m,j}(\zeta_q) & 0\\ 0 & \pm b_{m,j}(\xi_{q'})\end{bmatrix}\right) \qquad (5\text{-}24)$$

(+:S-type −:A-type)

where the elements are presented in Eqs.(5-7) through (5-9). Considering that m and n in Eq.(5-24) take all integers (i.e., $m,n=1,2,3,\ldots$), the following formulas are used in A and B.

$$\sum_{n=1}^{\infty}\frac{1}{f_{mn}(\lambda)}\begin{Bmatrix}\sinh n\pi\alpha_p \sin n\pi\alpha_\beta\\ n\sinh n\pi\alpha_p\cos n\pi\alpha_\beta\\ n^2\cosh n\pi\alpha_p\cos n\pi\alpha_\beta\end{Bmatrix}=\frac{1}{m_1\sinh m_1\pi}\begin{Bmatrix}\sinh m_1\pi\binom{1-\alpha_p}{\alpha_p}\sinh m_1\pi\binom{\alpha_\beta}{1-\alpha_\beta}\\ m_1\sinh m_1\pi\binom{1-\alpha_1}{-\alpha_p}\cosh m_1\pi\binom{\alpha_\beta}{1-\alpha_\beta}\\ -m_1^2\cosh m_1\pi\binom{1-\alpha_p}{\alpha_p}\cosh m_1\pi\binom{\alpha_\beta}{1-\alpha_\beta}\end{Bmatrix}-\frac{1}{m_2\sinh m_2\pi}\begin{Bmatrix}m_1\\ \downarrow\\ m_2\end{Bmatrix} \tag{5-25}$$

$$\sum_{n=1}^{\infty}\frac{1}{f_{mn}(\lambda)}\begin{Bmatrix}\phi_{n,i}(\vec{\gamma}_p)\sin n\pi\alpha_p\\ \phi_{n,i}(\vec{\gamma}_p)n\cosh n\pi\alpha_p\end{Bmatrix}=\frac{1}{m_1\sinh m_1\pi}\begin{Bmatrix}\psi_{n,i}\binom{1-\vec{\gamma}_p}{\vec{\gamma}_p}\sinh m_1\pi\binom{\alpha_\beta}{1-\alpha_\beta}\\ \psi_{n,i}\binom{1-\vec{\gamma}_p}{-\vec{\gamma}_p}m_1\cosh m_1\pi\binom{\alpha_\beta}{1-\alpha_\beta}\end{Bmatrix}-\frac{1}{m_2\sinh m_2\pi}\begin{Bmatrix}m_1\\ \downarrow\\ m_2\end{Bmatrix} \tag{5-26}$$

Then, the elements of Eq.(5-24) are given as

$$A_{m,i}(\vec{\gamma}_p,\alpha_\beta,\lambda)=\frac{1}{m_1\sinh m_1\pi}\begin{bmatrix}\psi_{m,i}\binom{1-\gamma_p}{\gamma_p}\sinh m_1\pi\binom{\alpha_\beta}{1-\alpha_\beta} & \psi_{m,i}\binom{1-\gamma_p}{-\gamma_p}m_1\cosh m_1\pi\binom{\alpha_\beta}{1-\alpha_\beta}\\ \psi_{m,i}\binom{1-\gamma_p}{\gamma_p}\sinh m_1\pi\binom{\alpha_\beta}{1-\alpha_\beta} & \psi_{m,i}\binom{1-\gamma_p}{-\gamma_p}m_1\cosh m_1\pi\binom{\alpha_\beta}{1-\alpha_\beta}\end{bmatrix}-\frac{1}{m_2\sinh m_2\pi}\times\left[m_1\to m_2\right] \tag{5-27}$$

$$B_m(\beta_p',\alpha_\beta,\lambda)=\frac{1}{m_1\sinh m_1\pi}\begin{bmatrix}\sinh m_1\pi\binom{1-\beta_p'}{\beta_p'}\sinh m_1\pi\binom{\alpha_\beta}{1-\alpha_\beta} & m_1\sinh m_1\pi\binom{1-\beta_p'}{-\beta_p'}\cosh m_1\pi\binom{\alpha_\beta}{1-\alpha_\beta}\\ m_1\cosh m_1\pi\binom{1-\beta_p'}{\beta_p'}\sinh m_1\pi\binom{-\alpha_\beta}{1-\alpha_\beta} & -m_1^2\cosh m_1\pi\binom{1-\beta_p'}{\beta_p'}\cosh m_1\pi\binom{\alpha_\beta}{1-\alpha_\beta}\end{bmatrix}$$

$$-\frac{1}{m_2\sinh m_2\pi}\left[m_1\to m_2\right] \tag{5-28}$$

The mode shapes are determined by

$$W(x,y)=\left(N_{(1),ij}^{(\beta\beta'\alpha_\beta)}-N_{(2),ij}^{(\beta\beta'\alpha_\beta)}\right)\begin{Bmatrix}(\ell_p/\pi)\,Q_{x,j}^{(\beta)}\\ (\ell_p/a)\,M_{x,j}^{(\beta)}\\ (\ell_{p'}/\pi)\,Q_{y,i}^{(\beta')}\\ (\ell_{p'}/b)\,M_{y,i}^{(\beta')}\end{Bmatrix} \tag{5-29}$$

where $N_{(\omega,ij)}^{(\alpha\beta\gamma\delta)} = \sum_{m=1}^{\infty} \frac{1}{m_i \sinh m_i\pi}$

$$\times \left\{ \sin m\pi X \left\{ \begin{array}{l} \phi_{m,i}(\eta_p)\sinh m_i\pi\binom{1-Y}{Y}\sinh m_i\pi\binom{\alpha_\beta}{1-\alpha_\beta} \\ \phi_{m,i}(\eta_p)m_i\sinh m_i\pi\binom{1-Y}{-Y}\cosh m_i\pi\binom{\alpha_\beta}{1-\alpha_\beta} \\ \phi_{n,i}(\xi_p')\sinh m_i\pi\binom{1-Y}{Y}\sinh m_i\pi\binom{\beta_\beta'}{1-\beta_\beta'} \\ \phi_{n,i}(\xi_p')m_i\sinh m_i\pi\binom{1-Y}{-Y}\cosh m_i\pi\binom{\beta_\beta'}{1-\beta_\beta'} \end{array} \right\} + \sin m\pi Y \left\{ \begin{array}{l} \phi_{m,i}(\eta_p)\sinh m_i\pi\binom{1-X}{X}\sinh m_i\pi\binom{\alpha_\beta}{1-\alpha_\beta} \\ \phi_{m,i}(\eta_p)m_i\sinh m_i\pi\binom{1-X}{-X}\cosh m_i\pi\binom{\alpha_\beta}{1-\alpha_\beta} \\ \phi_{m,i}(\xi_p')\sinh m_i\pi\binom{1-X}{X}\sinh m_i\pi\binom{\beta_\beta'}{1-\beta_\beta'} \\ \phi_{m,i}(\xi_i')m_i\sinh m_i\pi\binom{1-X}{-X}\cosh m_i\pi\binom{\beta_\beta'}{1-\beta_\beta'} \end{array} \right\}^T \right\} \quad (5\text{-}30)$$

5-4 Cross-shaped plate

5-4-1 Application of the method

Figure 5-4 shows a clamped cross-shaped plate which is geometrically symmetric about the XX and YY axis. Several segments are located on the original plate to make a closed cross-shaped form. Since symmetric and antisymmetric vibration modes about these axes occur on this plate, it is sufficient to consider a quarter part of the plate and locate the the following four segments there.

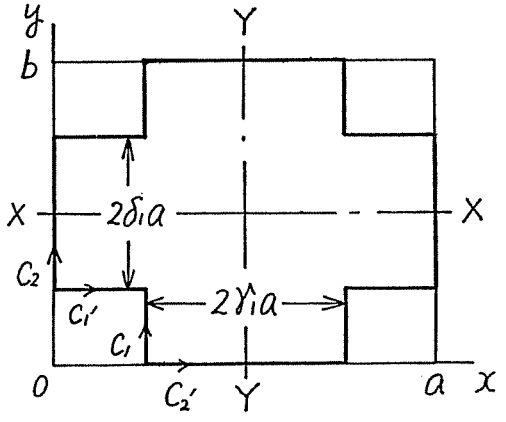

Fig.5-4

$$C_1: \alpha_1 = \frac{1}{2} - \gamma_1,\ \eta_1(z) = \left(\frac{1}{2} - \delta_1\right) z$$

$$C_2: \alpha_2 = 0,\ \eta_2(z) = \left(\frac{1}{2} - \delta_1\right) + \delta_1 z$$

$$C_1': \xi_1'(z) = \left(\frac{1}{2} - \gamma_1\right) z,\ \beta_1' = \frac{1}{2} - \delta_1$$

$$C_2': \xi_2'(z) = \left(\frac{1}{2} - \gamma_1\right) + \gamma_1 z,\ \beta_2 = 0$$

$$(0 \le z \le 1) \quad (5\text{-}31)$$

Both deflection and rotation are rigidly constrained along the segments C_1 and C_1', and only rotation is constrained along the segments C_2 and C_2'. When Eqs.(5-31) are substituted into Eqs.(5-16) through (5-19), relationships between the arguments must be considered as presented in Table 5-1.

Table 5-1

$\alpha_1 = \alpha_1$	$\alpha_1 > \alpha_2$	$\eta_1 < \beta_1'$	$\eta_1 > \beta_2'$
$\alpha_2 < \alpha_1$	$\alpha_2 = \alpha_2$	$\eta_2 > \beta_1'$	$\eta_2 > \beta_2'$
$\xi_1' < \alpha_1$	$\xi_1' > \alpha_2$	$\beta_1' = \beta_1'$	$\beta_1' > \beta_2'$
$\xi_2' > \alpha_1$	$\xi_2' > \alpha_2$	$\beta_2' < \beta_1'$	$\beta_2' = \beta_2'$

Equations (5-12,13) are applicable for $\alpha_i = \alpha_i$ or $\beta_i = \beta_i$ ($i = 1,2$) except for

$$\sum_{n(e,o)} \frac{n}{f_{mn}(\lambda)} \sin n\pi\beta_p' \cos n\pi\beta_q' = \frac{1}{2} \sum_{n(e,o)} \frac{n}{f_{mn}(\lambda)} \sin 2n\pi\beta_p' \quad (\beta_p' = \beta_q')$$

$$= \frac{1}{m_1 \sinh m_1\pi} \left(\frac{m_1}{2} \sinh m_1\pi (1 - 2\beta_p') \pm m_1 \sinh m_1\pi\beta_p' \cosh m_1\pi\beta_p' \right)$$

$$(+ : n = \text{odd}, - : n = \text{even})$$

$$- \frac{1}{m_2 \sinh m_2\pi} \left(m_1 \to m_2 \right) \tag{5-32}$$

and

$$\sum_{m(e,o)} \frac{m}{f_{mn}(\lambda)} \sin m\pi\alpha_p \cos m\pi\alpha_q = \frac{1}{2} \sum_{m(e,o)} \frac{m}{f_{mn}(\lambda)} \sin 2m\pi\alpha_p \quad (\alpha_p = \alpha_q)$$

$$= \frac{\mu^2}{n_1 \sinh n_1\pi} \left(\frac{n_1}{2} \sinh n_1\pi (1 - 2\alpha_p) \pm n_1 \sinh n_1\pi\alpha_p \cosh n_1\pi\alpha_q \right)$$

$$(+ : n = \text{odd}, - : n = \text{even})$$

$$- \frac{\mu^2}{n_2 \sinh n_2\pi} \left(n_1 \to n_2 \right) \tag{5-33}$$

Then, the frequency equation is given by

$$\left({}^{(p_g p'_{g'})}M_{(1),ij} - {}^{(p_g, p'_{g'})}M_{(2),ij} \right) \begin{Bmatrix} (\ell_1/\pi)\ Q^{(1)}_{x,i} \\ (\ell_1/a)\ M^{(1)}_{x,i} \\ (\ell_2/a)\ M^{(2)}_{x,i} \\ (\ell_1'/\pi)\ Q^{(1)}_{y,i} \\ (\ell_1/b)\ M^{(1)}_{y,i} \\ (\ell_2'/b)\ M^{(2)}_{y,i} \end{Bmatrix} = 0 \qquad (5\text{-}34)$$

where ${}^{(p_g p'_{g'})}M_{(1),ij} =$

$$\sum_{m(\neq 0)} \begin{bmatrix} \mathcal{A}_m(\alpha_p) & 0 \\ 0 & \mathcal{B}_{m,i}(\zeta_{p'}) \end{bmatrix} \left(\begin{bmatrix} 0 & \mathcal{G}_{m,i}(\gamma_p, \beta_{g'}, \lambda) \\ 0 & \mathcal{H}_m(\beta_{p'}, \beta_{g'}, \lambda) \end{bmatrix} \pm \begin{Bmatrix} \bar{\mathcal{B}}_{m,i}(\gamma_p) \\ \bar{\mathcal{A}}_m(\beta_{p'}) \end{Bmatrix} \begin{Bmatrix} 0 \\ \bar{\mathcal{A}}_m(\beta_{g'}) \end{Bmatrix}^T \right) \begin{bmatrix} 0 & 0 \\ 0 & \mathcal{B}_{n,j}(\zeta_{g'}) \end{bmatrix}$$

$$(\pm : n = \text{odd}_{\text{even}})$$

$$+\mu^2 \sum_{n(\neq 0)} \begin{bmatrix} \mathcal{B}_{n,i}(\gamma_p) & 0 \\ 0 & \mathcal{A}_n(\beta_{p'}) \end{bmatrix} \left(\begin{bmatrix} \mathcal{H}_n(\alpha_p, \alpha_{g'}, \lambda) & 0 \\ \mathcal{G}_{n,i}(\zeta_{p'}, \alpha_{g'}, \lambda) & 0 \end{bmatrix} \pm \begin{Bmatrix} \bar{\mathcal{A}}_n(\alpha_p) \\ \bar{\mathcal{B}}_{n,i}(\zeta_{p'}) \end{Bmatrix} \begin{Bmatrix} \bar{\mathcal{A}}_n(\alpha_{g'}) \\ 0 \end{Bmatrix}^T \right) \begin{bmatrix} \mathcal{B}_{n,j}(\gamma_{g'}) & 0 \\ 0 & 0 \end{bmatrix}$$

$$(\pm : m = \text{odd}_{\text{even}}) \qquad (5\text{-}35)$$

with

$$\mathcal{A}_m(\alpha_p) = \begin{bmatrix} \sin m\pi\alpha_1 & 0 & 0 \\ 0 & m\cos m\pi\alpha_1 & 0 \\ 0 & 0 & m \end{bmatrix}, \quad \mathcal{B}_{m,i}(\zeta_{p'}) = \begin{bmatrix} \phi_{m,i}(\zeta_{1'}) & 0 & 0 \\ 0 & \phi_{m,i}(\zeta_{1'}) & 0 \\ 0 & 0 & \phi_{m,i}(\zeta_{2'}) \end{bmatrix} \qquad (5\text{-}36)$$

$$\bar{a}_{m}(\beta_{p}')=\begin{bmatrix} \sinh m_1\pi\beta_1' & 0 & 0 \\ 0 & m_1\cosh m_1\pi\beta_1' & 0 \\ 0 & 0 & m_1 \end{bmatrix}, \quad \bar{b}_{m,i}(\gamma_p)=\begin{bmatrix} \psi_{m,i}(\gamma_1) & 0 & 0 \\ 0 & \psi_{m,i}(\gamma_1) & 0 \\ 0 & 0 & \psi_{m,i}(\gamma_2) \end{bmatrix} \tag{5-37}$$

$$G_{m,i}(\gamma_p,\beta_q',\lambda)=\frac{1}{m_1\sinh m_1\pi}\begin{bmatrix} \psi_{m,i}(\gamma_1)\sinh m_1\pi(1-\beta_1') & -\psi_{m,i}(\gamma_1)m_1\cosh m_1\pi(1-\beta_1') & \psi_{m,i}(1-\gamma_1)m_1 \\ \psi_{m,i}(\gamma_1)\sinh m_1\pi(1-\beta_1') & -\psi_{m,i}(\gamma_1)m_1\cosh m_1\pi(1-\beta_1') & \psi_{m,i}(1-\gamma_1)m_1 \\ \psi_{m,i}(1-\gamma_2)\sinh m_1\pi\beta_1' & \psi_{m,i}(1-\gamma_2)m_1\cosh m_1\pi\beta_1' & \psi_{m,i}(1-\gamma_2)m_1 \end{bmatrix} \tag{5-38}$$

$$H_{m}(\beta_{p}',\beta_{q}',\lambda)=\frac{1}{m_1\sinh m_1\pi}\begin{bmatrix} \sinh m_1\pi(1-\beta_1')\sinh m_1\pi\beta_1' & \frac{m_1}{2}\sinh m_1\pi(1-2\beta_1') & m_1\sinh m_1\pi(1-\beta_1') \\ & -m_1^2\cosh m_1\pi(1-\beta_1')\cosh m_1\pi\beta_1' & -m_1^2\cosh m_1\pi(1-\beta_1') \\ \text{Sym.} & & -m_1^2\cosh m_1\pi \end{bmatrix} \tag{5-39}$$

$\bar{a}_{m}(\beta_{p}')$, $\bar{b}_{m,i}(\gamma_p)$, $a_{n}(\alpha_p)$, $b_{n,i}(\gamma_p)$, $G_{m,i}(\beta_p',\alpha_q,\lambda)$ and $H_{m}(\alpha_p,\alpha_q,\lambda)$ can be obtained simply by substituting the arguments into Eqs.(5-36) through (5-39).

The parameter $m_1=\sqrt{m^2-\lambda^2/\pi^2}/\mu$ and $n_1=\sqrt{\mu^2n^2-\lambda^2/\pi^2}$ can be imaginary for $m<\lambda/\pi$ and $\mu n<\lambda/\pi$, respectively. In that case, partitioned matrices (5-37) through (5-39) become

$$\overline{a}_{lm}(\beta_p')=\begin{bmatrix} \sin m_1\pi\beta_1' & 0 & 0 \\ 0 & m_1\cos m_1\pi\beta_1' & 0 \\ 0 & 0 & m_1 \end{bmatrix}, \quad \overline{b}_{m,i}(\gamma_p)=\begin{bmatrix} \phi_{m,i}(\gamma_1) & 0 & 0 \\ 0 & \phi_{m,i}(\gamma_1) & 0 \\ 0 & 0 & \phi_{m,i}(\gamma_2) \end{bmatrix} \tag{5-40}$$

$$G_{m,i}(\gamma_p,\beta_q',\lambda)=\frac{1}{m_1\sin m_1\pi}\begin{bmatrix} \phi_{m,i}(\gamma_1)\sin m_1\pi(1-\beta_1') & -\phi_{m,i}(\gamma_1)m_1\cos m_1\pi(1-\beta_1') & \phi_{m,i}(1-\gamma_1)m_1 \\ \phi_{m,i}(\gamma_1)\sin m_1\pi(1-\beta_1) & -\phi_{m,i}(\gamma_1)m_1\cos m_1\pi(1-\beta_1) & \phi_{m,i}(1-\gamma_1)m_1 \\ \phi_{m,i}(1-\gamma_2)\sin m_1\pi\beta_1' & \phi_{m,i}(1-\gamma_2)m_1\cos m_1\pi\beta_1' & \phi_{m,i}(1-\gamma_2)m_1 \end{bmatrix} \tag{5-41}$$

$$H_m(\beta_p',\beta_q',\lambda)=\frac{1}{m_1\sin m_1\pi}\begin{bmatrix} \sin m_1\pi(1-\beta_1')\sin m_1\pi\beta_1' & \frac{m_1}{2}\sin m_1\pi(1-2\beta_1') & m_1\sin m_1\pi(1-\beta_1') \\ & -m_1^2\cos m_1\pi(1-\beta_1')\cos m_1\pi\beta_1' & -m_1^2\cos m_1\pi(1-\beta_1') \\ \text{Sym.} & & -m_1^2\cos m_1\pi \end{bmatrix} \tag{5-42}$$

5-4-2 Results and discussion

Figure 5-5 shows the frequency parameters $\lambda = a(\omega\sqrt{\rho/D})^{1/2}$ and nodal patterns of cross-shaped plates clamped along the edges. The results obtained for a clamped square plate in Sec.2-3 are also presented to trace the changes of the frequencies and patterns with the shape parameter. SS, SA and AA type modes are obtained for the plate,and AS type modes take the identical frequencies of SA type modes (degeneracy) because of the geometrical symmetry of the plate and aspect ratio $\mu = 1.0$. As the parameter $\gamma_1 = \delta_1$ decrease from 0.5 (square) and the shape of the plate becomes more irregular, the frequencies monotonously increase due to the decrease of area and the effect of the shape. The nodal patterns necessarily change from the normal modes given for a square plate. No nodal patterns are presented for the fundamental modes in the figure. The results presented were calculated by use of 30 x 30 matrix (i.e., $i \times j = 5 \times 5$) with $m(n) = 32$. The convergence of the solution will be examined for a L-shaped plate in Sec.5-6.

The variation of the frequencies can be seen more vividly in Fig.5-6, wherein the parameter $\gamma_1 = \delta_1$ determining shape of the plate is taken as the abscissa. The values of SS, SA(AS) and AA type modes are shown by solid lines, chain lines and broken lines, respectively. As seen from the figure, the rate of change of the frequencies varies from one mode to another.

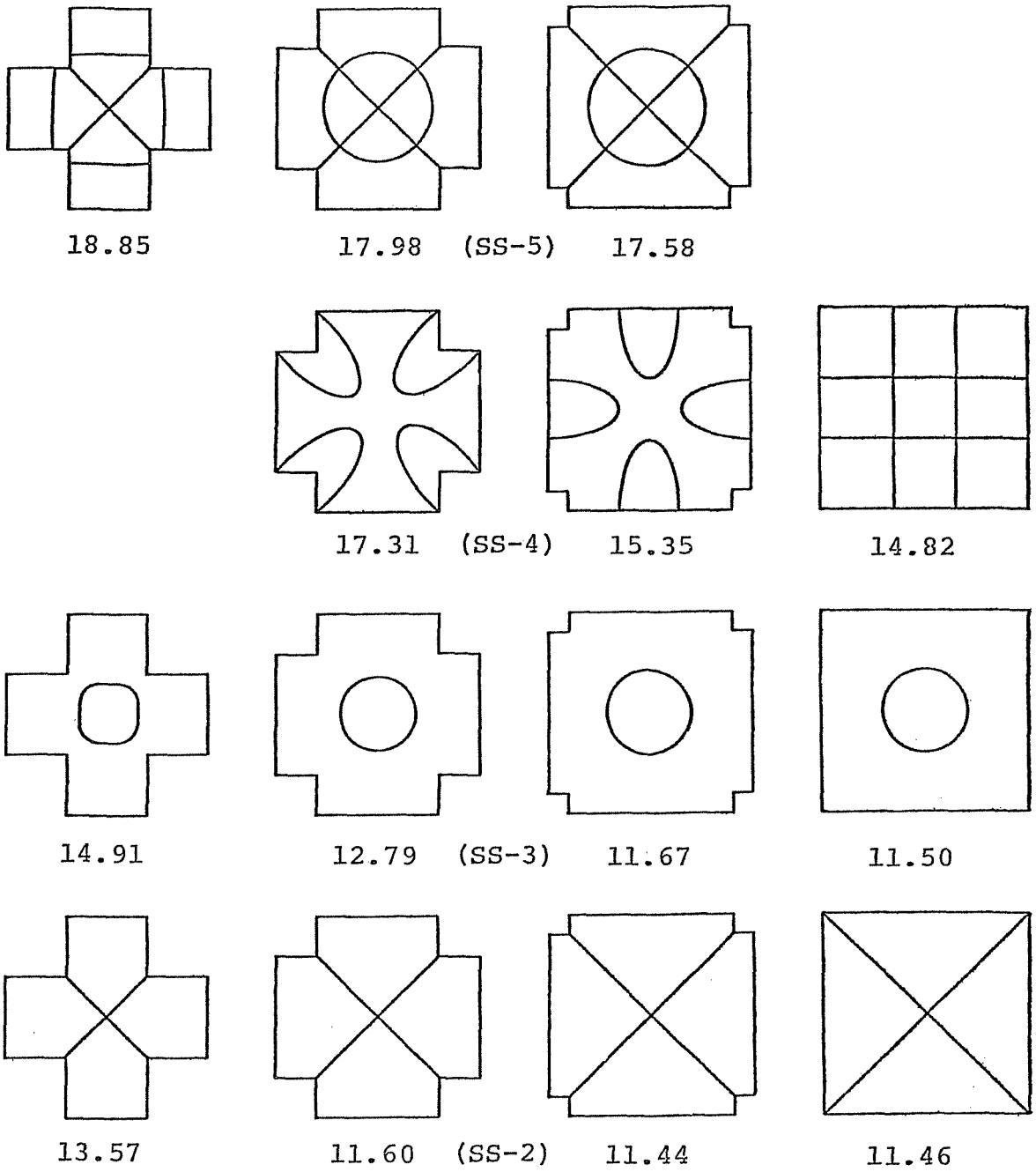

Fig.5-5 Frequency parameters and nodal patterns of a clamped cross-shaped plate (SS mode).

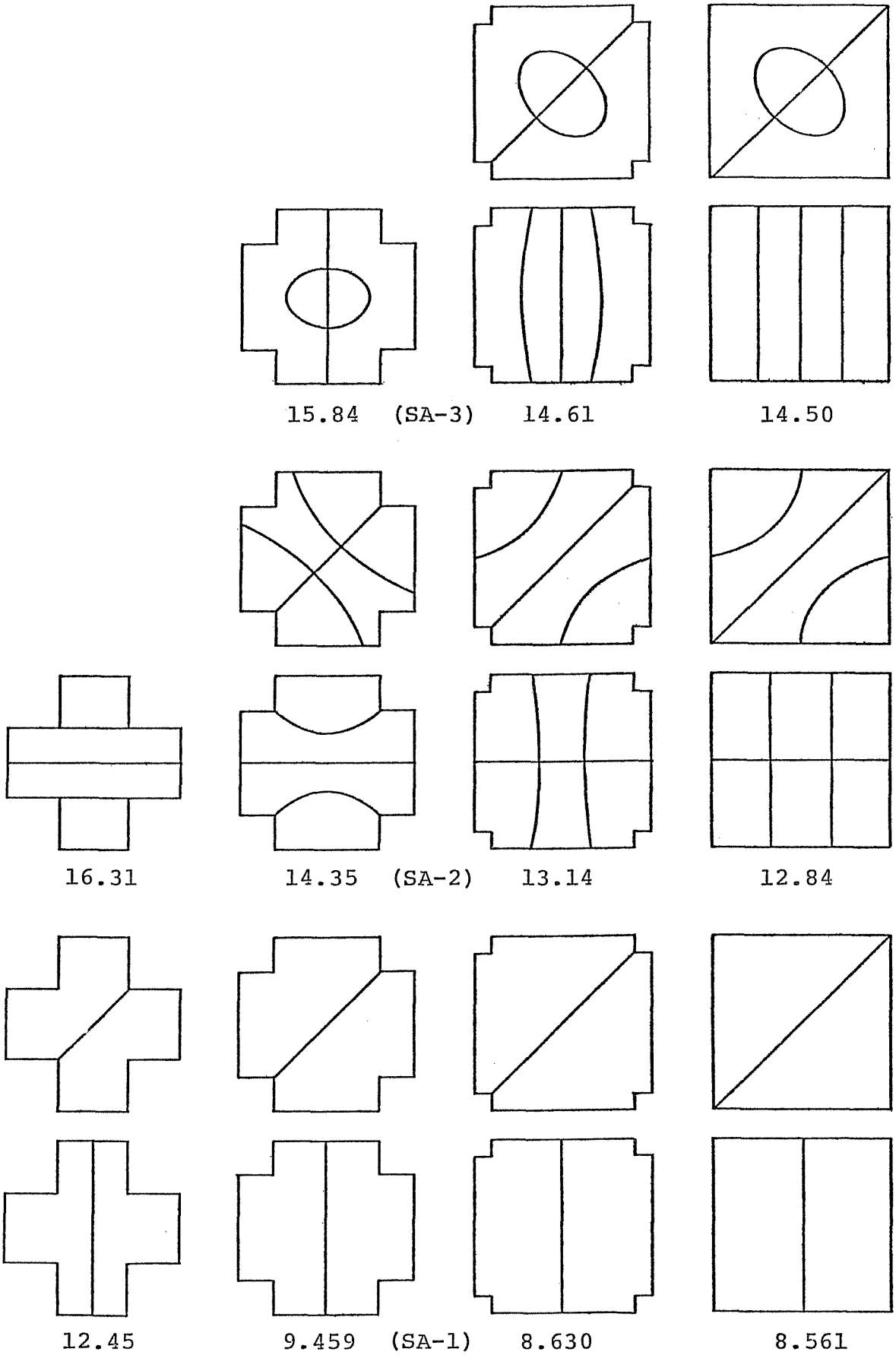

Fig.5-5 (continued) (SA mode)

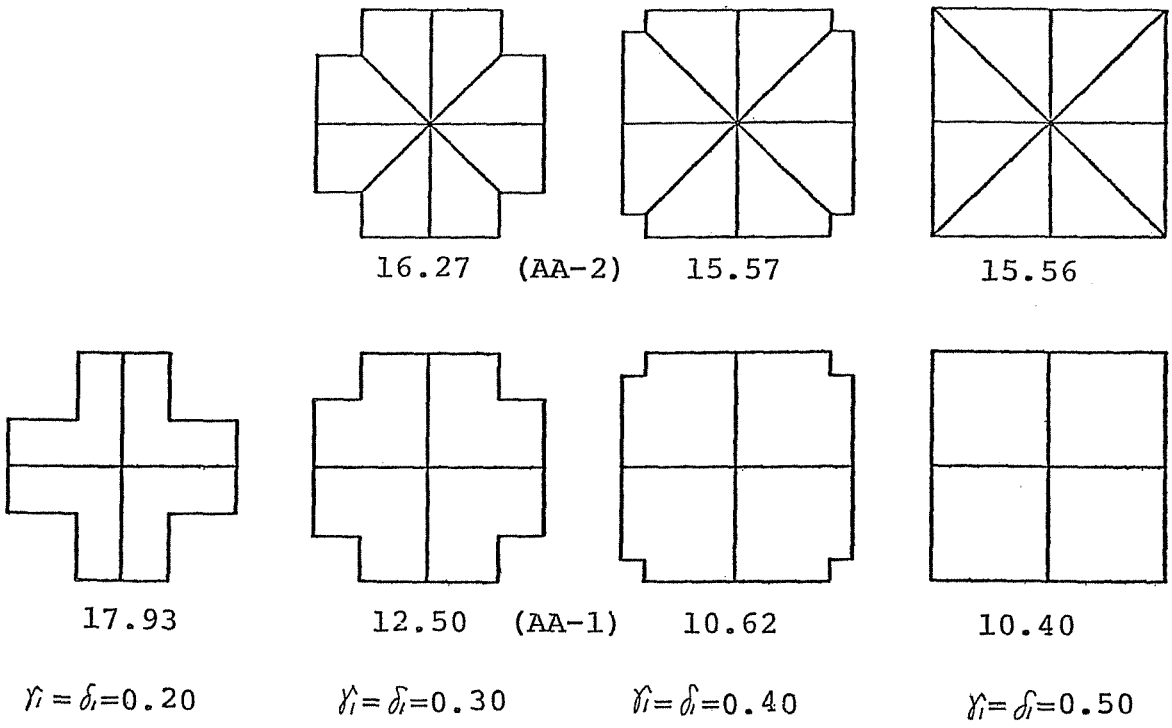

Fig.5-5 (continued) (AA mode)

5-5 I-shaped plate

5-5-1 Application of the method

Figure 5-7 shows a I-shaped plate clamped at the edges. Since four types of vibration arise here as in a cross-shaped plate, only a quarter part of the plate is considered and the following segments are placed.

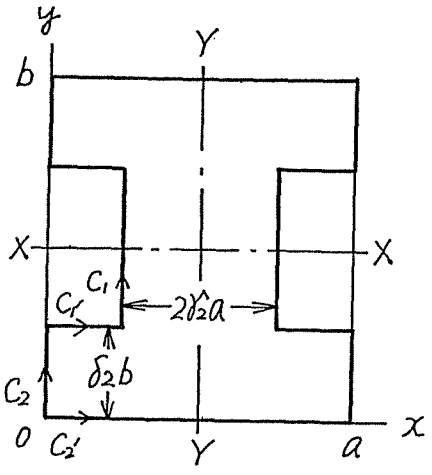

Fig.5-7

$$
\begin{aligned}
&C_1: \quad \alpha_1 = \frac{1}{2} - \gamma_2, \quad \eta_1(\xi) = \delta_2 + \left(\frac{1}{2} - \delta_2\right)\xi \\
&C_2: \quad \alpha_2 = 0, \quad \eta_2(\xi) = \delta_2 \xi \\
&C_1': \quad \xi_1'(\xi) = \left(\frac{1}{2} - \delta_2\right)\xi, \quad \beta_1' = \delta_2 \\
&C_2': \quad \xi_2'(\xi) = \frac{1}{2}\xi, \quad \beta_2' = 0 \\
&\qquad (0 \le \xi \le 1)
\end{aligned}
\tag{5-43}
$$

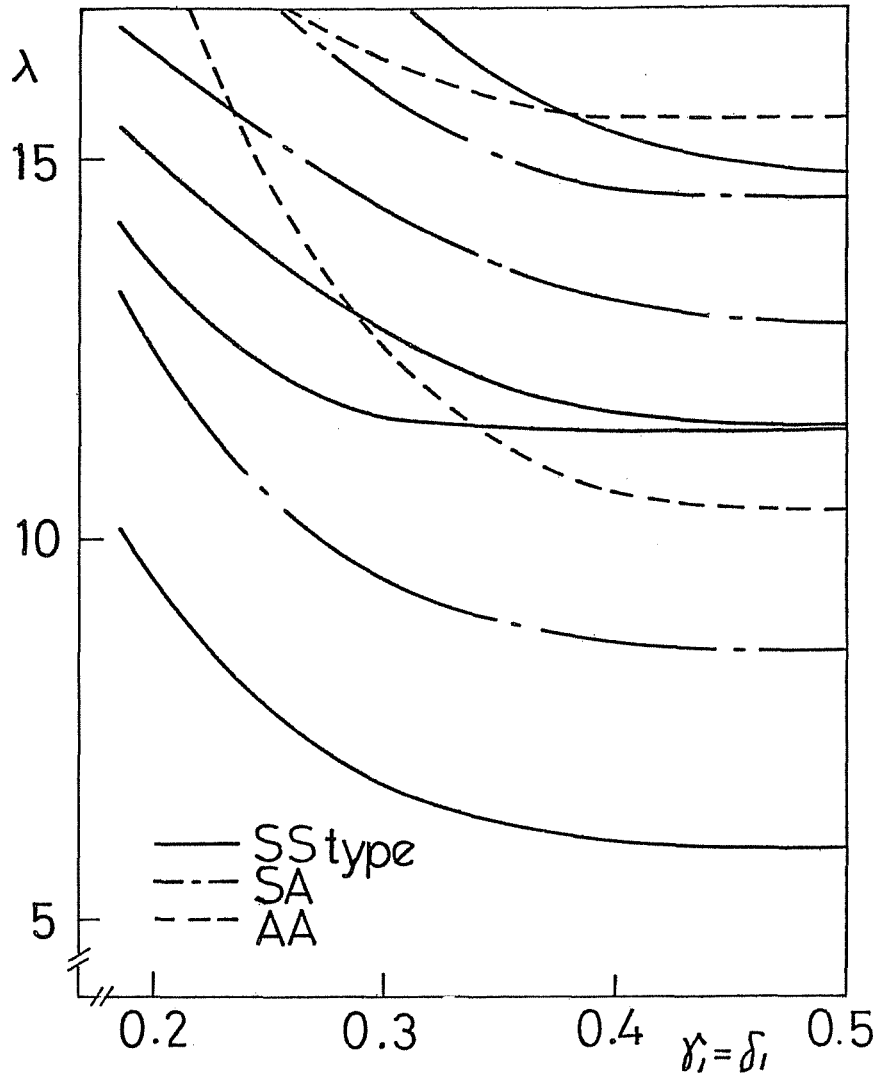

Fig.5-6 Variation of frequency parameters of a clamped cross-shaped plate (μ=1.0, $\gamma_1=\delta_1$)

Both deflection and rotation are rigidly constrained along the segments C_1 and C_1', and only rotation along C_2 and C_2'. The relationships among the arguments must be known to derive the frequency matrix.

Table 5-2

$\alpha_1 = \alpha_1$	$\alpha_1 > \alpha_2$	$\eta_1 > \beta_1'$	$\eta_1 > \beta_2'$
$\alpha_2 < \alpha_1$	$\alpha_2 = \alpha_2$	$\eta_2 < \beta_1'$	$\eta_2 > \beta_2'$
$\xi_1' < \alpha_1$	$\xi_1' > \alpha_2$	$\beta_1' = \beta_1'$	$\beta_1' > \beta_2'$
$\xi_2' \gtrless \alpha_1$	$\xi_2' > \alpha_2$	$\beta_2' < \beta_1'$	$\beta_2' = \beta_2'$

Considering the relations in the table, elements of the matrix (5-6) are determined according to the same procedure in the previous section. Since the relation between ξ_2' and α_1 cannot be determined uniquely ($\xi_2' \gtrless \alpha_1$), the matrix elements involving these arguments must be integrated as follows.

$$\sum_{m(\neq 0)} \frac{1}{f_{mn}(\lambda)} \begin{Bmatrix} \phi_{m,i}(\xi_2') \sin m\pi\alpha_1 \\ \phi_{m,i}(\xi_2')\, m \cos m\pi\alpha_1 \end{Bmatrix} = \frac{\mu^2}{n_1 \sinh n_1\pi} \left(\begin{Bmatrix} \sinh n_1\pi(1-\alpha_1) \int_0^{2\alpha_1} \sinh n_1\pi\xi_2' \sin i\pi z\, dz \\ -n_1 \cosh n_1\pi(1-\alpha_1) \int_0^{2\alpha_1} \sinh n_1\pi\xi_2' \sin i\pi z\, dz \end{Bmatrix} \right.$$

$$+ \begin{Bmatrix} \sinh n_1\pi\alpha_1 \int_{2\alpha_1}^{1} \sinh n_1\pi(1-\xi_2') \sin i\pi z\, dz \\ n \cosh n_1\pi\alpha_1 \int_{2\alpha_1}^{1} \sinh n_1\pi(1-\xi_2') \sin i\pi z\, dz \end{Bmatrix} \pm \left. \begin{Bmatrix} \sinh n_1\pi\alpha_1 \int_0^{1} \sinh n_1\pi\xi_2' \sin i\pi z\, dz \\ n_1 \cosh n_1\pi\alpha_1 \int_0^{1} \sinh n_1\pi\xi_2' \sin i\pi z\, dz \end{Bmatrix} \right)$$

$$(\pm : m = {}^{odd}_{even})$$

$$- \frac{\mu^2}{n_2 \sinh n_1\pi} \left(n_1 \to n_2 \right)$$

$$= \frac{\mu^2}{n_1 \sinh n_1\pi} \frac{1}{\pi} \frac{1}{i^2+(n_1/2)^2} \left\{ \begin{array}{l} \frac{n_1}{2} \sin 2\alpha_1 i\pi \sinh n_1\pi - i(-1)^i \sinh \frac{n_1\pi}{2} \sinh n_1\pi\alpha_1 \\ i \cos 2\alpha_1 i\pi \sinh n_1\pi - i(-1)^i \sinh \frac{n_1\pi}{2} \cosh n_1\pi\alpha_1 \end{array} \right\} - \left\{ n_1 \to n_2 \right\} \tag{5-44}$$

The frequency equation obtained for a I-shaped plate takes the same form as Eqs.(5-34,35), where the elements are given as

$$a_{m}(\alpha_p) = \begin{bmatrix} \sin m\pi\alpha_1 & 0 & 0 \\ 0 & m\cos m\pi\alpha_1 & 0 \\ 0 & 0 & m \end{bmatrix}, \quad b_{m,i}(\xi_p') = \begin{bmatrix} \phi_{m,i}(\xi_1') & 0 & 0 \\ 0 & \phi_{m,i}(\xi_1') & 0 \\ 0 & 0 & \phi_{m,i}(\xi_2') \end{bmatrix} \tag{5-45}$$

$$\overline{a_{m}}(\alpha_p) = \begin{bmatrix} \sinh m_1\pi\beta_1' & 0 & 0 \\ 0 & m_1\cosh m_1\pi\beta_1' & 0 \\ 0 & 0 & m_1 \end{bmatrix}, \quad \overline{b}_{m,i}(\eta_p) = \begin{bmatrix} \psi_{m,i}(\eta_1) & 0 & 0 \\ 0 & \psi_{m,i}(\eta_1) & 0 \\ 0 & 0 & \psi_{m,i}(\eta_2) \end{bmatrix} \tag{5-46}$$

$$G_{m,i}(\eta_p, \beta_q', \lambda) = \frac{1}{m_1 \sinh m_1\pi} \begin{bmatrix} \psi_{m,i}(1-\eta_1)\sinh m_1\pi\beta_1' & \psi_{m,i}(1-\eta_1) m_1\cosh m_1\pi\beta_1' & \psi_{m,i}(1-\eta_1) m_1 \\ \psi_{m,i}(1-\eta_1)\sinh m_1\pi\beta_1' & \psi_{m,i}(1-\eta_1) m_1\cosh m_1\pi\beta_1' & \psi_{m,i}(1-\eta_1) m_1 \\ \psi_{m,i}(\eta_2)\sinh m_1\pi(1-\beta_1') & -\psi_{m,i}(\eta_2) m_1\cosh m_1\pi(1-\beta_1') & \psi_{m,i}(1-\eta_2) m_1 \end{bmatrix} \tag{5-47}$$

$$\mathbb{H}_m(\beta_p',\beta_z',\lambda)=\frac{1}{m_1\sinh m_1\pi}\begin{bmatrix}\sinh m_1\pi(1-\beta_i')\sinh m_1\pi\beta_i' & \frac{m_1}{2}\sinh m_1\pi(1-2\beta_i') & m_1\sinh m_1\pi(1-\beta_i')\\ & -m_1^2\cosh m_1\pi(1-\beta_i')\cosh m\pi\beta_i' & -m_1^2\cosh m_1\pi(1-\beta_i')\\ \text{Sym.} & & -m_1^2\cosh m_1\pi\end{bmatrix} \tag{5-48}$$

$$\mathbb{G}_{n,i}(\xi_p',\alpha_z,\lambda)=\frac{1}{n_1\sinh n_1\pi}\begin{bmatrix}\psi_{n,i}(\xi_i')\sinh n_1\pi(1-\alpha_1) & -\psi_{n,i}(\xi_i')n_1\cosh n_1\pi(1-\alpha_1) & \psi_{n,i}(1-\xi_i')n_1\\ \psi_{n,i}(\xi_i')\sinh n_1\pi(1-\alpha_1) & -\psi_{n,i}(\xi_i')n_1\cosh n_1\pi(1-\alpha_1) & \psi_{n,i}(1-\xi_i')n_1\\ e_1 & e_2 & \psi_{n,i}(1-\xi_2')n_1\end{bmatrix} \tag{5-49}$$

with

$$e_1=\frac{1}{\pi}\frac{1}{i^2+(\frac{n_1}{2})^2}\left\{\frac{n_1}{2}\sin 2\alpha_1 i\pi\sinh n_1\pi-i(-1)^i\sinh\frac{n_1\pi}{2}\sinh n_1\pi\alpha_1\right\} \tag{5-50}$$

$$e_2=\frac{1}{\pi}\frac{1}{i^2+(\frac{n_1}{2})^2}\left\{i\cos 2\alpha_1 i\pi\sinh n_1\pi-i(-1)^i\sinh\frac{n_1\pi}{2}\cosh n_1\pi\alpha_1\right\}$$

The other elements are obtained simply by substituting the given arguments into these equations. When $m_1=\sqrt{m^2-\lambda^2/\pi^2}/\mu$ and $n_1=\sqrt{\mu^2n^2-\lambda^2/\pi^2}$ become imaginary for $m<\lambda/\pi$ and $\mu n<\lambda/\pi$, respectively, hyperbolic functions in $\overline{a}_m$, $\overline{b}_{m,i}$, $\mathbb{G}_{m,i}$ and $\mathbb{H}_m$ should be rewritten by using trigonometric functions.

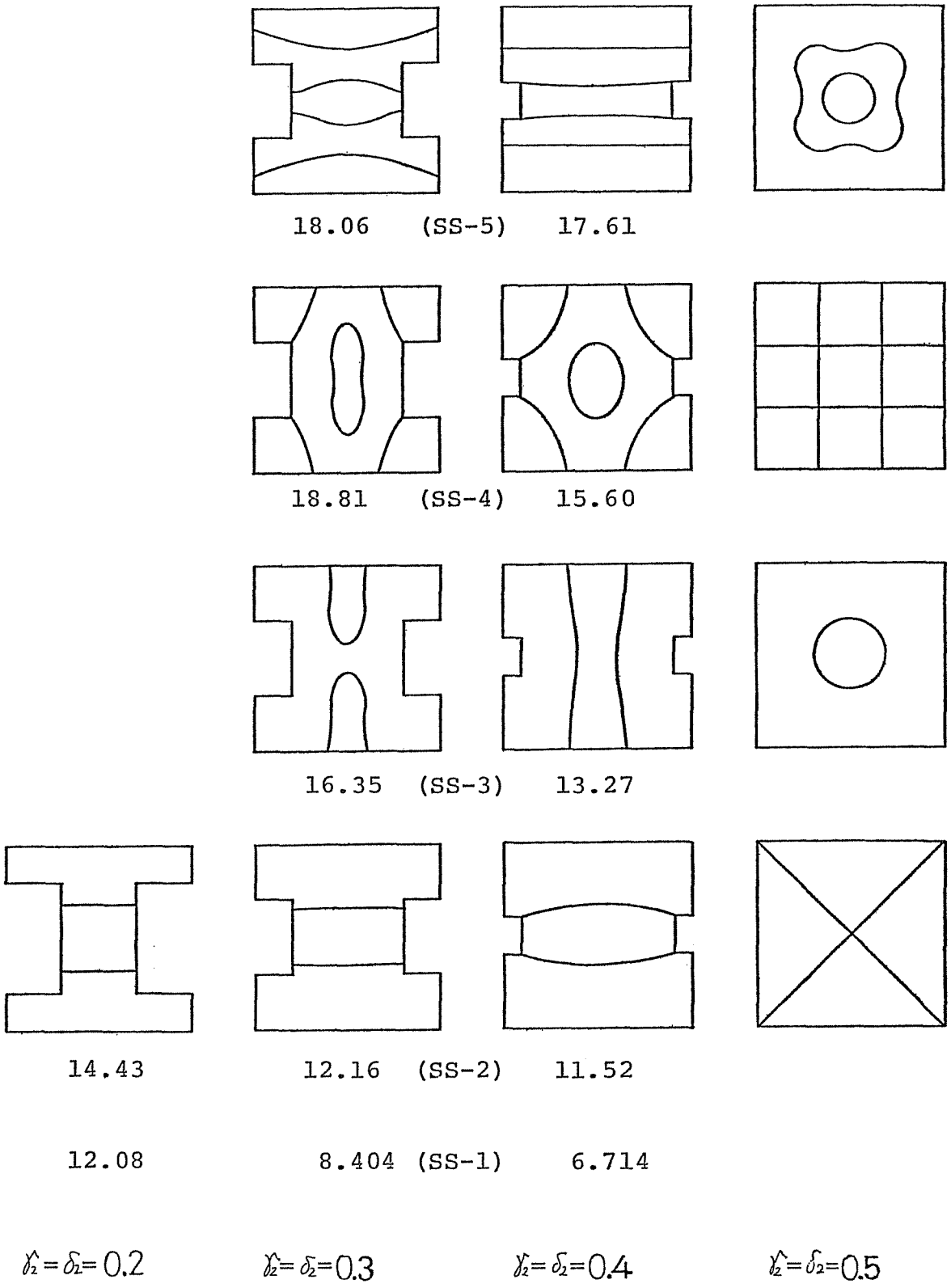

Fig.5-8 Frequency parameters and nodal patterns of a clamped I-shaped plate (SS mode).

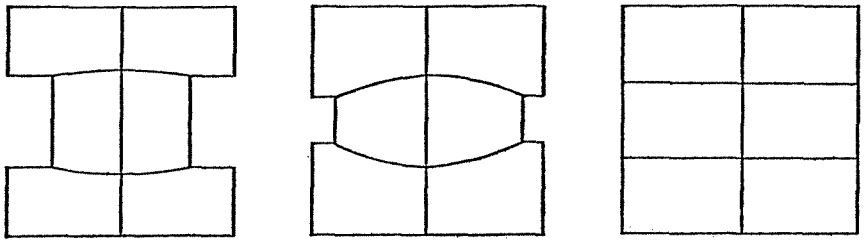

14.95 (AS-2) 13.17

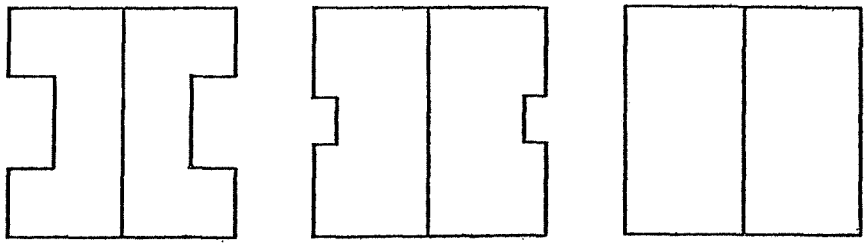

12.99 (AS-1) 9.962

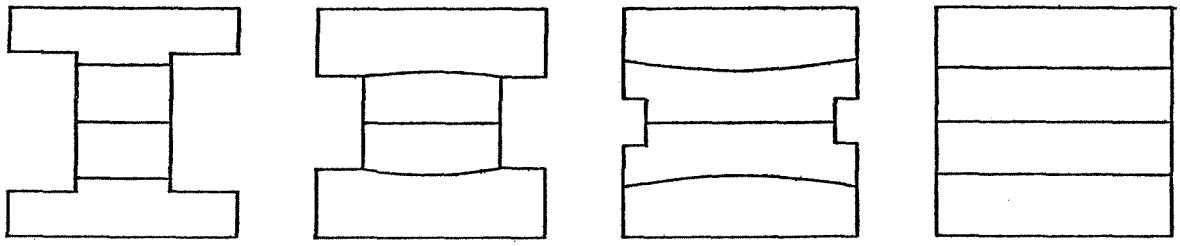

16.56 14.81 (SA-3) 14.64

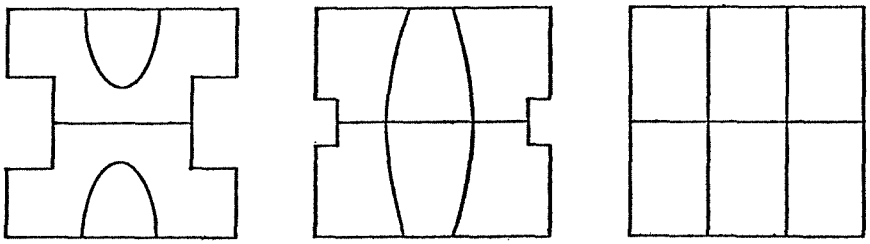

16.64 (SA-2) 13.53

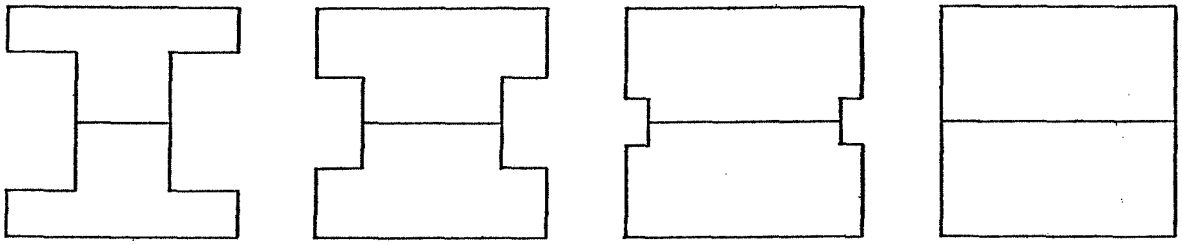

12.93 9.855 (SA-1) 8.790

$\delta_2=\delta_2=0.2$ $\delta_2=\delta_2=0.3$ $\delta_2=\delta_2=0.4$ $\delta_2=\delta_2=0.5$

Fig.5-8 (continued) (SA and AS mode)

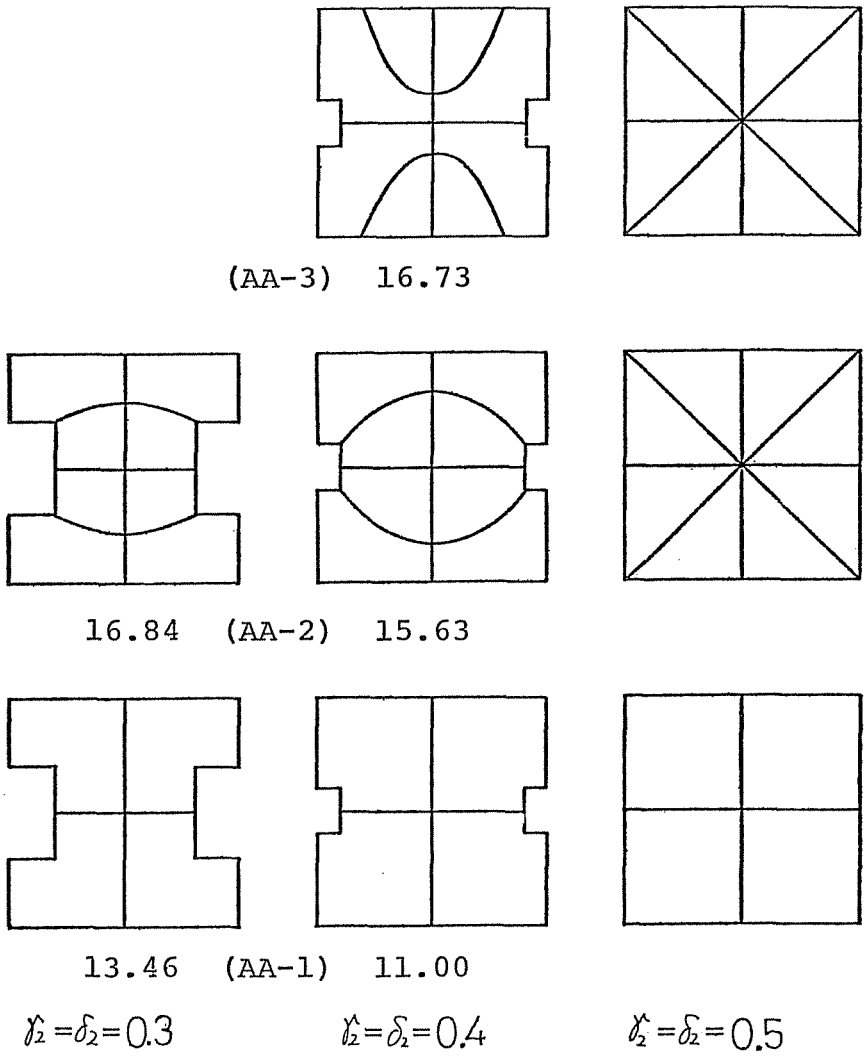

Fig.5-8 (continued) (AA mode)

5-5-2 Results and discussion

The frequency parameters $\lambda=a(\omega\sqrt{\rho/D})^{1/2}$ and nodal patterns are presented for clamped I-shaped plates in Fig.5-8. Since geometrical symmetry does not exist with respect to the diagonal axes in this case, four distinct modes of vibration appear on the plate and degeneracy does not occur. The results were calculated by use of 30 x 30 matrix (i.e., $i \times j = 5\times5$) with $m(n)=32$. Variations of the frequencies are shown in Fig.5-9 and it is noted that the rate of change is more conspicuous than that of cross-shaped plates.

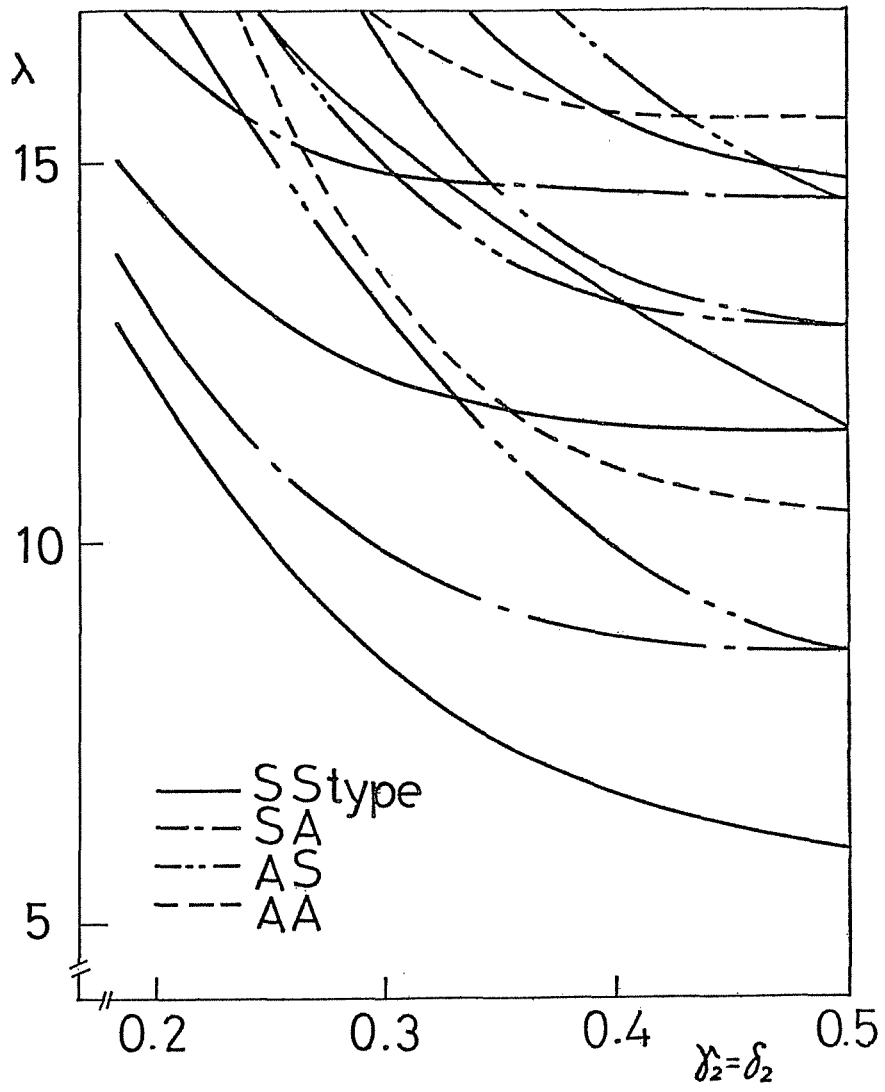

Fig.5-9 Variation of frequency parameters of a clamped I-shaped plate (μ =1.0, $\hat{\gamma}_2 = \delta_2$)

5-6 L-shaped plate

5-6-1 Application of the method

Figure 5-10 shows a clamped L-shaped plate which is symmetric about a diagonal axis ZZ. Since symmetric and antisymmetric modes of vibration arise about the axis, it is sufficient to consider a half part of the plate. The following segments are located on an original plate.

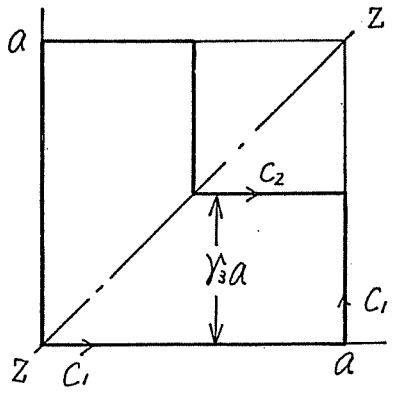

Table 5-10

$$
\begin{aligned}
&C_1: \ \alpha_1 = 1, \ \eta_1(z) = \gamma_3 z \\
&C_1': \ \xi_1' = z, \ \beta_1' = 0 \quad (0 \le z \le 1) \\
&C_2': \ \xi_2' = \gamma_3 + (1-\gamma_3) z, \ \beta_2' = \gamma_3
\end{aligned}
\tag{5-51}
$$

Both deflection and rotation are taken to be zero along the segment C_2', and only rotation is taken to be zero along C_1 and C_1'. Substituting Eqs.(5-51) into Eqs.(5-24) through (5-28) yields

$$
\left(M_{(1),ij}^{(\varphi_i \beta_i')} - M_{(2),ij}^{(\varphi_2' \beta_2')} \right)
\begin{Bmatrix}
(l_1/a) M_{x,i}^{(1)} \\
(l_i/b) M_{y,i}^{(i)} \\
(l_2'/\pi) Q_{y,i}^{(2')} \\
(l_2'/b) M_{y,i}^{(2')}
\end{Bmatrix} = 0
\tag{5-52}
$$

where

$$M_{(v,ij)}^{(\alpha\beta\beta')} = \sum_{m=1}^{\infty} \left(\begin{bmatrix} a_{m}(\alpha_p) & 0 \\ 0 & b_{m,i}(\zeta_{p'}) \end{bmatrix} \begin{bmatrix} G_{m,i}(\zeta_p, \alpha_q, \lambda) & G_{m,i}(\zeta_p, \beta_{q'}, \lambda) \\ H_m(\beta_{p'}, \alpha_q, \lambda) & H_m(\beta_{p'}, \beta_{q'}, \lambda) \end{bmatrix} \begin{bmatrix} \pm b_{m,j}(\zeta_q) & 0 \\ 0 & b_{m,j}(\xi_{q'}) \end{bmatrix} \right.$$

$$\left. + \begin{bmatrix} b_{m,i}(\zeta_p) & 0 \\ 0 & a_{m}(\beta_{p'}) \end{bmatrix} \begin{bmatrix} H_m(\alpha_p, \alpha_q, \lambda) & H_m(\alpha_p, \beta_{q'}, \lambda) \\ G_{m,i}(\xi_{p'}, \alpha_q, \lambda) & G_{m,i}(\xi_{p'}, \beta_{q'}, \lambda) \end{bmatrix} \begin{bmatrix} b_{m,j}(\zeta_q) & 0 \\ 0 & \pm b_{m,j}(\xi_{q'}) \end{bmatrix} \right) \quad (5\text{-}53)$$

$(+ : S \text{ type}, - : A \text{ type})$

with

$$a_m(\alpha_p) = \left[m \cos m\pi \right] \quad , \quad b_{m,i}(\zeta_p) = \left[\phi_{m,i}(\zeta_i) \right] \quad (5\text{-}54)$$

$$a_m(\beta_{p'}) = \begin{bmatrix} m & 0 & 0 \\ 0 & \sin m\pi\beta_{2'} & 0 \\ 0 & 0 & m\cos m\pi\beta_{2'} \end{bmatrix}, \quad b_{m,i}(\xi_{p'}) = \begin{bmatrix} \phi_{m,i}(\xi_{1'}) & 0 & 0 \\ 0 & \phi_{m,i}(\xi_{2'}) & 0 \\ 0 & 0 & \phi_{m,i}(\xi_{2'}) \end{bmatrix} \quad (5\text{-}55)$$

$$G_{m,i}(\zeta_p, \alpha_q, \lambda) = \frac{-1}{\sinh m_i \pi} \left[\psi_{m,i}(\zeta_i) \right] \quad (5\text{-}56)$$

$$G_{m,i}(\zeta_p, \beta_{q'}, \lambda) = \frac{1}{m_i \sinh m_i \pi} \left[\psi_{m,i}(\zeta_i) m_i \quad \psi_{m,i}(\zeta_i) \sinh m_i\pi(1-\beta_{2'}) \quad -\psi_{m,i}(\zeta_i) \cosh m_i\pi(1-\beta_{2'}) \right] \quad (5\text{-}57)$$

$$H_m(\beta_p', \alpha_q, \lambda) = \frac{-1}{\sinh m_1\pi} \begin{bmatrix} m_1 \\ \sinh m_1\pi\beta_2' \\ m_1\cosh m_1\pi\beta_2' \end{bmatrix} \tag{5-58}$$

$$H_m(\beta_p', \beta_q', \lambda) = \frac{1}{m_1\sinh m_1\pi} \begin{bmatrix} -m_1^2\cosh m_1\pi & m_1\sinh m_1\pi(1-\beta_2') & -m_1^2\cosh m_1\pi(1-\beta_2') \\ m_1\sinh m_1\pi(1-\beta_2') & \sinh m_1\pi(1-\beta_2')\sinh m_1\pi\beta_2' & \frac{m_1}{2}\sinh m_1\pi(1-2\beta_2') \\ -m_1^2\cosh m_1\pi(1-\beta_2') & \frac{m_1}{2}\sinh m_1\pi(1-2\beta_2') & -m_1^2\cosh m_1\pi(1-\beta_2')\cosh m_1\pi\beta_2' \end{bmatrix} \tag{5-59}$$

$$H_m(\alpha_p, \alpha_q, \lambda) = \frac{-1}{\sinh m_1\pi} \begin{bmatrix} m_1\sinh m_1\pi \end{bmatrix} \tag{5-60}$$

$$H_m(\alpha_p, \beta_q', \lambda) = \frac{-1}{\sinh m_1\pi} \begin{bmatrix} m_1 & \sinh m_1\pi\beta_2' & m_1\cosh m_1\pi\beta_2' \end{bmatrix} \tag{5-61}$$

$$G_{m,i}(\xi_p', \alpha_q, \lambda) = \frac{-1}{\sinh m_1\pi} \begin{bmatrix} \psi_{n,i}(\xi_1') \\ \psi_{n,i}(\xi_2') \\ \psi_{n,i}(\xi_2') \end{bmatrix} \tag{5-62}$$

$$G_{m,i}(\xi_p', \beta_q', \lambda) = \frac{1}{n_1\sinh n_1\pi} \begin{bmatrix} n_1\psi_{n,i}(1-\xi_1') & \frac{n_1}{\pi}\frac{\sin i\pi\beta_2'}{i^2+n_1^2}\sinh n_1\pi & \frac{n_1 i}{\pi}\frac{\cos i\pi\beta_2'}{i^2+n_1^2}\sinh n_1\pi \\ n_1\psi_{n,i}(1-\xi_2') & \psi_{n,i}(1-\xi_2')\sinh n_1\pi\beta_2' & \psi_{n,i}(1-\xi_2')\, n_1\cosh n_1\pi\beta_2' \\ n_1\psi_{n,i}(1-\xi_2') & \psi_{n,i}(1-\xi_2')\sinh n_1\pi\beta_2' & \psi_{n,i}(1-\xi_2')\, n_1\cosh n_1\pi\beta_2' \end{bmatrix} \tag{5-63}$$

5-6-2 Results and discussion

Table 5-3 presents the convergence characteristics of frequency parameter λ for the lowest five modes of a clamped L-shaped plate, when terms $i \times j$ of Fourier series increase. The frequency parameters converge within the range of four significant figures for A-1, S-2 and A-2 mode, and it is noted that all the frequency parameters tend to converge although the rate of convergence is different depending upon the modes. In the numerical examples, 6 terms of Fourier series were used. The convergence for the infinite series in m,n was quite satisfactory, since the frequency equation was expressed by single series in m or n only. $m(n)=32$ terms of the infinite series, which is sufficient to assure the complete convergence, were used for the calculation here.

The frequency parameters and corresponding nodal patterns obtained here for a L-shaped plate are presented with the experimental results in the next section. Variation of the frequencies with the shape parameter γ_3 is shown in Fig. 5-11.

Table 5-3 Convergence of the frequency parameters λ

$i \times j$ \ mode	S-1	A-1	S-2	S-3	A-2
2x2	7.273	9.095	10.19	11.65	12.00
4x4	7.449	9.139	10.24	11.99	12.23
6x6	7.502	9.145	10.25	12.08	12.24
8x8	7.527	9.145	10.25	12.11	12.24
10x10	7.543	—	—	12.13	—
12x12	7.556			12.15	

($\gamma_3=0.6, m=32$)

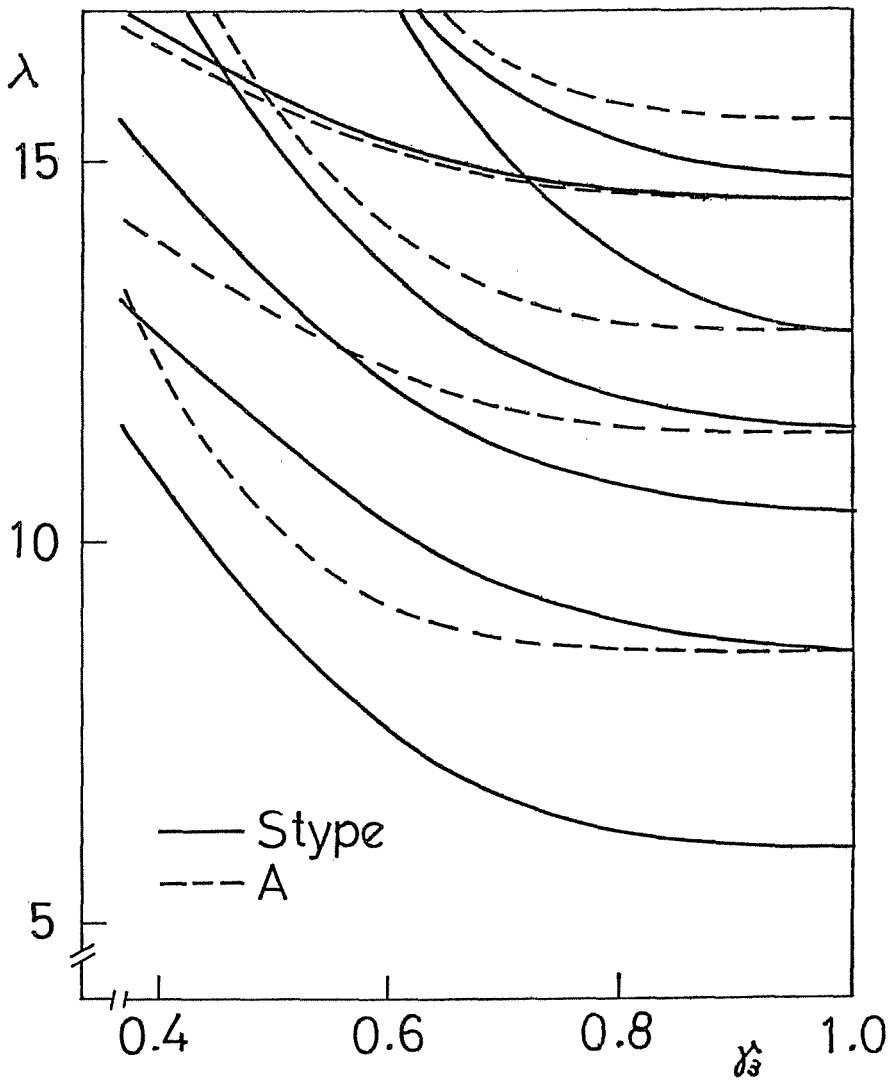

Fig.5-11 Variation of frequency parameters for a clamped L-shaped plate (μ=1.0)

5-7 L-shaped plate (Experiment)

5-7-1 Review on the experimental studies

The experimental methods on plate vibration are discussed and the results obtained by the Chladni method are presented in this section. The experimental methods are divided into two categories: the well-known Chladni method and a technique by use of holographic interferometry.

The Chladni method is a simple and useful experimental procedure to obtain nodal patterns of flat plates. When a plate is excited at a certain frequency corresponding to a natural frequency of the plate, some nodal lines (i.e., zero-deflection lines) appear and fine sands splinkle on the plate and move to the lines. After some seconds, a nodal pattern is formed with the particles. It is naturally known that this method cannot be applied to curved plates. Chladni, in his pioneer work [140] in 1802, gave illustrations of 52 figures for a square plate, 43 circular, 30 hexagonal, 52 rectangular, 26 elliptical, 15 semi-circular and 25 triangular. After a century and a half, Waller [118] made an extensive study of Chladni's figures in uniform metal plates of various different shapes. A new means was introduced to excite a plate using a chip of solid carbon dioxide. Since then, the Chladni method has been frequenctly used, in many cases, to show validity of numerical results obtained by analytical solutions. Ochs and Snowdon [141,142] presented experimental works to obtain transmissibility across rectangular and circular plates with constraints. Some interesting

Chladni's figure are shown. One of the recent works dealing with the Chladni's figure of circular plates is by Ravenhall and Som [143]. Three different test specimens of brass, aluminium and steel, are used and an empirical formula is presented, utilizing the relationship which exists between the number of nodal lines and the frequencies. Steinberg [144] collected experimental results of plates of various shapes having different arrangements.

In contrast with a long history of the Chladni method, the holographic interferometric technique has a short history of a quarter century. A remarkable progress has been made and its recent development is given in [145]. Since detailed descriptions on the method are beyond the scope of the present work, its principle and experimental apparatus should be referred to [146,147,148,149]. Besides the works by Maruyama and Ichinomiya [150,151], this technique is widely applied, for example, to a point-supported square plate [152], a rib-stiffened rectangular plate [153] and a triangular plate [112].

5-7-2 Experimental procedure

The experimental apparatus used here is illustrated in Fig.5-12. A thin steel plate was clamped between two thick steel plates having L-shaped inner boundary. The test plate was excited by means of an electromagnet exciter, which was positioned at various locations under the plate depending upon modes of vibration. Powders of cork were used, instead

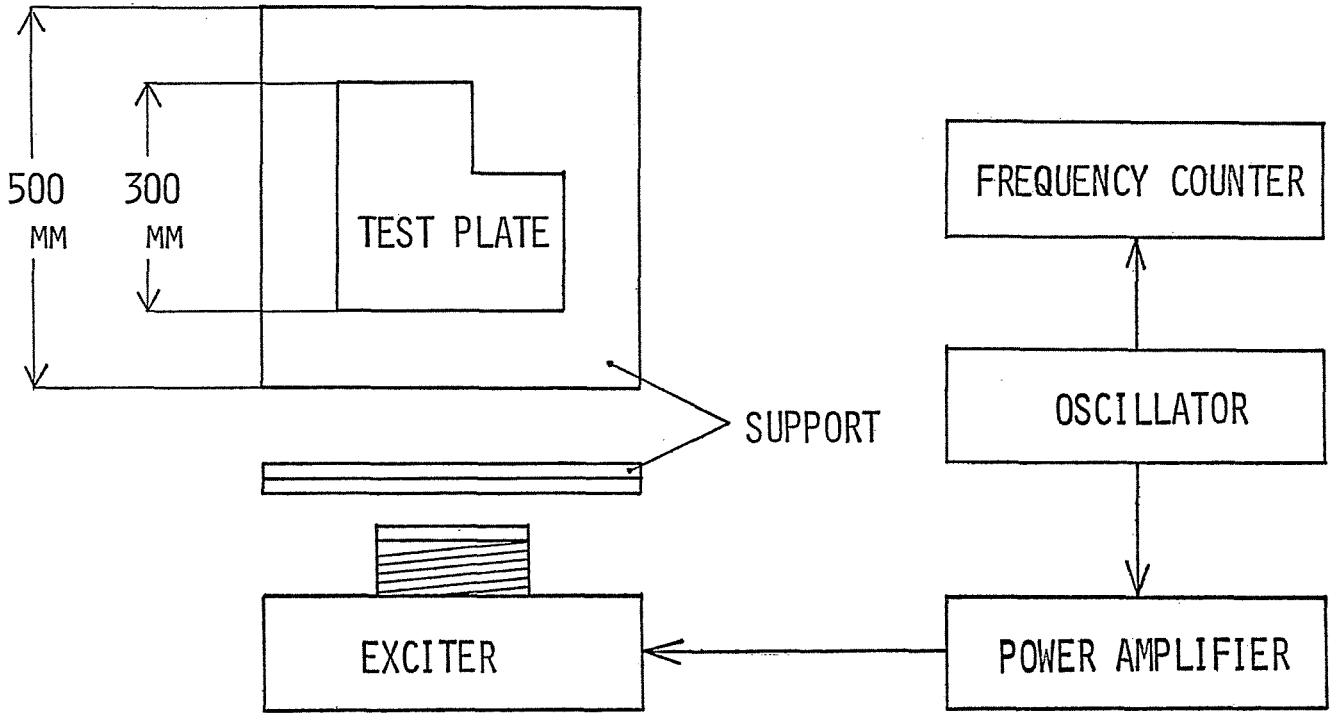

Fig.5-12 Experimental apparatus

of sands, in this experiment to increase the contrast of the patterns for photographic purpose, and also to avoid adding extra mass of powder to the plate. Otherwise this additional mass may shift the natural frequencies. The frequency dial of the oscillator was adjusted until a frequency was reached to the state, in which the particles splinkled on some areas of the plate while remaining still on nodal lines. This indicated that one of the natural frequencies was reached and the particles defined a nodal pattern. Another indication was the sound which occurred at a resonant frequency. The accurate resonant frequency was checked by using a digital counter. This procedure was repeated for other frequencies.

It was the most formidable part to make a test plate set-up shown in Fig.5-13, and also the most important part in the experiment because it considerably depends on the initial success of achieving the boundary conditions whether an excellent agreement is obtained between theory and experiment. A procedure of making the set-up was as follows. A L-shaped inner boundary was roughly cut from two steel plates with dimensions 500mm by 500mm by 9mm. These two thick plates were connected with 12mm and 8mm screw bolts. Then, inner boundary was precisely formed by a milling machine. Because of diameter of the milling drill, corners of the inner boundary remained round, but it is expected that these round corners practically have no effects on the frequencies since the plate deflection is almost zero in the vicinity of the corners.

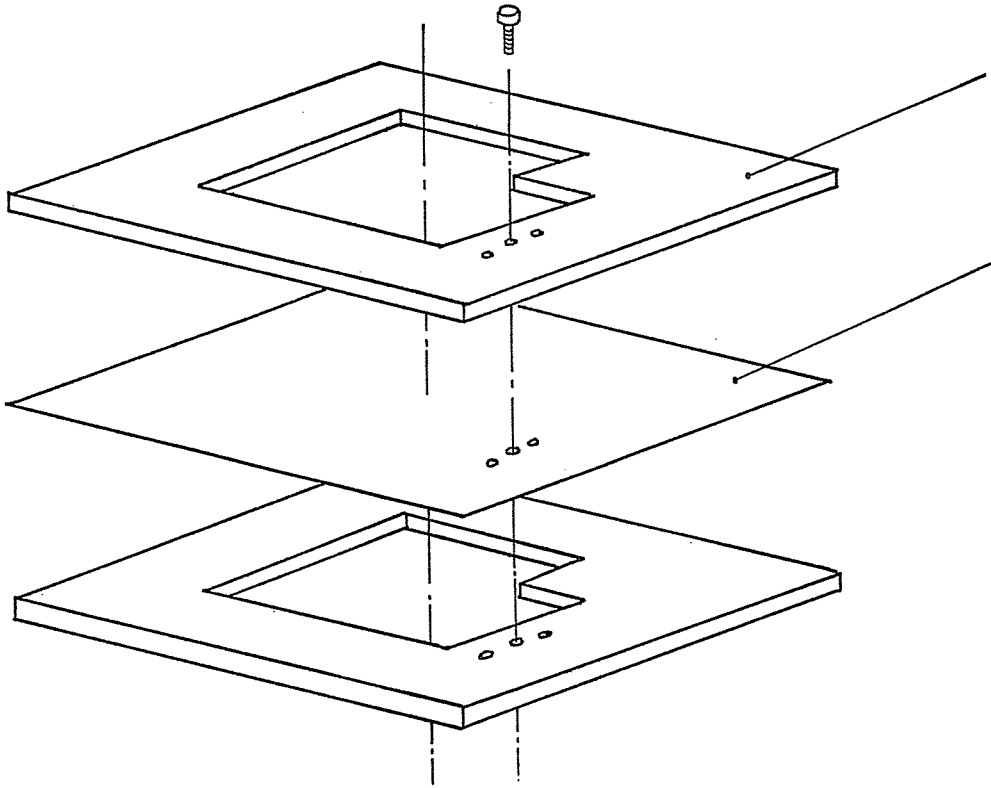

Fig.5-13 Test plate set-up

In the idealized boundary condition of clamp used in the analysis, it is assumed that deflection and rotation are perfectly zero along the edge. In the experiment, however, the supports clamping the test plate are also elastic, even though they are thick, and the idealized condition is never made. Some steel bars with ⊔-shaped cross section were attached around the inner boundary, as shown in Fig.5-14, to increase stiffness of the support and it turned out that this reinforcement actually increased the frequencies of the test plate.

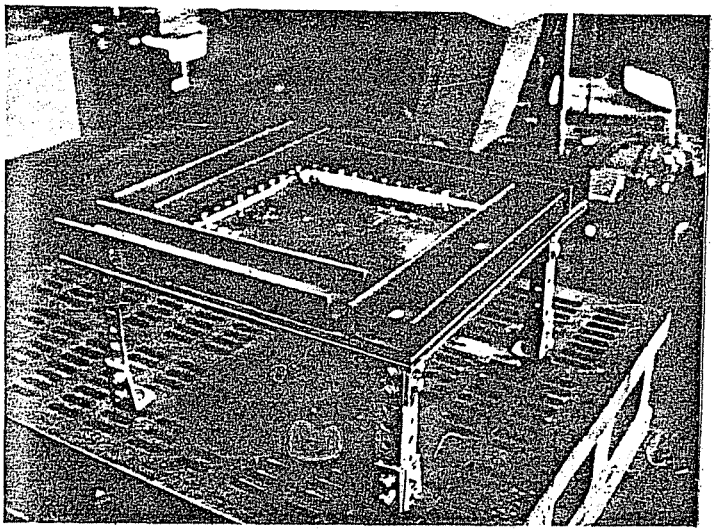

Fig.5-14 Test plate set-up

5-7-3 Results and discussion

Figure 5-15 shows photographs of Chladni's figure generated on the test plates with the shape parameter γ_3 = 0.6 and 0.8. Photographs are presented with the frequencies at which the figures were made and the results obtained by an analytical method. Resonant frequencies are converted into nondimensional parameters. For all the modes, frequency parameters obtained by the experiment are lower than those by the analytical method. This difference can be attributed to the experimental error, particularly due to the incomplete boundary conditions used. The maximum difference between analytical and experimental values is found in the 8th mode (A-4) of 7.2 percent for γ_3=0.6, and the 3rd mode (S-2) of 5.6 percent for γ_3=0.8. Conversely, the minimum difference is in the first (S-1) and 5th mode (A-2) of 2.8 percent for γ_3=0.6, and the 15th mode of 2.1 percent for γ_3=0.8. The difference is increased as γ_3 is taken to be smaller and the plate becomes more irregular. In both cases of γ_3=0.6 and γ_3=0.8, good agreement was reached for the fundamental modes. It has to be pointed out that the percentage difference doubles when the frequencies are expressed in terms of cycle-per-second (Hz) due to the relation $f = c\lambda^2$. The constant C can be given by calculating

$$\lambda^4 = \frac{a^4\omega^2\rho}{D} = \frac{48\pi^2 a^4 \rho(1-\nu^2)}{Eh^3} \times f^2 \qquad (5\text{-}64)$$

where Young's modulus: E= 2.1x10^4 [kg/mm^4], mass per unit area: ρ/h = 0.80x10^{-9} [kg·sec^2/mm^4], a =300mm, ν =0.30 and h =

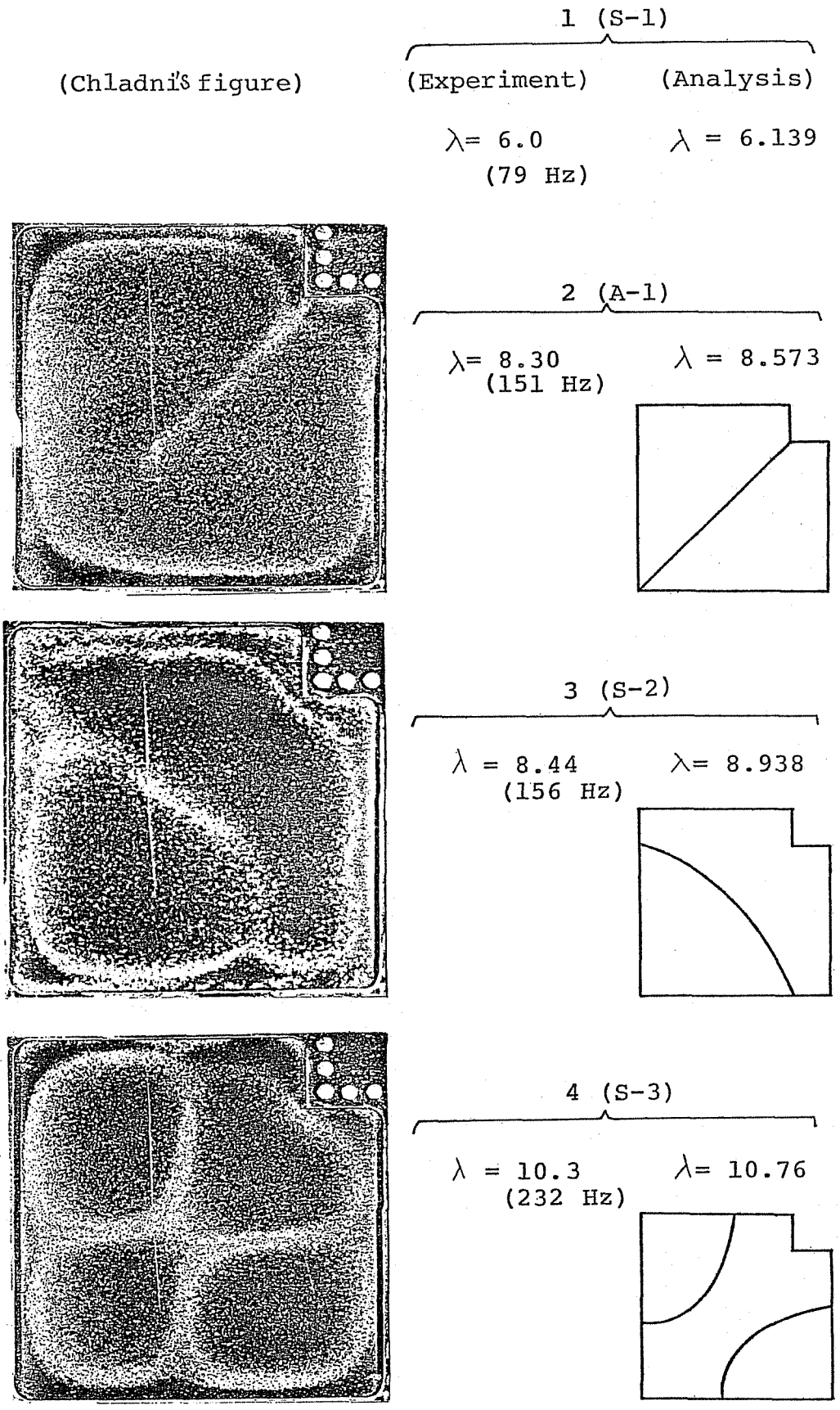

Fig.5-15 Frequency parameters and nodal patterns obtained by the Chladni method and the analytical solution for clamped L-shaped plates (ν_s=0.80).

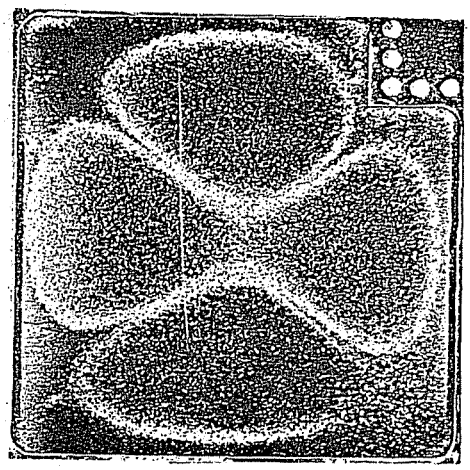

5 (A-2)

(Experiment) (Analysis)

λ= 11.2 (275 Hz)

λ = 11.50

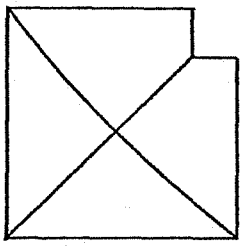

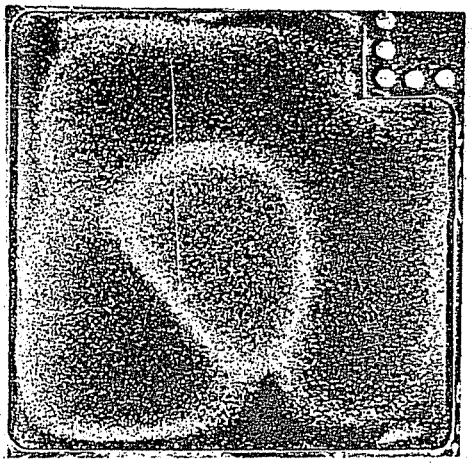

6 (S-4)

λ= 11.4 (283 Hz)

λ = 11.83

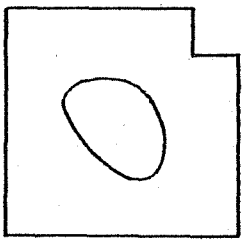

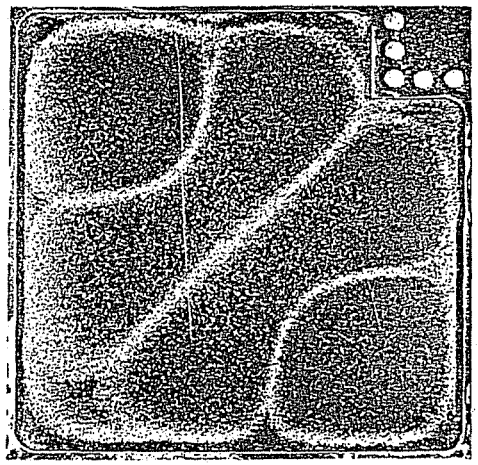

7 (A-3)

λ= 12.5 (343 Hz)

λ= 12.88

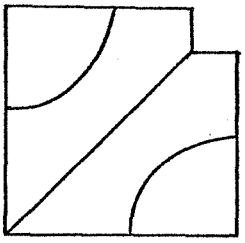

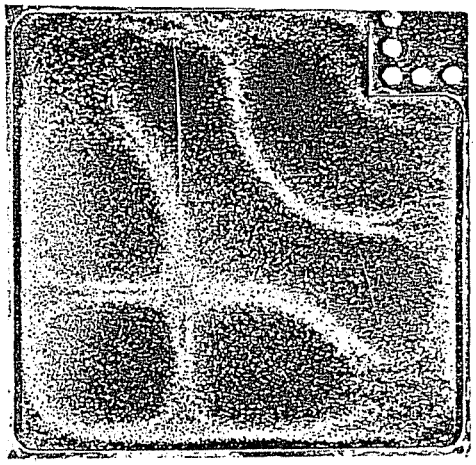

8 (S-5)

λ = 13.2 (379 Hz)

λ= 13.75

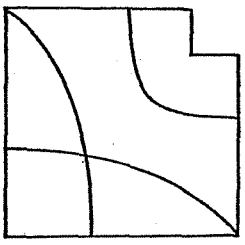

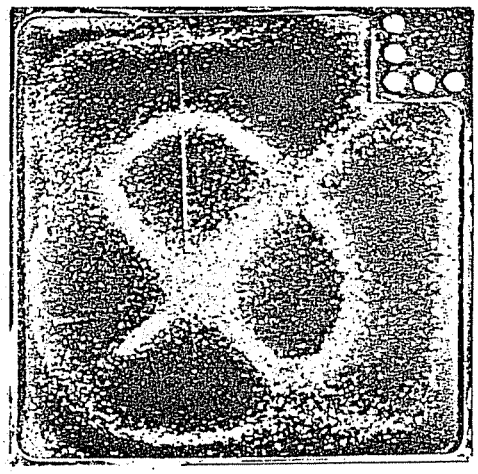

9 (A-4)

(Experiment) (Analysis)

λ= 14.0 (428 Hz) λ= 14.59

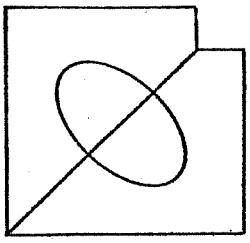

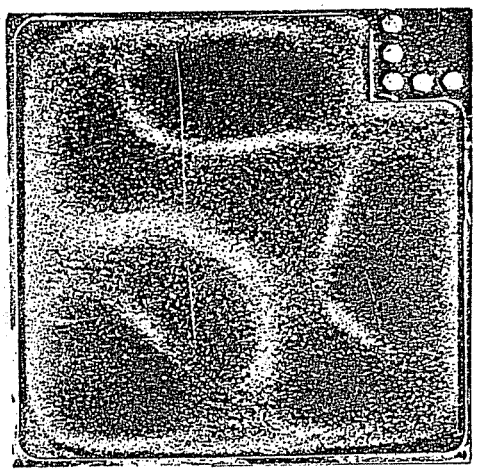

10 (S-6)

λ= 14.2 (441 Hz) λ = 14.60

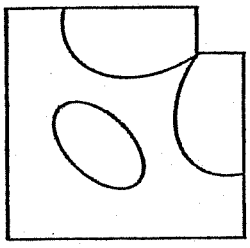

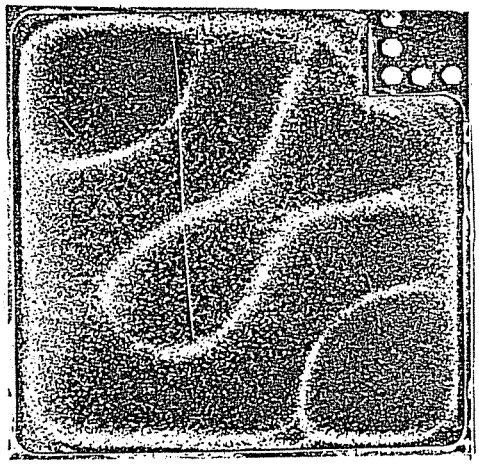

11 (S-7)

λ = 14.8 (480 Hz) λ = 15.24

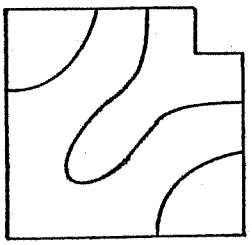

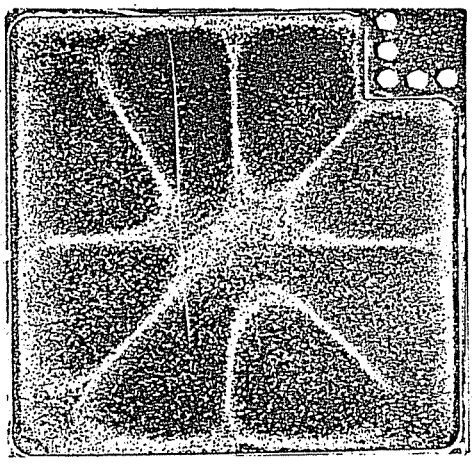

12 (A-5)

λ= 15.1 (500 Hz) λ= 15.72

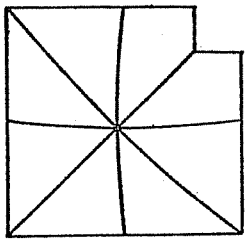

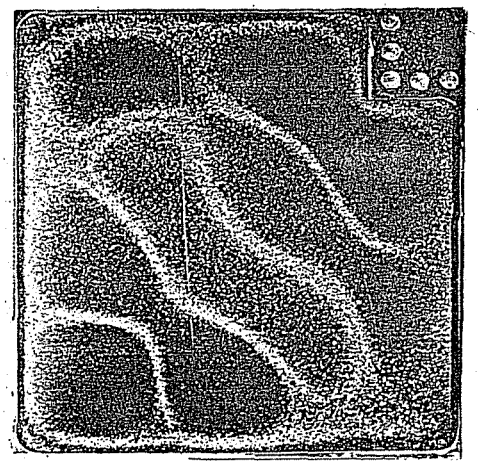

13 (S-8)

(Experiment) $\lambda = 16.2$ (577 Hz)

(Analysis) $\lambda = 16.62$

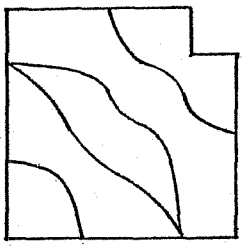

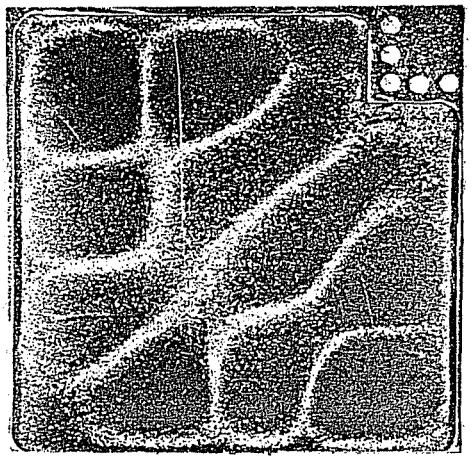

14 (A-6)

$\lambda = 16.8$ (619 Hz)

$\lambda = 17.25$

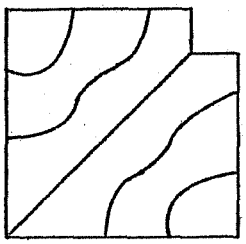

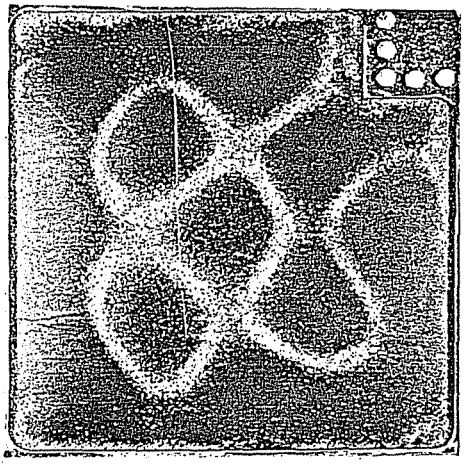

15 (S-9)

$\lambda = 17.2$ (645 Hz)

$\lambda = 17.56$

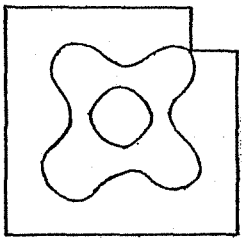

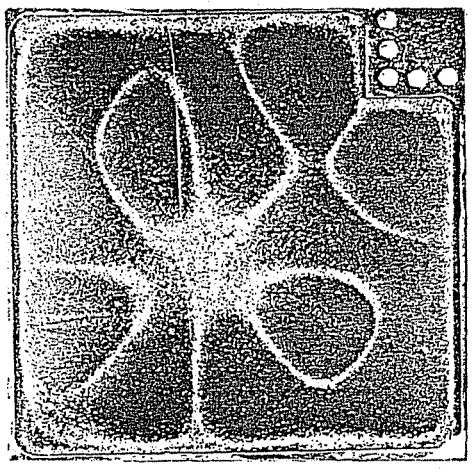

17* (A-7)

$\lambda = 18.1$ (721 Hz)

$\lambda = 18.75$

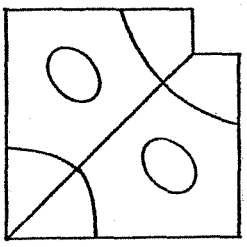

*The 16th mode was not found in the analytical results.

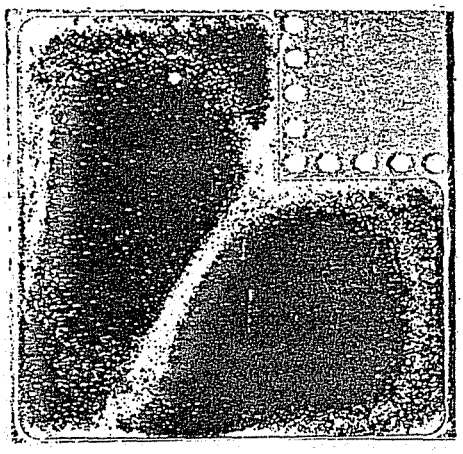

1 (S-1)

(Chladni's figure) (Experiment) (Analysis)

λ = 7.34 (118 Hz) λ = 7.556

2 (A-1)

λ = 8.86 (172 Hz) λ = 9.145

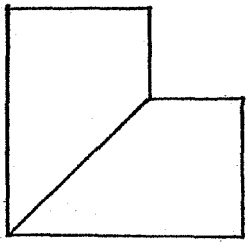

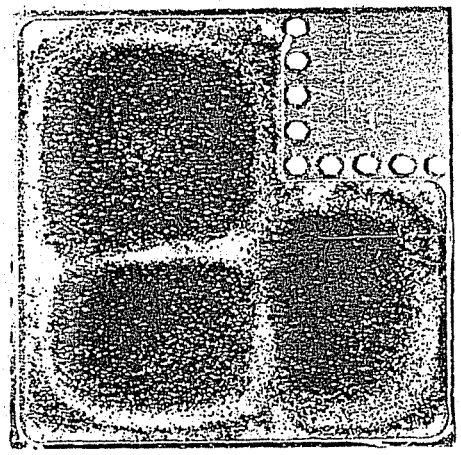

3 (S-2)

λ = 9.75 (208 Hz) λ = 10.25

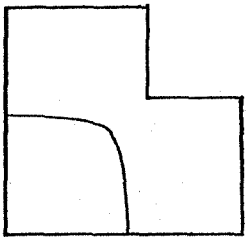

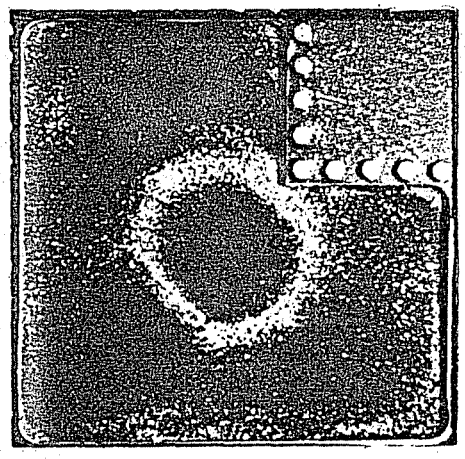

4 (S-3)

λ = 11.8 (306 Hz) λ = 12.15

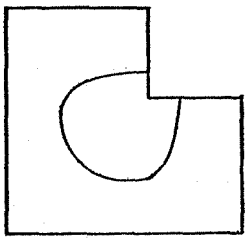

Fig.5-15 (continued) ($\hat{\gamma}_3$=0.60).

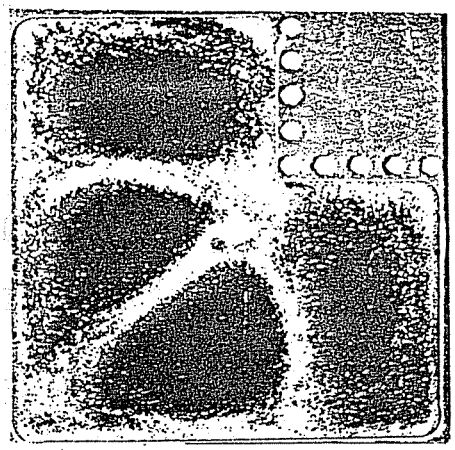

5 (A-2)

(Experiment) (Analysis)

λ = 11.9 (309 Hz) λ = 12.24

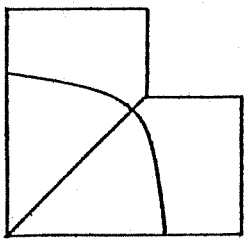

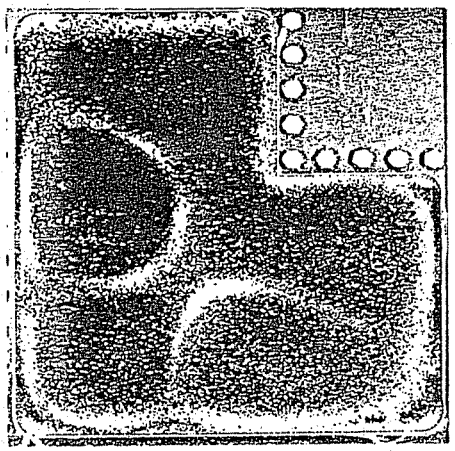

6 (S-4)

λ = 12.8 (360 Hz) λ = 13.59

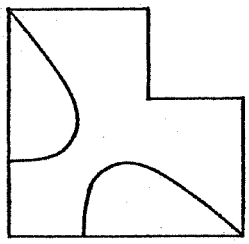

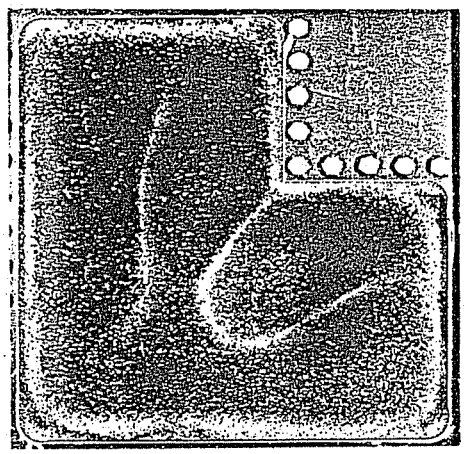

7 (A-3)

λ = 13.5 (399 Hz) λ = 14.12

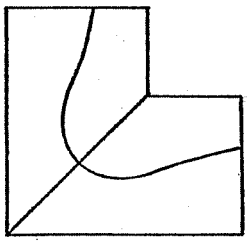

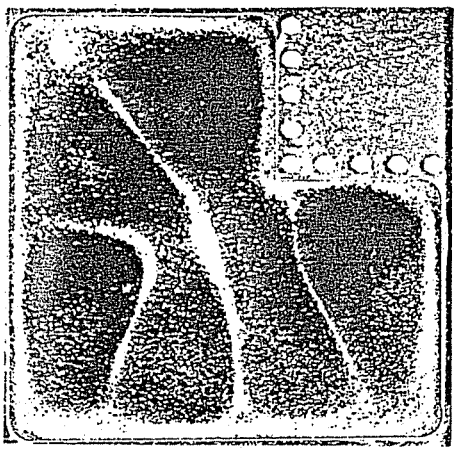

8 (A-4)

λ = 14.1 (438 Hz) λ = 15.20

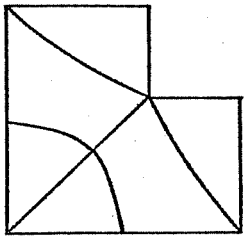

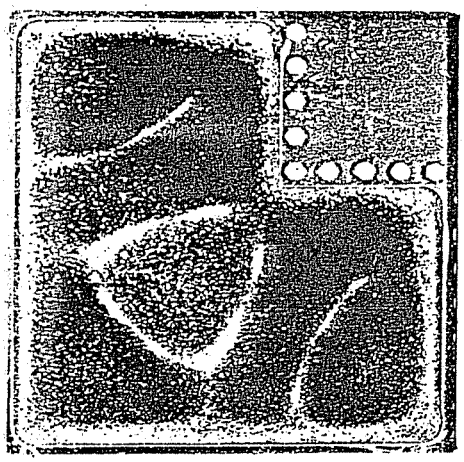

9 (S-5)

(Experiment) $\lambda = 14.6$ (464 Hz)

(Analysis) $\lambda = 15.22$

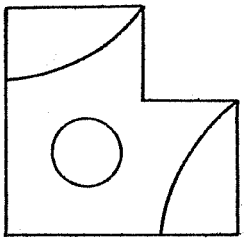

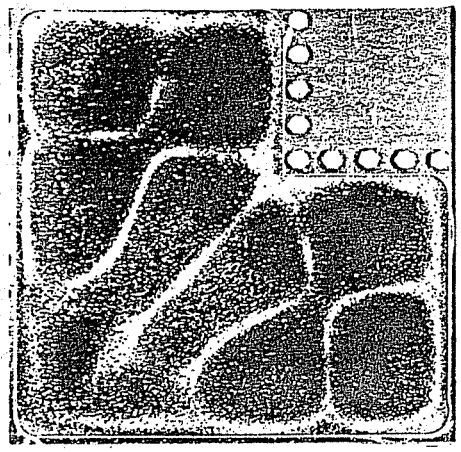

10 (A-5)

$\lambda = 16.6$ (601 Hz)

$\lambda = 17.22$

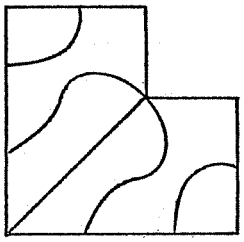

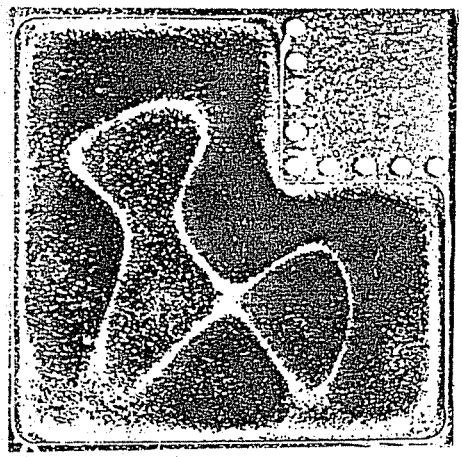

11 (S-6)

$\lambda = 16.8$ (621 Hz)

$\lambda = 17.62$

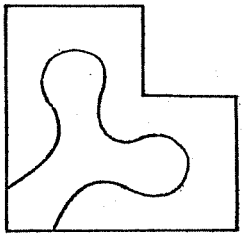

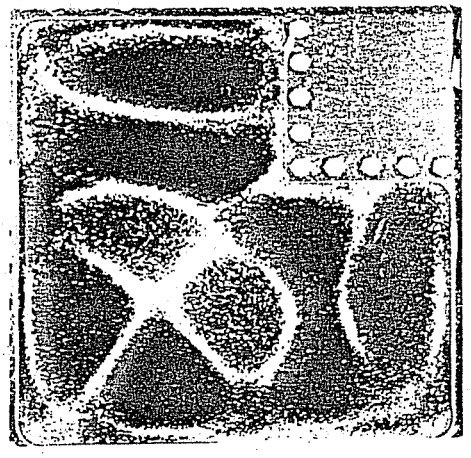

12 (A-6)

$\lambda = 17.1$ (644 Hz)

$\lambda = 18.09$

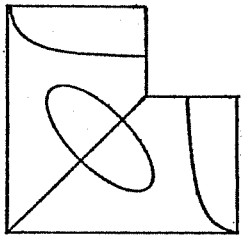

h =0.80mm, and therefore

$$C = \frac{0.80}{(300)^2\pi}\left(\frac{2.1 \times 10^4}{48 \times 0.80 \times 10^{-9} \times 0.91}\right)^{1/2} = 2.19 \quad (5\text{-}65)$$

As seen in the photographs, some nodal patterns are distorted and are difficult to define the exact shapes. This phenomenon can be attributed to non-uniformity in plate thickness and nonhomogeneity in the plate material, and also to difficulty in forming geometrical symmetry of the test plate.

CHAP.6 PLATES OF OTHER SHAPES (BIBLIOGRAPHY)

6-1 Introduction

Available references are introduced in this chapter on vibration of plates of various shapes which were not analyzed in the present study. Besides the plate shapes considered in the previous chapters, several different plate shapes are possible and actually found in practical situations of engineering.

No exact solutions exist and little has been done for the problems of trapezoidal and parallelogramic plates. The method presented by the author for clamped polygonal and irregularly shaped plates is readily applicable to the trapezoidal and parallelogramic plates with combinations of simply supported and clamped edges. Although no numerical calculations were done in this chapter, the frequency equations for the plates are presented for future study.

For annular plates, the exact solutions can be found in terms of Bessel functions, and a reasonable number of numerical results has been obtained for the case when the plate boundary is uniform. However, no results were found for annular plates having nonuniform boundary conditions. The analytical method developed by the author for circular plates with various boundary conditions can be extended to the plates with nonuniform edges.

A similar remark can be made for sectorial and annular sectorial plates. The exact solution is obtainable for

a special case of sector having two straight edges simply supported, but the accurate results are limited. The present method can be applied to sectorial and annular sectorial plates with nonuniform boundary conditions on the circular edges.

An elliptical plate, a generalization of a circular plate, has the exact solutions which are expressed in terms of Mathieu functions. Inasmuch as elliptical plates have far less practical significance than other plates, only a limited number of literature was found.

Rectangular plates with narrow cracks (slit, slot) or holes have received sparce treatment. This may be attributed to difficulty in obtaining analytical solutions, despite the fact that these plates are frequently found in many technical fields.

6-2 Trapezoidal plate

Klein [154] first solved the problem of a symmetric trapezoidal plate simply supported all around by use of collocation method (point matching) and presented the fundamental frequencies. Excellent studies are recently obtained by Chopra and Durvasula for symmetric [109] and unsymmetric [110] trapezoids, and the natural frequencies and nodal patterns are calculated up to higher modes by the Galerkin method and Fourier sine series in transformed coodinates. Orris and Petyt [111] introduced quadrilateral and triangular plate bending elements and applied to simply supported and

clamped trapezoidal plates, but the results presented are limited to a certain range of parameters. Donaldoson [155,156] presented an approximate method of analysis for the forced vibration of a quadrilateral or triangular plate under arbitrary conditions. Sepaha et al.[157] dealt with a trapezoidal cantilever plate.

A thorough and accurate numerical study remains to be done for trapezoidal plates with clamped edges along the entire edges and some other remaining boundary conditions. Table 6-1 and 2 include the frequency equations for the determination of natural frequencies and nodal patterns for symmetric and unsymmetric trapezoidal plates, respectively. The possible boundary conditions by the present method are shown in Fig.6-1.

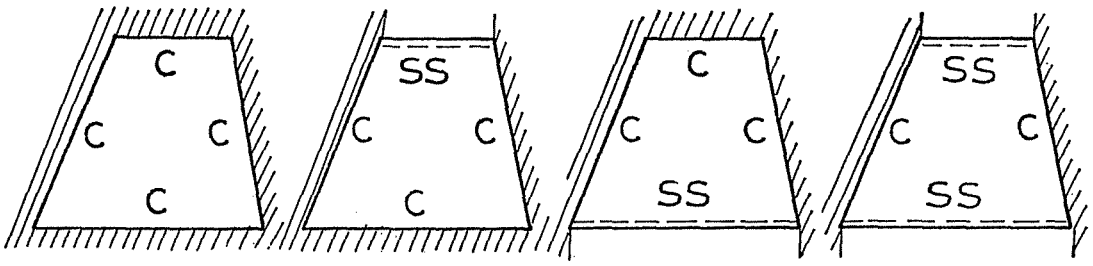

Fig.6-1 Possible boundary conditions

Table 6-1 Symmetric trapezoid

S type	A type
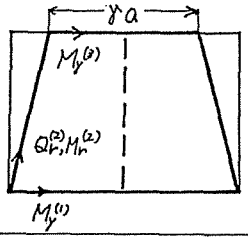	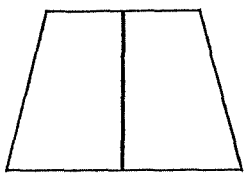

$$\left(\sum_m \sum_n \frac{1}{f_{mn(\lambda)}} \begin{Bmatrix} h^{(1)}_{mn,i} \\ g^{(2)}_{mn,i} \\ h^{(2)}_{mn,i} \\ h^{(3)}_{mn,i} \end{Bmatrix} \left\{ h^{(1)}_{mn,j} \;\; g^{(2)}_{mn,j} \;\; h^{(2)}_{mn,j} \;\; h^{(3)}_{mn,j} \right\} \right) \begin{Bmatrix} M^{(1)}_{y,j} \\ (a/\pi) Q^{(2)}_j \\ M^{(2)}_{r,j} \\ M^{(3)}_{r,j} \end{Bmatrix} = 0 \qquad (6\text{-}1)$$

where

$$g^{(p)}_{mn,i} = \int_0^1 \sin m\pi\xi_p \sin n\pi\eta_p \sin i\pi z \, dz$$

$$h^{(p)}_{mn,i} = m \sin\theta_p \int_0^1 \cos m\pi\xi_p \sin n\pi\eta_p \sin i\pi z \, dz + \mu n \cos\theta_p \int_0^1 \sin m\pi\xi_p \cos n\pi\eta_p \sin i\pi z \, dz$$

$\xi_1 = z/2$, $\eta_1 = 0$ $(\theta_1 = 0)$; $\xi_2 = \frac{z}{2}(1-\gamma)$, $\eta_2 = z$ $(\theta_2 = \tan^{-1}(2/\mu(1-\gamma)))$

$\xi_3 = \frac{1}{2}(1-\gamma) + \frac{\gamma}{2} z$, $\eta_3 = 1$ $(\theta_3 = 0)$

$m = 1, 3, \cdots$	$m = 2, 4, \cdots$

$n = 1, 2, 3, \cdots$

Table 6-2 Unsymmetric trapezoid

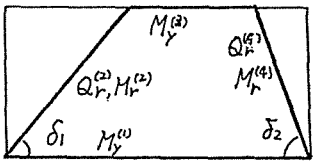

$$\left(\sum_m \sum_n \frac{1}{f_{mn(\lambda)}} \begin{Bmatrix} h^{(1)}_{mn,i} \\ g^{(2)}_{mn,i} \\ h^{(2)}_{mn,i} \\ h^{(3)}_{mn,i} \\ g^{(4)}_{mn,i} \\ h^{(4)}_{mn,i} \end{Bmatrix} \begin{Bmatrix} h^{(1)}_{mn,j} \\ g^{(2)}_{mn,j} \\ h^{(2)}_{mn,j} \\ h^{(3)}_{mn,j} \\ g^{(4)}_{mn,j} \\ h^{(4)}_{mn,j} \end{Bmatrix}^T \right) \begin{Bmatrix} M^{(1)}_{y,j} \\ (a/\pi) Q^{(2)}_{r,j} \\ M^{(2)}_{r,j} \\ M^{(3)}_{y,j} \\ (a/\pi) Q^{(4)}_{r,j} \\ M^{(4)}_{r,j} \end{Bmatrix} = 0 \qquad (6\text{-}2)$$

$\xi_1 = z$, $\eta_1 = 0$ $(\theta_1 = 0)$; $\xi_2 = z \cot\delta_1/\mu$, $\eta_2 = z$ $(\theta_2 = \delta_2)$

$\xi_3 = \frac{1}{\mu}\{(\mu + \cot\delta_1) - (\cot\delta_1 + \cot\delta_2) z\}$, $\eta_3 = 1$

$\xi_4 = 1 - z \cot\delta_2/\mu$, $\eta_4 = z$ $(\theta_4 = \pi - \delta_2)$

$m, n = 1, 2, 3, \cdots$

Equations (6-1) and (6-2) are derived for the plates clamped all around, and the element $M^{(1)}_y$ and/or $M^{(3)}_y$ in the equations are eliminated for other sets of the boundary conditions shown in Fig.6-1.

6-3 Parallelogramic plate

More publications have been obtained for the parallelogramic plate than for the trapezoidal plate. As pointed out in [1], most of research prior to 1966 dealt with the cantilevered parallelogramic plate to simulate airplane wings. Durvasula solved the problem of clamped [158] and simply supported [159] trapezoidal plates by using the Galerkin method and beam functions, satisfying the boundary conditions of zero deflection and normal slope on all edges. Durvasula and Abdel Fattah [160] presented an experimental work for the problem and compared nodal patterns determined by using fine grains of iron filings with the previous analytical results. Nair and Durvasula [163] considered parallelogramic plates with different edge conditions involving simple support and clamp by the Ritz method. Comprehensive results are presented for the natural frequencies and nodal patterns for differnt combinations of side ratio and skew angle. These authors [164] applied the partitioned (subdomain) method to a clamped parallelogram and comparison was made with the values obtained by the Galerkin method. Mizusawa et al. [165] analyzed the problem by the Rayleigh-Ritz method with B-spline function. Cuntze [161] and Rami Reddy [162] also treated the parallelogramic plate.

Table 6-3 presents the frequency equation for a clamped parallelogramic plate, and the element $M_y^{(1)}$ and/or $M_y^{(3)}$ are eliminated to consider other combinations of the boundary conditions as explained for the trapezoidal plate.

Table 6-3 Parallelogramic plate

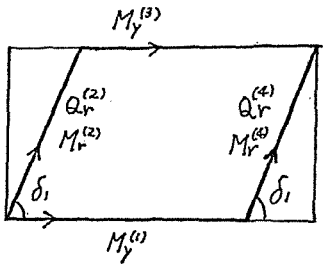

$$\left(\sum_m \sum_n \frac{1}{f_{mn}(\lambda)} \begin{Bmatrix} h_{mn,i}^{(1)} \\ g_{mn,i}^{(2)} \\ h_{mn,i}^{(2)} \\ h_{mn,i}^{(3)} \\ g_{mn,i}^{(4)} \\ h_{mn,i}^{(4)} \end{Bmatrix} \left\{ h_{mn,j}^{(1)} \; g_{mn,j}^{(2)} \; h_{mn,j}^{(2)} \; h_{mn,j}^{(3)} \; g_{mn,j}^{(4)} \; h_{mn,j}^{(4)} \right\} \right) \begin{Bmatrix} M_y^{(1)} \\ (a/\pi) Q_r^{(2)} \\ M_r^{(2)} \\ M_y^{(3)} \\ (a/\pi) Q_r^{(4)} \\ M_r^{(4)} \end{Bmatrix} = 0 \qquad (6\text{-}3)$$

$$\xi_1 = z \cot\delta_2 / \mu, \quad \eta_1 = 0 \quad (\theta_1 = 0)$$

$$\xi_2 = z \cot\delta_1 / \mu, \quad \eta_2 = z \quad (\theta_2 = \delta_1)$$

$$\xi_3 = \frac{1}{\mu} \{ \cot\delta_1 + (\mu - \cot\delta_1) z \}, \quad \eta_4 = 1 \quad (\theta_3 = 0)$$

$$\xi_4 = 1 - z \cot\delta_1 / \mu, \quad \eta_4 = z \quad (\theta_4 = \delta_1)$$

$$m, n = 1, 2, 3, \cdots$$

6-4 Annular plate

A comprehensive study was made by Raju [166] to yield the natural frequencies of annular plates having nine possible combinations of boundary conditions along the inner and outer boundary. Marchi and Diaz [167,168] treated axisymmetric vibration of annular plates by means of the integral-transform method, and the method was extended to a plate with elastic edge conditions.

Ramaiah and Vijayakumar [169] considered the location of nodal circles on annular plates and showed that annular plates of narrow width behave like long rectangular plates of the same width. Wilson and Garg [170] compared natural frequencies of annular plate segments with those obtained by using curved beam theory. Eastep and Hemmig [171] employed perturbation series of the modes of a circular plate and boundary curve by truncated Fourier series, and applied the method to an eccentric annulus.

Notable studies were obtained by Nagaya [172,173,174] on circular plates with eccentric holes (eccentric annulus). The Fourier expansion method was used, satisfying the inner boundary conditions exactly and the outer boundary conditions by truncated Fourier series approximately. This problem was also treated by the finite element method [175].

6-5 Sectorial and annular sectorial plate

An exact solution is obtainable for a sectorial and annular sectorial plate simply supported on the straight edges, but it appears that the known results are limited to the case whose solutions correspond to integer order Bessel functions due to the lack of Bessel function subroutine program for noninteger order. Westmann [176] considered a sector having a free circular edge by the Rayleigh method with one term approximation. Ramakrishnan and Kunukkasseril [177] considered annular sectors with two simply supported edges but, as pointed out above, the results are given only for the sector angle of 30°,45°,60° and 90°.

Ramaiah and Vijayakumar [178] used the Rayleigh-Ritz method with suitable coordinate transformation for the annular sector. The natural frequencies for various values of sector angle were obtained for all the nine combinations of clamp, simple support and free boundary conditions along the two circular edges. Rubin [179] solved the resulting equation of the plate with two straight edges simply supported by the Frobenius method.

For clamped sectorial plates, Ben-Amoz [180] applied the Rayleigh-Ritz method assuming a deflection function which satisfies the clamped edge conditons at the circular edge exactly. Rubin [181] presented variation of frequencies with the sector angle by the method of minimum potential energy. Bhattacharya and Bhowmic [182] employed Kantrovich method to present an approximate solution for a sector plate having two clamped straight edges and arbitrary conditions along the remaining edges. No numerical results, however, are given in the paper. Mukhopadhyay [183] employed a semi-analytic solution for the problem.

6-6 Elliptical plate

Shibaoka [184] and McNitt [185] published analytical works for vibration of a clamped elliptical plate by the energy method. Mazumdar [186] dealt with clamped and simply supported plates by the method of constant deflection lines. Pnueli [133] introduced a method to determine lower bounds of the solution and it was applied to a clamped

elliptic plate, and Johns [72] presented a simple formula to determine the fundamental frequency of the clamped plate. Nayfeh et al. [132] used a perturbation technique for clamped elliptical plates, and the frequencies and nodal patterns were presented for the lowest six modes.

For a simply supported ellipse, Leissa [187] employed the Rayleigh-Ritz method with a polynomial solution and the fundamental frequencies over a range of aspect ratio and Poisson's ratio were shown. Sato [188] used the exact solution in terms of Mathieu functions for the simply supported plate, and also treated an elliptical plate elastically restrained along the edge [189].

Waller [190] determined experimentally resonant modes of free elliptical plates. An analytical work was done by Beres [191] using the Rayleigh-Ritz method with a 25-term polynomial function, and the numerical results were compared with those in [190]. Sato [192] considered a confocal elliptical ring-shaped plate using Mathieu functions and the experimental results were also presented. Forsching [193] dealt with a cantilever semi-elliptical plate.

6-7 Rectangular plate with narrow slits

Plates with narrow slits (crack, slot) may be found in the applications of structural engineering. Due to the complicated analysis involved in the procedure, only a few references have been found for vibration of the plates. Solecki [194] formulated the problem but no numerical results were given. Lynn and Kumbasar [195] dealt with simply supported rectangular plates having a narrow slit parallel to

the edge, and variation of the frequencies was shown with the length of a slit. Keer and Sves [196] developed a method to analyze the bending of cracked plates, and Keer and Stahl [197] extended the method to vibration problem of the plates. Hirano and Okazaki [198] presented an analytical work of a rectangular plate with cracks parallel to the edges and simply supported on the other opposite edges. In all these references, however, only rectangular plates were concerned and no results were found for circular plates with slits.

6-8 Rectangular plate with holes

Plates with holes can be used to decrease the total mass of the plates in structural engineering. Takahashi [199] and Kumai [200] have dealt with a rectangular plate with a circular hole by using the Rayleigh-Ritz and point matching method, respectively. Basdekas and Chi [201] presented an approach to analyze dynamic response of plates with holes of various shape. Monahan et al. [202] treated the problem by the finite element method. Kristiansen and Soedel [203] obtained the fundamental frequencies of clamped square plates having some different holes. Paramasivam and Sridhar Rao [204,205] employed a finite difference and applied to a square plate with stiffened square holes. Hegarty and Ariman [206] used a least-square point matching method to analyze a rectangular plate with a central circular hole. Akus and Ali [207] made use of variational principles in conjunction with a finite difference to deal with a rectangu-

lar plate with one or two rectangular cutouts. Rajamani and Prabhakaran applied a method in [201] to the determination of dynamic response of composite plates with cutouts simply supported [208] and clamped [209] along the edges.

CHAP.7 CONCLUSIONS

The present study dealt with free, transverse vibration of thin, isotropic homogeneous plates of various shapes. The effects of such complicating factors as anisotropy, inplane forces, variable thickness, surrounding media, large (nonlinear) deflections, shear deformation, rotary inertia and material nonhomogeneity were not considered. Two types of analytical solutions were derived, utilizing the Fourier series, to study vibrational characteristics of the plates. The solutions were obtained in the following procedures.

Considering a rectangular plate with internal line elastic supports and regarding the reaction force and moment along the supports as unknown harmonic force and moment, the stationary response of the plate was expressed in terms of Green function. The force and moment distributed along the supports were expanded into Fourier sine series with unknown coefficients, and the homogeneous algebraic equation for the coefficients was derived by the constraint conditions along the supports. The natural frequencies and mode shapes were determined by calculating the eigenvalues and eigenvectors of the equation. (Solution (a))

Considering a circular plate, the general boundary conditions including the effects of non-uniform elastic springs and edge mass were expanded into Fourier series. The exact solutions of the differential equation govern-

ing plate vibration were substituted into the expanded boundary conditions, and the frequency equation of the plate was derived after some algebraic manipulations. (Solution (b))

In Chapter 1, solution (a) was developed for vibration of a rectangular plate elastically supported along some segments parallel to the edges. The solution was first applied to a clamped rectangular plate and the numerical results were compared to those obtained by other authors. Applying the method to a simply supported plate with a cross-shaped support and to a plate clamped at the outer edge and an internal rectangular support, the effects of varying the length and stiffness of the supports were evaluated numerically and their physical significances were discussed.

In Chapter 2, solution (b) was used to analyze vibration of circular plates having various boundary conditions. Fundamental equations were first derived for circular plates having uniform boundary conditions, and the numerical calculations were carried out only for the case when a reasonable number of accurate results was not found. Considering a simply supported plate having non-uniform rotational elastic constraints, the frequency equation was given in a simple form, and the natural frequencies and nodal patterns were calculated. As a more general case, a free circular plate elastically constrained by both translational and rotational springs along parts of the edge was considered. Variations of the natural

frequencies and nodal patterns were presented with the change of constraint parameters. This analytical method was extended to a free circular plate with nonuniform mass added to its boundary, and how the frequencies decrease with the addition of partial edge mass was clarified quantitatively.

In Chapter 4, solution (a) was conducted for vibration of a simply supported rectangular plate clamped along some segments located at arbitrary positions. The general solution thus obtained was applied to a clamped polygonal plate by locating some clamping segments so that they form a regular polygon on the original plate. The detailed frequency equations were derived for a clamped triangular, pentagonal, hexagonal, septagonal and octagonal plate, and the natural frequencies and nodal patterns were presented up to higher modes. The numerical examples revealed that the natural frequencies and nodal patterns of the polygonal plates could be separated into some groups, and the vibrational characteristics of the polygonal plates with more sides than six are quite similar to those of a clamped circular plate with the equal area. In contrast, the effect of plate shape was found distinctly in triangular, square and hexagonal plates.

In Chapter 5, making use of an anlysis presented in Chap.2 and an idea used in Chap.4, frequency equations were given for such irregularly shaped plates as cross-shaped, I-shaped and L-shaped plates. Since it was expected that the solutions, expressed in terms of double

Fourier series, would cause bad convergence, the frequency equations were then rewritten in a single series form. By this analytical manipulation, accurate numerical results were obtained and the natural frequencies and corresponding nodal patterns were presented with the parameters denoting geometric irregularity of the plate shape. An experimental investigation was carried out for a L-shaped plate, and the frequencies and nodal patterns determined by the Chladni method agreed well with the analytical results, showing the validity of the analysis.

A thorough survey was conducted attempting to collect related technical papers published mainly in this decade. The latest papers published up to the middle of 1979 were included. This survey clearly uncovered that vibration problems of the plates considered in this study have been received sparce treatment, in spite of the practical significance in engineering, because they have been considered quite difficult to obtain analytical solutions. Therefore, it seems obvious that this study is a considerable contribution in this field. The plates which were not analyzed in the study but might be included within the dissertation title were summarized for future use in Chapter 6 as a bibliography.

Analytical procedures described in the study are useful in extending the methods to further applications, and the resulting frequency equations were shown in convenient forms so that practical engineers can readily use. The numerical results presented both in tabular and graphi-

cal forms are useful for comparison and physical interpretation by other researchers, and may offer fundamental data for the design needs. For convenience, natural frequencies were expressed using the same definition throughout the study.

Concerning future aspects of the problem, the following comments can be made. The solution (a) has an excellent advantage of its applicability to clamped plates of arbitrary shape, and it is possible to make a computer program package for general use. Furthermore, the author believes that this method is extendable to simply supported plates of arbitrary shape. The solution (b) also has applications to annular and sectorial plates with various edge conditions. Although the complicating effects of plate such as anisotropy, varying thickness and so forth were excluded in the study, the analytical procedures developed here may provide basic ideas in accommodating these effects in the analysis. Particularly, orthotropy of plate can be easily considered in the analysis by using eigenfunctions of a simply supported orthotropic rectangular plate in solution (a).

REFERENCES

(1) Leissa,A.W.,"Vibration of plates," NASA SP-160 (1969).

(2) Leissa,A.W.,et al. "A comparison of approximate methods for the solution of plate bending problems," AIAA J., 7(5),pp.920-928 (1969).

(3) Leissa,A.W.,"Recent research in plate vibrations:classical theory," Shock Vibr. Dig.,9(10),pp.13-24 (1977).

(4) Leissa,A.W.,"Recent research in plate vibrations.1973-1976:complicating effects," Shock Vibr. Dig.,10(12),pp. 21-35 (1978).

(5) Young,D.,"Vibration of rectangular plates by the Ritz method," J. Appl. Mech.,17(4),pp.448-453 (1950).

(6) Iguchi,S.,"Die Eigenwertprobleme für die elastische rechteekige Platte," Mem. Fac. Eng., Hokkaido University, pp.305-372 (1938).

(7) Warburton,G.B.,"The vibration of rectangular plates," Proc. Inst. Mech. Eng., Ser.A,168(12),pp.371-384 (1954).

(8) Leissa,A.W.,"The free vibration of rectangular plates," J. Sound Vibr.,31(3),pp.257-293 (1973).

(9) Laura,P.A. and Saffell,Jr.B.F.,"Study of small-amplitude vibrations of clamped rectangular plates using polynomial approximations," J. Acous. Soc. Amer.,41(4),pp.836-839 (1967).

(10) Laura,P.A. and Duran,R.,"A note on forced vibrations of a clamped rectangular plate," J. Sound Vibr.,42(1),pp. 129-135 (1975).

(11) Warburton, G.B.,"Comment on "A note on forced vibrations of a clamped rectangular plate"," J. Sound Vibr.,45(3),pp. 461-466 (1976).

(12) Laura, P.A., Luisoni, L.E. and Filipich, C.,"A note on the determination of the fundamental frequency of vibration of thin, rectangular plates with edges possessing different rotational flexibility coefficients," J. Sound Vibr.,55(3), pp.327-333 (1977).

(13) Filipich, C.P., Reyes, J.A. and Rossi, R.E.,"Free vibrations of rectangular plates elastically restrained against rotation and translation simultaneously at the four edges," J. Sound Vibr.,56(2),pp.299-302 (1978).

(14) Laura, P.A., Luisoni, L.E. and Ficcadenti, G.,"On the effect of different edge flexibility coefficients on transverse vibrations of thin, rectangular plates," J. Sound Vibr.,57(3),pp.333-340 (1978).

(15) Laura, P.A. and Grossi, R.,"Transverse vibration of a rectangular plate elastically restrained against rotation along three edges and free on the fourth edge," J. Sound Vibr.,59(3),pp.355-368 (1978).

(16) Bassily, S.F. and Dickinson, S.M.,"On the use of beam functions for problems of plates involving free edges," J. Appl. Mech.,42(4),pp.858-864 (1975).

(17) Vijayakumar, K. and Ramaiah, G.K.,"Analysis of vibration of clamped square plates by the Rayleigh-Ritz method with asymptotic solutions from a modified Bolotin method," J. Sound Vibr.,56(1),pp.127-135 (1978).

(18) Dickinson, S.M.,"On the use of simply supported plate functions in Rayleigh method applied to the flexural vibration of rectangular plates," J. Sound Vibr.59(1), pp.143-146 (1978).

(19) Egle, D.M.,"The resonant response of a rectangular plate with an elastic edge restraint," Trans. ASME,Ser. B.,94(2),pp.517-525 (1972).

(20) Snowdon, J.C.,"Forced vibration of internally damped rectangular and square plates with simply supported boundaries," J. Acous. Soc. Amer., 56(4),pp.1177-1184 (1974).

(21) Snowdon, J.C.,"Vibration of simply supported rectangular and square plates to which lumped masses and dynamic vibration absorber are attached," J. Acous. Soc. Amer., 57(3),pp.646-654 (1975).

(22) Ochs, J.B. and Snowdon, J.C.,"Transmissibility across simply supported thin plates: part 1,rectangular and square plates with and without damping layers," J. Acous. Soc. Amer., 58(4),pp.832-840 (1975).

(23) Ochs, J.B. and Snowdon, J.C.,"Transmissibility across simply supported thin plates: part 2,rectangular plates with loading masses and straight ribs," J. Acous. Soc. Amer., 59(2),pp.350-363 (1976).

(24) Gorman, D.J. and Sharma, R.K.,"A comprehensive approach to the free vibration analysis of rectangular plates by use of the method of superposition," J. Sound Vibr., 47(1),pp.126-128 (1976).

(25) Gorman, D.J.,"Free vibration analysis of cantilever plates by the method of superposition," J. Sound Vibr., 49(4),pp.453-467 (1976).

(26) Gorman, D.J.,"Free-vibration analysis of rectangular plates with clamped-simply supported edge conditions by the method of superposition," J. Appl. Mech.,44(4), pp.743-749 (1977).

(27) Gorman, D.J.,"Free vibration analysis of the completely free rectangular plate by the method of superposition," J. Sound Vibr., 57(3),pp.437-447 (1978).

(28) Jones, R. and Milne, B.J.,"Application of the extended Kantrovich method to the vibration of clamped rectangular plates," J. Sound Vibr., 45(3),pp.309-316 (1976).

(29) Kerr, A.D.,"An extended Kantrovich method for the solution of eigenvalue problems," Intl. J. Solids Structs., 5, pp.559-572 (1972).

(30) Mukhopadhyay, M.,"A semi-analytic solution for free vibration of rectangular plates," J. Sound Vibr., 60(1), pp.71-85 (1978).

(31) Kurata, M. and Okamura, H.,"Natural vibrations of partially clamped plates," Proc. ASCE, 89(EM3),pp.169-186 (1963).

(32) Gajendar, N.,"Free vibrations of partially clamped rectangular plates," Bultene Teknik Universitesi, 20(2), pp.72-88 (1967).

(33) Ota, T. and Hamada, M.,"Fundamental frequencies of

simply supported but partially clamped square plates," Bull. JSME, 6(23),pp.397-403 (1963).

(34) Keer, L.M. and Stahl, B.,"Eigenvalue problems of rectangular plates with mixed edge conditions," J. Appl. Mech., 39(2),pp.513-520 (1972).

(35) Venkateswara Rao, G., Raju, I.S. and Murthy, T.V.G.K., "Vibration of rectangular plates with mixed boundary conditions," J. Sound Vibr., 30(2),pp.257-260 (1973).

(36) Tomotika, S.,"The transverse vibration of a square plate clamped at four edges," Phil. Mag., Ser.7 21(142),pp. 745-760 (1936).

(37) Ödman, S.T.A.,"Studies of boundary value problem.part III. characteristic functions of rectangular plates," Proc.NR24, Swedish Cement and Concrete Res. Inst., Roy. Inst. Tech. (Stochholm),pp.7-62 (1955).

(38) De Vito, L. et al.,"Sul calcolo degli autovalori della piastra quadrata incastrate lungo il bordo," Rendiconti di Scienze fisiche, mathematiche e naturali XL,pp.725-733 (1966).

(39) Bazley, N.W., Fox, D.O. and Stadter, J.T.,"Upper and lower bounds for the frequencies of rectangular clamped plates," Zeitschrift für angewandte Mathematik und Mechanik, 47(3),pp.191-198 (1967).

(40) Bazley, N.W.,"Upper and lower bounds for the frequencies of rectangular free plates," Zeitschrift für Angewandte Mathematic und Phisik, 18(4),pp.445-460 (1967).

(41) Marangoni, R.D., Cook, L.M. and Basavanhally, N.,"Upper and lower bounds to the natural frequencies of vibration of clamped rectangular orthotropic plates," Intl. J. Solids Structs., 14,pp.611-623 (1978).

(42) Cox, H.L. and Boxer, J.,"Vibration of rectangular plates point-supported at the corners," J. Aeron. Quart., 11(1), pp.41-50 (1960).

(43) John, D.J. and Nataraja, V.T.,"On the fundamental frequency of a square plate symmetrically supported at four points," J. Sound Vibr., 10(3),pp.404-410 (1969).

(44) John, D.J. and Nataraja, R.,"Vibration of a square plate symmetrically supported at four points," J. Sound Vibr., 25(1),pp.75-82 (1972).

(45) Reed, R.E.,"Comparison of methods in calculating frequencies of corner-supported rectangular plates," NASA TND-3030 (1965).

(46) Dowell, E.H.,"Free vibrations of a linear structure with arbitrary support conditions," J. Appl. Mech., 38,pp.595-600 (1971).

(47) Venkateswara Rao, G., Raju, I.S. and Amba-Rao, C.L.," Vibrations of point supported plates," J. Sound Vibr., 29(3),pp.387-391 (1973).

(48) Venkateswara Rao, G., Raju, I.S. and Murthy, T.V.G.K., "On the fundamental frequency of point supported plates," J. Sound Vibr., 40(4),pp.561-562 (1975).

(49) Sadasiva Rao, Y.V.K., Venkateswara Rao, G. and Amba Rao, C.L.,"Experimental study of vibrations of a four-point supported square plate," J. Sound Vibr., 32(2),pp.286-288 (1974).

(50) Leuner, T.R.,"An experimental-theoretical study of free vibrations of plates on elastic point supports," J. Sound Vibr., 32(4),pp.481-490 (1974).

(51) Damie, S.K. and Feeser, L.J.,"Vibration of four point-supported plates by a finite element method," J. Aero. Soc. India, 24(3),pp.375-377 (1972).

(52) Yang, W.H.,"Vibration of a plate with internal constraints," J. Appl. Mech., 41(4),pp.1072-1074 (1974).

(53) Klein, L.,"Vibrations of constrained plates by a Rayleigh-Ritz method using Lagrange multipliers," Quart. J. Mech. Appl. Math., 30(1),pp.51-70 (1977).

(54) Stahl, B. and Keer, L.M.,"Vibration and buckling of a rectangular plate with an internal support," Quart. J. Mech. Appl. Math., 25(4),pp.467-478 (1972).

(55) Takahashi, K. and Chishaki, T.,"Free vibrations of a rectangular plate on oblique supports," J. Sound Vibr., 60(2),pp.299-304 (1978).

(56) Irie, T., Yamada, G. and Narita, Y.,"Free vibration of a rectangular plate supported on the sides and some segments," Bull. JSME, 20(147),pp.1085-1092 (1977).

(57) Jacquot, R.G.,"The vibration of regularly supported elastic surface systems subject to additional point constraints," J. Sound Vibr., 32(4),pp.459-466 (1974).

(58) Poisson, S.D.,"Sur le Mouvement des Corps Élastiques," Mémoires de l'Academie Royal des Sciences de l'Institut de France," 8,p.357 (1829).

(59) Kirchhoff, G.,"Über das Gleichgewichit und die Bewegung einer elastischen Schebe," J. für die reine und angewandte Math., Crelle 40, p.51 (1850).

(60) Blanch, G.,"Notes on zeros of $I_{n+1}(x)\ J_n(x)+J_{n+1}(x)\ I_n(x)=0$," Math. Tables and Other Aids to Comput., 6(37),p.58 (1952).

(61) Carrington, H.,"The frequencies of vibration of flat circular plates fixed at the circumference," Phil. Mag., 50(6),pp.1261-1264 (1925).

(62) Maruyama, K.,"Measurements of vibrational modes of thin plate by holographic interferometry;part 1.clamped circular plate," Bull. Hokkaido Institute of Technology, 3,pp.185-196 (1970).

(63) Colwell, R.C. and Hardy, H.C.,"The frequencies and nodal systems of circular plates," Phil.Mag., 24(165),pp.1041-1055 (1937).

(64) Airey, J.,"The vibration of circular plates and their relation to Bessel function," Proc. Roy. Soc. (London), 23,pp.225-232 (1911).

(65) Itao, K. and Crandall, S.H.,"Natural modes and natural frequencies of uniform, circular, free edge plates," J. Appl. Mech., 46(2), pp.448-453 (1979).

(66) Gontkevich, V.S.,"Natural vibrations of plates and shells," A.P.Filippov,ed.,Nauk. Dumka (Kiev), (1964) (Transl. by Lockheed Missiles & Space Co.).

(67) Wah, T.,"Vibration of circular plates," J. Acous. Soc. Amer., 34(3),pp.275-281 (1962).

(68) Pardoen, G.C.,"Static, vibration and buckling analysis of axisymmetric circular plates using finite elements," Compt. Struct., 3(2),pp.355-375 (1973).

(69) Pardoen, G.C.,"Asymmetric vibration and stability of Circular plates," Compt. Struct., 9(1),pp.89-96 (1978).

(70) Jones, R.,"An approximate expression for the fundamental frequency of vibration of elastic plates," J. Sound Vibr. 38(4),pp.503-504 (1975).

(71) Mazumdar, J.,"Transverse vibration of elastic plates by the method of constant deflection," J. Sound Vibr., 18 (2),pp.147-155 (1971).

(72) Johns, D.J.,"Comments on "An approximate expression for the fundamental frequency of vibration of elastic plates"," J. Sound Vibr., 41(3),pp.385-387 (1975).

(73) Jacquot, R.G. and Lindsay, J.E.,"On the influence of Poisson's ratio on circular plate natural frequencies," J. Sound Vibr., 52(4),pp.603-605 (1977).

(74) Kantham, C.L.,"Bending and vibration of elastically restrained circular plates," J. Franklin Inst., 265(6),pp. 483-491 (1958).

(75) Laura, P.A., Paloto, J.C. and Santos, R.D.,"A note on the vibration and stability of a circular plate elastically restrained against rotation," J. Sound Vibr., 41(1),pp. 177-180 (1975); Erratum, 45(2),pp.302-303 (1976).

(76) Laura, P.A. and Geros, R.,"Further results on the vibration and stability of a circular plate elastically restrained against rotation," J. Sound Vibr., 41(3),pp.388-390 (1975).

(77) Laura, P.A., Luisoni, L.E. and Arias, A.,"Antisymmetirc modes of vibration of a circular plate elastically restrained against rotation and subjected to a hydrostatic state of in-plane stress," J. Sound Vibr., 47(3),pp.433-437 (1976).

(78) Laura, P.A., Pombo, J.L. and Luisoni, L.E.,"Forced vibrations of a circular plate elastically restrained against rotation," J. Sound Vibr., 45(2),pp.225-235 (1976).

(79) Laura, P.A., Arias, A. and Luisoni, L.E.,"Fundamental freqency of vibration of a circular plate elastically restrained against rotation and carrying a concentrated mass," J. Sound Vibr., 45(2),pp.298-301 (1976).

(80) Laura, P.A., Luisoni, L.E. and Lopes, J.J.,"A note on free and forced vibrations of circular plates: the effect of support flexibility," J. Sound Vibr., 47(2),pp.287-291 (1976).

(81) Singa Rao, K. and Amba Rao, C.L.,"Lateral vibration and stability relationship of elastically restrained circular plates," AIAA J., 10(12),pp.1689-1690 (1972).

(82) Snowdon, J.C.,"Forced vibration of internally damped circular plates with supported and free boundaries," J. Acous. Soc. Amer., 47(3),pp.882-891 (1970).

(83) Snowdon, J.C.,"Forced vibration of internally damped circular and annular plates with clamped boundaries," J. Acous. Soc. Amer., 50(3),pp.846-858 (1971).

(84) Saito, H. and Nakazawa, M.,"Free vibration of a circular plate on an elastic support," Trans. JSME, 32(235),pp.457-463 (1966),(in Japanese).

(85) Leissa, A.W. and Narita, Y.,"Natural frequencies of simply supported circular plates," J. Sound Vibr.,(to appear).

(86) Nowacki, W. and Olesiak, Z.,"Vibration, buckling and bending of a circular plate clamped along part of its periphery and simply supported on the remaining part," Bull. Acad. Pol. Sci., IV 4(4),pp.247-258 (1956).

(87) Bartlett, C.C.,"The vibration and buckling of a circular plate clamped on part of its boundary and simply supported on the remainder," Quart. J. Mech. Appl. Math., 16(4),pp. 431-440 (1963).

(88) Noble, B.,"The vibration and buckling of a circular plate clamped on part of its boundary and simply supported on the remainder," Proc. 9th Midwest. Conf. Solid and Fluid Mech., (1965).

(89) Hirano, Y. and Okazaki, K.,"Vibration of a circular plate having partly clamped or partly simply supported boundary," Bull. JSME, 19(132), pp.610-618 (1976).

(90) Hemmig, F.G.,"Investigation of natural frequencies of circular plates with mixed boundary conditions," Air Force Inst. Tech., School of Engng. Rep.,No.GAE/MC 175-11 (1975).

(91) Leissa, A.W., Laura, P.A. and Gutierrez, R.H.,"Transverse vibrations of circular plates having nonuniform edge constraints," J. Acous. Soc. Amer., 66(1),pp.180-184 (1979).

(92) Narita, Y. and Leissa, A.W.,"Transverse vibration of simply supported circular plates having partial elastic constraints," J. Sound Vibr.,(to appear).

(93) Bodine, R.Y.,"Vibrations of a circular plate supported by a concentric ring of arbitrary radius," J. Acous. Soc. Amer. 41(6),p.1551 (1967).

(94) Bodine, R.Y.,"The fundamental frequencies of a thin flat circular plate simply supported along a circle of arbitrary radius," J. Appl. Mech., 26, pp.666-668 (1959).

(95) Singh, A.V. and Mizra, S.,"Free axisymmetric vibration of a circular plate elastically supported along two concentric circles," J. Sound Vibr., 48(3),pp.425-429 (1976).

(96) Nagaya, K., Hirano, Y. and Okazaki, K.,"Transverse vibration of a circular plate on an eccentric annular elastic support," Bull. JSME, 22(167),pp.642-647 (1979).

(97) Chi, C. et al.,"Vibrational modes of the circular mirror with three support points," Opt. Soc. Amer., (Tucson, Ariz),(1971).

(98) Nakazawa, M.,"Free vibrations of a circular plate supported at several points of the boundary," Trans. JSME, 33(256),pp.1951-1961 (1967),(in Japanese).

(99) Chi, C.,"Modes of vibration in a circular plate with three simple support points," AIAA J., 10(2),pp.142-147 (1972).

(100) Irie, T. and Yamada, G.,"Free vibration of circular plate elastically supported at some points," Bull. JSME, 21(161),pp.1602-1609 (1978).

(101) Ichinomiya, O. and Maruyama, K.,"Experimental determinations of the natural frequencies and mode shapes of point-supported circular plates," Bull. Hokkaido Institute of Technology, 6,pp.9-14 (1973).

(102) Irie, T. and Yamada, G.,"The free vibration of a circular plate elastically supported on some arcs," Proc. 11th Conf. Dynamics of Machines (Prague, Czechoslovakia), pp.173-178 (1977).

(103) Okazaki, K. et al.,"Vibrations and bucklings of a circular plate with various constraints on its annular circle," Bull. JSME, 22(163),pp.31-40 (1979).

(104) Narita, Y. and Leissa, A.W.,"Transverse vibration of free circular plates elastically constrained along parts of the edge," J. Solids Structs. (to appear).

(105) Kirk, C.L. and Leissa, A.W.,"Vibration characteristics of a circular plate with a concentric reinforcing ring," J. Sound Vibr.,5(2),pp.278-284 (1967).

(106) Takahashi, S.,"The vibration of a circular plate with a rigid ring," Bull. JSME, 10(39),pp.463-471 (1967).

(107) Takahashi, S.,"The vibration of a circular plate with weights or a bar on its boundary," Bull. JSME, 10(40), pp.626-634 (1967).

(108) Stuart, R.J. and Carney III, J.F.,"Vibration of circular plates with edge-beams," Proc. ASCE, 99(EM4),pp.907-912 (1973).

(109) Chopra, I. and Durvasula, S.,"Vibration of simply-supported trapezoidal plates,I.symmetric trapezoids," J. Sound Vibr., 19(4),pp.379-392 (1971).

(110) Chopra, I. and Durvasula, S.,"Vibration of simply-supported trapezoidal plates,II.unsymmetic trapezoids," J. Sound Vibr., 20(2),pp.125-134 (1972).

(111) Orris, R.M. and Petyt, M.,"A finite element study of the vibration of trapezoidal plates," J. Sound Vibr.,27(3), pp.325-344 (1973).

(112) Williams, R., Yeow, Y.T. and Brinson, H.F.,"An analytical and experimental study of vibrating equilateral triangular plates," Exptl. Mech., 15(9),pp.339-346 (1975).

(113) Cox, H.L. and Klein, B.,"Fundamental frequencies of clamped triangular plates," J. Acous. Soc. Amer., 27(2), pp.266-268 (1955).

(114) Hersch, J.,"Une Méthode pour l'Évaluation par Défaut de la Premiere Valeur Propre de la Vibration ou du Flambage des Plaques Encastrées," Bull. Acad. Sci. (Paris), 13,pp.3943-3945 (1960).

(115) Ota, T., Hamada, M. and Tarumoto, T.,"Fundamental frequency of an isosceles-triangular plate," Bull. JSME, 4(15),pp.478-481 (1961).

(116) Reid, W.P.,"Vibrating triangular plate," Appl. Sci. Res., 17(4/5),pp.291-295 (1967).

(117) Koerner, D.R. and Snell, R.R.,"Vibration of cantilevered right triangular plates," Proc. ASCE, 93(ST5),pp.561-566 (1967).

(118) Waller, M.D.,"Vibrations of free plates:line symmetry; corresponding modes," Proc. Roy. Soc. (London), A 211, pp.265-276 (1952).

(119) Kaczkowski, Z.,"Stabilität und Eigenschwingungen einer Platte von der Form eines regelmässigen Polygons," Ost. Ingr. Arch., 15,pp.103-109 (1961).

(120) Conway, H.D.,"The bending, buckling, and flexural vibration of simply supported polygonal plates by point-matching," J. Appl. Mech., 28(2),pp.288-291 (1961).

(121) Conway, H.D.,"Analogies between the buckling and vibration of polygonal plates and membranes," Canadian Aero. J., 6(7),p.263 (1960).

(122) Walkinshaw, D.S. and Kennedy, J.S.,"On forced response of polygonal plates," Ing. Arch., 38(6),pp.358-369 (1969).

(123) Shahady, P.A., Passarelli, R. and Laura, P.A.,"Application of complex-variable theory to the determination of the fundamental frequency of vibrating plates," J. Acous. Soc. Amer., 42(4),pp.806-809 (1967).

(124) Yu, J.C.M.,"Application of conformal mapping and variational method to the study of natural frequencies of polygonal plates," J. Acous. Soc. Amer., 49(3),pp.781-785 (1971).

(125) Laura, P.A. and Marinelli, E.,"Comments on "Application of conformal mapping and variational method to the study of natural frequencies of polygonal plates"," J. Acous. Soc. Amer., 51(1),p.38 (1972).

(126) Roberts, S.B.,"Buckling and vibrations of polygonal and rhombic plates," Proc. ASCE, 97(EM2),pp.305-315 (1971).

(127) Cheung, Y.K. and Cheung, M.S.,"Flexural vibrations of rectangular and other polygonal plates," Proc. ASCE, 97 (EM2),pp.391-411 (1971).

(128) Gutierrez, R.H., Laura, P.A. and Steinberg, D.S.,"Determination of the second natural frequency of simply supported regular polygonal plates," J. Sound Vibr., 55 (1),pp.146-149 (1977).

(129) Irie, T., Yamada, G. and Narita, Y.,"Free vibration of clamped polygonal plates," Bull. JSME, 21(162),pp.1696-1702 (1978).

(130) Laura, P.A. and Gutierrez, R.H.,"Fundamental frequency of vibration of clamped plates of arbitrary shape subjected to a hydrostatic state of in-plane stress," J. Sound Vibr., 48(3),pp.327-332 (1976).

(131) Laura, P.A., Gutierrez, R.H. and Steinberg, D.S., "Vibration of simply supported plates of arbitrary shape carrying concentrated masses and subjected to a hydrostatic state of in-plane stresses," J. Sound Vibr., 55(1),pp.49-53 (1977).

(132) Nayfeh, A.H. et al.,"Vibrations of nearly annular and circular plates," J. Sound Vibr., 47(1),pp.75-84 (1976).

(133) Pnueli, D.,"Lower bounds to the gravest and all higher frequencies of homogeneous vibrating plates of arbitrary shape," J. Appl. Mech., 42(4),pp.815-820 (1975).

(134) Grinsted, B.,"Nodal pattern analysis," Proc. Inst. Mech. Eng.,Ser.A, 166,pp.309-326 (1952).

(135) Ruscoe, A.D.,"Communication on nodal pattern analysis," Proc. Inst. Mech. Eng.,pp.174-176 (1954).

(136) Vivoli, J. and Filippi, P.,"Eigenfrequencies of thin plates and layer potentials," J. Acous. Soc. Amer., 55 (3),pp.562-567 (1974).

(137) Khurasia, H.B. and Rawtani, S.,"Vibration-analysis of circular-arc aerofoil shaped plates," Intl. J. Mech. Sci., 20(5),p.283 (1978).

(138) Рвачев, В.Л. and Ракова, Л.В., "Расчет собственных форм и частот поперечных колебаний пластинки сложной формы," Прикладная механика, VI (4), pp. 80-85 (1977), (in Russian).

(139) Maruyama, K. and Ichinomiya, O.,"Experimental determination of transverse vibration modes of thin I-shaped plates," Exptl. Mech., 19(8),pp.271-275 (1979).

(140) Chladni, E.F.F., Die Akustik (2nd ed.),p.128 (1802).

(141) Ochs, J.B. and Snowdon, J.C.,"Transmissibility across simply supported thin plates,I.rectangular and square plates with and without damping layers," J. Acous. Soc. Amer., 58(4),pp.832-840 (1975).

(142) Ochs, J.B., Snowdon, J.C. and Kerlin, R.L.,"Transmissibility across clamped circular plates with central loading masses and various rib configulations," J. Acous. Soc. Amer., 59(6),pp.1347-1360 (1976).

(143) Ravenhall, F.W. and Som, A.K.,"Some recent observations on Chladni's figures," Acustica, 29(1),pp.14-21 (1973).

(144) Steinberg, D.S.,"Avoiding vibration in odd-shaped printed-circuit boards," Mach. Des., 48(12),pp.116-119 (1976).

(145) Sampson, R.C.,"Holographic-interferometry applications in experimental mechanics," Exptl. Mech., 10,pp.313-320 (1970).

(146) Powell, R. and Stetson, K.,"Interferometric vibration analysis by wavefront reconstruction," J. Opt. Soc. Amer., 55(12),pp.1593-1598 (1965).

(147) Monahan, M.A. and Bromley, K.,"Vibration analysis by holographic interferometry," J. Acous. Soc. Amer.,44 (5),pp.1225-1231 (1968).

(148) Aprahamian, R. and Evensen, D.A.,"Applications of holography to dynamics:high-frequency vibrations of beams," J. Appl. Mech., 37(2),pp.287-291 (1970).

(149) Aprahamian, R. and Evensen, D.A.,"Applications of holography to dynamics: high-frequency vibrations of plates," J. Appl. Mech., 37(4),pp.1083-1090 (1970).

(150) Maruyama, K.,"Measurements of vibrational modes of thin plate by holographic interferometry, part 1. clamped circular plate," Bull. Hokkaido Institute of Technology, 3,pp.185-196 (1975).

(151) Maruyama, K. and Ichinomiya, O.,"Experimental determination of natural frequencies and mode shapes of rectangular plates," Bull. Hokkaido Institute of Technology, 7,pp.23-34 (1979).

(152) Leuner, T.R.,"An experimental-theoretical study of free vibrations of plates on elastic point supports," J. Sound Vibr., 32(4),pp.481-490 (1974).

(153) Olson. M.D. and Hazell, C.R.,"Vibration studies on some integral rib-stiffened plates," J. Sound Vibr., 50(1), pp.43-61 (1977).

(154) Klein, B.,"Vibration of simply supported isosceles trapezoidal flat plates," J.Acous. Soc. Amer., 27(6),pp. 1059-1060 (1955).

(155) Donaldson, B.K.,"A new approach to the forced vibration of thin plates," J. Sound Vibr., 30(4),pp.397-417 (1973).

(156) Donaldson, B.K. and Chander, S.,"Numerical results for extended field method applications," J. Sound Vibr., 50 (4),pp.437-444 (1973).

(157) Sepaha, S.P. and Durvasula, S.,"Vibration of trapezoidal cantilever plates with partial root chord support," J. Indian Inst. Sci., 54(1),pp.43-54 (1972).

(158) Durvasula, S.,"Natural frequencies and modes of clamped skew plates," AIAA J., 7(6),p.1164 (1969).

(159) Durvasula, S.,"Free vibration of simply supported parallelogramic plates," J. Aircraft, 6,pp.66-68 (1969).

(160) Durvasula, S. and Abdel Fattah, A.A.,"An experimental study of vibration of clamped skew plates," Inst. Engrs. (Australia), Mech. Chem. Engng. Trans., MC 5(2),pp.59-63 (1969).

(161) Cuntze, R.,"Determination of natural frequencies of thin, oblique, isotropic plates," Zeit. Angew. Math. Mech.,49 (5),pp.306-309 (1969), (in German).

(162) Rami Reddy, K. and Amba Rao, C.L.,"Lateral vibration and stability relationship of elastically restrained skew plates," J. Acous. Soc. India, 24(3),pp.371-374 (1972).

(163) Nair, P.S. and Durvasula, S.,"Vibration of skew plates," J. Sound Vibr., 26(1),pp.1-19 (1973).

(164) Durvasula, S. and Nair, P.S.,"Application of partition method to vibration problems of plates," J. Sound Vibr., 37(3),pp.429-445 (1974).

(165) Mizusawa, T., Kajita, T. and Naruoka, M.,"Vibration of skew plates by using B-spline functions," J. Sound Vibr., 62(2),pp.301-308 (1979).

(166) Raju, P.N.,"Vibrations of annular plates," J. Aeron. Soc. India, 14(2),pp.37-52 (1962).

(167) Marchi, E. and Diaz, M.,"Elastic vibrations in the crowns of thin plates:part 1," Atti della Accademia delle Scienze di Torino, 101(5),pp.739-747 (1966/67).

(168) Zgrablich, G. and Diaz, M.,"Elastic vibrations in crowns of thin circular plates:part 2," Atti della Accademia delle Scienze di Torino, 101(5),pp.763-770 (1966/67).

(169) Ramaiah, G.K. and Vijayakumar, K.,"A note on flexural vibrations of annular plates of narrow width," J. Sound Vibr., 51(4),pp.574-576 (1977).

(170) Wilson, J.F. and Garg, D.P.,"Frequencies of annular plate and curved beam elements," AIAA J., 16(3),pp.270-272 (1978).

(171) Eastep, F.E. and Hemmig, F.G.,"Estimation of fundamental frequency of non-circular plates with free, circular cutouts," J. Sound Vibr., 56(2),pp.155-165 (1978).

(172) Nagaya, K.,"Transverse vibration of a plate having an eccentric inner boundary," J. Appl.Mech., 44(1),pp.165-166 (1977).

(173) Nagaya, K.,"Dynamics of viscoelastic plate with curved boundaries of arbitrary shape," J. Appl. Mech., 45(3), pp.629-635 (1978).

(174) Nagaya, K.,"Vibration of a viscoelastic plate having a circular outer boundary and an eccentric circular inner boundary for various edge conditions," J. Sound Vibr., 63(1),pp.73-86 (1979).

(175) Khurasia, H.B. and Rawtani, S.,"Vibration analysis of circular plates with eccentric holes," J. Appl. Mech., 45(1),pp.215-217 (1978).

(176) Westmann, R.A.,"A note on free vibrations of triangular and sector plates," J. Aerospace Sci., 29(9),pp.1139-1140 (1962).

(177) Ramakrishnan, R. and Kunukkasseril, V.X.,"Free vibration of annular sector plates," J. Sound Vibr., 30(1),pp.127-129 (1973).

(178) Ramaiah, G.K. and Vijayakumar, K.,"Natural frequencies of circumferentially truncated sector plates with simply supported straight edges," J. Sound Vibr., 34(1),pp.53-61 (1974).

(179) Rubin, C.,"Vibrating modes for simply supported polar-orthotropic sector plates," J. Acous. Soc. Amer., 58(4), pp.841-845 (1975).

(180) Ben-Amoz, M.,"Note on deflections and flexural vibrations of clamped sectorial plates," J. Appl. Mech., 26(1),pp. 136-137 (1959).

(181) Rubin, C.,"Nodal circles and natural frequencies for the isotropic wedge," J. Sound Vibr., 39(4),pp.523-526 (1975).

(182) Bhattacharya, A.P. and Bhowmic, K.N.,"Free vibration of a sectorial plate," J. Sound Vibr., 41(4),pp.503-505 (1975).

(183) Mukhopadhyay, M.,"A semi-analytic solution for free vibration of annular sector plates," J. Sound Vibr., 63(1), pp.87-96 (1979).

(184) Shibaoka, Y.,"On the transverse vibration of an elliptic plate with clamped edge," J. Phys. Soc. Japan, 11(7), pp.797-803 (1956).

(185) McNitt, R.P.,"Free vibration of a clamped elliptic plate," J. Aerospace Sci., 29(9),p.1124 (1962).

(186) Mazumdar, J.,"Transverse vibration of elastic plates by method of constant deflection lines," J. Sound Vibr., pp.147-155 (1971).

(187) Leissa, A.W.,"Vibration of a simply supported elliptical plate," J. Sound Vibr., 6(1),pp.145-148 (1967).

(188) Sato, K.,"Free flexural vibrations of an elliptical plate with simply supported edge," J. Acous. Soc. Amer., 52(3), pp.919-927 (1972).

(189) Sato, K.,"Free flexural vibrations of an elliptical plate with edge restrained elastically," Bull. JSME, 19(129), pp.260-264 (1976).

(190) Waller, M.D.,"Vibration of free elliptical plates," Proc. Phys. Soc., 63,p.451 (1950).

(191) Beres, D.P.,"Vibration analysis of a completely free elliptical plate," J. Sound Vibr., 34(3),pp.441-443 (1974).

(192) Sato, K.,"Free flexural vibrations of a ring-shaped plate bounded by confocal ellipses," J. Acous. Soc. Amer., 56 (4),pp.1172-1176 (1974).

(193) Forsching, H.,"Natural frequencies of isotropic cantilever semi-elliptical and semicircular plates," Inge. Arch., 36(3),pp.192-204 (1967),(in German).

(194) Solecki, R.,"Bending and vibration of an isotropic rectangular plate with a hinged slot," Acta Polytech. Scandinavia, 12,pp.3-19 (1962).

(195) Lynn, P.P. and Kumbasar, N.,"Free vibrations of thin rectangular plates having narrow cracks with simply supported edges," Gen Radio Exptr., 4,pp.911-928 (1967).

(196) Keer, L.M. and Sves, C.,"On the bending of cracked plates," Intl. J. Solids Structs., 6,pp.1545-1559 (1970).

(197) Stahl, B. and Keer, L.M.,"Vibration and stability of cracked rectangular plates," Intl. J. Solids Structs., 8(1),pp.69-91 (1972).

(198) Hirano, Y. and Okazaki, K.,"Vibration of cracked rectangular plates," Trans. JSME, 45(397),pp.975-984 (1979).

(199) Takahashi, S.,"Vibration of rectangular plates with circular holes," Bull. JSME, 1(4),pp.380-385 (1958).

(200) Kumai, T.,"The flexural vibrations of square plate with a central circular hole," Proc. 2nd Jap. Natl. Congr. Appl.Mech.,pp.339-342 (1952).

(201) Basdekas, N.L. and Chi, M.,"Dynamic response of plates with cutouts," Shock vibr. Bull., 41,pp.435-441 (1970).

(202) Monahan, Lt.J., Nemergut, P.J. and Maddux, G.E.,"Natural frequencies and mode shapes of plates with interior cutouts," Schock Vibr. Bull., 41,pp.37-49 (1970).

(203) Kristiansen, U. and Soedel, W.,"Fundamental frequencies of cutout square plates with clamped edges," Trans. ASME, Ser.B 93,pp.343-345 (1971).

(204) Paramasivam, P. and Sridhar Rao, J.K.,"Free vibrations of square plates with stiffened square openings," Intl. J. Mech. Sci., 15(2),pp.117-122 (1973).

(205) Paramasivam, P.,"Free vibration of square plates with square openings," J. Sound Vibr., 30(2),pp.173-178 (1973).

(206) Hegarty, R.F. and Ariman, T.,"Elasto-dynamic analysis of rectangular plates with circular holes," Intl. J. Solids Structs., 11(7/8),pp.895-906 (1975).

(207) Akus, G. and Ali, R.,"Determination of dynamic characteristics of rectangular plates with cutouts using a finite difference formulation," J. Sound Vibr., 44(1), pp.147-158 (1976).

(208) Rajamani, A. and Prabhakaran, R.,"Dynamic response of composite plates with cut-outs, part I:simply-supported plates," J. Sound Vibr., 54(4),pp.549-564 (1977).

(209) Rajamani, A. and Prabhakaran, R.,"Dynamic response of composite plates with cut-outs, part II:clamped-clamped plates," J. Sound Vibr., 54(4),pp.565-576 (1977).